

**GERM CELL TUMOR TREATMENT
RESISTANCE AND LIQUID BIOPSY-BASED
microRNA BIOMARKERS**

Dennis Michael Timmerman

ISBN: 978-94-6483-687-5

DOI: <https://doi.org/10.33540/2055>

Cover design: Kimberly Timmerman

Lay-out and print: Ridderprint | www.ridderprint.nl

© Copyright 2024: Dennis Timmerman, Utrecht, Nederland

All rights reserved. No part of this publication may be reproduced, stored in a retrieval system, or transmitted in any form or by any means, electronic, mechanical, by photocopying, recording, or otherwise, without the prior written permission of the author.

Germ cell tumor treatment resistance and liquid biopsy-based microRNA biomarkers

Kiemceltumor behandelingsresistentie en vloeibare biopsie-gebaseerde microRNA-biomarkers

(met een samenvatting in het Nederlands)

Proefschrift

ter verkrijging van de graad van doctor aan de
Universiteit Utrecht
op gezag van de
rector magnificus, prof. dr. H.R.B.M. Kummeling,
ingevolge het besluit van het college voor promoties
in het openbaar te verdedigen op

dinsdag 23 januari 2024 des middags te 4.15 uur

door

Dennis Michael Timmerman

geboren op 23 september 1995
te Dordrecht

Promotor:

Prof. dr. L. H. J. Looijenga

Beoordelingscommissie:

Dr. O. R. Brouwer

Prof. dr. J. H. J. Hoeijmakers

Prof. dr. L. M. O. de Kort (voorzitter)

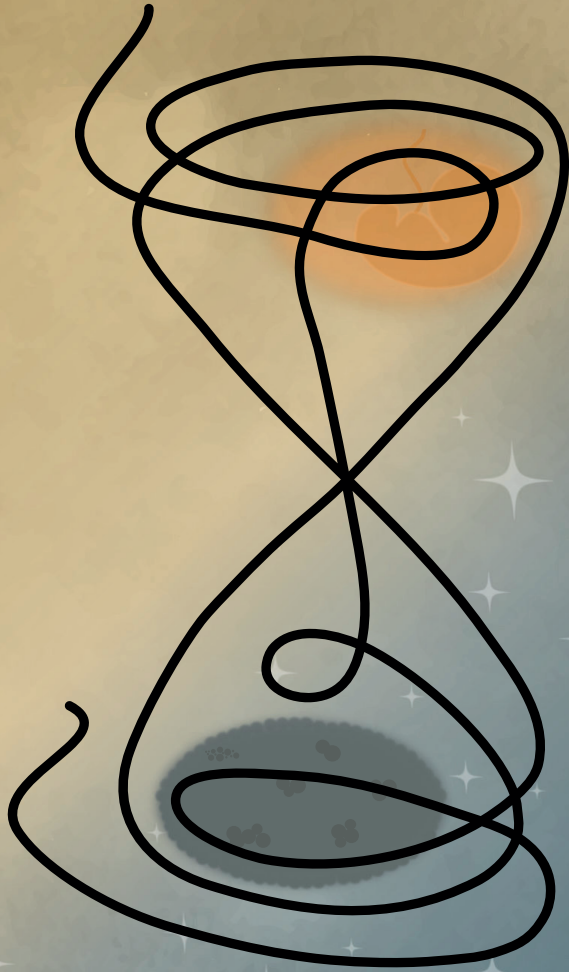
Prof. dr. M. M. Maurice

Prof. dr. J. J. Molenaar

TABLE OF CONTENTS

Chapter 1	General introduction	9
Chapter 2	Mechanisms of TP53 Pathway Inactivation in Embryonic and Somatic Cells—Relevance for Understanding (Germ Cell) Tumorigenesis	27
Chapter 3	The Role of TP53 in Cisplatin Resistance in Mediastinal and Testicular Germ Cell Tumors	91
Chapter 4	Chromosome 3p25.3 gain is associated with cisplatin resistance and is an independent predictor of poor outcome in male malignant germ cell tumors	115
Chapter 5	Comparative Analyses of Liquid-Biopsy MicroRNA371a-3p Isolation Protocols for Serum and Plasma	135
Chapter 6	miR371a-3 cluster functionality in germ cell tumor cell lines	157
Chapter 7	Analysis of a mouse germ cell tumor model establishes pluripotency-associated miRNAs (mouse miR-290-295/human miR-371-373) as conserved serum biomarkers for germ cell cancer detection	199
Chapter 8	General discussion	229
Addendum	English summary	244
	Nederlandse samenvatting	247
	Curriculum Vitae	251
	PhD Portfolio	252
	Dankwoord	253

Chapter



1

Chapter 1

General introduction

INTRODUCTION

Origin and histology

Germ cell tumors (GCTs) are neoplasms derived from embryonic precursors of the germ line, called the primordial germ cells (PGCs), as well as derivatives thereof, and can arise anywhere in the mid-line of the body, for example, in the gonads, but also extragonadal in the (retro)peritoneum and the mediastinum, as well as intracranially, in the brain (Looijenga and Oosterhuis, 1999; Oosterhuis and Looijenga, 2005; Oosterhuis and Looijenga, 2019). Although GCTs can occur both in males and females, in this thesis the focus will be mostly on the male variant, of which the majority occur in the testis, hereafter referred to as Testicular GCTs ((T)GCTs). (T)GCTs can be divided into two groups based on the origin, i.e., presence or absence, of the precursor lesion called 'germ cell neoplasm *in situ*' (GCNIS) (Berney *et al.*, 2016; Moch *et al.*, 2016; Cheng *et al.*, 2018) which is a term derived from the term 'carcinoma *in situ* of the testis' mentioned first in 1972 (Skakkebaek, 1972) as well as "intratubular germ cell neoplasia unclassified/undifferentiated/undetermined" (Ulbright, 2005). Even though, biologically, (T)GCTs can be divided into seven groups (Oosterhuis and Looijenga, 2019), the most well understood, studied and common are the Type I and Type II. Type I (T)GCTs are the non-GCNIS-related tumors and are most common in prepubertal (pediatric) patients, giving rise to teratomas and/or yolk-sac tumors (YST). Type II (T)GCTs are the GCNIS-related and are histologically and clinically divided into seminomas or non-seminomatous GCTs (NSGCTs) which can harbor both embryonic and extra-embryonic structures and therefore can present as either pure or mixed elements of embryonal carcinoma (EC), choriocarcinoma (CC) or YSTs (both extra-embryonal), and teratomas (embryonal) (Sesterhenn and Davis, 2004; Oosterhuis and Looijenga, 2005; Berney *et al.*, 2016; Moch *et al.*, 2016; Cheng *et al.*, 2018; Oosterhuis and Looijenga, 2019). Mixtures of seminoma and the various components of nonseminoma can occur. The distinction between Type I and Type II (T)GCTs is of importance in treatment stratification as Type II (T)GCTs often have a more poor-prognosis and require more aggressive treatment (chemotherapy and/or radiotherapy) depending on the stage of clinical presentation, whilst Type I GCTs are more often treated with surgery alone. This is related to the intrinsic chemotherapy resistance of fully differentiated teratomas, both regarding those as Type I and Type II (Marina *et al.*, 1999; Ulbright *et al.*, 2005; Siddiqui *et al.*, 2019; Hulsker *et al.*, 2021).

Prevalence

TGCTs, i.e., Type II, are the most common solid malignancy in young Caucasian males aged between 15 and 44 years old, accounting for approximately 1% of male cancers worldwide (Trabert *et al.*, 2015). Yearly, in the US, it is estimated that 9910 new cases of

TGCTs are diagnosed, including roughly 5% (460) of patients that eventually succumb to the disease (Siegel *et al.*, 2022). Although patients staged in ‘good prognosis’ groups according to the International Germ Cell Cancer Collaborative Group (IGCCCG) risk classification model, have an expected cure rate exceeding 95%, overall survival in ‘poor prognosis’ patients does not exceed 70% or even lower (International Germ Cell Cancer Collaborative Group, 1997; Olofsson *et al.*, 2011; Gillessen *et al.*, 2019). Of note, patients harboring a nonsemitomatous mediastinal GCT are by definition considered ‘poor prognosis’ by the IGCCCG due to the aggressiveness of these tumors (International Germ Cell Cancer Collaborative Group, 1997; Bokemeyer *et al.*, 2002). These statistics, combined with the young age at which these malignancies occur, culminate in the most potential years of life lost due to this disease (Song *et al.*, 2020).

Treatment

The main treatment modality for (T)GCT tumor patients typically involves a combination of surgery and radiotherapy or chemotherapy, consisting of three to four cycles of Bleomycin, Etoposide and Cisplatin (BEP) in adults, of which cisplatin is the key component of this treatment (Olofsson *et al.*, 2011; Jacobsen and Honecker, 2015; Honecker *et al.*, 2018). This DNA-crosslinking platin-based chemotherapeutic agent has been around since the 70s (Rosenberg *et al.*, 1965; Reed, 1998) and was first reported in the use for TGCTs in a Phase I study demonstrating that 9 out of 11 (T)GCT patients responded well to this drug, with complete remission in three cases (Higby *et al.*, 1974). A more comprehensive study in 50 TGCT patients a few years later, investigated the use of cisplatin in combination with vinblastine and bleomycin, demonstrating 74% complete remissions using this regimen resulting in, together with the 26% partial remissions and surgical intervention, an overall disease-free status of 85% (Einhorn and Donohue, 1977).

Side-effects

Unfortunately, treating relatively young patients with cisplatin can come with various side-effects, of which some, are permanent. Many patients experience ototoxicity (hearing loss), but also nephrotoxicity, pulmonary toxicity, and even cardiovascular disease pose threats to patient well-being (Travis *et al.*, 2010; Ahmad *et al.*, 2016). In addition, chemotherapy induced infertility is a major problem as well. Cryopreservation of sperm is not possible for prepubertal patients, due to the absence of spermatogenesis at this age, while cryopreservation in general is possible for females in this age group (Chow *et al.*, 2016; Goossens *et al.*, 2020). Lastly, survivors of (T)GCTs have a significantly increased risk to develop second primary malignancies for at least 35 years after treatment (Travis *et al.*, 2005). Considering that most of these patients are particularly young, the chances

of developing the second primary malignancies increase drastically, adding to increased death among testicular cancer survivors (Travis *et al.*, 2005).

Cisplatin vs Carboplatin

Due to cisplatin's many side-effects, researchers have looked for alternative therapies with similar efficacies while increasing patient well-being. One of these compounds is carboplatin, a cisplatin analogue harboring in principle the same mechanism of action while causing less ototoxicity and nephrotoxicity and having a similar penetrance through the blood-brain-barrier (Reed, 1998; Jacobs *et al.*, 2010; Ho *et al.*, 2016; Frazier *et al.*, 2018). In the late 80s four randomized clinical trials were conducted studying the difference between carboplatin and cisplatin in adult male non-seminoma TGCT patients (Bajorin *et al.*, 1993; Tjulandin *et al.*, 1993; Bokemeyer *et al.*, 1996; Horwich *et al.*, 1997), all reporting that cisplatin outperforms carboplatin in the clinic, by reducing both the risk of events and the risk of death (Frazier *et al.*, 2018). Similar results were obtained for seminomas, comparing single-agent carboplatin treatment to cisplatin-based combination treatments demonstrated inferior overall survival (OS) and progression-free survival (PFS) in carboplatin treated patients (Bokemeyer *et al.*, 2004). However, a systematic review by Shaikh and colleagues reported that while carboplatin might not be suitable for the treatment of adult (T)GCT patients, it could be promising in pediatric cases due to increased number of cycles, frequency, and higher dose treatment protocols (Shaikh *et al.*, 2013). They report that, over three studies, 88% of children treated with carboplatin remained event-free (Shaik *et al.*, 2013). Due to these results carboplatin is more and more advocated for the treatment of pediatric non-teratoma (Type I) GCTs, i.e., yolk sac tumors, demonstrating equivalent outcomes compared to cisplatin, with lower long-term toxicities (Jain *et al.*, 2022). Furthermore, carboplatin-based regimens have also shown good survival rates, comparable to cisplatin, while demonstrating low ototoxicity in intracranial pediatric GCT patients (Worawongsakul *et al.*, 2020). Because carboplatin is still under investigation as alternative for cisplatin for the use in the clinic, with active trials ongoing, we will use the term "cisplatin" throughout this thesis, focusing on the standard of care treatment modality currently in the clinic for adult (T)GCT patients.

Pluripotency

(T)GCTs resemble embryonic stem (ES) cells and derivatives in many ways, from their intrinsic pluripotent characteristics allowing them to differentiate into any kind of somatic tissue (teratomas), to their totipotency, allowing them to form even extra-embryonal structures, like the yolk-sac and the chorion (early fetal placenta), as well as the germ cell lineage itself. The explanation why (T)GCTs resemble ES cells is their cell of origin.

As (T)GCTs arise from early germ-layer progenitors, called the PGCs or derivatives, they are very closely related to ES cells (**Figure 1**). Furthermore, the more mature germ cells generated eventually in the gonads, can, once fertilized, give rise to an entire new organism including the extra-embryonic structures, one can imagine the totipotent features present in germ cell progenitors, and tumors thereof (Oosterhuis and Looijenga, 2005; Cheng *et al.*, 2018; Oosterhuis and Looijenga, 2019). One of the main features of (T) GCTs, in which they can be characterized histologically, is the presence of the stem cell component, i.e., embryonal carcinomas (Looijenga and Oosterhuis, 1999). These cells indeed closely resemble ES cells, illustrated by the co-expression of pluripotency markers OCT3/4 (POU5F1) and SOX2 (SOX17 in seminomas) (Looijenga *et al.*, 2003; Oosterhuis and Looijenga, 2005; De Jong *et al.*, 2008; Cheng *et al.*, 2018; Oosterhuis and Looijenga, 2019).

Biomarkers

Even though (T)GCTs can be relatively easy diagnosed by histology, less invasive diagnostic markers are applied in the clinic as well, like serum tumors markers (STMs). Histology requires patient tumor material, either acquired by biopsy or resection, while STMs can be measured for example via blood and are therefore less invasive, and more efficient in application. The STMs currently used in the clinic for (T)GCT patients are AFP (alpha-fetoprotein), a protein normally produced in the liver and the yolk-sac, β -HCG (beta-human chorionic gonadotropin), a hormone produced by the placenta during pregnancy and, although to a lesser extent, LDH (lactate dehydrogenase), an enzyme of which elevated levels can indicate tissue damage, including cancer cell induced damage (Cheng *et al.*, 2018; Almstrup *et al.*, 2020; Leão *et al.*, 2022). However, these have limitations in their level of informativity, both regarding sensitivity as well as specificity. Therefore, there is space for improvement, to allow improved diagnosis as well as follow up of these patients, the latter both in the context of surveillance and systemic therapy. In this context, interesting targets have been identified, including microRNAs (miRNAs). These are small non-coding RNAs that are approximately 21 – 25 nucleotides in size, involved post-transcriptional regulation of gene activity and especially important in for example embryonal development (Gross *et al.*, 2017). Although the general mechanism of miRNAs is to a certain level understood, their vast abundance, rapid turnover, and many (putative) targets make them difficult to map regarding their actual functionality. Approximately two decades ago, a specific cluster of miRNAs, known as the miR371a-3 cluster (containing hsa-miR371a, hsa-miR372 and hsa-miR373), was discovered to not only be expressed in embryonic tissue, but harbor oncogenic capacities when overexpressed, in particular in (T)GCTs (Voorhoeve *et al.*, 2006; Gillis *et al.*, 2007). Many studies into this cluster have reported that it is a quite specific biomarker for (T)GCTs (teratomas excluded) (Voorhoeve *et al.*, 2006; Gillis *et al.*, 2007; Murray *et al.*, 2011; Rijlaarsdam *et al.*, 2015; Syring

et al., 2015; Mego *et al.*, 2019). Not only are these miRNAs highly sensitive (only present in (T)GCT patients) and specific (not present in healthy donors), they are secreted by (T)GCTs (**Figure 1**), with the consistent exception of teratoma, and can be detected from liquid-biopsy based samples from patients (e.g. blood (serum/plasma), seminal fluid and cerebrospinal fluid), making them useful as diagnostic markers, treatment follow-up, early relapse and the detection of residual metastatic disease (Gillis *et al.*, 2007; Murray *et al.*, 2011; Rijlaarsdam *et al.*, 2015; Syring *et al.*, 2015; van Agthoven *et al.*, 2017; Dieckmann *et al.*, 2019; Mego *et al.*, 2019; Almstrup *et al.*, 2020; Leão *et al.*, 2022).

Mouse models

There are only limited GCT mouse models available, likely because of the lack of PGC specific promotor sequences. One novel prominent genetically engineered mouse model (GEMM) is the gPAK mouse (Pierpont *et al.*, 2017; Lundaker *et al.*, 2021). These mice develop tumors specifically in early spermatogonia due to a *Stra8-Cre* transgene induced recombination of *LoxP* sites and conditional expression of mutant *Kras*^{G12D} (following a *LoxP-STOP-LoxP* cassette) and a conditional knock out of *Pten* (harboring flanking *LoxP* sites on exon 5) in early mitotic spermatogonia (Pierpont *et al.*, 2017; Lundaker *et al.*, 2021). Secondly, GCT cell line xenografting offers a decent alternative to GEMMs.

TP53 status

Another interesting resemblance between (T)GCTs and ES cells is their overall wild-type *TP53* status. Unlike most solid malignancies, which demonstrate a mutation-rate of about 50% in *TP53* (Kandoth *et al.*, 2013), treatment naïve (T)GCTs rarely harbor *TP53* mutations, irrespective of histology (Kersemaekers *et al.*, 2002; Oosterhuis and Looijenga, 2005; Bagrodia *et al.*, 2016; Oosterhuis and Looijenga, 2019). This wild-type *TP53* status, combined with their embryonal origin, also corroborates the low/inefficient DNA damage response of (T)GCTs where, like in ES cells, apoptosis is preferred over repair (Kersemaekers *et al.*, 2002; Filion *et al.*, 2009; Gutekunst *et al.*, 2011; Jacobsen and Honecker, 2015; Bloom *et al.*, 2019). As both (T)GCTs and ES cells prefer apoptosis over DNA-repair as a means of genome protection, they display a hypersensitive apoptotic response to DNA-damage, fueled by their pluripotent phenotype and P53 dependency (Bauer *et al.*, 2010; Koster *et al.*, 2011; Gutekunst *et al.*, 2013; Lobo *et al.*, 2020). This is considered the cornerstone of the excellent clinical outcomes achieved with cisplatin in (T)GCTs. Interestingly, *TP53* status in ES cells is a double-sided coin. While germline or *de novo* *TP53* mutations in ES cells cause Li-Fraumeni, a syndrome giving rise to many tissue-specific tumors in the early life of these patients (Light *et al.*, 2023), cultured human pluripotent stem cells are prone to acquire *TP53* mutations *in vitro* giving them a selective advantage in culture (Merkle

et al., 2017). Furthermore, GCTs with somatic transformation, that is cancers arising from differentiated cells of (usually) teratoma tissue that acquire new malignant (somatic) characteristics (Motzer *et al.*, 1998), lose their selection against *TP53* mutations (i.e. like most somatic cancers these cells often harbor *TP53* mutations in contrast to their original (T)GCT origin), illustrating again the embryonal similarities between (T)GCTs and ES cells (Houldsworth *et al.*, 1998).

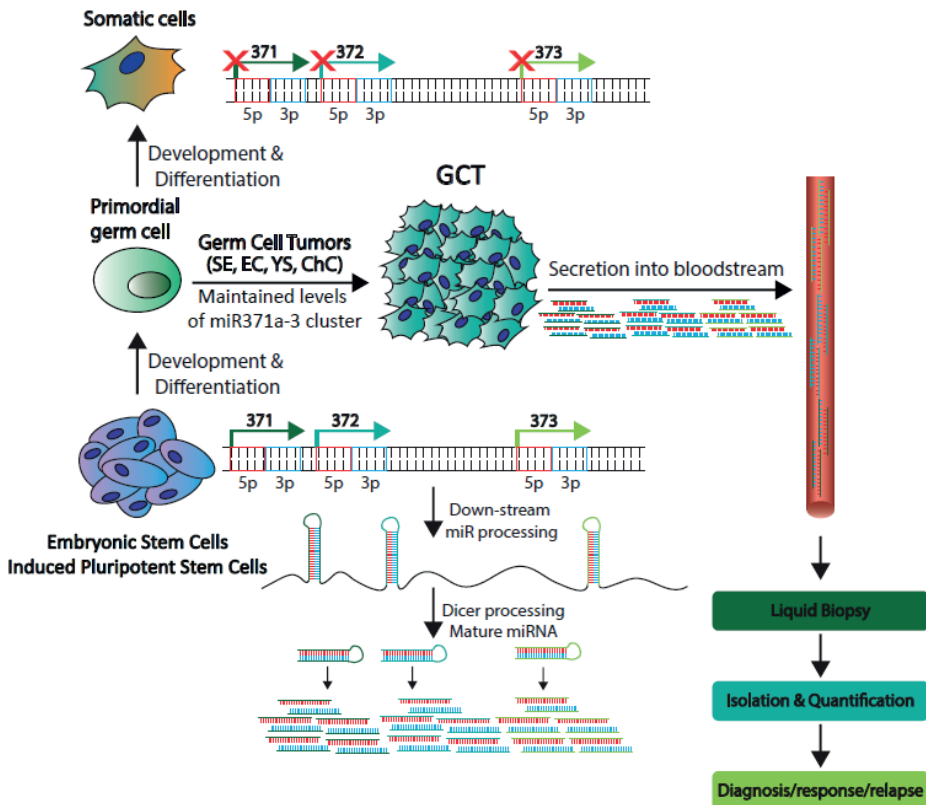


Figure 1. The differences in miR371a-3 cluster expression between ES cells, GCTs and somatic cells.

Resistance

The main clinical problem with (T)GCTs related to the use of cisplatin, besides the aforementioned long-term side-effects, is the potential intrinsic or acquired tumor resistance (**Figure 2**). Where over 95% of patients with a good prognosis malignancy survive, this number decreases to about 70% to even 50% in 'poor prognosis' patients, partially classed as such due to treatment resistance (Olofsson *et al.*, 2011). Moreover, as there is no proven effective alternative treatment modality currently available for (T)

GCTs (that does not require cisplatin), cisplatin-resistant patients will yet receive more cisplatin during high-dose chemotherapy salvage treatment, and therefore, about 50% of treatment resistant patients (~10% of all patients) eventually succumb to their disease (Einhorn, 2002; Einhorn *et al.*, 2007; Oechsle *et al.*, 2011; Oing *et al.*, 2018; Loveday *et al.*, 2020). Although it is known that common drivers of resistance and tumor development, like *TP53*, can play a role in tumor resistance in (T)GCTs, the number of patients harboring these mutations is relatively low and does not account for all resistant cases (Bauer *et al.*, 2010; Bagrodia *et al.*, 2016).

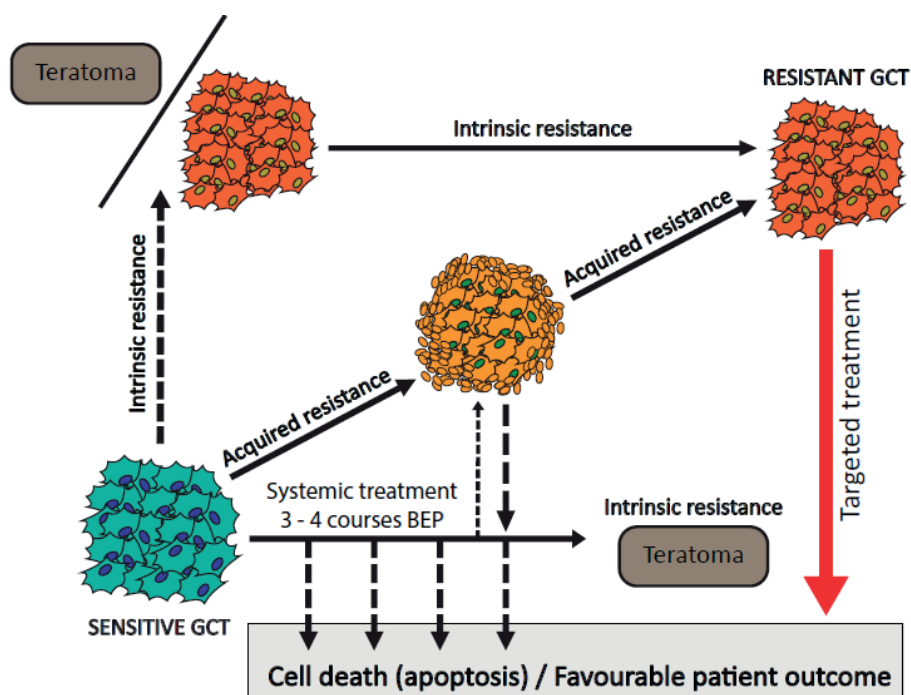


Figure 2. Model displaying different mechanisms to acquire resistance in GCTs.

Copy number alterations

One feature stereotypical to (Type II) TGCTs is their polyploidy. TGCTs have been known to be polyploid for almost three decades, and especially TGCTs are known to undergo (almost) whole-genome duplication (tetraploidization), followed by loss of various chromosomes during early onset of the disease (Oosterhuis *et al.*, 1989; de Jong *et al.*, 1990; Looijenga *et al.*, 1991; Dorssers *et al.*, 2019; Oosterhuis and Looijenga, 2019). Although it is known that (T)GCTs can harbor many copy number alterations (CNAs), there is an urgent

need to identify clinically relevant commonalities in these chromosomal rearrangements, especially the ones leading to cisplatin resistance. So far, the only well-known common alteration is the gain of isochromosome 12p (i12p), almost universal in Type II TGCTs, with the higher prevalence in non-seminomas compared to seminomas, although without a link to cisplatin resistance (Geurts van Kessel *et al.*, 1989; Van Echten *et al.*, 1995; Oosterhuis and Looijenga, 2019). Over the years many chromosomal arrangements have been suggested to play a role in cisplatin resistance, however, no common gain or loss was found, likely due to the high heterogeneity in (T)GCTs chromosomal constitution, as well as diversity in inclusion in the various studies published (Ma *et al.*, 2011, Bakardjieva-Mihaylova *et al.*, 2019; Singh *et al.*, 2019; Loveday *et al.*, 2020). Therefore, there is a clinical need to discover recurrent chromosomal arrangements to identify and stratify cisplatin resistant patients based on their CNA profiles.

THESIS SCOPE AND OUTLINE

The scope of this thesis is to address two domains of (T)GCT research, with potentially significant clinical impact. On one side using (T)GCT derived cell lines, genetic editing tools like CRISPR-Cas9 and publicly available patient data sets combined with our own cohorts, to study the underlying mechanism(s) of treatment resistance of (T)GCTs. Secondly, focusing on the possibilities as well as limitations of using the miR371a-3 cluster members as diagnostic marker as well as tool for treatment response monitoring and relapse detection. Since the discovery of the effectiveness of platin-based treatment for (T)GCTs, research into treatment resistance and disease relapse detection has been hampered by the consensus that these cancers are in fact considered curable. Unfortunately, cisplatin as treatment for (T)GCT is a double-edged sword; on one side being the main treatment modality cancer curable for most patients, while, on the other side, in addition to the significant and sometime life-long toxic side-effects, its efficacy is strongly reduced for refractory patients presenting with cisplatin resistant disease. Research into (early) detection of relapsed (T)GCTs using biomarkers and cisplatin resistant cases has increased over the years, however, mostly the latter, still largely left unsolved.

In **Chapter 2**, we discuss mechanisms of P53 pathway inactivation in both embryonic and somatic cells. The goal of this review is to understand the mechanisms at play in which (T)GCTs that, in origin, are embryonal, are malignant while maintaining a wild-type *TP53* status. Where 50% of solid cancers harbor some form of P53 pathway inactivation, either through direct (in)activating mutations of *TP53*, or through amplifications of important P53 regulators *MDM2* and *MDM4*, *TP53* mutations are rarely observed in (T)GCTs. In this review we speculate the (T)GCTs embryonal origin is the foundation for this phenotype postulating that (T)GCTs cells are at the crossroad between malignant, somatic, and

embryonal cells, at one side protecting their genome through an elevated apoptotic state (and often wild-type *TP53* status), and on the other side retaining pluripotent potential and unrestricted proliferation.

Chapter 3 continues down the road of the involvement of *TP53* in (T)GCTs, specifically in the context of resistance to cisplatin. In this chapter we use parental and cisplatin resistant isogenic clones of two commonly used non-seminoma (T)GCT cell lines, NCCIT (*TP53*^{Mut/-}) and 2102Ep (wild-type *TP53*), derived from different anatomical locations, the mediastinum, and the testis respectively. Using CRISPR Cas9 genome editing we introduced mutations in the *TP53* gene in both cell lines leading to premature STOP-codon and loss of the P53 protein. We demonstrate that, independent of anatomical location, or acquired cisplatin resistance, loss of P53 contributes to cisplatin resistance. Additionally, these results hold clinical value as, even though rarely seen in testicular (T) GCTs, mediastinal GCTs, considered to be more aggressive, more often present with *TP53* mutations. We postulate that mediastinal GCTs harbor intrinsic P53 driven resistance to cisplatin probably acquired through a stronger tumor selection due to an unfavorable environment (compared to testicular GCTs).

In **Chapter 4** we further investigate cisplatin resistance in (T)GCT cell lines and patients. Using a set of (T)GCT cell lines with isogenic cisplatin resistant subclones we identify, using whole genome sequencing, a recurring chromosomal amplification on the short arm of chromosome 3 in all resistant subclones. This is particularly relevant because these resistant subclones were generated independently from each other, even with (slightly) different protocols. We identify amplification of chromosome 3p25.3 to be an independent predictor of (T)GCT cisplatin resistance, rarely present in primary tumors, but more often found in relapsed/refractory tumors. Using a large public (MSKCC) dataset we demonstrate that 3p.25.3 amplification specifically marks cisplatin resistance in non-seminomas (and not seminomas) and patients harboring this amplification have a significantly worse progression free survival and overall survival. Finally, stratifying patients based on this amplification adds prognostic value adding to both classical IGCCCG staging and *MDM2/TP53* status. This finding offers possibilities to identify patients with an increased risk to have or develop cisplatin-refractory disease and allow initiation of studies to develop more effective treatment modalities for these patients in daily clinical practice.

In **Chapter 5** we focus on technical aspects of detection of (T)GCT biomarker miR371a. In this comparative study we investigate serum and plasma as liquid biopsy starting material and profile miR371a levels in both testicular (T)GCT patients and healthy donors using two isolation methods, the miRNeasy Serum/Plasma kit from Qiagen and the TaqMan anti-miRNA bead capture procedure from ThermoFisher. We report that there is little to no difference between serum and plasma, and both are suitable as starting material for liquid biopsies, however, for low volumes, the bead capture isolation method

is preferable due to its lower starting volumes and higher specificity. These data are relevant in the context of the currently ongoing prospective clinical trial regarding the use of this molecular marker in clinical practice.

Chapter 6 further explores the biological and mechanistic role of the miR371a-3 cluster in (T)GCTs. Using CRISPR Cas9 we generate miR371a knock-out clones in both NCCIT and 2102Ep cells. Comprehensive profiling, including cell growth and viability, cisplatin resistance, RNAseq, and *in vivo* xenografts shows no difference in wild-type cells or knock-out clones, illustrating that even though miR371a is virtually expressed in all malignant (T)GCTs (teratomas excluded) it is not required for tumor growth and maintenance. Additionally, we find upregulation of hypoxic pathways in miR371a knock-out clones, likely related to reduced miR371a-5p levels. Furthermore, upon knock-out of miR372 and miR373 in NCCIT cells we find one clone harboring a double knock-out. Although showing a slightly slower growth rate and increased mRNA and protein levels of LATS2, *in vivo* xenografting shows similar tumor growth between the double knock-out and wildtype clone. Triple knock-outs (371/372/373) derived from the double knock-out were generated and showed no difference in general cell survival and growth, indicating that the cluster is not essential in established (T)GCT cell lines. Moreover, this suggests that the expression of the cluster could be a passenger effect that occurs during oncogenic development, or more specifically, is simply not lost due to no positive selection on loss of this cluster in (T)GCTs.

In **Chapter 7** we use a previously described genetically engineered mouse model that develops *Cre*-induced GCTs to study the presence of mouse homologues of the human miR371a-3 cluster (miR291a-5) in murine induced mixed GCTs (featuring EC and teratoma histology). In this study we demonstrate that EC cells from these mice have elevated levels of murine miR371a-3 cluster homologues miR291a, miR292 and miR293, the first of which corresponding with human miR372/373 and the latter two with miR371a. We report that the induction of differentiation in these cells with either thioridazine or salinomycin significantly decreased the levels of these miRs. Furthermore, when treating gPAK mice with this same compound we find that the levels of these miRs drastically decrease. Finally, we find that elevated levels of these miRs in the serum of pregnant dams is a marker for tumor bearing fetuses *in utero*, a finding with important clinical applications for pregnant women carrying GCT risk group children.

Finally, we discuss the impact of this thesis in **Chapter 8**, placing the works in context of the (T)GCT field.

REFERENCES

1. Ahmad SS, Reinius MA, Hatcher HM, Ajithkumar TV. Anticancer chemotherapy in teenagers and young adults: managing long term side effects. *BMJ*. Published online September 7, 2016:i4567.
2. Almstrup K, Lobo J, Mørup N, *et al*. Application of miRNAs in the diagnosis and monitoring of testicular germ cell tumours. *Nat Rev Urol*. 2020;17(4):201-213.
3. Bagrodia A, Lee BH, Lee W, *et al*. Genetic determinants of cisplatin resistance in patients with advanced germ cell tumors. *JCO*. 2016;34(33):4000-4007.
4. Bajorin DF, Sarosdy MF, Pfister DG, *et al*. Randomized trial of etoposide and cisplatin versus etoposide and carboplatin in patients with good-risk germ cell tumors: a multiinstitutional study. *J Clin Oncol*. 1993;11(4):598-606.
5. Bauer S, Mühlenberg T, Leahy M, *et al*. Therapeutic potential of mdm2 inhibition in malignant germ cell tumours. *European Urology*. 2010;57(4):679-687.
6. Berney DM, Looijenga LHJ, Idrees M, *et al*. Germ cell neoplasia in situ (Gcnis): evolution of the current nomenclature for testicular pre-invasive germ cell malignancy. *Histopathology*. 2016;69(1):7-10.
7. Bloom JC, Loehr AR, Schimenti JC, Weiss RS. Germline genome protection: implications for gamete quality and germ cell tumorigenesis. *Andrology*. 2019;7(4):516-526.
8. Bokemeyer C, Köhrmann O, Tischler J, *et al*. A randomized trial of cisplatin, etoposide and bleomycin (Peb) versus carboplatin, etoposide and bleomycin (Ceb) for patients with “good-risk” metastatic non-seminomatous germ cell tumors. *Ann Oncol*. 1996;7(10):1015-1021.
9. Bokemeyer C, Nichols CR, Droz JP, *et al*. Extragonadal germ cell tumors of the mediastinum and retroperitoneum: results from an international analysis. *J Clin Oncol*. 2002;20(7):1864-1873.
10. Bokemeyer C, Kollmannsberger C, Stenning S, *et al*. Metastatic seminoma treated with either single agent carboplatin or cisplatin-based combination chemotherapy: a pooled analysis of two randomised trials. *Br J Cancer*. 2004;91(4):683-687.
11. Bakardjieva-Mihaylova V, Skvarova Kramarzova K, Slamova M, *et al*. Molecular basis of cisplatin resistance in testicular germ cell tumors. *Cancers (Basel)*. 2019;11(9):1316.
12. Cheng L, Albers P, Berney DM, *et al*. Testicular cancer. *Nat Rev Dis Primers*. 2018;4(1):29.
13. Chow EJ, Stratton KL, Leisenring WM, *et al*. Pregnancy after chemotherapy in male and female survivors of childhood cancer treated between 1970 and 1999: a report from the Childhood Cancer Survivor Study cohort. *Lancet Oncol*. 2016;17(5):567-576.
14. De Jong B, Oosterhuis JW, Castedo SM, Vos A, te Meerman GJ. Pathogenesis of adult testicular germ cell tumors. A cytogenetic model. *Cancer Genet Cytogenet*. 1990;48(2):143-167.
15. De Jong J, Stoop H, Gillis AJM, *et al*. Differential expression of SOX17 and SOX2 in germ cells and stem cells has biological and clinical implications. *J Pathol*. 2008;215(1):21-30.
16. Dieckmann KP, Radtke A, Geczi L, *et al*. Serum levels of microRNA-371a-3p (M371 test) as a new biomarker of testicular germ cell tumors: results of a prospective multicentric study. *J Clin Oncol*. 2019;37(16):1412-1423.
17. Dorssers LCJ, Gillis AJM, Stoop H, *et al*. Molecular heterogeneity and early metastatic clone selection in testicular germ cell cancer development. *Br J Cancer*. 2019;120(4):444-452.
18. Einhorn LH. Curing metastatic testicular cancer. *Proc Natl Acad Sci U S A*. 2002;99(7):4592-4595.

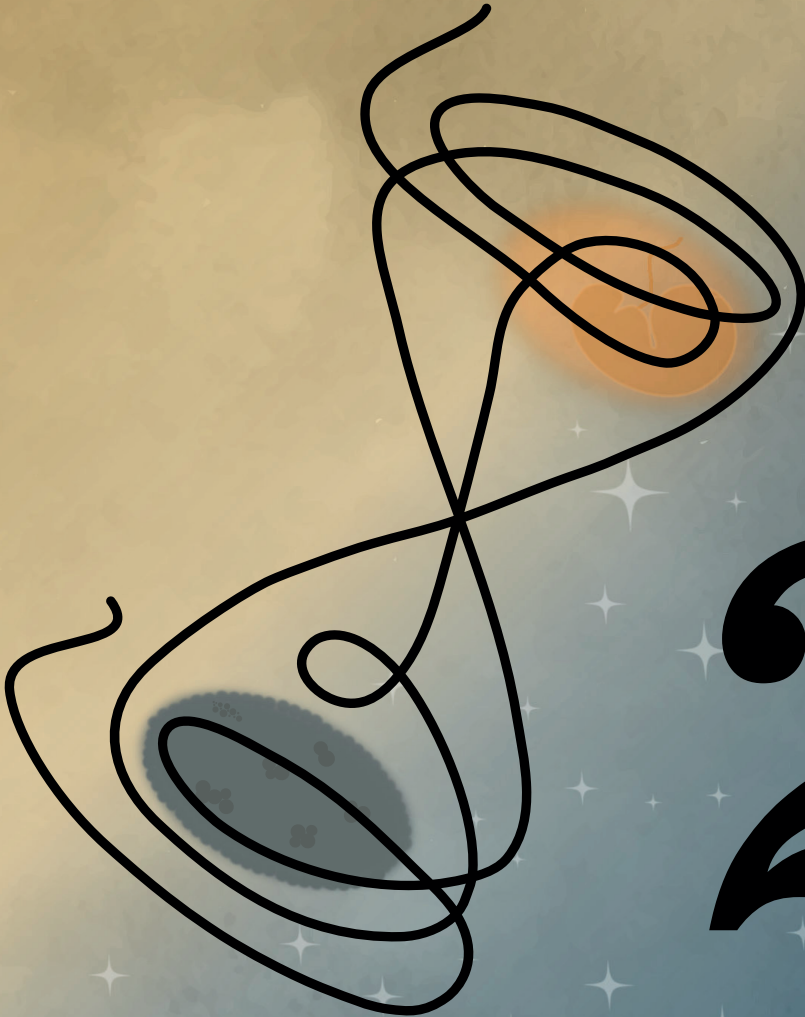
19. Einhorn LH, Brames MJ, Juliar B, Williams SD. Phase ii study of paclitaxel plus gemcitabine salvage chemotherapy for germ cell tumors after progression following high-dose chemotherapy with tandem transplant. *JCO*. 2007;25(5):513-516.
20. Einhorn LH, Donohue J. Cis-diamminedichloroplatinum, vinblastine, and bleomycin combination chemotherapy in disseminated testicular cancer. *Ann Intern Med*. 1977;87(3):293-298.
21. Frazier AL, Stoneham S, Rodriguez-Galindo C, *et al*. Comparison of carboplatin versus cisplatin in the treatment of paediatric extracranial malignant germ cell tumours: A report of the Malignant Germ Cell International Consortium. *European Journal of Cancer*. 2018;98:30-37.
22. Filion TM, Qiao M, Ghule PN, *et al*. Survival responses of human embryonic stem cells to DNA damage. *J Cell Physiol*. 2009;220(3):586-592.
23. Geurts van Kessel A, van Drunen E, de Jong B, Oosterhuis JW, Langeveld A, Mulder MP. Chromosome 12q heterozygosity is retained in i(12p)-positive testicular germ cell tumor cells. *Cancer Genet Cytogenet*. 1989;40(1):129-134.
24. Gillessen S, Collette L, Daugaard G, *et al*. Redefining the IGCCCG classification in advanced non-seminoma. *Annals of Oncology*. 2019;30:v357-v358.
25. Gillis A, Stoop H, Hersmus R, *et al*. High-throughput microRNAome analysis in human germ cell tumours. *J Pathol*. 2007;213(3):319-328.
26. Goossens E, Jahnukainen K, Mitchell RT, *et al*. Fertility preservation in boys: recent developments and new insights †. *Hum Reprod Open*. 2020;2020(3):hoaa016.
27. Gross N, Kropp J, Khatib H. MicroRNA signaling in embryo development. *Biology*. 2017;6(4):34.
28. Gutekunst M, Oren M, Weilbacher A, *et al*. P53 hypersensitivity is the predominant mechanism of the unique responsiveness of testicular germ cell tumor (Tgct) cells to cisplatin. Gartel AL, ed. *PLoS ONE*. 2011;6(4):e19198.
29. Gutekunst M, Mueller T, Weilbacher A, *et al*. Cisplatin hypersensitivity of testicular germ cell tumors is determined by high constitutive noxa levels mediated by oct-4. *Cancer Research*. 2013;73(5):1460-1469.
30. Higby DJ, Wallace HJ, Albert DJ, Holland JF. Diaminodichloroplatinum: a phase I study showing responses in testicular and other tumors. *Cancer*. 1974;33(5):1219-1215.
31. Ho GY, Woodward N, Coward JIG. Cisplatin versus carboplatin: comparative review of therapeutic management in solid malignancies. *Critical Reviews in Oncology/Hematology*. 2016;102:37-46.
32. Honecker F, Aparicio J, Berney D, *et al*. ESMO Consensus Conference on testicular germ cell cancer: diagnosis, treatment and follow-up. *Annals of Oncology*. 2018;29(8):1658-1686.
33. Horwich A, Sleijfer DT, Fosså SD, *et al*. Randomized trial of bleomycin, etoposide, and cisplatin compared with bleomycin, etoposide, and carboplatin in good-prognosis metastatic nonseminomatous germ cell cancer: a Multiinstitutional Medical Research Council/European Organization for Research and Treatment of Cancer Trial. *J Clin Oncol*. 1997;15(5):1844-1852.
34. Houldsworth J, Xiao H, Murty V, *et al*. Human male germ cell tumor resistance to cisplatin is linked to TP53 gene mutation. *Oncogene*. 1998;16(18):2345-2349.
35. Houldsworth J, Korkola JE, Bosl GJ, Chaganti RSK. Biology and genetics of adult male germ cell tumors. *JCO*. 2006;24(35):5512-5518.
36. Jacobs S, McCully CL, Murphy RF, Bacher J, Balis FM, Fox E. Extracellular fluid concentrations of cisplatin, carboplatin, and oxaliplatin in brain, muscle, and blood measured using microdialysis in nonhuman primates. *Cancer Chemother Pharmacol*. 2010;65(5):817-824.

37. Jacobsen C, Honecker F. Cisplatin resistance in germ cell tumours: models and mechanisms. *Andrology*. 2015;3(1):111-121.
38. Hulsker CCC, El Mansori I, Fiocco M, *et al*. Treatment and survival of malignant extracranial germ cell tumours in the paediatric population: a systematic review and meta-analysis. *Cancers (Basel)*. 2021;13(14):3561.
39. International germ cell consensus classification: a prognostic factor-based staging system for metastatic germ cell cancers. International germ cell cancer collaborative group. *J Clin Oncol*. 1997;15(2):594-603.
40. Jain R, Menon P, Bansal D, *et al*. Outcome of pediatric germ cell tumor with comparison of carboplatin and cisplatin based regimens: A 10-year analysis. *Pediatric Hematology and Oncology*. 2022;39(3):267-277.
41. Kandath C, McLellan MD, Vandin F, *et al*. Mutational landscape and significance across 12 major cancer types. *Nature*. 2013;502(7471):333-339.
42. Kersemaekers AMF, Mayer F, Molier M, *et al*. Role of p53 and mdm2 in treatment response of human germ cell tumors. *JCO*. 2002;20(6):1551-1561.
43. Koster R, Timmer-Bosscha H, Bischoff R, Gietema JA, de Jong S. Disruption of the MDM2–p53 interaction strongly potentiates p53-dependent apoptosis in cisplatin-resistant human testicular carcinoma cells via the Fas/FasL pathway. *Cell Death Dis*. 2011;2(4):e148-e148.
44. Leão R, Albersen M, Looijenga LHJ, *et al*. Circulating micrornas, the next-generation serum biomarkers in testicular germ cell tumours: a systematic review. *European Urology*. 2021;80(4):456-466.
45. Light N, Layeghifard M, Attery A, *et al*. Germline TP53 mutations undergo copy number gain years prior to tumor diagnosis. *Nat Commun*. 2023;14(1):77.
46. Lobo J, Jerónimo C, Henrique R. Cisplatin resistance in testicular germ cell tumors: current challenges from various perspectives. *Cancers*. 2020;12(6):1601.
47. Looijenga LH, Oosterhuis JW, Ramaekers FC, *et al*. Dual parameter flow cytometry for deoxyribonucleic acid and intermediate filament proteins of residual mature teratoma. All tumor cells are aneuploid. *Lab Invest*. 1991;64(1):113-117.
48. Looijenga LHJ, Oosterhuis JW. Pathogenesis of testicular germ cell tumours. *Reviews of Reproduction*. 1999;4(2):90-100.
49. Looijenga LHJ, Stoop H, de Leeuw HPJC, *et al*. POU5F1 (OCT3/4) identifies cells with pluripotent potential in human germ cell tumors. *Cancer Res*. 2003;63(9):2244-2250.
50. Loveday C, Litchfield K, Proszek PZ, *et al*. Genomic landscape of platinum resistant and sensitive testicular cancers. *Nat Commun*. 2020;11(1):2189.
51. Lyndaker AM, Pierpont TM, Loehr AR, Weiss RS. A genetically engineered mouse model of malignant testicular germ cell tumors. *Methods Mol Biol*. 2021;2195:147-165.
52. Ma YT, Cullen MH, Hussain SA. Biology of germ cell tumors. *Hematol Oncol Clin North Am*. 2011;25(3):457-471, vii.
53. Marina NM, Cushing B, Giller R, *et al*. Complete surgical excision is effective treatment for children with immature teratomas with or without malignant elements: A Pediatric Oncology Group/Children's Cancer Group Intergroup Study. *J Clin Oncol*. 1999;17(7):2137-2143.
54. Mego M, van Agthoven T, Gronesova P, *et al*. Clinical utility of plasma miR-371a-3p in germ cell tumors. *J Cell Mol Med*. 2019;23(2):1128-1136.

55. Merkle FT, Ghosh S, Kamitaki N, *et al.* Human pluripotent stem cells recurrently acquire and expand dominant negative P53 mutations. *Nature*. 2017;545(7653):229-233.
56. Moch H, Cubilla AL, Humphrey PA, Reuter VE, Ulbright TM. The 2016 who classification of tumours of the urinary system and male genital organs—part a: renal, penile, and testicular tumours. *European Urology*. 2016;70(1):93-105.
57. Motzer RJ, Amsterdam A, Prieto V, *et al.* Teratoma with malignant transformation: diverse malignant histologies arising in men with germ cell tumors. *J Urol*. 1998;159(1):133-138.
58. Murray MJ, Halsall DJ, Hook CE, Williams DM, Nicholson JC, Coleman N. Identification of microRNAs From the miR-371~373 and miR-302 clusters as potential serum biomarkers of malignant germ cell tumors. *Am J Clin Pathol*. 2011;135(1):119-125.
59. Oechsle K, Kollmannsberger C, Honecker F, *et al.* Long-term survival after treatment with gemcitabine and oxaliplatin with and without paclitaxel plus secondary surgery in patients with cisplatin-refractory and/or multiply relapsed germ cell tumors. *European Urology*. 2011;60(4):850-855.
60. Oing C, Giannatempo P, Honecker F, Oechsle K, Bokemeyer C, Beyer J. Palliative treatment of germ cell cancer. *Cancer Treatment Reviews*. 2018;71:102-107.
61. Olofsson SE, Tandstad T, Jerkeman M, *et al.* Population-based study of treatment guided by tumor marker decline in patients with metastatic nonseminomatous germ cell tumor: a report from the swedish-norwegian testicular cancer group. *JCO*. 2011;29(15):2032-2039.
62. Oosterhuis JW, Castedo SM, de Jong B, *et al.* Ploidy of primary germ cell tumors of the testis. Pathogenetic and clinical relevance. *Lab Invest*. 1989;60(1):14-21.
63. Oosterhuis JW, Looijenga LHJ. Testicular germ-cell tumours in a broader perspective. *Nat Rev Cancer*. 2005;5(3):210-222.
64. Oosterhuis JW, Looijenga LHJ. Human germ cell tumours from a developmental perspective. *Nat Rev Cancer*. 2019;19(9):522-537.
65. Pierpont TM, Lyndaker AM, Anderson CM, *et al.* Chemotherapy-induced depletion of oct4-positive cancer stem cells in a mouse model of malignant testicular cancer. *Cell Reports*. 2017;21(7):1896-1909.
66. Reed E. Platinum-DNA adduct, nucleotide excision repair and platinum based anti-cancer chemotherapy. *Cancer Treatment Reviews*. 1998;24(5):331-344.
67. Rijlaarsdam MA, van Agthoven T, Gillis AJM, *et al.* Identification of known and novel germ cell cancer-specific (Embryonic) miRs in serum by high-throughput profiling. *Andrology*. 2015;3(1):85-91.
68. Rosenberg B, Vancamp L, Krigas T. Inhibition of cell division in escherichia coli by electrolysis products from a platinum electrode. *Nature*. 1965;205:698-699.
69. Sesterhenn IA, Davis CJ. Pathology of germ cell tumors of the testis. *Cancer Control*. 2004;11(6):374-387.
70. Siddiqui BA, Zhang M, Pisters LL, Tu SM. Systemic therapy for primary and extragonadal germ cell tumors: prognosis and nuances of treatment. *Transl Androl Urol*. 2020;9(S1):S56-S65.
71. Siegel RL, Miller KD, Fuchs HE, Jemal A. Cancer statistics, 2022. *CA A Cancer J Clinicians*. 2022;72(1):7-33.
72. Shaikh F, Nathan PC, Hale J, Uleryk E, Frazier L. Is there a role for carboplatin in the treatment of malignant germ cell tumors? A systematic review of adult and pediatric trials. *Pediatr Blood Cancer*. 2013;60(4):587-592.

73. Singh R, Fazal Z, Freemantle SJ, Spinella MJ. Mechanisms of cisplatin sensitivity and resistance in testicular germ cell tumors. *Cancer Drug Resist.* 2019;2(3):580-594.
74. Skakkebaek NE. Possible carcinoma-in-situ of the testis. *Lancet.* 1972;2(7776):516-517.
75. Song M, Hildesheim A, Shiels MS. Premature years of life lost due to cancer in the united states in 2017. *Cancer Epidemiology, Biomarkers & Prevention.* 2020;29(12):2591-2598.
76. Syring I, Bartels J, Holdenrieder S, Kristiansen G, Müller SC, Ellinger J. Circulating serum miRNA (Mir-367-3p, mir-371a-3p, mir-372-3p and mir-373-3p) as biomarkers in patients with testicular germ cell cancer. *J Urol.* 2015;193(1):331-337.
77. Tjulandin SA, Garin AM, Mescheryakov AA, *et al.* Cisplatin-etoposide and carboplatin-etoposide induction chemotherapy for good-risk patients with germ cell tumors. *Ann Oncol.* 1993;4(8):663-667.
78. Trabert B, Chen J, Devesa SS, Bray F, McGlynn KA. International patterns and trends in testicular cancer incidence, overall and by histologic subtype, 1973-2007. *Andrology.* 2015;3(1):4-12.
79. Travis LB, Fosså SD, Schonfeld SJ, *et al.* Second cancers among 40,576 testicular cancer patients: focus on long-term survivors. *J Natl Cancer Inst.* 2005;97(18):1354-1365.
80. Travis LB, Beard C, Allan JM, *et al.* Testicular cancer survivorship: research strategies and recommendations. *J Natl Cancer Inst.* 2010;102(15):1114-1130.
81. Ulbright TM. Germ cell tumors of the gonads: a selective review emphasizing problems in differential diagnosis, newly appreciated, and controversial issues. *Mod Pathol.* 2005;18 Suppl 2:S61-79.
82. van Aghthoven T, Eijkenboom WMH, Looijenga LHJ. Microrna-371a-3p as informative biomarker for the follow-up of testicular germ cell cancer patients. *Cell Oncol (Dordr).* 2017;40(4):379-388.
83. van Echten J, Oosterhuis JW, Looijenga LH, *et al.* No recurrent structural abnormalities apart from i(12p) in primary germ cell tumors of the adult testis. *Genes Chromosomes Cancer.* 1995;14(2):133-144.
84. Voorhoeve PM, le Sage C, Schrier M, *et al.* A genetic screen implicates mirna-372 and mirna-373 as oncogenes in testicular germ cell tumors. *Cell.* 2006;124(6):1169-1181.
85. Worawongsakul R, Sirachainan N, Rojanawatsirivej A, *et al.* Carboplatin-based regimen in pediatric intracranial germ-cell tumors (lc-gcts): effectiveness and ototoxicity. *Neurooncol Pract.* 2020;7(2):202-210.

Chapter



2

Chapter 2

Mechanisms of TP53 Pathway Inactivation in Embryonic and Somatic Cells—Relevance for Understanding (Germ Cell) Tumorigenesis

Dennis M. Timmerman ^{1,†}, Tessa L. Remmers ^{1,†}, Sanne Hillenius ^{1,†} and Leendert H. J. Looijenga ^{2,*}

¹ Princess Máxima Center for Pediatric Oncology, Heidelberglaan 25, 3584 CS Utrecht, The Netherlands; D.M.Timmerman-6@prinsesmaximacentrum.nl (D.M.T.); tessa.l.remmers@gmail.com (T.L.R.); s.hillenius@students.uu.nl (S.H.)

² Princess Máxima Center for Pediatric Oncology, Heidelberglaan 25, 3584 CS Utrecht, The Netherlands

* Correspondence: L.Looijenga@prinsesmaximacentrum.com; Tel.: +31-(0)-88 972-5211

† These authors contributed equally.

ABSTRACT

The P53 pathway is the most important cellular pathway to maintain genomic and cellular integrity, both in embryonic and non-embryonic cells. Stress signals induce its activation, initiating autophagy or cell cycle arrest to enable DNA repair. The persistence of these signals causes either senescence or apoptosis. Over 50% of all solid tumors harbor mutations in *TP53* that inactivate the pathway. The remaining cancers are suggested to harbor mutations in genes that regulate the P53 pathway such as its inhibitors Mouse Double Minute 2 and 4 (MDM2 and MDM4, respectively). Many reviews have already been dedicated to P53, MDM2, and MDM4, while this review additionally focuses on the other factors that can deregulate P53 signaling. We discuss that P14^{ARF} (ARF) functions as a negative regulator of MDM2, explaining the frequent loss of ARF detected in cancers. The long non-coding RNA Antisense Non-coding RNA in the *INK4* Locus (ANRIL) is encoded on the same locus as *ARF*, inhibiting ARF expression, thus contributing to the process of tumorigenesis. Mutations in tripartite motif (TRIM) proteins deregulate P53 signaling through their ubiquitin ligase activity. Several microRNAs (miRNAs) inactivate the P53 pathway through inhibition of translation. CCCTC-binding factor (CTCF) maintains an open chromatin structure at the *TP53* locus, explaining its inactivation of CTCF during tumorigenesis. P21, a downstream effector of P53, has been found to be deregulated in different tumor types. This review provides a comprehensive overview of these factors that are known to deregulate the P53 pathway in both somatic and embryonic cells, as well as their malignant counterparts (i.e., somatic and germ cell tumors). It provides insights into which aspects still need to be unraveled to grasp their contribution to tumorigenesis, putatively leading to novel targets for effective cancer therapies.

Keywords: P53 pathway; cancers; mutations; embryonic and somatic cells

INTRODUCTION

Embryonic Stem Cells and Germ Cell Tumors Versus Somatic Cells

The development of multicellular, sexually reproductive organisms starts with the fusion of a spermatozoa and an oocyte that created a diploid zygote (depicted in Figure 1). Then, the zygote divides, forming a cluster of undifferentiated cells (i.e., blastomeres) known as the morula. The first step of lineage differentiation occurs during the subsequent blastocyst stage in which the embryoblast (i.e., the inner cell mass) and the trophectoderm are formed [1,2]. The trophectoderm develops into all extra-embryonic structures, whereas the embryoblast, which consists of pluripotent embryonic stem (ES) cells, develops into all embryonic structures [2]. ES cells are transiently present, can self-renew and give rise to all three embryonic germ layers during gastrulation (i.e., the ecto-, meso-, and endoderm), which ultimately will give rise to all cell lineages of the adult organism [2]. Additionally, ES cells give rise to the primordial germ cells (PGC) in the embryonic yolk sac, which subsequently migrate toward developing gonads to give rise to the germ line [2,3] (see Figure 1).

The pluripotent nature of ES cells is characterized by the expression of pluripotency markers including but not limited to OCT4, NANOG, SOX2, and REX1 (Figure 1) [4]. In contrast, somatic cells are differentiated and thus lineage-restricted and unipotent [5]. Therefore, these cells seldomly give rise to other progeny than the identity of the cells themselves [5]. In addition, due to their capacity to self-renew, ES cells can be cultured indefinitely in vitro while retaining their embryonic state as well as a stable genome. This immortality is facilitated by active telomerase, which is an enzyme that extends telomeric repeats that are otherwise lost due to the end-replication problem after each cell cycle (approximately 50–150 base pairs are lost per cycle) [6,7] (Figure 1). Conversely, somatic cells have a restricted lifespan due to the lack of active telomerase and induce cellular senescence when a critical telomere length is reached [6,7]. Furthermore, ES cells also regulate the cell cycle differently as these lack Cyclin D expression yet continuously express Cyclin A and E, which leads to a significantly shortened G_1 -phase when compared to somatic cells [8]. This characteristic also facilitates the tendency for ES cells to initiate apoptosis rather than cell cycle arrest and DNA repair when DNA damage occurs, the latter of which occurs predominantly in the G_1 phase after cell cycle arrest [9,10]. The preference for apoptosis in these early embryonic cells is considered a failsafe mechanism to preserve the genetic integrity of their multitudinous progeny. In rare occasions, ES cells can initiate DNA repair; however, these cells then opt for error-free homologous recombination (HR) to repair double-strand breaks, whereas somatic cells predominantly employ error-prone non-homologous end joining (NHEJ) [9]. Finally, a zygote is known to lose its inherited DNA methylation pattern immediately after fertilization and subsequent changes in DNA methylation occur during early embryonic development as various

cell lineages arise. Thus, DNA methylation patterns between ES and somatic cells vary significantly [11,12].

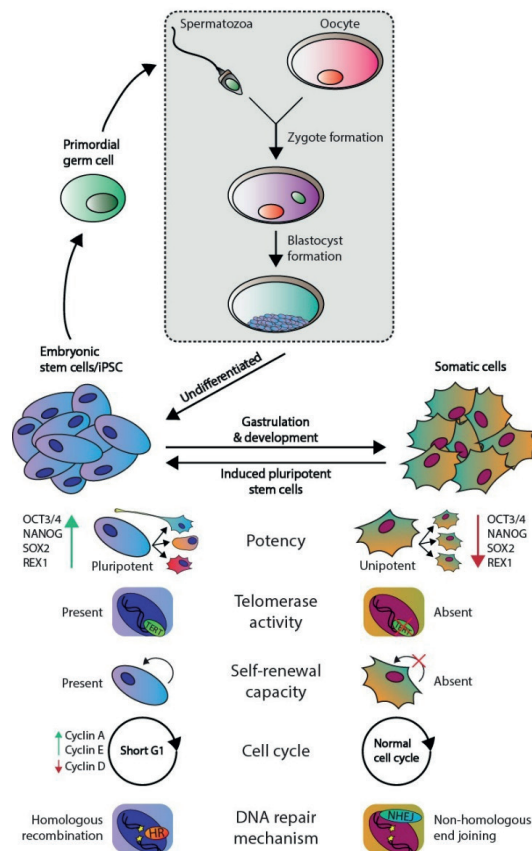


Figure 1. Phenotypic differences between embryonic and somatic cells. Fertilization of an oocyte by a spermatozoon forms a zygote, which subsequently develops the blastocyst. The blastocyst contains embryonic stem (ES) cells that eventually give rise to all somatic cell types. ES and somatic cells can be distinguished according to multiple aspects: their potency, telomerase activity, self-renewal capacity, cell cycle regulation, and preferred DNA repair mechanism. Both germ cells and germ cells tumors are derived from ES derived PGCs and therefore harbor the same embryonal characteristics.

Of note, a discovery made over a decade ago demonstrated that differentiated somatic human cells (e.g., adult human fibroblasts) could be reprogrammed to a pluripotent state reminiscent of ES cells (i.e., nuclear reprogramming) [13]. These cells are known as induced pluripotent stem cells (iPSCs) and, in theory, they can also be maintained in a pluripotent state indefinitely. iPSCs are originally generated in vitro by

overexpressing a cocktail of four essential genes (*OCT3/4*, *c-MYC*, *SOX2*, and *KLF4*) in the differentiated cells [14].

Moreover, many of the characteristics of ES cells are strongly conserved in germ cell tumors (GCTs), which represent a heterogeneous cluster of solid tumors that originate from both ES cells and PGCs [3]. Of note, the parallels observed between ES cells and GCTs do not apply to the teratomas, which is a GCT subtype that consists of fully differentiated cells and harbor significant differences in their (epi)genetic makeup and clinical response (i.e., inherent chemotherapeutic resistance) compared to other GCT subtypes [3,15–17]. An example of the similarities observed between ES cells and GCTs is that the latter also express multiple pluripotency markers including *OCT3/4* and *NANOG* and have active telomerase activity, again with the exception of teratoma [3,16,17]. Moreover, it is widely accepted that in response to DNA damage, GCTs also favor apoptosis, which is thought to underlie their unique sensitivity to platinum-based chemotherapeutics, including cisplatin (a key component of GCT treatment) [9,10,18]. This is supported by additional evidence demonstrating that GCTs have low expression of genes involved in cell cycle arrest and a deregulated G1-S phase checkpoint, thus potentially also preventing the activation of DNA repair pathways [18–23]. Moreover, the apoptotic response of ES cells and GCTs in response to DNA damage has been attributed to the well-known P53 pathway; however, at least in GCTs, it remains a topic of debate [18,21,24–37]. The P53 pathway has been dubbed the guardian of the genome due to its integral role in maintaining genomic integrity among all cell types. This pathway acts in response to cellular stress and lies at the apex of a plethora of downstream signaling pathways including cell cycle arrest, DNA repair, and apoptosis. The deregulation of this pathway has been observed in cancer and is strongly associated to many aspects of tumorigenesis. For instance, GCTs most often express high levels of wild-type (WT) *TP53*, and it has been suggested that the P53 pathway is (partially) responsible for their characteristic to enter apoptosis in response to platinum-based chemotherapeutics (e.g., cisplatin) which is reminiscent of ES cells in response to DNA damage [10,18,21,23,25–29,33–37]. In addition, it has been suggested that the P53 pathway is deregulated through multiple mechanisms in GCTs that have acquired resistance to chemotherapy, including cisplatin [15,18,38–42].

In short, the importance of the P53 pathway and its differential regulation between somatic and ES cells (and in parallel GCTs, except teratoma) underlines the purpose of this review, which is to provide an up-to-date overview of the important roles, regulators, and downstream effectors of the P53 pathway. In addition, multiple mechanisms that are known to inactivate this pathway and contribute to tumorigenesis will be highlighted.

Protecting Genomic Integrity

Genomic changes during development serve as the driving force of evolution; however, these may also negatively impact multiple cell lineages with possible detrimental effects on both the individual and their offspring. Therefore, protection of the genomic integrity is paramount for a species to survive and commences during early embryonic development [23]. For example, the oocyte expresses and deposits multiple mRNAs that protect the zygote against DNA damage during the first cellular divisions [43]. As mentioned before, there have been several indications of a robust protective mechanism in ES cells including the removal of mutated ES cells from the stem cell pool through apoptosis, which is a characteristic that is seemingly conserved in GCTs [7,12,44]. Alternatively, ES cells may also be instructed to differentiate through transcriptional inhibition of the pluripotency factor *NANOG*, which also effectively removes ES cells from the stem cell pool [45]. These mechanisms in combination with lacking a G₁ checkpoint are thought to result in a 100-fold lower frequency of accumulating mutations in at least murine ES cells compared to mouse embryonic fibroblasts, which resemble the somatic cells [9,23]. Conversely to ES cells and GCTs, somatic cells utilize different pathways (DNA repair rather than apoptosis) to protect their genome that enable these to survive while risking an increased mutational load [9,23].

P53 Pathway

As mentioned before, the P53 pathway is essential in maintaining genomic integrity. Central to this pathway is the P53 protein that is regarded as a tumor suppressor and originates from the *TP53* gene. Several key discoveries regarding P53 are depicted in Figure 2, as well as its relevance in GCTs [22–38,46–59]. In response to cellular stress, the P53 protein is activated and accumulates in the cell after which it mainly functions as a transcription factor that transactivates a plethora of downstream targets [49]. These target genes are key players in one of many downstream pathways including cell cycle arrest, DNA repair, apoptosis, senescence, and autophagy [51,60,61]. The P53 protein counts 393 amino acids (AA) and consists of multiple domains, starting with a transactivation domain (TAD) at the amino-terminus (N-terminus), a directly neighboring proline-rich domain (PRD), a large DNA-binding domain (DBD), a tetramerization domain (TD), and a carboxy-terminus (C-terminus) regulatory domain (REG) [62,63] (depicted in Figure 3). Once activated and accumulated in the cell, the P53 protein functions and binds DNA as a tetramer, which is facilitated by the TD [64]. When tetramerized, the DBD contains three loops, L1, L2, and L3 respectively [65]. Both L2 and L3 are bound by a zinc ion, effectively linking both loops and enabling L3 to bind to the minor groove of the DNA, while a helix in the DBD is complementary to the major groove [65,66].

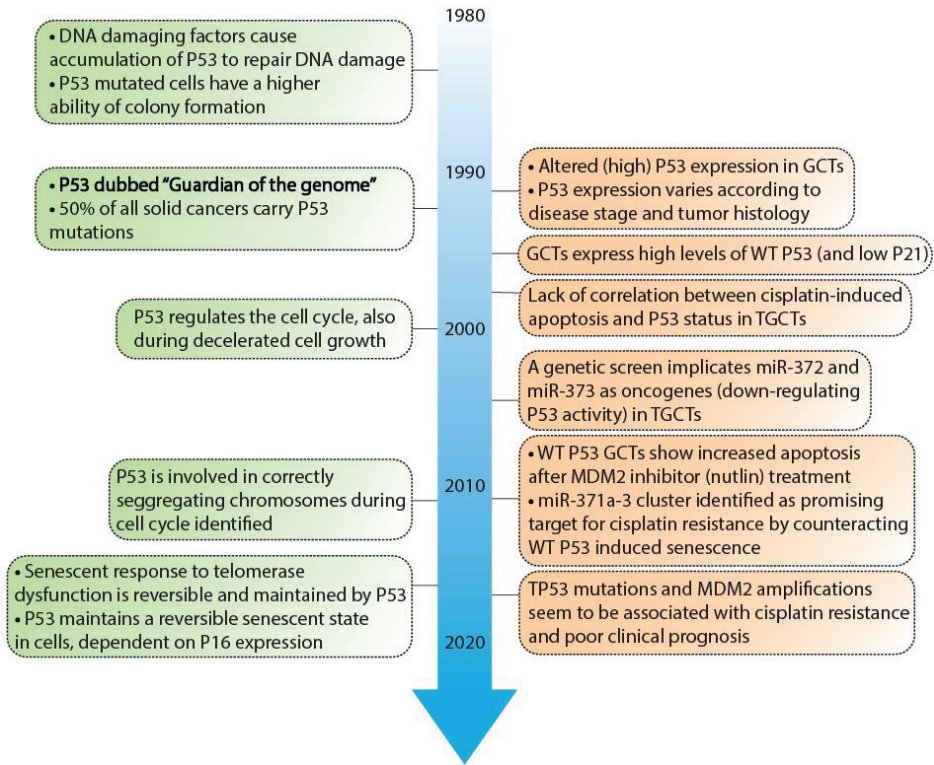


Figure 2. Timeline depicting key discoveries in P53 signaling and germ cell tumors. A timeline of the discoveries regarding P53 as a guardian of the genome (green) and studies regarding TP53 in GCT development and resistance (orange). References key discoveries P53 (green): 49–58, references key discoveries TP53 in GCT development (orange): 25–41, 59–62.

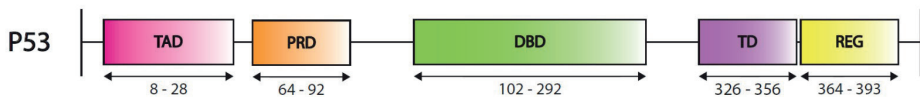


Figure 3. Schematic overview of the P53 protein. Indicated are (from N- to T-terminus) TAD: Transactivation domain, PRD: Proline-rich domain, DBD: DNA-binding domain, TD: Tetramerization domain and REG: Regulatory domain. Numbers indicate the amino acids included in each domain.

There are many different forms of cellular stress such as DNA damage that activate upstream regulators of p53, leading to the activation of the p53 pathway. For example, Ataxia-telangiectasia mutated (ATM) kinase serves as an important DNA damage sensor, as it recognizes and binds to double-strand DNA breaks and subsequently activates the P53 pathway, ultimately resulting in the activation of NHEJ or HR DNA repair mechanisms

[55,67]. ATM phosphorylates histone H2AX, which is a variant of histone H2A that recruits molecules responsible for H3K9 methylation [55]. In turn, methylated H3K9 leads to the acetylation and activation of ATM [55]. Among other substrates, ATM phosphorylates and activates Checkpoint Kinase 1 and 2 (CHK1 and CHK2, respectively) [55]. In turn, CHK1 and 2 function as transcriptional activators by phosphorylating and activating the P53 protein [68]. The subsequent section will further outline several downstream targets and their related pathways including cell cycle arrest, senescence, apoptosis, and autophagy (also summarized in Figure 4).

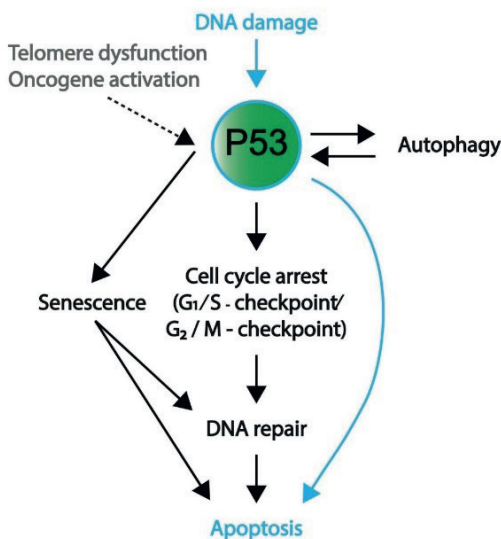


Figure 4. A schematic overview representing the favored mechanism of P53 activation in embryonic cells and somatic cells. DNA damage, both in embryonic (blue) and somatic (black) cells, will induce P53 activation. To protect genomic integrity, embryonic cells favor apoptosis over DNA repair. Conversely, somatic cells preferentially engage in cell cycle arrest and DNA repair; however, if DNA damage persists, these cells will enter apoptosis or become senescent. Furthermore, telomere dysfunction and oncogene activation are other means to activate P53 signaling (mostly in somatic cells). In addition to apoptosis, P53 activation and its downstream pathways can result in autophagy, senescence, and cell cycle arrest.

Induction of Cell Cycle Arrest

As indicated, DNA damage leads to the accumulation of P53, which induces cell cycle arrest, and subsequent DNA repair cell cycle arrest can occur at both the G₁/S and G₂/M checkpoints and is mostly effectuated by p21 (*CDKN1A*), which is a target of P53 [69]. Activated P53 binds to the promotor of p21 and initiates its transcription [70,71]. p21 inhibits the function of cyclin-dependent kinases (CDKs) CDK2 and CDK4/6 present at the G₁/S transition, which results in the hypomethylation of pRB-related proteins p107

and p130 [69,72]. The transcription of cell cycle-promoting genes will subsequently be repressed, inducing a temporary block of cell cycle arrest that enables the cell to initiate DNA repair mechanisms.

Senescence or Apoptosis as a Final Measure to Protect Genomic Integrity

Chronic cellular stress signals such as telomere dysfunction, persisting DNA damage, and oncogene activation result in prolonged P53 activation and subsequent P21 expression, which in turn may induce cellular senescence or apoptosis (the latter of which is the main outcome in ES cells and GCTs) [72]. In contrast to cell cycle arrest, senescence is a stable state of arrest, and both processes are initiated by P53, again illustrating the tumor-suppressive functions of this protein [55,72]. Conversely, a senescent cell is able to re-enter the cell cycle after loss of P53 and has been shown to contribute to tumorigenesis, as it results in fast cell proliferation [27,28,73]. Prolonged P21 expression eventually induces the expression of P16^{INK16A} (hereafter referred to as P16), which similarly functions as a CDK inhibitor for CDK4/6, thereby indirectly inhibiting pRb-family members [72]. P16 expression is known to be regulated by epigenetic factors including DNMT3, which facilitates de novo methylation of the P16 promotor, inhibiting its expression, which is maintained by DNMT1 [55]. Demethylation of the promotor consequently induces P16 expression [55]. In addition to P16, senescence is also regulated by P53-independent pathways including NF- κ B, which is responsible for the expression of proinflammatory cytokines that are secreted during senescence/this cellular state [55,72]. Notably, senescent cells are non-responsive to apoptotic signals, which is demonstrated by the continued activation of cAMP response element-binding (CREB), which functions as a transcription factor for the anti-apoptotic BCL-2 protein [55]. Alternatively, persisting cellular stress signals may induce apoptotic pathways, and further information of these pathways is described in Box 1.

Autophagy

Lastly, P53 can induce autophagy, which underlines its additional role in cellular metabolism. Autophagy enables cells to maintain homeostasis by the removal and recycling of (faulty) organelles [74]. Recycling results in an increase of anabolic intermediates that can subsequently be used in multiple pathways [74,75]. There are many connections between P53 and autophagy, as illustrated in Figure 5, as autophagy is able to inactivate P53 through different mechanisms such as proteosomal degradation [76]. In addition, the autophagy protein ATG7 has been reported to bind P53 and activate the transcription of P21, resulting in cell cycle arrest [74]. Conversely, P53 promotes the transcription of genes

involved in autophagy, which suggests a negative feedback loop between the autophagy proteins and P53 [74]. Additionally, a more indirect crosstalk between p53 and autophagy via the mTOR pathway is known to occur in multiple tissue types including skeletal muscle, heart, white fat, liver, and kidney tissue [33]. Here, P53 promotes the transcription of negative regulators of the IGF–AKT–mTOR pathway, resulting in higher levels of BECLIN-1, which is part of the phosphatidylinositol-3 kinase (PI3K) complex and plays an important role in the formation of autophagosomes [77,78]. Notably, a loss of BECLIN-1 results in an increased risk of tumorigenesis, which underlines its importance in autophagy and maintaining genomic integrity [78].

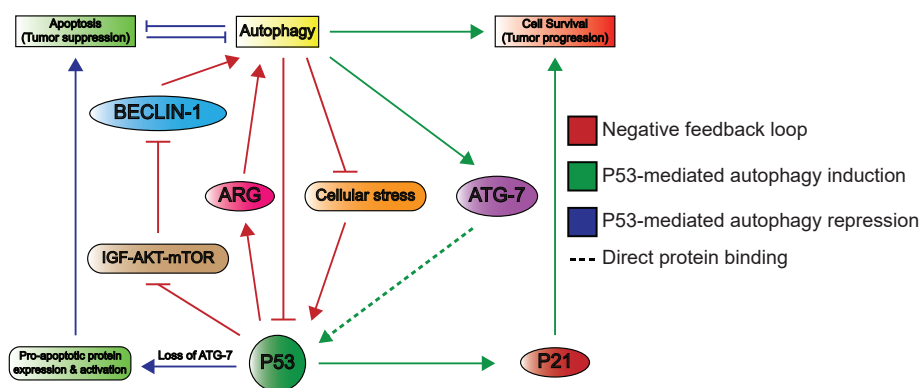


Figure 5. An overview of the crosstalk between P53 and autophagy. Autophagy can repress P53 through the inhibition of upstream activating proteins as well as P53 itself. This forms a negative feedback loop (red) as P53 induces autophagy through the inhibition of the IGF–AKT–mTOR pathway and subsequent increase in BECLIN-1 levels, which plays a role in autophagosome formation. P53 also induces the expression of autophagy-related genes (ARG). Autophagy induces cell survival, which is effectuated by the binding of ATG7 to P53, ultimately leading to P53-dependent P21 expression and subsequent cell cycle arrest (green). The loss of ATG-7 results in apoptosis (blue), as P53 induces the expression and activation of pro-apoptotic proteins. Apoptosis and autophagy have mutually inhibitory effects on one another.

INHIBITORY MECHANISMS OF THE P53 PATHWAY

As the P53 pathway is fundamental in maintaining genomic integrity in the face of cellular stress signals, it is unsurprising that approximately 50% of all solid cancers contain inactivating mutations within the *TP53* gene [50]. Additionally, it is hypothesized that nearly all cancers have a compromised P53 pathway, as the remaining 50% of cancers that lack *TP53* mutations often have mutated genes that lie either up- or downstream of P53 and may also lead to the inactivation of the P53 pathway [15,16]. In the following

sections, different mutations and modifications of P53 and its main negative regulators Mouse Double Minute 2 and 4 (MDM2 and MDM4, respectively) will be described in further detail. Additionally, alternative mechanisms are also highlighted to provide a complete overview of the large variety of mechanisms that inactivate the p53 pathway.

Box 1. The P53-mediated mitochondrial apoptotic pathway.

Under unstressed conditions, apoptosis is inhibited by anti-apoptotic proteins BCL-2, BCL-X_L, BCL-W, MCL1, and A1, which interact with and inhibit pro-apoptotic proteins such as BAX and BAK [79]. These pro- and anti-apoptotic proteins are members of the BCL-2 family and contain up to four BCL-2 homology (BH) domains [79,80]. BH3-only proteins contain only the BH3 domain and are pro-apoptotic proteins within the BCL-2 family [81]. When DNA damage persists, P53 activation results in the expression of pro-apoptotic protein BAX and BH3-only proteins PUMA and NOXA. The latter two in combination with P53 induce apoptosis by releasing BAX and BAK from their inhibitory binding with various anti-apoptotic proteins [81–83]. Additionally, NOXA is seen to degrade anti-apoptotic proteins MCL1 and A1, to further induce apoptosis [82]. The free pro-apoptotic proteins BAX and BAK translocate to the mitochondria (which is also stimulated through binding to PUMA), to induce mitochondrial outer membrane permeabilization (MOMP), leading to release of cytochrome c [74,81]. Secreted cytochrome c subsequently promotes the oligomerization of APAF1, which is also transcribed by P53, to initiate apoptosome formation [72,78]. Finally, different caspases will be recruited and activated through cleavage, including executioner caspases 3 and 7 to carry out apoptosis by cleaving all proteins in the cell [78,84].

TP53 Modifications

TP53 Mutations

It has been estimated that the entire human genome contains approximately three million single nucleotide polymorphisms (SNPs), which suggests that an SNP occurs every 1000 nucleotides [85,86]. The *TP53* gene contains 19 kilobases, which suggests that it contains 19 SNPs; however, currently, 2060 *TP53* mutations have been identified in multiple different tumors and tumor cell lines, indicating a strong selection for mutations within this locus [87]. In fact, all 393 AA of the P53 protein are shown to be mutated in the International Agency of Research on Cancer I [66,87]. However, approximately 85% of all mutations, depending on the cancer type, are found within the DBD between residues 102 and 292 [66,87,88]. Approximately 10% of these DBD mutations are nonsense mutations that prevent the formation of the P53 protein, and another 80% of these

mutations are missense [30,87]. Missense mutations are caused by the substitution of a single nucleotide within a gene, resulting in a different AA sequence while retaining the translation into a full-length protein. The extent to which *TP53* mutations contribute to tumorigenesis has been studied extensively. For example, many investigators have studied the temporal occurrence of *TP53* mutations; however, as many of these studies were performed retrospectively, no clear-cut conclusions were drawn [89,90]. Moreover, while the full-length protein is maintained, missense mutations are known to alter the structural conformation of the protein which may influence its binding affinity to proteins, DNA, or both [91]. In the context of *TP53*, biochemical analysis of different missense mutations demonstrated a partial loss of its DNA binding capacity, which may in turn affect its ability to transactivate target genes [92]. For example, the p53175P mutation has been shown to render P53 incapable of initiating apoptosis while remaining fully competent to contribute to cell cycle arrest [93].

Notably, approximately eight missense mutations account for 28% of all *TP53* DBD missense mutations, which are known as hotspot mutational sites [66,87,94–96]. This not only suggests a profound selection for mutations within the *TP53* locus but within specific sites of the DBD. Of note, in refractory GCTs, rare *TP53* mutations also appear to occur in the DBD [38]. An example of a hotspot mutations is an SNP at residue 175 where arginine is substituted by a histidine (R175H), which occurs in approximately 4–5% of all tumors and has been shown to impair the folding of the P53 protein [65,66]. This destabilizes the protein and interferes with its function as a tumor suppressor [92]. This mutation has also been shown to demonstrate a gain-of-function (GOF) phenotype, which indicates the acquisition of neomorphic functions that contribute to cellular transformation such as a disrupted cell cycle, invasiveness, and immortality [97–99]. It has been hypothesized that *TP53* missense mutations are selected for based on their impact on protein structure and subsequent oncogenic effects rather than being dependent on specific protein residues [98,100]. For instance, in glioblastoma, an infrequently occurring *TP53* mutation was identified that does not alter the protein structure [101]. However, this mutant was substituted in vitro for a frequently occurring oncogenic *TP53* missense that affects protein structure, and selection for the latter mutant was subsequently observed.

TP53 missense mutants have been shown to exert additional effects as well. For example, in some tumors, it was demonstrated that the mono-allelic R175H mutation was followed by the deletion of the second allele, causing a loss-of-heterozygosity (LOH) which in turn stabilized the R175H mutant and facilitated its GOF phenotype [102]. Additionally, this mutant was shown to exert a dominant negative effect in which the mutant protein sequesters WT protein during tetramerization and effectively inhibits the ability of WT protein to bind to DNA and engage its tumor-suppressive functions [51,52]. It has also been suggested that the dominant negative effect of P53 missense mutants is due to their higher propensity to form aggregates with the WT P53 protein but also

with its homologs P63 and P73, disrupting their function [39]. These tumorigenic effects (i.e., LOH, GOF and a dominant negative effect) have been observed for multiple *TP53* missense mutants and remain an area of intense research [94,103–105]. Notably, P63 and P73 have also been implicated in GCTs (specifically testicular GCTs) [18,106–108]. For example, in contrast to germ cells, testicular GCTs did not express GTAp63, which has been attributed to epigenetic silencing, suggesting a possible mechanism that facilitates GCT development [106]. Moreover, while Δ Np73 was shown to inhibit NOXA expression in testicular GCTs after cisplatin exposure, the opposite was observed for TAp73 (also in the absence of P53), the latter may partially explain the propensity for GCTs to enter apoptosis in response to cisplatin [107]. Further information regarding the P53 homologs is summarized in Box 2.

Box 2. Background information of the P53 homologs P63 and P73.

The role of P53 (*TP53*) has been studied intensely; however, the P53 homologs P63 (*TP63*) and P73 (*TP73*) have also gained significant attention in the context of genomic integrity, embryogenesis, and cancer development since their discovery in the late 1990s [109–115]. These three proteins constitute the P53 family and share sequence homology most significantly within the TAD, DBD, and TD, having different chromosomal localizations [109–116]. Evidence suggests that *TP53* arose from an ancestral *TP63/73*-like gene throughout evolution [113,117,118]. Furthermore, two main protein variants of P63 and P73 have been identified caused by alternative promoter usage: the full-length protein (TAp63 and TAp73, respectively) and a protein product, lacking the TAD at the N-terminus, although they may retain transactivation activity through the presence of alternative TADs (Δ Np63 and Δ Np73, respectively) [113–116,119–121].

In short, the TA variant of P63 and P73 share the highest degree of sequence homology to P53 and have similar functions (depending on the isoform), including the transactivation of multiple P53 targets such as MDM2 (which in turn also negatively regulates P63 and P73), P21, PUMA, NOXA, and Bax, thus also playing a role in cell cycle arrest, DNA repair, and apoptosis [107,109,110,112–115,122–125]. For example, TAp73 and TAp63 have been implicated in DNA-damage induced apoptosis in oocytes, suggesting a role in maintaining the genomic integrity of the female germline [113,126–128]. Similarly, a more recently identified new P63 isoform, GTAp63, was found to be highly expressed in male germ cells, which induce apoptosis (including the transactivation of PUMA and NOXA) after cisplatin-induced DNA damage [106].

Box 2. Background information of the P53 homologs P63 and P73. (*continued*)

In contrast to the TA variants, the ΔN variants of P63 and P73 mostly act as dominant negative inhibitors of the transcriptionally active members of the P53 family including P53 itself, which highlights a complex degree of interaction between different members of the P53 family [113–115]. In addition, the TA and ΔN variants of P63 and P73 are also subjected to alternative mRNA splicing, generating multiple isoforms with overlapping and distinct functions that add to the diversity and complexity of the P53 family [113–116].

Moreover, P63 is known to have fundamental roles in epidermal development, whereas P73 is vital for neuronal development and maintenance, which is also evident from mouse studies where p63 or p73 knockout mice present with severe congenital defects in the respective organ systems (e.g., the skin and the brain) [113,129–134]. Moreover, P63 germline mutations have been associated with various syndromes, including ectodermal dysplasia [113,131].

In the context of tumorigenesis, the involvement of P63 and P73 has sparked considerable debate which is in part due to the low frequency of mutations, which contrasts the high frequency of P53 mutations in cancer [113–116,135]. However, it is generally accepted that the TA variants mainly function as tumor suppressors whereas the ΔN variants are mostly oncogenic and are often overexpressed in multiple cancer types; however, exceptions have been observed, and much remains to be investigated and confirmed [113–115,135,136].

P53 Isoforms

The *TP53* gene consists of 13 exons that are subjected to alternative splicing [137]. This mechanism combined with two transcription start sites and an internal ribosomal entry site results in 12 possible isoforms of P53 [138,139]. Tumors harboring low rates of *TP53* mutations were demonstrated to have higher expression of different P53 isoforms, which are also most often truncated at the N-terminus [139]. These isoforms lack the transcriptional function of the full-length P53 protein [140]. For example, $\Delta 40P53$ lacks the first transactivation domain, while the second TAD as well as the DNA binding domain are intact [141]. Moreover, this specific isoform is resistant to ubiquitination, rendering it more stable than the full-length protein [142]. Therefore, while $\Delta 40P53$ does not have transcriptional activity of its own, it can influence the full-length P53 protein by either repressing or activating it, depending on the cellular circumstances [142].

A second frequently occurring isoform is $\Delta 133P53$, where both TADs are missing, as well as the PRD and a part of the DBD [141]. It has been demonstrated that this isoform

is capable of inactivating full-length P53 in a dominant negative manner, which may explain the observation that the expression of $\Delta 133$ P53 represses apoptosis [139]. Additionally, due to a modified DBD, $\Delta 133$ P53 induces the expression of different genes that contribute to tumorigenesis, including genes that promote angiogenesis and cellular reprogramming, which have been observed to be highly expressed in human glioblastoma cells [143]. On the other hand, in ovarian cancer, it has been shown that an increased expression of $\Delta 133$ P53 correlates with improved survival and a lower change of recurrence [144]. Finally, another isoform that was recently discovered is $\Delta 160$ P53, which lacks the same domains as $\Delta 133$ P53 but lacks a larger segment of the DBD [138]. While there is still little known about the consequences of higher levels of $\Delta 160$ P53, it was recently discovered that it is able to promote cellular invasion [145].

2

P53 Post-Translational Modifications and Regulatory Elements

In addition to isoforms, the P53 protein is continuously subjected to a variety of post-translational modifications (PTMs) that are context-, tissue-, and cell-specific [146,147]. The most common PTMs are the methylation of arginine and lysine residues, phosphorylation of serines and threonines residues, and ubiquitination, acetylation, and sumoylation of lysine residues. Specific PTM patterns are present under physiological circumstances to regulate P53 activity, and aberrant patterns may disrupt P53 function and contribute to tumorigenesis. Different PTMs of P53 and its main negative regulators MDM2 and MDM4 are depicted in Figure 6 [148,149]. Further information of these negative regulators is described in Section 2.2.

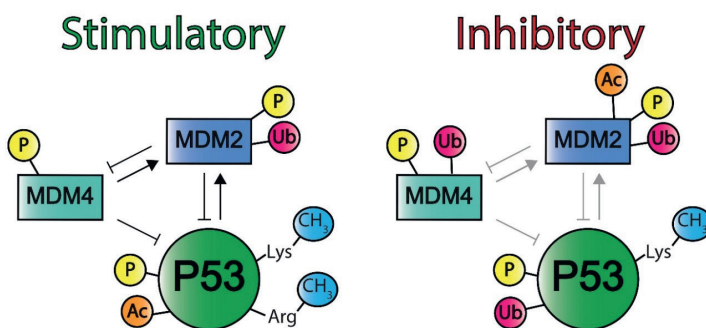


Figure 6. The different post-translational modifications of P53 and Mouse Double Minute 2 and 4. P53 can be activated (left) through phosphorylation (P), acetylation (Ac), and methylation (CH₃) on lysine and arginine residues. Mouse Double Minute 2 (MDM2) can be phosphorylated and ubiquitinated (Ub) and Mouse Double Minute 4 (MDM4) can be phosphorylated. Post-translational modifications (PTMs) can also inhibit these proteins, which also decreases the regulation of each other (right). Phosphorylation, ubiquitination, and lysine methylation inactivate P53. Phosphorylation, acetylation, and ubiquitination inhibit MDM2, and phosphorylation and ubiquitination obstruct MDM4 activity. Of note, human genes and proteins are annotated in all capital letters (e.g., MDM2 and MDM2, respectively), whereas the murine homologs are annotated with a single capital letter (e.g., Mdm2 and Mdm2, respectively).

It has been demonstrated that multiple PTMs are simultaneously required to influence P53 activity, and crosstalk between these modifications has been observed [150]. For example, modifications can block each other and thus determine the activity of P53 combined [151].

Although little is known about the exact effects of P53 methylation, several enzymes have been characterized as either mono- or dimethylate lysine residues [152,153]. On one hand, methylation has been shown to activate P53 by stabilizing the protein and induce transcriptional activity [153]. However, repression of the DNA binding activity of P53 has also been observed [152]. Notably, crosstalk between methylation sites has also been suggested, as stimulatory methylation of a first lysine residue was shown to block the inhibitory methylation of a second lysine residue [154].

The combination of which lysine residues are modified and the number of methyl groups that are added to each lysine ultimately determines P53 activity. Thus far, the methylation of arginine residues appears to be solely regulated by protein arginine methyltransferase 5 (PRMT5), which targets three residues within the TD [155]. The induction of DNA damage causes the translocation of PRMT5 toward P53 to modify the protein, resulting in cell cycle arrest and a DNA damage response [155]. These specific residues have been seen to be mutated in tumors and inhibit the tetrameric formation of P53 [148].

The phosphorylation of P53 mainly occurs at the N- and C-terminal, and most residues are phosphorylated upon cellular stress to activate P53 [156]. However, several

threonine and serine residues are continuously phosphorylated that target P53 for degradation, which is especially important in the absence of cellular stress [157,158]. DNA damage either induces phosphorylation or dephosphorylation of specific residues and enables cell cycle arrest and DNA repair. Phosphorylation is mediated through multiple redundant enzymes, as the same AA can be phosphorylated by multiple kinases and a single kinase is able to phosphorylate different residues [159–161]. Mutations in P53 could potentially lead to increased phosphorylation sites, which have also been seen to contribute to tumorigenesis. For instance, CDK4 can phosphorylate P53 at SNP R249S, resulting in Myc activation [149].

Ubiquitination of lysine residues, including those in P53, is established by three enzymes: an E1 ubiquitin-activating enzyme, an E2 ubiquitin-conjugating enzyme, and an E3 ubiquitin-ligating enzyme [162]. An important E3 ubiquitin ligase that functions as one of the main negative regulators of P53 is MDM2, which can ubiquitinate P53 at six residues present in the C-terminus [163]. Mono-ubiquitination translocates P53 toward the cytoplasm, where it may inhibit autophagy by promoting apoptosis in a transcription-independent manner [164,165]. P53 poly-ubiquitinated by MDM2 will result in its degradation [166,167]. The importance of MDM2 in regulating P53 is illustrated by the numerous types of tumors harboring elevated levels of MDM2, resulting in increased degradation of WT P53 and thus contributing to tumorigenesis [166]. Moreover, MDM2 overexpression and TP53 mutations appear to be mutually exclusive, suggesting that both can independently and efficiently disrupt the P53 pathway and contribute to tumorigenesis [168–170].

Small Ubiquitin-like Modifier (SUMO) has a structural resemblance to ubiquitin, and both are attached to lysine residues via a comparable [171]. Sumoylation has been seen to promote P53 transcriptional activity, while it is not able to affect P53's stability or localization [172].

Finally, amongst other proteins, P53 can be acetylated by histone acetyl transferases (HATs), which were initially discovered to be involved in epigenetic acetylation [173]. P53 acetylation was shown to occur at the C-terminus, which promotes its binding to its target genes [173]. Moreover, acetylation stabilizes P53, as most of the known acetylation residues can also be subjected to MDM2-mediated ubiquitination [150]. MDM2 is not able to form a complex with acetylated P53, thereby protecting acetylated P53 from degradation [174,175]. To balance the acetylation of P53, histone deacetylases (HDACs) come into play, which suppress the transcriptional activity of P53 [176]. Certain deacetylases such as SIRT1 have been found to be upregulated in tumors; however, it has also been seen to have a tumor-suppressive role in others [177,178]. This counterintuitively suggests that de-acetylation may also stabilize P53 despite it rendering P53 vulnerable to ubiquitination at the same residues and requires further investigation.

Chromosomal Number Alterations

Many tumors present a mono-allelic *TP53* mutation and an additional loss of the remaining WT *TP53* allele [179]. Loss of the WT allele is known to result from its specific deletion or the duplication of the mutated allele. As mentioned before, it has been hypothesized that *TP53* missense mutations can drive the loss of the WT allele, which may be explained by the observations made with the R175H mutant in which the loss of the WT allele stabilized the mutant protein [50,98,99]. For example, in murine leukemia and lymphomas, it has been shown that this loss did not only cause the deletion of WT *TP53* but also of other genes that further exacerbated the tumorigenic phenotype [180]. In addition, the loss of the WT allele in these mice were found to be the result from a duplication of the mutated *TP53* allele rather than the deletion of the WT gene, a similar observation to an earlier performed database analysis [180,181]. Recently, it has been demonstrated that the loss of the WT P53 allele contributed to the tumor- and metastasis initiation with intestinal tumors in a mouse model [182]. This suggests that the loss of the WT allele contributes to tumorigenesis; however, the underlying mechanisms (i.e., mutant allele duplication or WT allele deletion) differ between cancers.

Negative Regulators of the P53 Pathway

MDM2

MDM2 is an E3 ubiquitin ligase that functions as an important negative regulator of P53 (illustrated in Figure 6) and is often modified in tumors with WT *TP53* [62]. Its importance in regulating P53 is underlined by the observation that *Mdm2*-null mice resulted in embryonic lethality [183–186]. The MDM2 protein consists of 491 AAs and contains multiple domains including an N-terminal P53 binding domain, an acidic domain, a zinc finger domain, and a C-terminal Really Interesting New Gene (RING) finger domain [187–189]. In addition, MDM2 contains nuclear localization and export sequences [190]. MDM2 can regulate P53 through mono- and polyubiquitination. Firstly, facilitated by its p53-binding domain, RING-finger domain, and nuclear localization sequences, MDM2 binds at the p53 TAD and subsequently monoubiquitinates specific lysine residues of the p53 REG domain, which translocates p53 from the nucleus to the cytosol and inhibits its functions as a transcription factor [163,166,167,190–194]. Secondly, MDM2-mediated polyubiquitination of p53 leads to its proteasomal degradation [163,166,194–196]. Notably, MDM2-mediated P53 ubiquitination is also facilitated by the phosphorylation of specific serine residues within acidic domain of MDM2 that enable its interaction (and thus that of p53) with proteasomes [197]. Furthermore, mono- or polyubiquitination of P53 by MDM2 is suggested to be a result of the level of MDM2 in the nucleus [192]. Notably, a negative feedback loop has been identified to control P53 protein levels as high levels of P53 induced *MDM2* gene expression of which the protein product subsequently mediates P53

ubiquitination and degradation [198]. Finally, MDM2 also has P53-independent functions such as targeting E-cadherin for degradation through its ubiquitin ligase activity, which has been associated with increased cellular invasiveness [199].

Elevated Levels of MDM2

MDM2 amplifications, observed in multiple cancers, have been shown to result in increased levels of its RNA and protein product [188]. Firstly, *MDM2* amplification affects the critical balance in P53 protein levels as MDM2-mediated P53 ubiquitination is increased, which has been observed in sarcoma amongst other tumor types [102,110]. Therefore, the therapeutic potential of disrupting the interaction between MDM2 and P53 has been intensely studied in tumors harboring an *MDM2* amplification, and small-molecule inhibitors such as Nutlin-3a demonstrate a successful reactivation of the P53-dependent apoptosis in osteosarcoma, colon cancer, and GCTs [28,41,201–203].

Regarding its P53-independent functions, lower levels of E-cadherin in combination with high expression of *MDM2* has been observed in breast and ovarian cancer [199,204]. Another P53-independent function of MDM2 is its ability to bind to RB, resulting in the expression of cell cycle promoters such as E2F from RB which has been shown to increase cellular proliferation [205].

Amplification is not the only cause of increased expression of *MDM2*. The frequently occurring SNP at nucleotide 309 (resulting in a T > G substitution), within the promotor of *MDM2*, leads to a higher affinity of transcription factor SP1 for the *MDM2* promotor and thus increased *MDM2* expression [206]. This mutation has also been correlated to a high risk for colorectal and prostate cancer [207,208]. Especially, colorectal cancer has been extensively studied for this SNP, indicating a higher risk in Asian populations when one or both alleles are mutated [209]. The reason SNP309 has not been shown to correlate in other cancers is due to another SNP at nucleotide 285, which frequently occurs in combination with SNP309 [210]. This SNP285 counteracts the increased affinity of SP1 for the *MDM2* promotor and has been observed in breast and ovarian cancers [211]. The SNP285 has been shown to be more frequently occurring in citizens from countries as Norway, the Netherlands, and UK compared to Finland and China, possibly explaining the correlation between SNP309 and tumorigenesis in colorectal cancer [209,211].

Isoforms of MDM2

As a result of alternative splicing, over 40 different isoforms of MDM2 have been identified in both tumor and healthy tissues, which often lack (part of) the P53 binding site [212]. For example, MDM2-B was shown to be expressed most frequently in tumors including ovarian and bladder cancers [213]. Moreover, Zheng and colleagues detected a higher

level of mutant P53 when this specific isoform was expressed [214]. This may be explained by the observation that MDM2-B cannot bind P53 but is capable of binding and inhibiting the full-length MDM2 protein, thus inhibiting P53 degradation [215]. In the case of a co-occurring *TP53* mutation, this leads to stabilization of mutant P53 resulting in an increased tumor volume and metastasis [214]. Additionally, many other MDM2 isoforms either have a truncation at the C-terminus or the alternative splicing causes the C-terminus to be out-of-frame; however, these do not occur as frequently as MDM2-B, which complicates gaining a deeper understanding of its effect [212].

Post-Translational Modifications of MDM2

Similar to P53, MDM2 is also subjected to PTMs, which regulate its downstream functions. Currently, three types of MDM2 PTMs have been identified, as illustrated in Figure 6. Firstly, MDM2 can be ubiquitinated, which includes auto-ubiquitination. In unstressed cells, this mechanism is responsible for maintaining a low concentration of MDM2 protein [216]. Although the auto-ubiquitination function of MDM2 is inhibited under stressed conditions, MDM2 degradation still occurs, suggesting that other E3 ubiquitin ligases can target MDM2 for degradation [217]. Notably, MDM2 auto-ubiquitination also stimulates MDM2 to bind to E2 ubiquitin-conjugating enzymes, which subsequently leads to increased P53 polyubiquitination and degradation [218]. Conversely, MDM2 de-ubiquitination is equally important and occurs through the ubiquitin hydrolase HAUSP, which inhibits MDM2 auto-ubiquitination and enables MDM2-mediated P53 degradation [219].

Secondly, MDM2 is subject to acetylation, which mostly occurs at two lysine residues: K466 and K467 [220]. Modification of these lysine residues, which are located within the RING-finger domain, was shown to be effectuated by histone acyltransferase CREB-binding protein (CBP) *in vitro*, which silenced the E3 ubiquitin ligase activity of MDM2 [220]. Moreover, these lysine residues are also located in the nucleolar localization signal; however, their acetylation did not affect MDM2 translocation toward the nucleolus [220]. Notably, the *in vitro* substitution of these lysine residues for glutamine resulted in diminished E2 ubiquitin ligase activity [220].

Thirdly, MDM2 serine residues can be phosphorylated and occurs at multiple residues through multiple different enzymes [221]. For instance, ATM kinase has already been mentioned for its role as a DNA damage sensor and inducing stabilization through phosphorylation of P53. However, murine studies demonstrated that it can also phosphorylate Mdm2 at serine 395 [222]. In a mouse model, Gannon and colleagues have shown that the phosphorylation of this residue weakens the ability of Mdm2 to ubiquitinate P53, leading to increased apoptosis [222]. In addition, AKT/PKB serine–threonine kinase has been observed to phosphorylate MDM2 at serine 166 and 188 [221]. After activation by PI3K, AKT-mediated phosphorylation promotes the translocation of

MDM2 toward the nucleus, where MDM2 can target P53 for nuclear degradation [221]. *AKT* has been shown to be overexpressed in tumors, resulting in MDM2 phosphorylation and increased P53 degradation, thus contributing to tumorigenesis [223].

Ribosomal Proteins Influencing MDM2

Additionally, other factors are involved in regulating MDM2 activity. One of these factors regards ribosomal biogenesis, i.e., the production and processing of RNA and proteins that form the 40S and 60S ribosomal compartments, which occurs within the nucleolus [224]. When this process is disrupted, ribosomal proteins may bind and inhibit MDM2, leading to P53 stabilization and cell cycle induction [225]. Multiple proteins are known to bind MDM2; however, these bind varying regions due to their differences in structure [226]. The negative regulation of MDM2 by ribosomal proteins contributes to the hypothesis that decreased ribosomal biogenesis (and thus decreased MDM2 inhibition) contributes to an increased cancer risk [227]. Conversely, high expression of ribosomal RNA and proteins has also been observed in cancer, which may be caused by concomitant increased oncogene expression and/or inhibition of tumor suppressors [228,229]. In malignant melanoma cell lines, the expression of different ribosomal proteins was higher compared to significantly less malignant cells [230]. In addition, ribosomal proteins mutations have also been linked to syndromes that predispose to cancer such as the 5q-syndrome (a subtype of myelodysplastic syndrome) [231].

MDM4

MDM4 is a homolog of MDM2 and is structurally similar [187]. For instance, MDM4 also contains a P53 binding domain and binds P53 at its TAD, thus blocking its function as a transcription factor [101,143]. Additionally, MDM4 was shown to bind P53 via other domains, including its acidic domain [144]. Loss of *MDM4* has been shown to increase the expression of many pro-apoptotic P53 target genes, which underlines its relevance in inhibiting P53 [232]. Moreover, in mouse embryonic fibroblasts, *Mdm4* was shown to block p300-induced P53 acetylation that normally stabilizes and activates the P53 protein, thus resulting in an inactivated protein [233]. In addition, similar to MDM2, MDM4 is fundamental to embryonic development in regulating P53-dependent apoptosis which was demonstrated by the embryonic lethality observed in MDM4- or MDM2-null mice [183,185,186,234,236]. Notably, MDM4 is detected at low levels in healthy adult tissues [237].

Several differences and non-overlapping functions have also been observed. Firstly, the loss of *Mdm2* could not be compensated by increased *Mdm4* expression and vice versa [238]. Moreover, MDM4 is a cytoplasmic proteins that lacks nuclear localization sequences and therefore depends on MDM2 to be translocated to the nucleus [239]. In addition, the

MDM4 RING finger domain lacks E3 ubiquitin ligase activity, which indicates that MDM4 cannot target P53 for degradation [240]. Nevertheless, MDM4 can bind and stabilize MDM2 through heterodimerization via the RING finger domains and thus indirectly contributes to P53 ubiquitination [240]. Conversely, it has also been suggested that this heterodimer is needed to degrade MDM4 and thus to stabilize P53 [241]. Additionally, MDM4 also has P53-independent actions, such as the inhibition of DNA damage repair mechanisms, which may result in genomic instability [242].

Elevated Levels of MDM4

The overexpression of *MDM4* has been observed in many different tumors, adding up to 2.9% of all cancers according to The Cancer Genome Atlas using cBioPortal, with higher frequencies observed of retinoblastoma and breast cancer as well as tumor cell lines [233,243–245]. The exact mechanisms underlying MDM4 upregulation are not completely understood [246]. Nevertheless, increased *MDM4* expression due to amplification results in fast proliferating and immortal cells, as WT P53 is transcriptionally inactivated [233]. Moreover, p300-mediated P53 acetylation is also impaired when MDM4 levels are elevated. Notably, MDM4 has also been demonstrated to contribute to cell growth and tumorigenesis in the absence of P53 [247]. This is thought to be a result of the P53-independent functions of MDM4, such as the ability to induce genomic instability through the inhibition of DNA damage repair [242].

SNPs and Overexpression of Transcriptional and Translational Regulators of MDM4

Estrogen receptor- α is an important transcription factor of *MDM4* and is frequently overexpressed in cancer [248]. In addition, cancer-related overexpression of K-RAS and IGF-I induce the expression of MDM4 and thus inhibit P53 [249].

Multiple SNPs within the *MDM4* locus have been correlated to increased tumor risk [250]. For instance, the rs4245739 polymorphism that results in an A > C substitution has been studied extensively and has been detected within ovarian, prostate, and breast cancer [251,252]. This SNP lies within the 3' UTR of *MDM4* and was found to form a new binding site in the MDM4 RNA for microRNA-191 and 887 [251,252]. MicroRNAs (miRNAs) are non-coding molecules of approximately 22 nucleotides that bind to complementary mRNA strands, resulting in their subsequent silencing or degradation [253–255]. Regarding *MDM4*, miRNAs-191 and -887 inhibited *MDM4* translation, thus reducing its protein level and stabilizing P53. Increased expression of these miRNAs has been observed in prostate cancer patients [252]. Moreover, a significant decrease in survival among ovarian patients was observed in those harboring this SNP [251].

Overexpression of MDM4-S

Many isoforms of MDM4 have been found and studied with nearly all being the result of alternative splicing [245]. For instance, MDM4-S is a transcript variant in which exon six has been skipped and therefore excluded from the final protein that targets it for nonsense-mediated mRNA decay, ultimately preventing the inactivation of P53 [246]. Additionally, in mice, this isoform was shown to correlate to decreased levels of full-length Mdm4, thus potentially increasing P53 levels and having a tumor suppressive effect [246]. This was additionally suggested to be caused by the decreased expression of the oncogene serine/arginine-rich splicing factor 3 (Srsf3), which facilitates the inclusion of exon six [246]. In a mouse model, the undifferentiated ES cells were shown to harbor high levels of Mdm4, which significantly decreased upon differentiation, and it was suggested that this resulted from increased exclusion of exon six and therefore increased Mdm4-S expression [246]. Moreover, the increased expression of Mdm4-S in melanoma appeared to reduce tumor growth, thus demonstrating its potential as a therapeutic target [246]. In contrast, other studies demonstrated that MDM4-S has an increased binding affinity for P53 compared to full-length MDM4, which may suggest increased P53 inhibition. For instance, decreased P53 levels as well as a higher level of MDM4-S relative to full-length MDM4 was detected in papillary thyroid carcinoma and soft tissue sarcoma [256,257], which in turn may also dispute both the tumor-suppressor function of MDM4-S and the oncogenic function of Srsf3.

Finally, Pant and colleagues observed increased MDM4-S expression in B-cell leukemia patients, however, they suggested that this isoform was a consequence of splicing defects in tumor cells rather than being a contributor to tumorigenesis [258]. These investigators also supported the notion that MDM4-S has the potential to become a biomarker for this cancer.

Post-Translational Modifications of MDM4

Similar to P53 and MDM2, MDM4 activity is also determined by the combination of PTMs, most notably phosphorylation and ubiquitination. For instance, the phosphorylation of tyrosine residue 99 (Y99), located within the P53 binding site, impairs the binding of MDM4 to P53, leading to P53 stabilization [259]. However, when this PTM is combined with the phosphorylation of tyrosine residue 55 (Y55) at the N-terminus, MDM4 is able to bind P53 and inhibit its function [259]. MDM4 can be phosphorylated by the DNA damage sensor ATM and its targets CHK1 and CHK2 [260,261]. The phosphorylation of serine residue 367 by CHK1 results in the translocation of MDM4 toward the cytoplasm, effectively inhibiting it from binding P53, whereas CHK2-mediated phosphorylation of serine residues 342 and 367 translocates MDM4 toward the nucleus [260]. Additionally, these phosphorylation sites are also recognized by MDM2 to mediate MDM4 ubiquitination and

degradation [260]. P14^{Arf} also functions as a negative regulator of MDM4 by facilitating MDM2-mediated MDM4 ubiquitination [262]. In different cancers, it has been shown that MDM4 ubiquitination is inhibited by a ribosomal RNA, namely non-coding 5S rRNA, which binds to the RING-finger domain of MDM4 [263].

Alternative Mechanisms to Inactivate the P53 Pathway

P21

P21 (*CDKN1A*), also known as WAF1 and CIP1, is an important transcriptional target of P53; however, it is also regulated through P53-independent mechanisms [70,71,264–266]. The *CDKN1A* gene consists of 2118 base pairs with three exons and produces a protein of 164 AAs [70]. As mentioned before, *CDKN1A* contributes to P53-dependent cell cycle arrest and apoptosis, and therefore, its expression is increased as P53 levels rise in response to cellular stress signals such as DNA damage [267]. P21 is primarily known to function as a CDK inhibitor (CDKi) by binding to a variety of cyclin–CDK complexes [71]. These complexes are crucial for cell cycle progression, with specific CDKs–cyclin complexes involved in different cell cycle phases [268,269]. Upon DNA damage, P21 facilitates cell-cycle arrest through the inhibition of CDK2 [267]. In addition, P21 also directly inhibits DNA replication and repair by binding proliferating-cell nuclear antigen (PCNA), which is an important processivity factor for these processes [172–174,270].

Moreover, during a cellular stress response, anti-apoptotic proteins such as BCL-2 are known to bind and sequester pro-apoptotic proteins BAX and BAK, which inhibits apoptosis and increases mitochondrial reactive oxygen species through activation of the PI3K–AKT–MMP2 pathway, ultimately increasing the invasive competence of the cell [271]. Similarly, P21 is known to interact with and inhibit multiple pro-apoptotic proteins in the cytoplasm, including multiple caspases [264,272–275]. However, paradoxically, P21 may also have pro-apoptotic functions, as it was demonstrated to complex with P53 and aid in sequestering anti-apoptotic proteins to form a trimer, which results in the release of pro-apoptotic proteins, leading to the induction of apoptosis and decreased ROS levels [276].

Furthermore, despite that P21 is not a transcription factor, it is capable of influencing the expression of a variety of genes [277]. For example, the inhibition of CDKs by P21 reduces the phosphorylation of and activates retinoblastoma proteins, leading to the inactivation of transcription factor E2F [278]. E2F functions as a transcription factor for a wide spectrum of genes, with functions including DNA repair, DNA damage checkpoint, and cell cycle progression [279].

While P21 has been researched extensively in relation to tumorigenesis, SNPs in this protein are rare, which complicates studying its effects [280]. Double knockout *Cdkn1a* mice did not show any developmental restrictions or increased tumorigenesis in the presence of WT P53 during the seven months in which they were studied [281]. However,

Martín-Caballero and colleagues created similar homozygous *Cdkn1a*-null mice, which they studied for two years [282]. A large part of the cohort died due to complications of increased proliferation of T-memory lymphocytes; however, a significant portion of the mice developed tumors including lymphomas, carcinomas, and sarcomas [282]. Moreover, compared to WT P21 mice, P21-null mice had a prolonged survival after irradiation, which may be due decreased tumor growth caused by an enhanced apoptotic response [282]. In addition, the loss of *CDKN1A* was demonstrated to contribute to tumorigenesis when combined with the loss of other tumor suppressors or activated pro-oncogenes. For instance, inactivation of both P21 and the INK4 pathway, which also functions in CDK inactivation, results in enhanced proliferation and increased susceptibility of tumorigenesis [283]. Additionally, *Cdkn1a*-null mutant mice crossed into an oncogenic Ras mutant background showed increased and accelerated tumor growth compared to WT P21 [284]. Furthermore, the inactivation of P21 has also been observed through the methylation of its gene, which is mediated by growth factor independent 1 (Gfi1)v [285], which has been observed to be highly expressed in a variety of tumors [286,287].

Paradoxically, increased P21 levels have also been associated to cancer and predisposing syndromes [264,265,275]. For example, high levels of P21 have been detected in ataxia telangiectasia, which is an illness caused by mutations in the *ATM* gene with increased formation of lymphomas and leukemias, and P21 was demonstrated to contribute to tumorigenesis in *Atm*-null mouse fibroblasts [288]. The loss of *Cdkn1a* partially compensated for the senescent phenotype and increased the sensitivity of the cells toward irradiation, indicating that the high expression of *Cdkn1a* contributes to tumorigenesis.

Increasing evidence is emerging that in contrast to the initial paradigm, P21 may not solely function as a tumor suppressor but also as an oncogenic protein (this has previously been reviewed in [264,273,275,289]). While these controversial functions have sparked considerable debate, it has been suggested that a plethora of factors including PTMs and its subcellular localization (nuclear versus cytoplasmic) may dictate the effects of P21, which may underlie why both its up- and downregulation is observed in different cancer types [264,274,275]. For example, it has been hypothesized that the nuclear localization of P21 is important for its tumor suppressor function, mostly through cell cycle arrest; however, when localized in the cytoplasm, P21 may function as an oncogene [264,274,275]. The oncogenic properties of P21 may firstly be related to its aforementioned anti-apoptotic functions that are associated to its cytoplasmic localization [264,273,275,290]. Furthermore, another mechanism that put P21 forward as an oncogene was demonstrated when in vitro high constitutive P21 expression resulted in the deregulation of replication license machinery, leading to replication stress and subsequent genomic instability [265,291]. Notably, this was observed in a P53-deficient background, which suggests that the P53 status of the cell also dictates whether P21 functions as an oncogene or tumor suppressor gene [265,266,275,291]. Of note, P21 is

known to be regulated by both P53-dependent and -independent mechanisms [264]. It was later also demonstrated that in addition to P21-mediated genomic stability, P21 may also contribute to a shift toward error-prone DNA repair pathways (most notably the RAD52-dependent error-prone break-induced replication pathway), which further contributes to genomic instability.

ARF

The INK4 locus encodes for multiple proteins including P16^{INK4A} from the *CDKN2A* gene (hereafter P16) and P14^{ARF} from the *ARF* gene (hereafter ARF) [292,293]. The latter was first discovered in mice when an alternative reading frame of the *P16^{ink4A}* gene in the INK4 locus of mice revealed the sequence of a second gene: *P19^{Arf}*, which is the murine homolog of *ARF* sharing 50% sequence homology [294]. This suggests that this protein is not strongly conserved. The sequences encoding for human *P16* and *ARF* overlap substantially and share the last two out of three exons [293]. However, P16 is part of the INK4 family of which all members function as CDK inhibitors whereas ARF does not, which is also evident due to its structural differences [293]. Instead, ARF functions as a tumor suppressor by inactivating MDM2 and thus stabilizing P53, which explains how the loss of *ARF* can increase tumor susceptibility [295,296]. It has been shown that ARF is mainly localized in the nucleolus, where it restricts MDM2 from its function to degrade P53 [297,298]. In addition, ARF is also thought to neutralize the E3 ubiquitin ligase activity of MDM2, including MDM2, that is already bound to P53 [292,299]. A P53-independent role of murine *P19^{Arf}* was demonstrated in a *P19^{Arf}/-* mouse that was crossed into a double *Tp53^{-/-}; Mdm2^{-/-}* background, which also increased tumor susceptibility, and subsequent reintroduction of *P19^{Arf}* into these triple knockout mice resulted in G1 cell cycle arrest [300,301]. This P53-independent function may partially explain the binding partners of *P19^{Arf}* [302]. One of these proteins is Aurora B, through which *P19^{Arf}* is thought to maintain chromosomal stability [303]. Furthermore, *P19^{Arf}* has been demonstrated to be involved in the development of the eyes and male germ cells and even the extra-embryonic structures, such as the yolk sac [304,305].

Inactivation of ARF has been observed in multiple tumors (also in a mutually exclusive manner with *TP53* mutations) [306]. For instance, approximately half of the malignant gliomas were shown to harbor an *ARF* deletion, either with or without the additional deletion of *P16* [306,307]. Of note, the deletion of the entire *CDKN2A* locus is not *ARF* specific and as P16 is also lost; however, deleterious mutations in exon 1 β , which is the *ARF* promoter, will only inactivate ARF [308]. For example, in renal cell carcinoma and tumors in the intestinal system, ARF expression was specifically silenced through promoter methylation [308–311]. Moreover, in cancer cell lines with an unmethylated *ARF* promoter, MDM2 was found to be localized in the nucleus, whereas a colorectal

cancer cell line with a hypermethylated *ARF* promoter revealed MDM2 to be localized in the cytoplasm as well [312]. Subsequent in vitro demethylation of the *ARF* promoter in this colorectal cancer cell line demonstrated a translocation of MDM2 from the cytoplasm toward the nucleus, where it was subsequently inactivated by *ARF*, leading to P53 activation.

The overexpression of *ARF* was also found to contribute to tumorigenesis in a number of tumor cell lines, which is suggested to be caused by the initiation of autophagy, as both autophagy and tumor growth decreased when *ARF* was inhibited [313]. Xie and colleagues studied the metastatic capability of prostate cancer in double *Pten*^{-/-}; *TP53*^{-/-}, knockout mice [314,315]. *P19*^{Arf} was shown to stabilize Slug, decreasing the expression of E-cadherin [314], and upregulate metalloproteinase 7 (MMP-7), which promotes the degradation of E-cadherin [315], both promoting epithelial–mesenchymal transition. With a similar double knockout background of *Pten*^{-/-}; *TP53*^{-/-}, overexpression of *P19*^{Arf} was frequently demonstrated to be present in chemo-resistant bladder cancer [316].

SNPs and indels specifically affecting *ARF* have been detected in a variety of tumors. These can be present in exon 1β (the *ARF* promoter), which has been demonstrated in a human colon cancer cell line carrying a nucleotide deletion that results in a truncated protein [310]. In addition, a primary colon carcinoma was shown to have a point mutation at codon 12 in exon 1β, which was thought to impair the binding of *ARF* to MDM2 and subsequently MDM2 nuclear translocation [310]. In melanoma, five mutational sites were identified that were suggested to inhibit *ARF* activity [317]. Such mutations are thought to increase MDM2 levels and thus the degradation of P53, thus contrasting the function of WT *ARF*.

TRIM

The tripartite motif (TRIM) proteins were discovered in 1992, long before their functions were elucidated [318,319]. These proteins mostly contain three zinc-finger domains, two B-boxes, a coiled-coil domain, and a RING-finger domain, which gives the protein E3 ubiquitin ligase activity [318]. Multiple TRIM proteins have been identified and most of them homodimerize through their coiled-coil domain [319,320]. As these proteins are overexpressed in many tumors they are hypothesized to contribute to tumorigenesis [321,322]. For instance, increased TRIM23 expression is correlated with a poor prognosis in colorectal cancer [322] and lung adenocarcinoma [323]. TRIM23 can bind to P53 through its RING-finger domain and mediate P53 ubiquitination and subsequent degradation [322]. In colorectal cancer, elevated TRIM23 levels were shown to correlate with tumor size and lymph node metastasis, which was suggested to be the result of impaired P53 signaling [322]. In lung adenocarcinoma, TRIM23 expression was shown to correlate with

resistance to the chemotherapeutic agent cisplatin which was suggested to be the result of induced GLUT1/3 expression and inhibition of NF- κ B [323].

Additionally, TRIM32 was shown to be overexpressed in lung cancer cells lines and was found to decrease apoptosis cell-cycle arrest and senescence and enhance proliferation and invasiveness [324,325]. Moreover, in a study with multiple tumorigenic cell lines, P53 was found to regulate TRIM32 expression as the promoter of TRIM32 harbored a P53 responsive element [325].

Lastly, TRIM59 upregulation has been observed in gastric cancer, non-small cell lung cancer and osteosarcoma [321,326–328]. In gastric cancer, this upregulation resulted in a decreased expression of P53 targets including P21, suggesting the inactivation of the P53 pathway [321]. Moreover, TRIM59 overexpression was found to correlate with the metastatic capacity of gastric tumor cells and a negative impact on the 5-year survival rates of patients [321]. Additionally, in cholangiocarcinoma and colorectal cancer, TRIM59 was demonstrated to promote cellular proliferation [327,329]. In all cell lines used, the inhibition of TRIM59 resulted in decreased phosphorylation of both PI3K and AKT, indicating that TRIM59 promotes cellular migration through these proteins [327,329].

Long Non-Coding RNAs

The majority of the genome consists of non-coding sequences, including long non-coding RNAs (lncRNAs), which are often longer than 200 nucleotides [330]. Most of the nearly 15,000 known lncRNAs are transcribed by RNA polymerase II, and these molecules are modified by 5' capping and poly-adenylation [331,332]. The expression of lncRNAs can be regulated by different mechanisms including transcription factors and epigenetic mechanisms [333,334]. lncRNAs are able to affect chromatin structure, thereby regulating gene expression and determining development, epigenetic reprogramming, and cellular pluripotency [331,335,336].

The P53 pathway can be inactivated through elevated expression of several lncRNAs, which has been demonstrated for Antisense Non-coding RNA In the *INK4* Locus (ANRIL) in prostate cancer [337]. Similar to ARF and P16, ANRIL is located in the *INK4* locus and was found to partially overlap with two genes, namely *P15^{INK4B}* and *ARF* [338], the latter of which is known to influence the P53 pathway [295]. In prostate cancer, ANRIL overexpression was shown to recruit CBX7 (a Polycomb Repressive Complex 1 protein) to the *INK4* locus to enhance methylation and decrease the expression of all genes contained within this locus, including ARF, which may suggest increased P53 degradation [337]. Conversely, decreased ANRIL expression due to SNPs in the corresponding gene was detected in melanoma and may contribute to tumorigenesis through its ability to downregulate *CDKN2B* expression [339].

Moreover, the lncRNA Maternally Expressed Gene 3 (*MEG3*) was also shown to bind and activate P53, which was demonstrated by increased activation of P53 target genes and decreased expression was detected in pituitary adenomas [231,237]. In mice, knockout of *Meg3* resulted in overexpression of *Vegf* and *Notch*, leading to increased angiogenesis [334]. This was explained by the earlier observation that P53 represses *VEGF* expression breast cancer [340].

MicroRNA

As previously mentioned, miRNAs are short sequences of approximately 22 nucleotides [253]. These are initially formed as long primary transcripts, which are cleaved by Drosha to process them toward stem-loop precursors of about 70 nucleotides known as pre-miRNAs [341]. These are subsequently cut into single-stranded, mature miRNAs by Dicer [342]. Double knockout of Dicer in mice caused lethality during early development, which was suggested to be caused by the loss of stem cells, thus underlining the importance of miRNAs during early embryonic development [343]. MiRNA can bind the 3' UTR of the mRNA and contribute to post-transcriptional regulation [255,344]. In short, mature miRNAs are incorporated into and RNA-induced silencing complex (RISC), which enables this complex to target mRNA that is at least partially complementary to the miRNA [254,345]. If the targeted mRNA has a high degree of complementarity, it will be cleaved and degraded, whereas low complementarity results in the inhibition of its translation [255].

Several miRNAs that target P53 have been identified, including miRNA-125 [346]. This specific miRNA was shown to be upregulated in prostate cancer cells [347] and myeloid leukemia [348]. In human cells as well as zebrafish embryos, miRNA-125 was able to bind to the P53 mRNA and inhibit its translation, possibly contributing to tumorigenesis [346]. Moreover, in prostate cancer cells with elevated miRNA-125 levels, inhibition of P53 was shown to result in increased growth [347]. It was found that the mRNA coding for apoptotic protein BAK contained a binding site for miRNA-125, which was confirmed by decreased BAK protein levels after ectopic expression of miRNA-125[347]. A similar mechanism was demonstrated for miRNA-24 in hepatocellular carcinoma, which was shown to target P53, and elevated miRNA-24 levels resulted in increased invasiveness [349].

Conversely, other miRNAs have been shown to increase P53 signaling through inhibition of P53 inhibitors such as MDM2 [350,351]. For example, the downregulation of miRNA-339-5p (hereafter miRNA-339) was observed in colorectal cancer [352] and breast cancer [353], and it was later demonstrated that this miRNA was able to bind the 3' UTR of MDM2 mRNA in human colorectal cancer cells [350]. Both mRNA and protein levels of MDM2 are decreased when miRNA-339 is elevated, suggesting high complementarity. Moreover, through the activation of P53, miRNA-339 was demonstrated to suppress the migration and invasion of colorectal cancer cells [350]. Additionally, miRNA-1827 was

also shown to bind MDM2 mRNA, and elevated expression resulted in senescence and apoptosis [351].

MiRNAs can also be present within a cluster in the genome such as the miRNA-371a, -372, -373, and -373* cluster. In human fibroblasts with overactivated RAS, elevated expression of miRNA-372 and -3 resulted in continued proliferation, which was more pronounced compared to *TP53* knockdown [56]. Moreover, miRNA 372 and -3 were found to be highly expressed in testicular GCTs and GCT cell lines that harbored WT *TP53* [56]. It was further hypothesized that miRNA-372 and 3 are able to inactivate P53 through translational inhibition of MDM2 inhibitory protein LATS2 [56]. It was also recently demonstrated that murine miRNA-291a-3p (the murine homolog for miRNA-371a) inhibited senescence in human dermal fibroblasts by targeting several components of the P53 pathway [354]. Moreover, the human miRNA-371a-3p demonstrated similar anti-senescence activity, suggesting that all miRNA members of this cluster may have similar functions involved in inactivating the P53 pathway [354]. In addition, this specific miRNA cluster may soon function as a biomarker for GCTs [57–59].

CTCF

An important tumor suppressor that is involved in epigenetic regulation is CCCTC-binding factor (CTCF) [355]. In chickens, CTCF was first found to bind CCCTC-sites in the oncogene *c-myc* and repress its expression [356], which was later also demonstrated in mammalian cells [357]. CTCF has 11 zinc-fingers within its DNA binding domain [358]; however, these are not all involved during every DNA-binding event [359,360]. Rather, multiple combinations are possible due to this large number of zinc-fingers, which enables CTCF to bind to approximately 125,000 cell type-specific, either inter- or intragenic or at the promotor [361]. CTCF is also essential during embryonic development as CTCF-null are non-viable [362]. This protein requires several post-translational modifications to function, including sumoylation by SUMO proteins [363] and poly(ADP-ribosyl)ation by PARP [364].

The hemizygous deletion of CTCF, which occurs more frequently than homozygous deletion, increased the susceptibility of spontaneous and radiation and chemically induced tumorigenesis [365]. Loss of the locus that contains the *CTCF* gene is frequently detected in breast and prostate cancer, which underlines its tumor suppressor activity [366]. *TP53* is one of the genes with a CTCF binding site in its promotor, and CTCF binding has been shown to obstruct histone methylation, which maintains an open chromatin structure and enables *TP53* transcription [367]. The *INK4* locus is also regulated by CTCF, as loss of CTCF increased the methylation and decreased the expression of CDKi P16 [368]. It was further demonstrated that CTCF can bind and repress *c-myc* expression, which in addition to inhibiting P16 and enabling *TP53* expression, further demonstrates its tumor suppressive role.

Additionally, CTCF has also been suggested to have oncogenic potential, as increased expression was related to tumorigenesis within several breast cancer cell lines and tumor samples [369]. It has been hypothesized that CTCF could enhance tumorigenesis through the inhibition of pro-apoptotic protein BAX, which was increased after CTCF knockdown in breast cancer cell lines [370]. P53-levels were also elevated after CTCF knockdown in the same breast cancer cell line, resulting in increased cell cycle arrest and apoptosis [371].

SUMMARIZING DISCUSSION

This review focuses on the P53 pathway as a guardian of the genome in cell types ranging from ES cells to somatic cells and describes different mechanisms that lead its inactivation and tumorigenesis (summarized in Figure 7). In response to cellular stress such as DNA damage, the P53 pathway is activated and initiates a plethora of downstream signaling pathways that ensure and maintain genomic integrity. For instance, P21 is a renowned downstream target that is involved in cell cycle arrest and cellular senescence [55,69,72]. In addition, autophagy and apoptosis can also be initiated to limit the damage [83]. It has been hypothesized that nearly all solid cancers harbor a disrupted P53 pathway, either directly through inactivating *TP53* mutations (occurring in roughly 50% of all tumors) or indirectly through alternative mechanisms such as described in this review [50,372]. An interesting exception to this pertains to GCTs in which *TP53* mutations rarely occur [33,35,36].

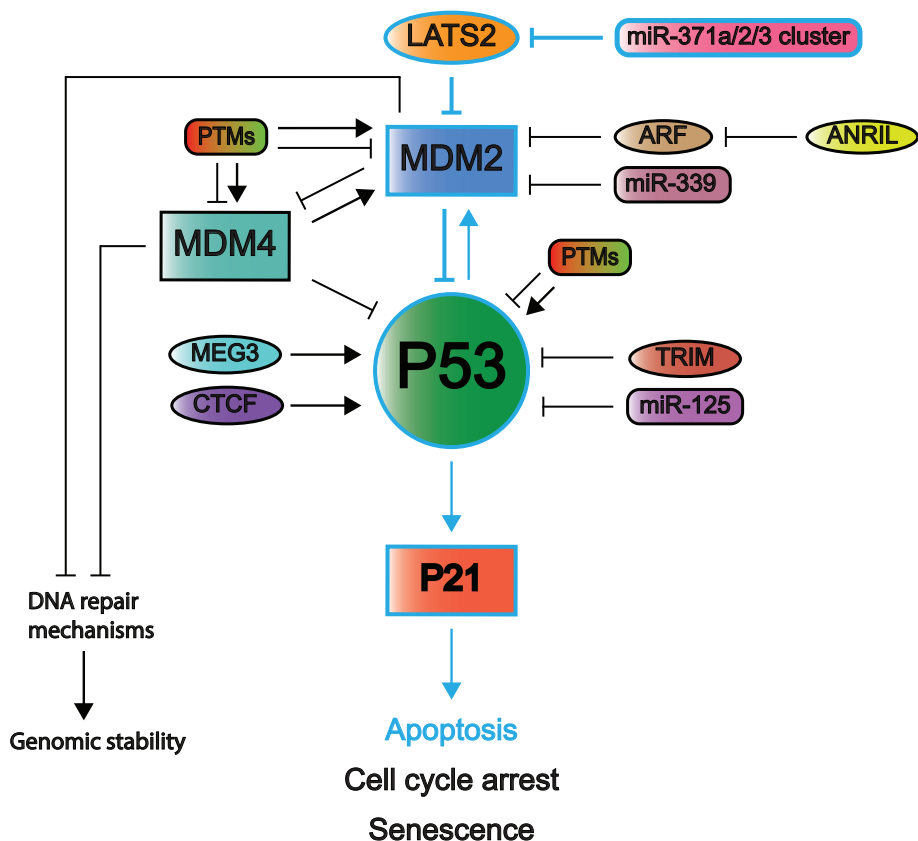


Figure 7. The regulatory mechanisms of the P53 pathway. P53 is regulated by MDM2 and MDM4, which are all affected by the PTMs and are also determining each other's activity. MDM2 is indirectly activated by miR-cluster 371a-3 and ANRIL, while it is inhibited by ARF and miR-339. MEG3, CTCF, TRIM proteins, and miR-125 can regulate P53 activity directly. All these regulatory mechanisms combined will lead to the inhibition or activation of P21 expression, leading to apoptosis, cell cycle arrest, or senescence. MDM2 and MDM4 are both able to inhibit DNA repair mechanisms, resulting in genomic instability.

Regarding *TP53*, SNPs and other mutations and multiple isoforms have been demonstrated to increase tumor susceptibility. Moreover, multiple P53 isoforms resulting from alternative splicing have been identified, most of which are truncated at the N-terminus, and these have also been associated with tumorigenesis [139]. For instance, isoform is capable of binding and inactivating full-length WT P53 in a dominant-negative manner [57]. Moreover, due to a modified DBD, this isoform has been shown to transactivate oncogenes in human glioblastoma cells; however, this may be tumor-specific, as the opposite was observed in ovarian cancers where the expression of this isoform correlated to increased survival rates [143,144].

The activity of full-length P53 is also regulated by extensive PTM patterns, including methylation, phosphorylation, acetylation, and sumoylation, which are also known to engage in cross-talk, as shown in Figure 6 [150]. Whereas some *TP53* mutations have been found to obstruct multiple PTMs, other mutations may result in new modifiable residues [149]. These PTM patterns can also change by increased or decreased expression of the enzymes effectuating these modifications, which has been demonstrated by P53's main E3 ubiquitin ligase MDM2 [191,199,204].

P53 activity is also strongly determined by its negative regulators such as MDM2. Elevated MDM2 levels have been shown to contribute to tumorigenesis through the increased degradation of P53 and tend to occur in a mutually exclusive manner with *TP53* mutations [168–170]. MDM2 levels can be increased through *MDM2* amplification but also through SNPs within its promoter [188,206]. For example, SNP309 is known to increase *MDM2* expression, as it enhances the affinity of transcription factor SP1 for the *MDM2* promoter. However, the effect of this SNP can be counteracted by the SNP285 SNP, which has been observed in ovarian and breast cancer [211]. SNP285 was demonstrated to be significantly higher expressed in Caucasians compared to Asian populations and may explain the stronger correlation between SNP309 and tumorigenesis in Asian populations [206,210]. However, a study within a Caucasian sample group showed a causative relation between SNP309 and earlier onset of prostate cancer [208]. Thus, further investigation is required to fully understand the co-occurrence of SNP309 and SNP285 in relation to cancer.

In addition, MDM2 activity is determined by a combination of PTMs, including phosphorylation and acetylation which, depending on the specific residues, either repress or enhance its activity [220,221]. Moreover, MDM2 can be degraded through ubiquitination and can also engage in auto-ubiquitination; however, the outcome of the latter remains controversial, as it has both been demonstrated to activate and degrade MDM2 [123–125]. It would be of interest to investigate whether the lysine residues subjected to auto-ubiquitination are similar to those subjected to ubiquitination by other enzymes.

A final mechanism that determines MDM2 activity is ribosomal proteins, which bind and inhibit MDM2 in response to cellular stress signals [225]. It would be expected that decreased levels of these ribosomal proteins could contribute to tumorigenesis due to enhanced MDM2-mediated P53 degradation. However, several cancers demonstrate an increased level of ribosomal proteins [228,229]. This is likely confounded by the fast proliferation rate of cancer cells, which also requires high levels of ribosomal proteins [228]. However, a predisposition to tumorigenesis has been seen within conditions with a malfunctioning ribosomal protein modification [373]. These ribosomal proteins could be obstructed of their interaction with MDM2, resulting in the activation of P53.

MDM4 is another important negative regulator of P53, and its overexpression has been observed in multiple cancers [233,243–245]. Its overexpression as well as increased

expression of the transcription factors that regulate its expression is mostly caused by gene amplification. Similar to MDM2 and P53, MDM4 also has an isoform frequently occurring in tumors, Mdm4-S, where exon 6 is excluded from the protein [246]. It has been demonstrated to be highly expressed in B-cell leukemia, for which it may potentially serve as a biomarker [258]. Although Mdm4-S is prone to nonsense-mediated decay, its degradation is obstructed in B-lymphocytes, which leads to elevated levels of this isoform [258,374]. This has been suggested to be the result of increased *c-myc* expression, which is overexpressed through amplification in many tumors [374,375]. Conversely, other cancers have been shown to demonstrate higher levels of full-length Mdm4 compared to Mdm4-S, resulting in stronger P53 degradation [246]. This in turn could be the result of increased expression of the Srsf3 enzyme, which is responsible for the inclusion of exon 6 and was also demonstrated to be overexpressed in multiple tumors [376,377].

A final means to regulate MDM4 is through MDM2-mediated ubiquitination, which in turn is stimulated by the binding of ARF [262]. ARF is frequently lost in cancer, leading to the stabilization of MDM4 and thus the repression of P53 [262]. Loss of ARF also results in the activation of MDM2; however, it appears to obstruct MDM2-mediated P53 degradation, which decreases P53 levels [292,299]. Thus, ARF both appears to stimulate MDM2-mediated MDM4 ubiquitination (and thus P53 activation), yet it obstructs MDM2-mediated P53 ubiquitination [262,299]. This suggests that ARF facilitates the binding of MDM2 to MDM4, which reduces the number of free MDM2 protein that can bind and inhibit P53. This may be explained by the ARF binding site on the MDM2 protein. ARF binds to the N-terminal of MDM2, which is also required for P53 binding; however, the RING-finger domains in the C-terminus of MDM2 remain unobstructed, enabling MDM2 to bind to MDM4 [187,240]. Moreover, in contrast to a loss of ARF, overexpression of ARF has also been detected in tumors, which in mice and prostate cancer cells was demonstrated to increase the invasiveness of cells [314,315]. Notably, the murine study that associated *P19^{Arf}* overexpression with increased invasiveness was performed in a P53-null background and therefore does not conclusively demonstrate the tumor suppressive roles of *P19^{Arf}*. Moreover, *P19^{Arf}* shares 50% sequence homology to human ARF, which further complicates their findings [293].

In addition to MDM2 and MDM4, another group of E3 ubiquitin ligase proteins known as tripartite motif proteins (TRIMs) were recently discovered to negatively regulate P53 [318,322]. TRIM23, TRIM32, and TRIM59 contribute to tumorigenesis when highly expressed, which is thought to be caused by inducing proliferation through multiple signaling pathways including the P53 pathway. For example, TRIM59 was overexpressed in gastric cancers and was suggested to inhibit the P53 pathway as the expression P53 targets including P21 was decreased [321]. In colorectal cancer and cholangiocarcinoma, TRIM59 was shown to promote proliferation, but this was thought to be through the PI3K/AKT or PI3K/AKT/mTOR signaling pathway, respectively [327,329]. It has been previously

described that the PI3K/AKT pathway is able to induce P21 expression in ovarian carcinoma cells [378], which suggests that TRIM59 also has P53-independent functions.

Long non-coding RNAs are also known to regulate gene expression, and several may be indirectly involved in regulating the P53 pathway. For example, ANRIL and ARF are transcribed from the same locus, and the former was shown to decrease expression of the latter [338]. ANRIL-mediated inhibition of ARF subsequently results in higher levels of MDM2, which may lead to decreased P53 levels. This hypothesis was supported by the findings in prostate cancer where increased ANRIL levels resulted in lower activity of the P53 pathway [337]. Notably, the involvement of ANRIL in cancer may be context-dependent, as a specific SNP in melanoma was found to downregulate ANRIL expression, whereas a different ANRIL mutation was found to increase its expression in glioma [339]. Thus, the contributions of ANRIL to tumorigenesis are still debatable and require further attention. MEG3 is a second lncRNA that is often downregulated in cancer. In pituitary tumors and breast cancer, MEG3 downregulation was associated with a decrease in P53 activity [334,379].

Additionally, several miRNAs have been found to be overexpressed in tumors, which may disrupt the P53 pathway through P53 downregulation as well as through MDM2 overexpression [347,351]. For instance, P53 and the pro-apoptotic protein BAK contain a miRNA-125 binding site, which suggests that this miRNA has an anti-apoptotic function [347]. Additionally, in WT P53 expressing GCTs, it was demonstrated that MDM2 activity can be regulated by the miRNA 371-3 cluster by downstream inhibition of LATS2 (an MDM2 inhibitor) thereby indirectly inhibiting P53 [56].

The final P53 regulator discussed in this review is the CCCTF-binding factor CTCF which maintains an open chromatin structure at the *TP53* locus, thus enabling expression [367].

Further evidence regarding its tumor suppressive function was demonstrated by the discovery that CDK1 *P16* is also under transcriptional control of CTCF [368]. *ARF* may also be regulated by CTCF, as it lies within the same locus as *P16*. Conversely, CTCF may also function as an oncogene, as CTCF knockdown resulted in an increased expression of P53 or the pro-apoptotic protein BAX in WT and mutant P53 breast cancer cell lines, respectively, which both increased apoptosis [370,371]. Moreover, CTCF is thought to repress *TP53* expression by inhibiting RNA polymerase II at the promotor [371]. However, it had been previously shown that CTCF interacts with RNA polymerase II to increase gene expression [380], which shows that the regulatory function of CTCF necessitates further investigation. In addition to the aforementioned mechanisms, it has been demonstrated that the P53 pathway may also be disrupted through aberrations of the P53 target P21. *CDKN1A* was initially proposed as a tumor suppressor gene for its role in cell cycle arrest. Therefore, it is unsurprising that decreased expression or loss of *CDKN1A* in combination with the loss of a second tumor suppressor gene or activated oncogene

has been observed in multiple tumors [283,284]. However, as increased P21 levels have also been observed in multiple tumor types, there is growing evidence that P21 may also paradoxically function as an oncogene, which may be localization, cell type- and context-dependent, as well as related to the P53 status [264–266,275].

The main functions of these regulators have been elucidated; however, important questions remain to be answered to gain a complete understanding of their underlying mechanisms and their potential contribution to tumorigenesis. For instance, MDM2 contains two frequently occurring SNPs: SNP309, which increases its expression, and SNP285, which compensates for the effects of the former SNP [210]. The frequency of these SNPs differs among Asian and Caucasian populations, and further investigation into their individual and combined effects could provide further insights into their contribution to tumorigenesis. Furthermore, the involvement of the MDM4 isoform MDM4-S also provokes unanswered questions. On one hand, high MDM4-S levels are thought to be a result of *c-myc* overexpression followed by blocked nonsense-mediated decay [258,375]. In contrast, other tumors demonstrate upregulation of *Srsf3*, resulting in more Mdm4 compared to Mdm4-S [246,376]. Therefore, a deeper understanding of MDM4-S regulation is required to understand its contribution to tumorigenesis. Additionally, ARF-mediated MDM2 regulation is still largely unclear, as MDM4 is still ubiquitinated by ARF-bound MDM2, whereas MDM2-mediated P53 degradation is inhibited. In addition, lncRNAs have been shown to contribute to tumorigenesis; however, the exact pathways through which they elicit this effect remain debatable, as was demonstrated for MEG3 [381]. Finally, CTCF is thought to keep an open chromatin structure at the *TP53* locus and stimulate RNA Polymerase II required for gene transcription [367,380]. However, knockdown of CTCF has also been shown to increase P53 expression [370,371]. As a final note, it is most likely that the combination of the regulatory proteins and molecules are required to determine the outcome of P53 pathway activity and that multiple, as depicted in Figure 7. Notably, as an abundance of mechanisms that deregulate the P53 pathway has been observed in both somatic cells and cancers, including P53 mutations, many studies are dedicated to identify novel targets that can restore this pathway and function as potential new cancer treatments. An overview of ongoing clinical trials regarding these types of approaches is summarized in Table 1.

Table 1. Ongoing clinical trials regarding novel targeting agents that modulate the P53 pathway.

Targeting Agents	Mechanism(s)	NCT Number
<i>Phase I</i>		
Vaccine therapy (i.e., gene therapy)	Virus-based adaption of <i>P53</i> expression in cancerous cells, mostly combined with chemotherapeutics	P53MVA: NCT02275039 Ad5CMVP53: NCT00004225
APR-246	A small molecule that binds mutant P53 and aids in folding to restore its wild-type conformation	NCT02098343
AMG-232 (KRT-232)	A small molecule that inhibits MDM2 and thereby activates P53	NCT03217266
ALRN-6924	A peptide that binds MDM2 and MDM4 to activate WT P53 in noncancerous cells, thus preventing side effects while enhancing chemotherapy effects in cancer cells.	NCT02264613
<i>Phase I/II</i>		
APG-115	MDM2 inhibitor that activates WT P53 with and without platinum-based chemotherapeutics	NCT03781986

In light of ES and somatic cells, it is evident that the P53 pathway is integral for ensuring genomic integrity; however, the subsequent downstream effects of this pathway are differentially regulated between these cell types. As mentioned before, somatic cells employ the P53 pathway to first induce cell cycle arrest and a DNA damage response (both error-free and -prone) to remain viable with the potential risk of accumulating harmful mutations, and they only initiate P53-mediated apoptosis when the damage cannot be repaired sufficiently [9,60,72]. In contrast, embryonic stem (ES) cells preferentially induce P53-mediated apoptosis as a failsafe mechanism to protect its multitude of cellular progeny and initiate a DNA damage response (mostly through error-free HR) only in a select few cases [9,10,23]. Similarly, GCTs contain many (epi)genetic and behavioral features that reflect their cells of origin, the ES cells and PGCs, and appear to initiate apoptosis in response to DNA damage, which is thought to explain their unique sensitivity to chemotherapeutics such as cisplatin [3,10,18]. To reiterate, teratomas are an exception to this rule, which is most likely due to their differentiated phenotype, rendering these tumors more comparable to somatic cells [3,15–17]. In GCTs, the preference to induce apoptosis has also been attributed to the P53 pathway, which as GCTs often have high WT *TP53* and *NOXA* expression concomitant with low expression of *CDKN1A* and other CDK inhibitors [18,21,23–29,33–37]. The low expression of other CDK inhibitors have also been observed in GCTs, which together with low P21 expression suggests a deregulated G1-S phase checkpoint reminiscent of ESCs, which are characterized by a short G1 phase [8,10,19–21,27]. Moreover, high *NOXA* and low *CDKN1A* expression may also be caused

by the pluripotency marker OCT3/4, which is highly expressed in GCTs and their cells of origin and has been shown to augment the pro-apoptotic function of the P53 pathway through the indirect downregulation of *CDKN1A* and upregulation of *NOXA* [382,383]. Thus, these observations combined suggest that GCTs, similar to ES cells, may be biased toward P53-mediated apoptosis rather than attempting to repair the acquired damage.

In addition, despite the curative success of GCTs due to their sensitivity to chemotherapeutics such as cisplatin, GCTs may acquire resistance which, with the lack of targeted treatment, is inherently difficult to treat and exemplifies a significant shortcoming in current GCT treatment [384]. Thus, a significant proportion of GCT research aims to identify the underlying cause of GCT resistance, and it has been suggested that the deregulation of the P53 pathway may be a contributing factor [15,18,39,40,42]. Correspondingly, multiple mechanisms of P53 pathway deregulation have been observed in GCTs including rare *TP53* mutations and elevated P21, MDM2, and/or MDM4 levels, which have also been associated with resistance to cisplatin [22,27,34,37,39,385]. Furthermore, albeit that *TP53* mutations are rare in GCTs, an enlightening unbiased retrospective study of 180 GCTs was performed, and multiple P53 and MDM2 aberrations were observed in a subset of patients with aggressive and cisplatin-resistant GCTs [38]. This is further supported by the observation that disruption of the MDM2–p53 complex with a small molecule MDM2 inhibitor (Nutlin-3) resulted in the induction of P53 and increased cisplatin sensitivity in GCT cell lines that express WT *TP53* [28,41,203]. Additionally, as mentioned before, the miRNA-371a to -373* cluster has been found to be highly expressed in GCTs with WT P53 and have been shown to function as oncogenes by indirectly inhibiting P53 through the degradation of *LATS2*, which prevents it from inhibiting MDM2 [56]. Both this miRNA cluster and the elevated MDM2 and MDM4 levels suggest that while *TP53* mutations are rare, alternative mechanisms may be at play to deregulate the P53 pathway which may ultimately contribute to GCT cisplatin resistance. Furthermore, elevated P21 expression has also been associated with GCT cisplatin resistance; however, P21 appeared to be localized to the cytoplasm and was most likely regulated in a P53-independent manner [39]. It was further demonstrated that the cytoplasmic localization enabled P21 to inhibit apoptosis through protein–protein interactions with pro-apoptotic proteins, which again highlights that P21 may function as both an oncogene (or in this case contributes to the resistance phenotype) and a tumor suppressor which is most likely determined by many factors including subcellular localization [39,264,274,275]. Thus, whereas the P53 pathway may be deregulated, P21 expression may still be induced through P53-independent mechanisms with potentially oncogenic effects. Lastly, although not currently investigated in GCTs, elevated P21 expression levels also appear to dictate the DNA damage repair landscape, resulting in the use of error-prone DNA repair pathways that consequently contribute to genomic instability, and it would be of further interest to investigate this in GCTs [265,266]. It

remains to be determined whether this also applies to GCTs, which, as mentioned before, are normally known to induce apoptosis rather than initiate DNA repair.

Nevertheless, the observations regarding the P53 pathway in GCTs thus far suggest that the transition from sensitive to (cisplatin)-resistant GCTs may be accompanied by the deregulation of the P53 pathway, enabling these cells to circumvent the characteristic preference for apoptosis and survive. This may additionally be exacerbated by the acquired ability to engage in cell cycle arrest and DNA repair.

In summary, the activity of the P53 pathway is dictated by a myriad of regulating factors that form an elaborate and complex network. This review describes several of these factors and how they correlate to tumorigenesis through the disruption of the P53 pathway. Many aspects of these factors remain elusive and require further investigation to fully understand their contributions to tumorigenesis in general. Additionally, the involvement of the P53 pathway specifically in GCTs remains incompletely understood, and several of the mechanisms that regulate this pathway that have been described in this review may also be implicated in this specific context, which warrants further investigation. Moreover, due to the similarities between GCTs and ES cells, it may be of particular interest to further investigate the regulation of the P53 pathway in these cells and to further elucidate how this differs from somatic cells, which in turn may aid in understanding the involvement of this pathway in both the pathogenesis and acquired chemotherapeutic resistance in GCTs. Finally, further investigation into the complexity of the regulation of the P53 pathway in both ES and somatic cells may aid in the identification of new targets, the design of new studies, and ultimately new treatment options for multiple cancer types, including GCTs.

Author Contributions: The study design was done by D.M.T. and L.H.J.L. Literature search and analysis was done by T.L.R. The work was finalized and critically reviewed by D.M.T., L.H.J.L., T.L.R. and S.H. All authors have read and agreed to the published version of the manuscript.

Funding: This research received no external funding.

Acknowledgments: The work was financially supported by the Princess Maxima Center for Pediatric Oncology, including a dedicated grant on the role of microRNA, treatment sensitivity and differentiation.

Conflicts of Interest: The authors declare no conflict of interest.

REFERENCES

1. Juan, H.-C.; Lin, Y.; Chen, H.-R.; Fann, M.-J. Cdk12 is essential for embryonic development and the maintenance of genomic stability. *Cell Death Differ.* **2016**, *23*, 1038–1048, doi:10.1038/cdd.2015.157.
2. Kobayashi, T.; Surani, M.A. On the origin of the human germline. *Development* **2018**, *145*, doi:10.1242/dev.150433.
3. Oosterhuis, J.W.; Looijenga, L.H.J. Human germ cell tumours from a developmental perspective. *Nat. Rev. Cancer* **2019**, *19*, 522–537, doi:10.1038/s41568-019-0178-9.
4. Dvash, T.; Ben-Yosef, D.; Eiges, R. Human Embryonic Stem Cells as a Powerful Tool for Studying Human Embryogenesis. *Pediatr. Res.* **2006**, *60*, doi:10.1203/01.pdr.0000228349.24676.17.
5. Vazin, T.; Freed, W.J. Human embryonic stem cells: Derivation, culture, and differentiation: A review. *Restor. Neurol. Neurosci.* **2010**, *28*, 589–603, doi:10.3233/RNN-2010-0543.
6. Wright, W.E.; Piatyszek, M.A.; Rainey, W.E.; Byrd, W.; Shay, J.W. Telomerase activity in human germline and embryonic tissues and cells. *Dev. Genet.* **1996**, *18*, 173–179, doi:10.1002/(SICI)1520-6408(1996)18:2<173::AID-DVG10>3.0.CO;2-3.
7. Liu, L.; Bailey, S.M.; Okuka, M.; Muñoz, P.; Li, C.; Zhou, L.; Wu, C.; Czerwicz, E.; Sandler, L.; Seyfang, A.; et al. Telomere lengthening early in development. *Nat. Cell Biol.* **2007**, *9*, doi:10.1038/ncb1664.
8. Liu, L.; Michowski, W.; Kołodziejczyk, A.; Sicinski, P. The cell cycle in stem cell proliferation, pluripotency and differentiation. *Nat. Cell Biol.* **2019**, *21*, 1060–1067, doi:10.1038/s41556-019-0384-4.
9. Bloom, J.C.; Loehr, A.R.; Schimenti, J.C.; Weiss, R.S. Germline genome protection: Implications for gamete quality and germ cell tumorigenesis. *Andrology* **2019**, *7*, andr.12651, doi:10.1111/andr.12651.
10. Fillion, T.M.; Qiao, M.; Ghule, P.N.; Mandeville, M.; Van Wijnen, A.J.; Stein, J.L.; Lian, J.B.; Altieri, D.C.; Stein, G.S. Survival Responses of Human Embryonic Stem Cells to DNA Damage. *J. Cell. Physiol.* **2009**, *220*, 586–592, doi:10.1002/jcp.21735.
11. Magnúsdóttir, E.; Gillich, A.; Grabole, N.; Surani, M.A. Combinatorial control of cell fate and reprogramming in the mammalian germline. *Curr. Opin. Genet. Dev.* **2012**, *22*, 466–474, doi:10.1016/j.gde.2012.06.002.
12. Greenberg, M.V.C.; Bourchis, D. The diverse roles of DNA methylation in mammalian development and disease. *Nature* **2019**, *20*, doi:10.1038/s41580-019-0159-6.
13. Takahashi, K.; Tanabe, K.; Ohnuki, M.; Narita, M.; Ichisaka, T.; Tomoda, K.; Yamanaka, S. Induction of Pluripotent Stem Cells from Adult Human Fibroblasts by Defined Factors. *Cell* **2007**, *131*, 861–872, doi:10.1016/j.cell.2007.11.019.
14. González, F.; Boué, S.; Carlos Izpisua Belmonte, J. Methods for making induced pluripotent stem cells: Reprogramming à la carte. *Nat. Publ. Gr.* **2011**, doi:10.1038/nrg2937.
15. Singh, R.; Fazal, Z.; Freemantle, S.J.; Spinella, M.J. Mechanisms of cisplatin sensitivity and resistance in testicular germ cell tumors HHS Public Access. *Cancer Drug Resist.* **2019**, *2*, 580–594, doi:10.20517/cdr.2019.19.
16. Van Echten, J.; Sleijfer, D.T.; Wiersema, J.; Schraffordt Koops, H.; Oosterhuis, J.W.; De Jong, B. Cytogenetics of Primary Testicular Nonseminoma, Residual Mature Teratoma, and Growing Teratoma Lesion in Individual Patients. *Cancer Genet. Cytogenet* **1997**, *96*, 1–6.
17. Van Echten, J.; Van Der Vloedt, W.S.; Sleijfer, D.T.; Oosterhuis, J.W.; De Jong, B. Comparison of the Chromosomal Pattern of Primary Testicular Nonseminomas and Residual Mature Teratomas after Chemotherapy. *Cancer Genet. Cytogenet* **1997**, *99*, 59–67.

18. Jacobsen, C.; Honecker, F. Cisplatin resistance in germ cell tumours : Models and mechanisms. *Andrology* **2015**, *3*, 111–121, doi:10.1111/andr.299.
19. Bártková, J.; Rajpert-de Meyts, E.; Skakkebaek, N.E.; Lukas, J.; Bartek, J.; Meyts, R.-D.E. Deregulation of the G1/S-phase control in human testicular germ cell tumours. *APMIS* **2003**, *111*, 252–266.
20. Bártková, J.; Thullberg, M.; Rajpert-De Meyts, E.; Skakkebaek, N.E.; Bartek, J. Cell cycle regulators in testicular cancer: Loss of P18INK4c marks progression from carcinoma in situ to invasive germ cell tumours. *Int. J. Cancer* **2000**, *85*, 370–375.
21. Romano, F.J.; Rossetti, S.; Conteduca, V.; Schepisi, G.; Cavaliere, C.; Di Franco, R.; La Mantia, E.; Castaldo, L.; Nocerino, F.; Ametrano, G.; et al. Role of DNA repair machinery and p53 in the testicular germ cell cancer: A review. *Oncotarget* **2016**, *7*, 85641–85649, doi:10.18632/oncotarget.13063.
22. Spierings, D.C.; Ge De Vries, E.; Stel, A.J.; Te Rietstap, N.; Vellenga, E.; De Jong, S. Low p21 Waf1/Cip1 protein level sensitizes testicular germ cell tumor cells to Fas-mediated apoptosis. *Oncogene* **2004**, *23*, 4862–4872, doi:10.1038/sj.onc.1207617.
23. Hong, Y.; Cervantes, R.B.; Tichy, E.; Tischfield, J.A.; Stambrook, P.J. Protecting genomic integrity in somatic cells and embryonic stem cells. *Mutat. Res.* **2007**, *614*, 48–55, doi:10.1016/j.mrfmmm.2006.06.006.
24. Datta, M.W.; Macri, E.; Signoretti, S.; Renshaw, A.A.; Loda, M. Transition from In Situ to Invasive Testicular Germ Cell Neoplasia is Associated with the Loss of p21 and Gain of mdm-2 Expression. *Mod. Pathol.* **2001**, *14*, 437–442.
25. Kerley-Hamilton, J.S.; Pike, A.M.; Li, N.; Drenzo, J.; Spinella, M.J. A p53-dominant transcriptional response to cisplatin in testicular germ cell tumor-derived human embryonal carcinoma. *Oncogene* **2005**, *24*, 6090–6100, doi:10.1038/sj.onc.1208755.
26. Spierings, D.; De Vries, E.; Vellenga, E.; De Jong, S. Loss of drug-induced activation of the CD95 apoptotic pathway in a cisplatin-resistant testicular germ cell tumor cell line. *Cell Death Differ.* **2003**, *10*, 808–822, doi:10.1038/sj.cdd.4401248.
27. Spierings, D.C.; Ge De Vries, E.; Vellenga, E.; De Jong, S. The attractive Achilles heel of germ cell tumours: An inherent sensitivity to apoptosis-inducing stimuli. *J. Pathol.* **2003**, *200*, 137–148, doi:10.1002/path.1373.
28. Gutekunst, M.; Oren, M.; Weilbacher, A.; Dengler, M.A.; Markwardt, C.; Thomale, J.; Aulitzky, W.E.; van der Kuip, H. P53 hypersensitivity is the predominant mechanism of the unique responsiveness of testicular germ cell tumor (TGCT) cells to Cisplatin. *PLoS ONE* **2011**, *6*, doi:10.1371/journal.pone.0019198.
29. Bártková, J.; Bártek, J.; Lukáš, J.; Vojtěšek, B.; Stašková, Z.; Rejthar, A.; Kovařík, J.; Midgley, C.A.; Lane, D.P. p53 Protein alterations in human testicular cancer including pre-invasive intratubular germ-cell neoplasia. *Int. J. Cancer* **1991**, *49*, 196–202, doi:10.1002/ijc.2910490209.
30. Burger, H.; Nooter, K.; Boersma, A.W.M.; Kortland, C.J.; Stoter, G. Lack of correlation between cisplatin-induced apoptosis, p53 status and expression of Bcl-2 family proteins in testicular germ cell tumour cell lines. *Int. J. Cancer* **1997**, *73*, 592–599.
31. Burger, H.; Nooter, K.; Boersma, A.W.M.; Wingerden, K.E. van; Looijenga, L.H.J.; Jochemsen, A.G.; Stoter, G. Distinct p53-independent apoptotic cell death signalling pathways in testicular germ cell tumour cell lines. *Int. J. Cancer* **1999**, *628*, 620–628.
32. Kersemaekers, A.M.F.; Mayer, F.; Molier, M.; Van Weeren, P.C.; Oosterhuis, J.W.; Bokemeyer, C.; Looijenga, L.H.J. Role of P53 and MDM2 in treatment response of human germ cell tumors. *J. Clin. Oncol.* **2002**, *20*, 1551–1561, doi:10.1200/JCO.20.6.1551.

33. Ulbright, T.M.; Orazi, A.; de Riese, W.; de Riese, C.; Messemer, J.E.; Foster, R.S.; Donohue, J.P.; Eble, J.N. The correlation of P53 protein expression with proliferative activity and occult metastases in clinical stage I non-seminomatous germ cell tumors of the testis. *Mod. Pathol.* **1994**, *7*, 64–68.
34. Riou, G.; Barrois, M.; Prost, S.; Terrier, M.J.; Theodore, C.; Levine, A.J. The p53 and mdm-2 genes in human testicular germ-cell tumors. *Mol. Carcinog.* **1995**, *12*, 124–131, doi:10.1002/mc.2940120303.
35. Schenkman, N.S.; Sesterhenn, I.A.; Washington, L.; Weghorst, C.M.; Buzard, G.S.; Srnastava, S.; Moul, J.W.; PRIIDyn, B. Increased p53 protein does not correlate to p53 gene mutations in microdissected human testicular germ cell tumors. *J. Urol.* **1995**, *154*, 617–621.
36. Guillou, L.; Estreicher, A.; Chaubert, P.; Hurlimann, J.; Kurt, A.-M.; Mettetz, G.; Iggo, R.; Gray, A.C.; Jichlinski, P.; Leisinger, H.-J.; et al. Germ cell tumors of the testis overexpress Wild-Type P53. *Am. J. Pathol.* **1996**, *149*, 1221–1228.
37. Lutzker, S.G. P53 tumour suppressor gene and germ cell neoplasia. *APMIS* **1998**, *106*, 85–89, doi:10.1111/j.1699-0463.1998.tb01323.x.
38. Bagrodia, A.; Lee, B.H.; Lee, W.; Cha, E.K.; Sfakianos, J.P.; Iyer, G.; Pietzak, E.J.; Gao, S.P.; Zabor, E.C.; Ostrovskaya, I.; et al. Genetic determinants of cisplatin resistance in patients with advanced germ cell tumors. *J. Clin. Oncol.* **2016**, *34*, 4000–4007, doi:10.1200/JCO.2016.68.7798.
39. Koster, R.; Di Pietro, A.; Timmer-Bosscha, H.; Gibcus, J.H.; Van Den Berg, A.; Suurmeijer, A.J.; Bischoff, R.; Gietema, J.A.; De Jong, S. Cytoplasmic p21 expression levels determine cisplatin resistance in human testicular cancer. *J. Clin. Invest.* **2010**, *120*, doi:10.1172/JCI41939DS1.
40. Koster, R.; van Vugt, M.A.; Timmer-Bosscha, H.; Gietema, J.A.; de Jong, S. Unravelling mechanisms of cisplatin sensitivity and resistance in testicular cancer. *Expert Rev. Mol. Med.* **2013**, *15*, 2013, doi:10.1017/erm.2013.13.
41. Koster, R.; Timmer-Bosscha, H.; Bischoff, R.; Gietema, J.A.; De Jong, S. Disruption of the MDM2-p53 interaction strongly potentiates p53-dependent apoptosis in cisplatin-resistant human testicular carcinoma cells via the Fas/FasL pathway. *Cell Death Dis.* **2011**, *2*, doi:10.1038/cddis.2011.33.
42. Lobo, J.; Alzamora, M.A.; Guimarães, R.; Cantante, M.; Lopes, P.; Braga, I.; Maurício, J.; Jerónimo, C.; Henrique, R. p53 and MDM2 expression in primary and metastatic testicular germ cell tumors: Association with clinical outcome. *Andrology* **2020**, *8*, 1233–1242, doi:10.1111/andr.12814.
43. Ménéz, Y.; Dale, B.; Cohen, M. DNA damage and repair in human oocytes and embryos: A review. *Zygote* **2010**, *18*, 357–365, doi:10.1017/S0967199410000286.
44. Xu, Y. A New Role for p53 in Maintaining Genetic Stability in Embryonic Stem Cells. *Cell Cycle* **2005**, *363*, 363–364, doi:10.1038/ncb1211.
45. Lin, T.; Chao, C.; Saito, I.; JMazur, S.; Murphy, M.E.; Appella, E.; Xu, Y. p53 induces differentiation of mouse embryonic stem cells by suppressing Nanog expression. *Nat. Cell Biol.* **2005**, *7*, 165, doi:10.1038/ncb1211.
46. Maltzman, W.; Czyzyk, L. UV Irradiation Stimulates Levels of p53 Cellular Tumor Antigen in Nontransformed Mouse Cells. *Mol. Cell. Biol.* **1984**, *4*, 1689–1694.
47. Kastan, M.B.; Onyekwere, O.; Sidransky, D.; Vogelstein, B.; Craig, R.W. Participation of p53 Protein in the Cellular Response to DNA Damage1. *Cancer Res.* **1991**, *51*, 6304–6311.
48. Baker, S.J.; Markowitz, S.; Fearon, E.R.; Willson, J.K. V.; Vogelstein, B. Suppression of Human Colorectal Carcinoma Cell Growth by Wild-Type p53. *Science* **1990**, *249*, 912–915.
49. Lane, D.P. Cancer. p53, guardian of the genome. *Nature* **1992**, *358*, 661–663.
50. Greenblatt, M.S.; Bennett, W.P.; Hollstein, M.; Harris, C.C. Mutations in the p53 Tumor Suppressor Gene: Clues to Cancer Etiology and Molecular Pathogenesis. *Cancer Res.* **1994**, *54*, 4855–4878.

51. Vogelstein, B.; Lane, D.; Levine, A.J. Surfing the p53 network. *Nature* **2000**, *408*, 307–310.
52. Schvartzman, J.M.; Duijf, P.H.G.; Sotillo, R.; Coker, C.; Benezra, R. Mad2 is a critical mediator of the chromosome instability observed upon Rb and p53 pathway inhibition. *Cancer Cell* **2011**, *19*, 701–714, doi:10.1016/j.ccr.2011.04.017.
53. Kasthuber, E.R.; Lowe, S.W. Putting p53 in Context. *Cell* **2017**, *170*, doi:10.1016/j.cell.2017.08.028.
54. Beauséjour, C.M.; Krtolica, A.; Galimi, F.; Narita, M.; Lowe, S.W.; Yaswen, P.; Campisi, J. Reversal of human cellular senescence: Roles of the p53 and p16 pathways. *EMBO J.* **2003**, *22*, 4212–4222.
55. Hernandez-Segura, A.; Nehme, J.; Demaria, M. Hallmarks of Cellular Senescence. *Trends Cell Biol.* **2018**, *28*, doi:10.1016/j.tcb.2018.02.001.
56. Voorhoeve, P.M.; Le Sage, C.; Schrier, M.; Gillis, A.J.M.; Stoop, H.; Nagel, R.; Liu, Y.-P.; Van Duijse, J.; Drost, J.; Griekspoor, A.; et al. A Genetic Screen Implicates miRNA-372 and miRNA-373 As Oncogenes in Testicular Germ Cell Tumors. *Cell* **2006**, *124*, 1169–1181, doi:10.1016/j.cell.2006.02.037.
57. Dieckmann, K.-P.; Spiekermann, M.; Balks, T.; Flor, I.; Lö Ning, T.; Bullerdiek, J.; Belge, G. MicroRNAs miR-371-3 in serum as diagnostic tools in the management of testicular germ cell tumours. *Br. J. Cancer* **2012**, *107*, doi:10.1038/bjc.2012.469.
58. Dieckmann, K.P.; Radtke, A.; Spiekermann, M.; Balks, T.; Matthies, C.; Becker, P.; Ruf, C.; Oing, C.; Oechsle, K.; Bokemeyer, C.; et al. Serum Levels of MicroRNA miR-371a-3p: A Sensitive and Specific New Biomarker for Germ Cell Tumours. *Eur. Urol.* **2017**, *71*, 213–220, doi:10.1016/j.eururo.2016.07.029.
59. Dieckmann, K.-P.; Radtke, A.; Geczi, L.; Matthies, C.; Anheuser, P.; Eckardt, U.; Sommer, J.; Zengerling, F.; Trenti, E.; Pichler, R.; et al. Serum Levels of MicroRNA-371a-3p (M371 Test) as a New Biomarker of Testicular Germ Cell Tumors: Results of a Prospective Multicentric Study. *J. Clin. Oncol.* **2019**, *37*, 1412–1423, doi:10.1200/JCO.18.01480.
60. Helton, E.S.; Chen, X. p53 Modulation of the DNA Damage Response. *J. Cell. Biochem.* **2007**, *100*, 883–896, doi:10.1002/jcb.21091.
61. Harris, S.L.; Levine, A.J. The p53 pathway: Positive and negative feedback loops. *Oncogene* **2005**, *24*, 2899–2908, doi:10.1038/sj.onc.1208615.
62. Marine, J.-C.; Francoz, S.; Maetens, M.; Wahl, G.; Toledo, F.; Lozano, G. Keeping p53 in check: Essential and synergistic functions of Mdm2 and Mdm4. *Cell Death Differ.* **2006**, *13*, 927–934, doi:10.1038/sj.cdd.4401912.
63. Harms, K.L.; Chen, X. The functional domains in p53 family proteins exhibit both common and distinct properties. *Cell Death Differ.* **2006**, *13*, 890–897, doi:10.1038/sj.cdd.4401904.
64. Toledo, F.; Wahl, G.M. Regulating the p53 pathway: In vitro hypotheses, in vivo veritas. *Nat. Rev. Cancer* **2006**, *6*, doi:10.1038/nrc2012.
65. Butler, J.S.; Loh, S.N. Structure, Function, and Aggregation of the Zinc-Free Form of the p53 DNA Binding Domain. *Biochemistry* **2003**, *42*, 2396–2403, doi:10.1021/bi026635n.
66. Cho, Y.; Gorina, S.; Jeffrey, P.D.; Pavletich, N.P. Crystal Structure of a p53 Tumor Suppressor-DNA Complex: Understanding Tumorigenic. *Science* **1994**, *265*, 346–355.
67. Stracker, T.H.; Roig, I.; Knobel, P.A.; Marjanović, M. The ATM signaling network in development and disease. *Front. Genet.* **2013**, *4*, doi:10.3389/fgene.2013.00037.
68. Hafner, A.; Bulyk, M.L.; Jambhekar, A.; Lahav, G. The multiple mechanisms that regulate p53 activity and cell fate. *Nat. Rev. Mol. Cell Biol.* **2019**, *20*, doi:10.1038/s41580-019-0110-x.
69. Engeland, K. Cell cycle arrest through indirect transcriptional repression by p53: I have a DREAM. *Cell Death Differ.* **2018**, *25*, 114–132, doi:10.1038/cdd.2017.172.

70. El-Deiry, W.S.; Tokino, T.; Velculescu, V.E.; Levy, D.B.; Parsons, R.; Trent, J.M.; Lin, D.; Edward Mercer, W.; Kinzler, K.W.; Vogelstein, B. WAF1, a Potential Mediator of p53 Tumor Suppression. *Cell* **1993**, *75*, 817–825.
71. Harper, J.W.; Adami, G.R.; Wei, N.; Keyomarsi, K.; Elledge, S.J. The p21 Cdk-Interacting Protein Cip1 Is a Potent Inhibitor of G1 Cyclin-Dependent Kinases. *Cell* **1993**, *75*, 805–816.
72. Chen, J. The cell-cycle arrest and apoptotic functions of p53 in tumor initiation and progression. *Cold Spring Harb. Perspect. Med.* **2016**, *6*, doi:10.1101/cshperspect.a026104.
73. Chen, Z.; Trotman, L.C.; Shaffer, D.; Lin, H.-K.; Dotan, Z.A.; Niki, M.; Koutcher, J.A.; Scher, H.I.; Ludwig, T.; Gerald, W.; et al. Crucial role of p53-dependent cellular senescence in suppression of Pten-deficient tumorigenesis. *Nature* **2005**, *436*, 725–730.
74. Kruiswijk, F.; Labuschagne, C.F.; Vousden, K.H. p53 in survival, death and metabolic health: A lifeguard with a licence to kill. *Nat. Rev. Mol. Cell Biol.* **2015**, *16*, 393, doi:10.1038/nrm4007.
75. Rabinowitz, J.D.; White, E. Autophagy and metabolism. *Science* **2010**, *330*, 1344–1348, doi:10.1126/science.1193497.
76. Choudhury, S.; Kolukula, V.K.; Preet, A.; Albanese, C.; Avantiaggiati, M.L. Dissecting the pathways that destabilize mutant p53: The proteasome or autophagy? *Cell Cycle* **2013**, *12*, 1022–1029, doi:10.4161/cc.24128.
77. Feng, Z.; Hu, W.; De Stanchina, E.; Teresky, A.K.; Jin, S.; Lowe, S.; Levine, A.J. The Regulation of AMPK B1, TSC2, and PTEN Expression by p53: Stress, Cell and Tissue Specificity, and the Role of These Gene Products in Modulating the IGF-1-AKT-mTOR Pathways. *Cancer Res.* **2007**, *67*, 3043–3053, doi:10.1158/0008-5472.CAN-06-4149.
78. Nikolettou, V.; Markaki, M.; Palikaras, K.; Tavernarakis, N. Crosstalk between apoptosis, necrosis and autophagy. *Biochim. Biophys. Acta* **2013**, *1833*, 3448–3459, doi:10.1016/j.bbamcr.2013.06.001.
79. Shamas-Din, A.; Kale, J.; Leber, B.; Andrews, D.W. Mechanisms of action of Bcl-2 family proteins. *Cold Spring Harb. Perspect. Biol.* **2013**, *5*, 1–21, doi:10.1101/cshperspect.a008714.
80. Maiuri, M.C.; Le Toumelin, G.; Criollo, A.; Rain, J.C.; Gautier, F.; Juin, P.; Tasdemir, E.; Pierron, G.; Troulinaki, K.; Tavernarakis, N.; et al. Functional and physical interaction between Bcl-XL and a BH3-like domain in Beclin-1. *EMBO J.* **2007**, *26*, 2527–2539, doi:10.1038/sj.emboj.7601689.
81. Hakisiz, P.; Kiliańska, Z.M. Puma, a critical mediator of cell death—One decade on from its discovery. *Cell. Mol. Biol. Lett.* **2012**, *17*, 646–669, doi:10.2478/s11658-012-0032-5.
82. Morsi, R.Z.; Hage-Sleiman, R.; Kobeissy, H.; Dbaibo, G. Noxa: Role in Cancer Pathogenesis and Treatment. *Curr. Cancer Drug Targets* **2018**, *18*, 914–928, doi:10.2174/1568009618666180308105048.
83. Green, D.R.; Kroemer, G. Cytoplasmic functions of the tumour suppressor p53. *Nature* **2009**, *458*, doi:10.1038/nature07986.
84. Riedl, S.J.; Salvesen, G.S. The apoptosome: Signalling platform of cell death. *Nat. Rev. Mol. Cell Biol.* **2007**, *8*, doi:10.1038/nrm2153.
85. Cargill, M.; Altshuler, D.; Ireland, J.; Sklar, P.; Ardlie, K.; Patil, N.; Lane, C.R.; Lim, E.P.; Kalyanaraman, N.; Nemesh, J.; et al. Characterization of single-nucleotide polymorphisms in coding regions of human genes. *Nat. Genet.* **1999**, *22*, 231–238.
86. Wang, D.G.; Fan, J.-B.; Siao, C.-J.; Berno, A.; Young, P.; Sapolsky, R.; Ghandour, G.; Perkins, N.; Winchester, E.; Spencer, J.; et al. Large-Scale Identification, Mapping, and Genotyping of Single-Nucleotide Polymorphisms in the. *Science* **1998**, *280*, 1077–1082.

87. Bouaoun, L.; Sonkin, D.; Ardin, M.; Hollstein, M.; Byrnes, G.; Zavadil, J.; Olivier, M. TP53 Variations in Human Cancers: New Lessons from the IARC TP53 Database and Genomics Data. *Hum. Mutat.* **2016**, *37*, 865–876, doi:10.1002/humu.23035.
88. Pavletich, N.P.; Chambers, K.A.; Pabo, C.O. The DNA-binding domain of 53 contains the four conserved regions the major mutation hot spots. *Genes Dev.* **1993**, *7*, 2556–2564.
89. Parkin, D.M.; Pisani, P.; Ferlay, J. Estimates of the worldwide incidence of 25 major cancers in 1990. *Int. J. Cancer* **1999**, *80*, 827–841.
90. Hieken, T.J.; Farolan, M.; Velasco, J.M.; D'Alessandro, S. Predicting the biologic behavior of ductal carcinoma in situ: An analysis of molecular markers. *Surgery* **2001**, *130*, 593–601, doi:10.1067/msy.2001.116921.
91. Offutt, T.L.; leong, P.U.; Demir, Ö.; Amaro, R.E. Dynamics and Molecular Mechanisms of p53 Transcriptional Activation. *Biochemistry* **2018**, *57*, 6537, doi:10.1021/acs.biochem.8b01005.
92. Bullock, A.N.; Henckel, J.; Fersht, A.R. Quantitative analysis of residual folding and DNA binding in mutant p53 core domain: Definition of mutant states for rescue in cancer therapy. *Oncogene* **2000**, *19*, 1245–1256, doi:10.1038/sj.onc.1203434.
93. Rowan, S.; Ludwig, R.L.; Haupt, Y.; Bates, S.; Lu, X.; Oren, M.; Vousden, K.H. Specific loss of apoptotic but not cell-cycle arrest function in a human tumor derived p53 mutant. *EMBO J.* **1996**, *15*, 827–838.
94. Baugh, E.H.; Ke, H.; Levine, A.J.; Bonneau, R.A.; Chan, C.S.; Abstract, G. Why are there hotspot mutations in the TP53 gene in human cancers? *Nat. Publ. Gr.* **2018**, *25*, 154–160, doi:10.1038/cdd.2017.180.
95. Nigro, J.M.; Baker, S.J.; Preisinger, A.C.; Jessup, J.M.; Hostetter, R.; Cleary, K.; Bigner, S.H.; Davidson, N.; Baylin, S.; Devilee, P.; et al. Mutations in the p53 gene occur in diverse human tumour types. *Nature* **1989**, *342*, 705–708.
96. Xu, J.; Reumers, J.; Couceiro, J.R.; De Smet, F.; Gallardo, R.; Rudyak, S.; Cornelis, A.; Rozenski, J.; Zwolinska, A.; Marine, J.C.; et al. Gain of function of mutant p53 by coaggregation with multiple tumor suppressors. *Nat. Chem. Biol.* **2011**, *7*, 285–295, doi:10.1038/nchembio.546.
97. Dittmer, D.; Pati, S.; Zambetti, G.; Chu, S.; Teresky, A.K.; Moore, M.; Finlay, C.; Levine, A.J. Gain of function mutations in p53. *Nat. Genet.* **1993**, *4*, 42–46.
98. Gualberto, A.; Aldape, K.; Kozakiewicz, K.; Tlsty, T.D. An oncogenic form of p53 confers a dominant, gain-of-function phenotype that disrupts spindle checkpoint control. *PNAS* **1998**, *95*, 5166–5171.
99. Hsiao, M.; Low, J.; Dorn, E.; Ku, D.; Pattengale, P.; Yeargin, J.; Haas, M. Gain-of-function mutations of the p53 gene induce lymphohematopoietic metastatic potential and tissue invasiveness. *Am. J. Pathol.* **1994**, *145*, 702–714.
100. Shaulian, E.; Zauberman, A.; Ginsberg, D.; Oren, M. Identification of a Minimal Transforming Domain of p53: Negative Dominance through Abrogation of Sequence-Specific DNA Binding. *Mol. Cell. Biol.* **1992**, *12*, 5581–5592.
101. Lee, J.-K.; Wang, J.; Sa, J.K.; Ladewig, E.; Lee, H.-O.; Lee, I.-H.; Ju Kang, H.; Rosenbloom, D.S.; Camara, P.G.; Liu, Z.; et al. Spatiotemporal genomic architecture informs precision oncology in glioblastoma. *Nat. Genet.* **2017**, *49*, 594–599, doi:10.1038/ng.3806.
102. Alexandrova, E.M.; Mirza, S.A.; Xu, S.; Schulz-Heddergott, R.; Marchenko, N.D.; Moll, U.M. p53 loss-of-heterozygosity is a necessary prerequisite for mutant p53 stabilization and gain-of-function in vivo. *Cell Death Dis.* **2017**, *8*, doi:10.1038/cddis.2017.80.
103. Freed-Pastor, W.A.; Prives, C. Mutant p53: One name, many proteins. *Genes Dev.* **2012**, *26*, 1268–1286, doi:10.1101/gad.190678.112.

104. Zhang, C.; Liu, J.; Xu, D.; Zhang, T.; Hu, W.; Feng, Z. Gain-of-function mutant p53 in cancer progression and therapy. *J. Mol. Cell Biol.* **2020**, *12*, 674–687, doi:10.1093/jmcb/mjaa040.
105. Liu, J.; Zhang, C.; Feng, Z. Tumor suppressor p53 and its gain-of-function mutants in cancer. *Acta Biochim Biophys Sin.* **2014**, *46*, 170, doi:10.1093/abbs/gmt144.
106. Beyer, U.; Moll-Rocek, J.; Moll, U.M.; Döbelstein, M. Endogenous retrovirus drives hitherto unknown proapoptotic p63 isoforms in the male germ line of humans and great apes. *PNAS* **2011**, *108*, 3624–3629, doi:10.1073/pnas.1016201108.
107. Grande, L.; Bretones, G.; Rosa-Garrido, M.; Garrido-Martin, E.M.; Hernandez, T.; Fraile, S.; Botella, L.; De Alava, E.; Vidal, A.; Garcia Del Muro, X.; et al. Transcription Factors Sp1 and p73 Control the Expression of the Proapoptotic Protein NOXA in the Response of Testicular Embryonal Carcinoma Cells to Cisplatin. *J. Biol. Chem.* **2012**, *287*, 26495–26505, doi:10.1074/jbc.M112.376319.
108. Lobo, J.; Jerónimo, C.; Henrique, R. Cisplatin Resistance in Testicular Germ Cell Tumors: Current Challenges from Various Perspectives. *Cancers* **2020**, *12*, doi:10.3390/cancers12061601.
109. Jost, C.A.; Marin, M.C.; Kaelin, W.G. p73 is a human p53-related protein that can induce apoptosis. *Nature* **1997**, *389*, 191–194.
110. Kaghad, M.; Bonnet, H.; Yang, A.; Creancier, L.; Biscan, J.C.; Valent, A.; Minty, A.; Chalou, P.; Lelias, J.M.; Dumont, X.; et al. Monoallelically expressed gene related to p53 at 1p36, a region frequently deleted in neuroblastoma and other human cancers. *Cell* **1997**, *90*, 809–819, doi:10.1016/S0092-8674(00)80540-1.
111. Schmale, H.; Bamberger, C. A novel protein with strong homology to the tumor suppressor p53. *Oncogene* **1997**, *15*, 1363–1367.
112. Yang, A.; Kaghad, M.; Wang, Y.; Gillett, E.; Fleming, M.D.; Dötsch, V.; Andrews, N.C.; Caput, D.; McKeon, F. p63, a p53 Homolog at 3q27-29, Encodes Multiple Products with Transactivating, Death-Inducing, and Dominant-Negative Activities. *Mol. Cell* **1998**, *2*, 305–316.
113. Dötsch, V.; Bernassola, F.; Coutandin, D.; Candi, E.; Melino, G. p63 and p73, the Ancestors of p53. *Cold Spring Harb. Perspect. Biol.* **2010**, *2*, doi:10.1101/cshperspect.a004887.
114. Wei, J.; Zaika, E.; Zaika, A. P53 family: Role of protein isoforms in human cancer. *J. Nucleic Acids* **2012**, *2012*, doi:10.1155/2012/687359.
115. Pflaum, J.; Schlosser, S.; Müller, M. P53 family and cellular stress responses in cancer. *Front. Oncol.* **2014**, *4*, doi:10.3389/fonc.2014.00285.
116. DeYoung, M.P.; Ellisen, L.W. p63 and p73 in human cancer: Defining the network. *Oncogene* **2007**, *26*, doi:10.1038/sj.onc.1210337.
117. Yang, A.; Kaghad, M.; Caput, D.; McKeon, F. On the shoulders of giants: p63, p73 and the rise of p53. *TRENDS Genet.* **2002**, *18*, 90–95.
118. Rutkowski, R.; Hofmann, K.; Gartner, A. Phylogeny and Function of the Invertebrate p53 Superfamily. *Cold Spring Harb. Perspect. Biol.* **2010**, *2*, doi:10.1101/cshperspect.a001131.
119. Duijf, P.H.G.; Vanmolkot, K.R.J.; Propping, P.; Friedl, W.; Krieger, E.; McKeon, F.; Dötsch, V.; Brunner, H.G.; Van Bokhoven, H. Gain-of-function mutation in ADULT syndrome reveals the presence of a second transactivation domain in p63. *Hum. Mol. Genet.* **2002**, *11*, 799–804.
120. Ghioni, P.; Bolognese, F.; Duijf, P.H.G.; Van Bokhoven, H.; Mantovani, R.; Guerrini, L. Complex Transcriptional Effects of p63 Isoforms: Identification of Novel Activation and Repression Domains. *Mol. Cell. Biol.* **2002**, *22*, 8659–8668, doi:10.1128/MCB.22.24.8659-8668.2002.

121. Helton, E.S.; Zhu, J.; Chen, X. The Unique NH 2-terminally Deleted (N) Residues, the PXXP Motif, and the PPXY Motif Are Required for the Transcriptional Activity of the N Variant of p63. *J. Biol. Chem.* **2006**, *281*, doi:10.1074/jbc.M507964200.
122. Pietsch, E.C.; Sykes, S.M.; McMahon, S.B.; Murphy, M.E. The p53 family and programmed cell death. *Oncogene* **2008**, *27*, 6507–6521, doi:10.1038/onc.2008.315.
123. Flores, E.R.; Tsai, K.Y.; Crowley, D.; Sengupta, S.; Yang, A.; McKeon, F.; Jacks, T. p63 and p73 are required for p53-dependent apoptosis in response to DNA damage. *Nature* **2002**, *416*, doi:10.1038/nature731.
124. Harms, K.; Nozell, S.; Chen, X. The common and distinct target genes of the p53 family transcription factors. *Cell. Mol. Life Sci.* **2004**, *61*, 822–842, doi:10.1007/s00018-003-3304-4.
125. Melino, G.; Bernassola, F.; Ranalli, M.; Yee, K.; Xing Zong, W.; Corazzari, M.; Knight, R.A.; Green, D.R.; Thompson, C.; Vousden, K.H. p73 Induces Apoptosis via PUMA Transactivation and Bax Mitochondrial Translocation. *J. Biol. Chem.* **2004**, *279*, doi:10.1074/jbc.M307469200.
126. Suh, E.-K.; Yang, A.; Kettenbach, A.; Bamberger, C.; Michaelis, A.H.; Zhu, Z.; Elvin, J.A.; Bronson, R.T.; Crum, C.P.; McKeon, F. p63 protects the female germ line during meiotic arrest. *Nature* **2006**, *444*, doi:10.1038/nature05337.
127. Amelio, I.; Grespi, F.; Annicchiarico-Petruzzelli, M.; Melino, G. P63 the Guardian of Human Reproduction. *Cell Cycle* **2012**, *11*, 4545–4551, doi:10.4161/cc.22819.
128. Gebel, J.; Tuppi, M.; Sängler, N.; Schumacher, B.; Dötsch, V. DNA Damaged Induced Cell Death in Oocytes. *Molecules* **2020**, *25*, doi:10.3390/molecules25235714.
129. Talos, F.; Abraham, A.; Vaseva, A.; Holembowski, L.; Tsirka, S.; Scheel, A.; Bode, D.; Döbelstein, M.; Brück, W.; Moll, U. p73 is an essential regulator of neural stem cell maintenance in embryonal and adult CNS neurogenesis. *Cell Death Differ.* **2010**, *17*, 1816–1829, doi:10.1038/cdd.2010.131.
130. Vanbokhoven, H.; Melino, G.; Candi, E.; Declercq, W. P63, a story of mice and men. *J. Invest. Dermatol.* **2011**, *131*, 1196–1207, doi:10.1038/jid.2011.84.
131. Soares, E.; Zhou, H. Master regulatory role of p63 in epidermal development and disease. *Cell. Mol. Life Sci.* **2018**, *75*, 1179–1190, doi:10.1007/s00018-017-2701-z.
132. Yang, A.; Schweitzer, R.; Sun, D.; Kaghad, M.; Walker, N.; Bronson, R.T.; Tabin, C.; Sharpe, A.; Caput, D.; Crum, C.; et al. p63 is essential for regenerative proliferation in limb, craniofacial and epithelial development. *Nature* **1999**, *398*, 714–718.
133. Mills, A.A.; Zheng, B.; Wang, X.-J.; Vogel, H.; Roop, D.R.; Bradley, A. P63 Is a P53 Homologue Required for Limb and Epidermal Morphogenesis. *Nature* **1999**, *398*, 708–713.
134. Yang, A.; Walker, N.; Bronson, R.; Kaghad, M.; Oosterwegel, M.; Bonnin, J.; Vagner, C.; Bonnet, H.; Dikkes, P.; Sharpe, A. P73-Deficient mice have neurological, phenotypic and inflammatory defects but lack spontaneous tumours. *Development* **2000**, *117*, 1321–1331.
135. Ramos, H.; Raimundo, L.; Saraiva, L. p73: From the p53 shadow to a major pharmacological target in anticancer therapy. *Pharmacol. Res.* **2020**, *162*, 1043–6618, doi:10.1016/j.phrs.2020.105245.
136. Melino, G.; Lu, X.; Gasco, M.; Crook, T.; Knight, R.A. Functional regulation of p73 and p63: Development and cancer. *TRENDS Biochem. Sci.* **2003**, *28*, 663–670, doi:10.1016/j.tibs.2003.10.004.
137. Lamb, P.; Crawford, L. Characterization of the Human p53 Gene. *Mol. Cell. Biol.* **1986**, *6*, 1379–1385.
138. Marcel, V.; Perrier, S.; Aoubala, M.; Ageorges, S.; Groves, M.J.; Diot, A.; Fernandes, K.; Tauro, S.; Bourdon, J.-C. $\Delta 160p53$ is a novel N-terminal p53 isoform encoded by $\Delta 133p53$ transcript. *FEBS Lett.* **2010**, *584*, 4463–4468, doi:10.1016/j.febslet.2010.10.005.

139. Bourdon, J.-C.; Fernandes, K.; Murray-Zmijewski, F.; Liu, G.; Diot, A.; Xirodimas, D.P.; Saville, M.K.; Lane, D.P. p53 isoforms can regulate p53 transcriptional activity. *Genes Dev.* **2005**, *19*, 2122–2137, doi:10.1101/gad.1339905.
140. Billant, O.; Léon, A.; Le Guellec, S.; Friocourt, G.; Blondel, M.; Voisset, C. The dominant-negative interplay between p53, p63 and p73: A family affair. *Oncotarget* **2016**, *7*, 69549–69564, doi:10.18632/oncotarget.11774.
141. Knezovi Florijan, M.; Ozreti, P.; Bujak, M.; Pezz, L.; Ciribilli, Y.; Ka stelán, Z.; Slade, N.; Hudolin, T. The role of p53 isoforms' expression and p53 mutation status in renal cell cancer prognosis. *Urol. Oncol.* **2019**, *37*, doi:10.1016/j.urolonc.2019.03.007.
142. Hafsi, H.; Santos-Silva, D.; Courtois-Cox, S.; Hainaut, P. Effects of $\Delta 40p53$, an isoform of p53 lacking the N-terminus, on transactivation capacity of the tumor suppressor protein p53. *BMC Cancer* **2013**, *13*, 134, doi:10.1186/1471-2407-13-134.
143. Bernard, H.; Garmy-Susini, B.; Ainaoui, N.; Van Den Berghe, L.; Peurichard, A.; Javerzat, S.; Bikfalvi, A.; Lane, D.P.; Bourdon, J.C.; Prats, A.-C. The p53 isoform, $\Delta 133p53a$, stimulates angiogenesis and tumour progression. *Oncogene* **2013**, *32*, 2150–2160, doi:10.1038/onc.2012.242.
144. Hofstetter, G.; Berger, A.; Schuster, E.; Wolf, A.; Hager, G.; Vergote, I.; Cadron, I.; Sehouli, J.; Braicu, E.I.; Mahner, S.; et al. $\Delta 133p53$ is an independent prognostic marker in p53 mutant advanced serous ovarian cancer. *Br. J. Cancer* **2011**, *105*, 1593–1599, doi:10.1038/bjc.2011.433.
145. Candeias, M.M.; Hagiwara, M.; Matsuda, M. Cancer-specific mutations in P53 induce the translation of $\Delta 160P53$ promoting tumorigenesis. *EMBO Rep.* **2016**, *17*, 1542–1551.
146. Zhang, Y.; Ma, W.-Y.; Kaji, A.; Bode, A.M.; Dong, Z. Requirement of ATM in UVA-induced Signaling and Apoptosis. *J. Biol. Chem.* **2001**, *277*, 3124–3131, doi:10.1074/jbc.M110245200.
147. Midgley, C.A.; Owens, B.; Briscoe, C.V.; Thomas, D.B.; Lane, D.P.; Hall, P.A. Coupling between gamma irradiation, p53 induction and the apoptotic response depends upon cell type in vivo. *J. Cell Sci.* **1995**, *108*, 1843–1848.
148. Kawaguchi, T.; Kato, S.; Otsuka, K.; Watanabe, G.; Kumabe, T.; Tominaga, T.; Yoshimoto, T.; Ishioka, C. The relationship among p53 oligomer formation, structure and transcriptional activity using a comprehensive missense mutation library. *Oncogene* **2005**, *24*, 6976–6981, doi:10.1038/sj.onc.1208839.
149. Liao, P.; Zeng, S.X.; Zhou, X.; Chen, T.; Zhou, F.; Cao, B.; Jung, J.H.; Sal, G. Del; Luo, S.; Lu, H. Mutant p53 Gains Its Function via c-Myc Activation upon CDK4 Phosphorylation at Serine 249 and Consequent PIN1 Binding. *Mol. Cell* **2017**, *68*, 1134–1146, doi:10.1016/j.molcel.2017.11.006.
150. Nakamura, S.; Roth, J.A.; Mukhopadhyay, T. Multiple Lysine Mutations in the C-Terminal Domain of p53 Interfere with MDM2-Dependent Protein Degradation and Ubiquitination. *Mol. Cell. Biol.* **2000**, *20*, 9391–9398.
151. Liu, Y.; Tavana, O.; Gu, W. p53 modifications: Exquisite decorations of the powerful guardian. *J. Mol. Cell Biol.* **2019**, *11*, 564–577, doi:10.1093/JMCB/MJZ060.
152. Shi, X.; Kachirskaja, I.; Yamaguchi, H.; West, L.E.; Wen, H.; Wang, E.W.; Dutta, S.; Appella, E.; Gozani, O. Modulation of p53 function by SET8-mediated methylation at lysine 382. *Mol. Cell* **2007**, *27*, 636–646, doi:10.1016/j.molcel.2007.07.012.
153. Chuikov, S.; Kurash, J.K.; Wilson, J.R.; Xiao, B.; Justin, N.; Ivanov, G.S.; Mckinney, K.; Tempst, P.; Prives, C.; Gamblin, S.J.; et al. Regulation of p53 activity through lysine methylation. *Nature* **2004**, *432*, 353–360.

154. Huang, J.; Perez-Burgos, L.; Placek, B.J.; Sengupta, R.; Richter, M.; Dorsey, J.A.; Kubicek, S.; Opravil, S.; Jenuwein, T.; Berger, S.L. Repression of p53 activity by Smyd2-mediated methylation. *Nature* **2006**, *444*, doi:10.1038/nature05287.
155. Jansson, M.; Durant, S.T.; Cho, E.-C.; Sheahan, S.; Edelman, M.; Kessler, B.; Thangue, N.B. La Arginine methylation regulates the p53 response. *Nat. Cell Biol.* **2008**, *10*, doi:10.1038/ncb1802.
156. Minamoto, T.; Buschmann, T.; Habelhah, H.; Matusevich, E.; Tahara, H.; Boerresen-Dale, A.-L.; Harris, C.; Sidransky, D.; Ronai, Z. Distinct pattern of p53 phosphorylation in human tumors. *Oncogene* **2001**, *20*, 3341–3347.
157. Gatti, A.; Li, H.-H.; Traugh, J.A.; Liu, X. Phosphorylation of Human p53 on Thr-55. *Biochemistry* **2000**, *39*, 9837–9842, doi:10.1021/bi992454i.
158. Waterman, M.J.F.; Stavridi, E.S.; Waterman, J.L.F.; Halazonetis, T.D. ATM-dependent activation of p53 involves dephosphorylation and association with 14-3-3 proteins. *Nat. Genet.* **1998**, *19*, 175–178, doi:10.1038/542.
159. Shieh, S.-Y.; Ahn, J.; Tamai, K.; Taya, Y.; Prives, C. The human homologs of checkpoint kinases Chk1 and Cds1 (Chk2) phosphorylate p53 at multiple DNA damage-inducible sites. *Genes Dev.* **2000**, *14*, 289–300.
160. Canman, C.E.; Lim, D.-S.; Cimprich, K.A.; Taya, Y.; Tamai, K.; Sakaguchi, K.; Appella, E.; Kastan, M.B.; Siliciano, J.D. Activation of the ATM Kinase by Ionizing Radiation and Phosphorylation of p53. *Science* **1998**, *281*, 1677–1679.
161. Tibbetts, R.S.; Brumbaugh, K.M.; Williams, J.M.; Sarkaria, J.N.; Cliby, W.A.; Shieh, S.-Y.; Taya, Y.; Prives, C.; Abraham, R.T. A role for ATR in the DNA damage-induced phosphorylation of p53. *Genes Dev.* **1999**, *13*, 152–157.
162. Herskho, A.; Heller, H.; Elias, S.; Ciechanover, A. Components of Ubiquitin-Protein Ligase System. *R. J. Biol. Chem.* **1983**, *258*, 8206–8214.
163. Rodriguez, M.S.; Desterro, J.M.P.; Lain, S.; Lane, D.P.; Hay, R.T. Multiple C-Terminal Lysine Residues Target p53 for Ubiquitin-Proteasome-Mediated Degradation. *Mol. Cell. Biol.* **2000**, *20*, 8458–8467.
164. Tasdemir, E.; Chiara Maiuri, M.; Galluzzi, L.; Vitale, I.; Djavaheri-Mergny, M.; D'amelio, M.; Criollo, A.; Morselli, E.; Zhu, C.; Harper, F.; et al. Regulation of autophagy by cytoplasmic p53. *Nat. Cell Biol.* **2008**, *10*, 676–687, doi:10.1038/ncb1730.
165. Stommel, J.M.; Marchenko, N.D.; Jimenez, G.S.; Moll, U.M.; Hope, T.J.; Wahl, G.M. A leucine-rich nuclear export signal in the p53 tetramerization domain: Regulation of subcellular localization and p53 activity by NES masking. *EMBO J.* **1999**, *18*, 1660–1672.
166. Momand, J.; Zambetti, G.P.; Olson, D.C.; George, D.; Levine, A.J. The mdm-2 oncogene product forms a complex with the p53 protein and inhibits p53-mediated transactivation. *Cell* **1992**, *69*, 1237–1245, doi:10.1016/0092-8674(92)90644-R.
167. Oliner, J.D.; Pietenpol, J.A.; Thiagalingam, S.; Gyuris, J.; Kinzler, K.W.; Vogelstein, B. Oncoprotein Mdm2 conceals the activation domain of tumour suppressor p53. *Nature* **1993**, *362*, 857–860.
168. Leach, F.S.; Tokino, T.; Meltzer, P.; Burrell, M.; Oliner, J.D.; Smith, S.; Hill, D.E.; Sidransky, D.; Kinzler, K.W.; Vogelstein, B. p53 Mutation and MDM2 Amplification in Human Soft Tissue Sarcomas. *Cancer Res.* **1993**, *53*, 2231–2234.
169. Jones, S.N.; Hancock, A.R.; Vogel, H.; Donehower, L.A.; Bradley, A. Overexpression of Mdm2 in mice reveals a p53-independent role for Mdm2 in tumorigenesis. *PNAS* **1998**, *95*, 15608–15612.
170. Momand, J.; Jung, D.; Wilczynski, S.; Niland, J. The MDM2 gene amplification database. *Nucleic Acids Res.* **1998**, *26*, 3453–3459.

171. Gostissa, M.; Hengstermann, A.; Fogal, V.; Sandy, P.; Schwarz, S.E.; Scheffner, M.; Sal, G. Del Activation of p53 by conjugation to the ubiquitin-like protein SUMO-1. *EMBO J.* **1999**, *18*, 6462–6471.
172. Bischof, O.; Schwamborn, K.; Martin, N.; Werner, A.; Sustmann, C.; Grosschedl, R.; Dejean, A. The E3 SUMO Ligase PIASy Is a Regulator of Cellular Senescence and Apoptosis. *Mol. Cell* **2006**, *22*, 783–794, doi:10.1016/j.molcel.2006.05.016.
173. Gu, W.; Roeder, R.G. Activation of p53 Sequence-Specific DNA Binding by Acetylation of the p53 C-Terminal Domain. *Cell* **1997**, *90*, 595–606.
174. Tang, Y.; Zhao, W.; Chen, Y.; Zhao, Y.; Gu, W. Acetylation Is Indispensable for p53 Activation. *Cell* **2008**, *16*, 612–626, doi:10.1016/j.cell.2008.03.025.
175. Li, M.; Luo, J.; Brooks, C.L.; Gu, W. Acetylation of p53 Inhibits Its Ubiquitination by Mdm2. *J. Biol. Chem.* **2002**, *277*, 50607–50611, doi:10.1074/jbc.C200578200.
176. Luo, J.; Su, F.; Chen, D.; Shiloh, A.; Gu, W. Deacetylation of p53 modulates its effect on cell growth and apoptosis. *Nature* **2000**, *408*, 377–381.
177. Zhao, W.; Kruse, J.-P.; Tang, Y.; Jung, S.Y.; Qin, J.; Gu, W. Negative regulation of the deacetylase SIRT1 by DBC1. *Nature* **2008**, *451*, 587–590, doi:10.1038/nature06515.
178. Huffman, D.M.; Grizzle, W.E.; Bamman, M.M.; Kim, J.-S.; Eltoum, I.A.; Elgavish, A.; Nagy, T.R. SIRT1 Is Significantly Elevated in Mouse and Human Prostate Cancer. *Cancer Res.* **2007**, *67*, doi:10.1158/0008-5472.CAN-07-0085.
179. Parikh, N.; Hilsenbeck, S.; Creighton, C.J.; Dayaram, T.; Shuck, R.; Shinbrot, E.; Xi, L.; Gibbs, R.A.; Wheeler, D.A.; Donehower, L.A. Effects of TP53 Mutational Status on Gene Expression Patterns Across Ten Human Cancer Types. *J. Pathol.* **2014**, *232*, 522–533, doi:10.1002/path.4321.
180. Liu, Y.; Chen, C.; Xu, Z.; Scuoppo, C.; Rillahan, C.D.; Gao, J.; Spitzer, B.; Bosbach, B.; Kasthuber, E.R.; Baslan, T.; et al. Deletions linked to TP53 loss drive cancer through p53-independent mechanisms. *Nature* **2016**, *531*, 471–475, doi:10.1038/nature17157.
181. Petitjean, A.; Achatz, M.; Borresen-Dale, A.L.; Hainaut, P.; Olivier, M. TP53 mutations in human cancers: Functional selection and impact on cancer prognosis and outcomes. *Oncogene* **2007**, *26*, 2157–2165, doi:10.1038/sj.onc.1210302.
182. Nakayama, M.; Hong, C.P.; Oshima, H.; Sakai, E.; Kim, S.J.; Oshima, M. Loss of wild-type p53 promotes mutant p53-driven metastasis through acquisition of survival and tumor-initiating properties. *Nat. Commun.* **2020**, *11*, 1–14, doi:10.1038/s41467-020-16245-1.
183. Jones, S.N.; Roe, A.E.; Donehower, L.A.; Bradley, A. Rescue of embryonic lethality in Mdm2-deficient mice by absence of p53. *Nature* **1995**, *378*, 206–208.
184. Kuerbitz, S.J.; Plunkett, B.S.; Walsh, W.V.; Kastan, M.B. Wild-type p53 is a cell cycle checkpoint determinant following irradiation. *Cell Biol.* **1992**, *89*, 7491–7495.
185. Montes de Oca Luna, R.; Wagner, D.S.; Lozanot, G. Rescue of early embryonic lethality in mdm2-deficient mice by deletion of p53. *Nature* **1995**, *378*, 203–206.
186. Moyer, S.M.; Larsson, C.A.; Lozano, G. Mdm proteins: Critical regulators of embryogenesis and homeostasis. *J. Mol. Cell Biol.* **2017**, *9*, 16–25, doi:10.1093/jmcb/mjx004.
187. Shvarts, A.; TSteegenga, W.; Riteco, N.; van Laar, T.; Dekker, P.; Bazuine, M.; CAvan Ham, R.; van der Houven van Oordt, W.; Hateboer, G.; Jvan der Eb, A.; et al. MDMX: A novel p53-binding protein with some functional properties of MDM2. *EMBO J.* **1996**, *15*, 5349–5357.
188. Oliner, J.D.; Kinzler, K.W.; Meltzer, P.S.; George, D.L.; Vogelstein, B. Amplification of a gene encoding a p53-associated protein in human sarcomas. *Nature* **1992**, *358*, 80–83.

189. Shadfan, M.; Lopez-Pajares, V.; Yuan, Z.-M. MDM2 and MDMX: Alone and together in regulation of p53. *Transl Cancer Res.* **2012**, *1*, 88–89.
190. Roth, J.; Dobbelstein, M.; Freedman, D.A.; Shenk, T.; Levine, A.J. Nucleo-cytoplasmic shuttling of the hdm2 oncoprotein regulates the levels of the p53 protein via a pathway used by the human immunodeficiency virus rev protein. *EMBO J.* **1998**, *17*, 554–564.
191. Fang, S.; Jensen, J.P.; Ludwig, R.L.; Vousden, K.H.; Weissman, A.M. Mdm2 Is a RING Finger-dependent Ubiquitin Protein Ligase for Itself and p53. *J. Biochem. Chem.* **2000**, *275*, 8945–8951.
192. Li, M.; Brooks, C.L.; Wu-Baer, F.; Chen, D.; Baer, R.; Gu, W. Mono-versus Polyubiquitination: Differential Control of p53 Fate. *Science* **2003**, *302*, 1972–1975.
193. Geyer, R.K.; Yu, Z.K.; Maki, C.G. The MDM2 RING-finger domain is required to promote p53 nuclear export. *Nat. Cell Biol.* **2000**, *2*, 569–573.
194. Marine, J.-C.; Lozano, G. Mdm2-mediated ubiquitylation: p53 and beyond. *Cell Death Differ.* **2010**, *17*, 93–102, doi:10.1038/cdd.2009.68.
195. Haupt, Y.; Mayat, R.; Kazantz, A.; Orent, M. Mdm2 promotes the rapid degradation of p53. *Nature* **1997**, *387*, 296–299.
196. Honda, R.; Tanaka, H.; Yasuda, H. Oncoprotein MDM2 is a ubiquitin ligase E3 for tumor suppressor p53. *Fed. Eur. Biochem. Soc.* **1997**, *420*, 25–27.
197. Kulikov, R.; Letienne, J.; Kaur, M.; Grossman, S.R.; Arts, J.; Blattner, C. Mdm2 facilitates the association of p53 with the proteasome. *PNAS* **2010**, *107*, 10038–10043, doi:10.1073/pnas.0911716107/-DCSupplemental.
198. Zauberman, A.; Barak, Y.; Ragimov, N.; Levy, N.; Oren, M. Sequence-specific DNA binding by p53: Identification of target sites and lack of binding to p53 MDM2 complexes. *EMBO J.* **1993**, *12*, 2799–2808.
199. Yang, J.-Y.; Zong, C.S.; Xia, W.; Wei, Y.; Ali-Sayed, M.; Li, Z.; Broglio, K.; Berry, D.A.; Hung, M.-C. MDM2 Promotes Cell Motility and Invasiveness by Regulating E-Cadherin Degradation. *Mol.* **2006**, *26*, 7269–7282, doi:10.1128/MCB.00172-06.
200. Oliner, J.D.; Saiki, A.Y.; Caenepeel, S. The role of MDM2 amplification and overexpression in tumorigenesis. *Cold Spring Harb. Perspect. Med.* **2016**, *6*, doi:10.1101/cshperspect.a026336.
201. Vassilev, L.T.; Vu, B.T.; Graves, B.; Carvajal, D.; Podlaski, F.; Filipovic, Z.; Kong, N.; Kammlott, U.; Lukacs, C.; Klein, C.; et al. In vivo Activation of the p53 Pathway by Small-Molecule Antagonists of MDM2. *Science* **2004**, *303*, 844–848.
202. Tovar, C.; Rosinski, J.; Filipovic, Z.; Higgins, B.; Kolinsky, K.; Hilton, H.; Zhao, X.; Vu, B.T.; Qing, W.; Packman, K.; et al. Small-molecule MDM2 antagonists reveal aberrant p53 signaling in cancer: Implications for therapy. *PNAS* **2006**, *103*, 1888–1893.
203. Bauer, S.; Mühlenberg, T.; Leahy, M.; Hoiczky, M.; Gauler, T.; Schuler, M.; Looijenga, L. Therapeutic Potential of Mdm2 Inhibition in Malignant Germ Cell Tumours. *Eur. Urol.* **2010**, *57*, 679–687, doi:10.1016/j.eururo.2009.06.014.
204. Chen, Y.; Wang, D.-D.; Wu, Y.-P.; Su, D.; Zhou, T.-Y.; Gai, R.-H.; Fu, Y.-Y.; Zheng, L.; He, Q.-J.; Zhu, H.; et al. MDM2 promotes epithelial-mesenchymal transition and metastasis of ovarian cancer SKOV3 cells. *Br. J. Cancer* **2017**, *117*, 1192–1201.
205. Sdek, P.; Ying, H.; Chang, D.L.F.; Qiu, W.; Zheng, H.; Touitou, R.; Allday, M.J.; Xiao, Z.-X.J. MDM2 Promotes Proteasome-Dependent Ubiquitin-Independent Degradation of Retinoblastoma Protein. *Mol. Cell* **2005**, *20*, 699–708, doi:10.1016/j.molcel.2005.10.017.

206. Bond, G.L.; Hu, W.; Bond, E.E.; Robins, H.; Lutzker, S.G.; Arva, N.C.; Bargonetti, J.; Bartel, F.; Taubert, H.; Wuerl, P.; et al. A Single Nucleotide Polymorphism in the MDM2 Promoter Attenuates the p53 Tumor Suppressor Pathway and Accelerates Tumor Formation in Humans. *Cell* **2004**, *119*, 591–602, doi:10.1016/j.cell.2004.11.022.
207. Bond, G.L.; Menin, C.; Bertorelle, R.; Alhopuro, P.; Aaltonen, L.A.; Levine, A.J. MDM2 SNP309 accelerates colorectal tumour formation in women. *J. Med. Genet.* **2006**, *43*, 950–952, doi:10.1136/jmg.2006.043539.
208. Sun, T.; Lee, G.-S.M.; Oh, W.K.; Pomerantz, M.; Yang, M.; Xie, W.; Freedman, M.L.; Kantoff, P.W. Single-nucleotide Polymorphisms in p53 Pathway and Aggressiveness of Prostate Cancer in a Caucasian Population. *Clin. Cancer Res.* **2010**, *16*, 5244–5251, doi:10.1158/1078-0432.CCR-10-1261.
209. Wang, W.; Du, M.; Gu, D.; Zhu, L.; Chu, H.; Tong, N.; Zhang, Z.; Xu, Z.; Wang, M. MDM2 SNP309 polymorphism is associated with colorectal cancer risk. *Sci. Rep.* **2014**, doi:10.1038/srep04851.
210. Knappskog, S.; Bjørnslett, M.; Myklebust, L.M.; Huijts, P.E.A.; Vreeswijk, M.P.; Edvardsen, H.; Guo, Y.; Zhang, X.; Yang, M.; Ylisaukko-Oja, S.K.; et al. Cancer Cell The MDM2 Promoter SNP285C/309G Haplotype Diminishes Sp1 Transcription Factor Binding and Reduces Risk for Breast and Ovarian Cancer in Caucasians. *Cancer Cell* **2011**, *19*, 273–282, doi:10.1016/j.ccr.2010.12.019.
211. Knappskog, S.; Lønning, P.E. MDM2 promoter SNP285 and SNP309; phylogeny and impact on cancer risk. *Oncotarget* **2011**, *2*, 251–258.
212. Bartel, F.; Taubert, H.; Harris, L.C. Alternative and aberrant splicing of MDM2 mRNA in human cancer. *Cancer Cell* **2002**, *2*, 9–15.
213. Sigalas, I.; Calvert, A.H.; Akdfrso, J.J.; Neal, D.E.; Lunec, J. Alternatively spliced mdm2 transcripts with loss of p53 binding domain sequences: Transforming ability and frequent detection in human cancer. *Nat. Med.* **1996**, *2*, 912–917.
214. Zheng, T.; Wang, J.; Zhao, Y.; Zhang, C.; Lin, M.; Wang, H.Y.; Liu, L.; Feng, Z.; Hu, W. Spliced MDM2 isoforms promote mutant p53 accumulation and gain-of-function in tumorigenesis. *Nat. Commun.* **2013**, *4*, doi:10.1038/ncomms3996.
215. Evans, S.C.; Viswanathan, M.; Grier, J.D.; Narayana, M.; El-Naggar, A.K.; Lozano, G. An alternatively spliced HDM2 product increases p53 activity by inhibiting HDM2. *Oncogene* **2001**, *20*, 4041–4049.
216. Stommel, J.M.; Wahl, G.M. Accelerated MDM2 auto-degradation induced by DNA-damage kinases is required for p53 activation. *EMBO J.* **2004**, *23*, 1547–1556, doi:10.1038/sj.emboj.7600145.
217. Itahana, K.; Mao, H.; Jin, A.; Itahana, Y.; Clegg, H.V.; Lindström, M.S.; Bhat, K.P.; Godfrey, V.L.; Evan, G.I.; Zhang, Y. Targeted inactivation of Mdm2 RING finger E3 Ubiquitin Ligase Activity in the Mouse Reveals Mechanistic Insights into p53 regulation. *Cancer Cell* **2007**, *12*, 355–366.
218. Ranaweera, R.S.; Yang, X. Auto-ubiquitination of Mdm2 Enhances Its Substrate Ubiquitin Ligase Activity. *J. Biol. Chem.* **2013**, *288*, 18939–18946, doi:10.1074/jbc.M113.454470.
219. Li, M.; Brooks, C.L.; Kon, N.; Gu, W. A dynamic role of HAUSP in the p53-Mdm2 pathway. *Mol. Cell* **2004**, *13*, 879–886.
220. Wang, X.; Taplick, J.; Geva, N.; Oren, M. Inhibition of p53 degradation by Mdm2 acetylation. *FEBS Lett.* **2004**, *561*, 195–201, doi:10.1016/S0014-5793(04)00168-1.
221. Mayo, L.D.; Donner, D.B. A phosphatidylinositol 3-kinase/Akt pathway promotes translocation of Mdm2 from the cytoplasm to the nucleus. *PNAS* **2001**, *98*, 11598–11603.
222. Gannon, H.S.; Woda, B.A.; Jones, S.N. ATM Phosphorylation of Mdm2 Ser394 Regulates the Amplitude and Duration of the DNA Damage Response in Mice. *Cancer Cell* **2012**, *21*, 668–679, doi:10.1016/j.ccr.2012.04.011.

223. Lopez-Pajares, V.; Kim, M.M.; Yuan, Z.-M. Phosphorylation of MDMX Mediated by Akt Leads to Stabilization and Induces 14-3-3 Binding. *J. Biol. Chem.* **2008**, *283*, 13707–13713, doi:10.1074/jbc.M710030200.
224. Anderson, J.S.; Lyon, C.E.; Fox, A.H.; Leung, A.K.L.; Lam, Y.W.; Steen, H.; Mann, M.; Lamond, A.I. Directed proteomic analysis of the human nucleolus. *Curr. Biol.* **2002**, *12*, 1–11.
225. Lindstrom, M.S.; Deisenroth, C.; Zhang, Y.; Lindström, M.S. Putting a Finger on Growth Surveillance: Insight into MDM2 Zinc Finger-Ribosomal Protein Interactions. *Cell Cycle* **2007**, *6*, 434–437, doi:10.4161/cc.6.4.3861.
226. Zhang, Y.; Lu, H. Signaling to p53: Ribosomal Proteins Find Their Way. *Cancer Cell* **2009**, *16*, 369–377, doi:10.1016/j.ccr.2009.09.024.
227. Gazda, H.T.; Sheen, M.R.; Vlachos, A.; Choesmel, V.; O'donohue, M.-F.; Schneider, H.; Darras, N.; Hasman, C.; Sieff, C.A.; Newburger, P.E.; et al. Ribosomal Protein L5 and L11 Mutations Are Associated with Cleft Palate and Abnormal Thumbs in Diamond-Blackfan Anemia Patients. *Am. J. Hum. Genet.* **2008**, *83*, 769–780, doi:10.1016/j.ajhg.2008.11.004.
228. Derenzini, M.; Trere, D.; Pession, A.; Montanaro, L.; Sirri, V.; Ochst, R.L. Nucleolar Function and Size in Cancer Cells. *Am. J. Pathol.* **1998**, *152*, 1291–1297.
229. Bee, A.; Ke, Y.; Forootan, S.; Lin, K.; Beesley, C.; Forrest, S.E.; Foster, C.S. Ribosomal Protein L19 Is a Prognostic Marker for Human Prostate Cancer. *Clin. Cancer Res.* **2006**, *12*, doi:10.1158/1078-0432.CCR-05-2445.
230. Ishiguro, T.; Nakajima, M.; Naito, M.; Muto, T.; Tsuruo, T. Identification of genes differentially expressed in B16 murine melanoma sublines with different metastatic potentials. *Cancer Res.* **1996**, *56*, 875–879.
231. Ebert, B.L.; Pretz, J.; Bosco, J.; Chang, C.Y.; Tamayo, P.; Galili, N.; Raza, A.; Root, D.E.; Attar, E.; Ellis, S.R.; et al. Identification of RPS14 as a 5q-syndrome gene by RNA interference screen HHS Public Access. *Nature* **2008**, *451*, 335–339, doi:10.1038/nature06494.
232. Martoriati, A.; Doumont, G.; Alcalay, M.; Bellefroid, E.; Pelicci, P.G.; Marine, J.-C. dapk1, encoding an activator of a p19 ARF-p53-mediated apoptotic checkpoint, is a transcription target of p53. *Oncogene* **2005**, *24*, 1461–1466, doi:10.1038/sj.onc.1208256.
233. Danovi, D.; Meulmeester, E.; Pasini, D.; Migliorini, D.; Capra, M.; Frenk, R.; de Graaf, P.; Francoz, S.; Gasparini, P.; Gobbi, A.; et al. Amplification of Mdmx (or Mdm4) Directly Contributes to Tumor Formation by Inhibiting p53 Tumor Suppressor Activity. *Mol. Cell. Biol.* **2004**, *24*, 5835–5843, doi:10.1128/MCB.24.13.5835-5843.2004.
234. Chavez-Reyes, A.; Parant, J.M.; Amelse, L.L.; Montes, R.; Luna, O.; Korsmeyer, S.J.; Lozano, G. Switching Mechanisms of Cell Death in mdm2-and mdm4-null Mice by Deletion of p53 Downstream Targets. *Cancer Res.* **2003**, *63*, 8664–8669.
235. This reference is reference 185.
236. Parant, J.; Chavez-Reyes, A.; Little, N.A.; Yan, W.; Reinke, V.; Jochemsen, A.G.; Lozano, G. Rescue of embryonic lethality in Mdm4-null mice by loss of Trp53 suggests a nonoverlapping pathway with MDM2 to regulate p53. *Nat. Genet.* **2001**, *29*, doi:10.1038/ng714.
237. De Clercq, S.; Gembarska, A.; Denecker, G.; Maetens, M.; Naessens, M.; Haigh, K.; Haigh, J.J.; Marine, J.-C. Widespread Overexpression of Epitope-Tagged Mdm4 Does Not Accelerate Tumor Formation In Vivo. *Mol. Cell. Biol.* **2010**, *30*, 5394–5405, doi:10.1128/mcb.00330-10.

238. Francoz, S.; Froment, P.; Bogaerts, S.; De Clercq, S.; Maetens, M.; Doumont, G.; Bellefroid, E.; Marine, J.-C. Mdm4 and Mdm2 cooperate to inhibit p53 activity in proliferating and quiescent cells in vivo. *PNAS* **2006**, *103*, 3232–3237.
239. Migliorini, D.; Danovi, D.; Colombo, E.; Carbone, R.; Pelicci, P.G.; Marine, J.-C. Hdmx Recruitment into the Nucleus by Hdm2 Is Essential for Its Ability to Regulate p53 Stability and Transactivation. *J. Biol. Chem.* **2001**, *277*, 7318–7323, doi:10.1074/jbc.M108795200.
240. Tanimura, S.; Ohtsuka, S.; Mitsui, K.; Shirouzu, K.; Yoshimura, A.; Ohtsubo, M. MDM2 interacts with MDMX through their RING finger domains. *FEBS Lett.* **1999**, *447*, 5–9.
241. Pant, V.; Xiong, S.; Iwakuma, T.; Quintás-Cardama, A.; Lozano, G. Heterodimerization of Mdm2 and Mdm4 is critical for regulating p53 activity during embryogenesis but dispensable for p53 and Mdm2 stability. *PNAS* **2011**, *108*, 11995–12000, doi:10.1073/pnas.1102241108.
242. Carrillo, A.M.; Bouska, A.; Arrate, M.P.; Eischen, C.M. Mdmx promotes genomic instability independent of p53 and Mdm2. *Oncogene* **2015**, *34*, 846–856, doi:10.1038/onc.2014.27.
243. Gao, J.; Arman Aksoy, B.; Dogrusoz, U.; Dresdner, G.; Gross, B.; Onur Sumer, S.; Sun, Y.; Jacobsen, A.; Sinha, R.; Larsson, E.; et al. Integrative Analysis of Complex Cancer Genomics and Clinical Profiles Using the cBioPortalS. *Sci. Signal.* **2013**, *6*, doi:10.1126/scisignal.2004088.
244. Cerami, E.; Gao, J.; Dogrusoz, U.; Gross, B.E.; Sumer, S.O.; Aksoy, A.; Jacobsen, A.; Byrne, C.J.; Heuer, M.L.; Larsson, E.; et al. The cBio Cancer Genomics Portal: An Open Platform for Exploring Multidimensional Cancer Genomics Data. *Cancer Discov.* **2012**, *2*, 401–404, doi:10.1158/2159-8290.CD-12-0095.
245. Ramos, Y.F.M.; Stad, R.; Attema, J.; Peltenburg, L.T.C.; Van Der Eb, A.J.; Jochemsen, A.G. Aberrant Expression of HDMX Proteins in Tumor Cells Correlates with Wild-Type p53. *Cancer Res.* **2001**, *61*, 1839–1842.
246. Dewaele, M.; Marine, J.; Invest, J.C.; Dewaele, M.; Tabaglio, T.; Willekens, K.; Bezzi, M.; Teo, S.X.; Low, D.H.P.; Koh, C.M. Antisense oligonucleotide—Mediated MDM4 exon 6 skipping impairs tumor growth. *J. Clin. Invest.* **2016**, *126*, 68–84, doi:10.1172/JCI82534.MDM4.
247. Miranda, P.J.; Buckley, D.; Raghu, D.; Pang, J.-M.B.; Takano, E.A.; Vijayakumaran, R.; Teunisse, A.F.; Posner, A.; Procter, T.; Herold, M.J.; et al. MDM4 is a rational target for treating breast cancers with mutant p53. *J. Pathol.* **2017**, *241*, 661–670, doi:10.1002/path.4877.
248. Swetzig, W.M.; Wang, J.; Das, G.M. Estrogen receptor alpha (ERα/ESR1) mediates the p53-independent overexpression of MDM4/MDMX and MDM2 in human breast cancer. *Oncotarget* **2016**, *7*, 16049–16069.
249. Gilkes, D.M.; Pan, Y.; Coppola, D.; Yeatman, T.; Reuther, G.W.; Chen, J. Regulation of MDMX Expression by Mitogenic Signaling. *Mol. Cell. Biol.* **2008**, *28*, 1999–2010, doi:10.1128/MCB.01633-07.
250. Haupt, S.; Mejía-Hernández, J.O.; Vijayakumaran, R.; Keam, S.P.; Haupt, Y. The long and the short of it: The MDM4 tail so far. *J. Mol. Cell Biol.* **2019**, *11*, 231–244, doi:10.1093/jmcb/mjz007.
251. Wynendaale, J.; Böhnke, A.; Leucci, E.; Nielsen, S.J.; Lambert, I.; Hammer, S.; Sbrzesny, N.; Kubitza, D.; Wolf, A.; Gradhand, E.; et al. An illegitimate microRNA target site within the 3' UTR of MDM4 affects ovarian cancer progression and chemosensitivity. *Cancer Res.* **2010**, *70*, 9641–9649, doi:10.1158/0008-5472.CAN-10-0527.
252. Stegeman, S.; Moya, L.; Selth, L.A.; Spurdle, A.B.; Clements, J.A.; Batra, J. A genetic variant of MDM4 influences regulation by multiple microRNAs in prostate cancer. *Endocr. Relat. Cancer* **2015**, *22*, 265–276, doi:10.1530/ERC-15-0013.

253. Lagos-Quintana, M.; Rauhut, R.; Lendeckel, W. Identification of Novel Genes Coding for Small Expressed RNAs. *Science* **2001**, *294*, 853–858.
254. Elbashir, S.M.; Lendeckel, W.; Tuschl, T. RNA interference is mediated by 21-and 22-nucleotide RNAs. *Genes Dev.* **2001**, *15*, 188–200, doi:10.1101/gad.862301.
255. Zeng, Y.; Yi, R.; Cullen, B.R. MicroRNAs and small interfering RNAs can inhibit mRNA expression by similar mechanisms. *PNAS* **2003**, *100*, 9779–9784.
256. Prodosmo, A.; Giglio, S.; Moretti, S.; Mancini, F.; Barbi, F.; Avenia, N.; Di Conza, G.; Schünemann, H.J.; Pistola, L.; Ludovini, V.; et al. Analysis of human MDM4 variants in papillary thyroid carcinomas reveals new potential markers of cancer properties. *J. Mol. Med.* **2008**, *86*, 585–596, doi:10.1007/s00109-008-0322-6.
257. Bartel, F.; Schulz, J.; Böhnke, A.; Blümke, K.; Kappler, M.; Bache, M.; Schmidt, H.; Würfl, P.; Taubert, H.; Hauptmann, S. Significance of HDMX-S (or MDM4) mRNA splice variant overexpression and HDMX gene amplification on primary soft tissue sarcoma prognosis. *Int. J. Cancer* **2005**, *117*, 469–475, doi:10.1002/ijc.21206.
258. Pant, V.; Larsson, C.A.; Aryal, N.; Xiong, S.; James You, M.; Quintas-Cardama, A.; Lozano, G. Tumorigenesis promotes Mdm4-S overexpression. *Oncotarget* **2017**, *8*, 25837–25847.
259. Vin Chan, J.; Xin Ping Koh, D.; Liu, Y.; Joseph, T.L.; Lane, D.P.; Verma, C.S.; Sing Tan, Y. Role of the N-terminal lid in regulating the interaction of phosphorylated MDMX with p53. *Oncotarget* **2017**, *8*, 112825–112840.
260. Chen, L.; Gilkes, D.M.; Pan, Y.; Lane, W.S.; Chen, J. ATM and Chk2-dependent phosphorylation of MDMX contribute to p53 activation after DNA damage. *EMBO J.* **2005**, *24*, 3411–3422, doi:10.1038/sj.emboj.7600812.
261. Lebron, C.; Chen, L.; Gilkes, D.M.; Chen, J. Regulation of MDMX nuclear import and degradation by Chk2 and 14-3-3. *EMBO J.* **2006**, *25*, 1196–1206, doi:10.1038/sj.emboj.7601032.
262. Li, X.; Gilkes, D.; Li, B.; Cheng, Q.; Pernazza, D.; Lawrence, N.; Chen, J. Abnormal MDMX degradation in tumor cells due to ARF deficiency. *Oncogene* **2012**, *9*, 3721–3732, doi:10.1038/onc.2011.534.
263. Li, M.; Gu, W. A critical role for the non-coding 5S rRNA in regulating Mdmx stability. *Mol. Cell* **2011**, *43*, 1023–1032, doi:10.1016/j.molcel.2011.08.020.
264. Abbas, T.; Dutta, A. p21 in cancer: Intricate networks and multiple activities. *Nat. Rev. Cancer* **2009**, *9*, 400–414, doi:10.1038/nrc2657.
265. Galanos, P.; Vougas, K.; Walter, D.; Polyzos, A.; Maya-Mendoza, A.; Haagensen, E.J.; Kokkalis, A.; Roumelioti, F.-M.; Gagos, S.; Tzetis, M.; et al. Protracted p53-independent stimulation of p21 WAF1/Cip1 fuels genomic instability by deregulating the replication licensing machinery Europe PMC Funders Group. *Nat. Cell Biol.* **2016**, *18*, 777–789, doi:10.1038/ncb3378.
266. Galanos, P.; Pappas, G.; Polyzos, A.; Kotsinas, A.; Svolaki, I.; Giakoumakis, N.N.; Glytsou, C.; Pateras, I.S.; Swain, U.; Souliotis, V.L.; et al. Mutational signatures reveal the role of RAD52 in p53-independent p21-driven genomic instability. *Genome Biol.* **2018**, *19*, doi:10.1186/s13059-018-1401-9.
267. Brugarolas, J.; Chandrasekaran, C.; Gordon, J.I.; Beach, D.; Jacks, T.; Hannon, G.J. Radiation-induced cell cycle arrest compromised by p21 deficiency. *Nature* **1995**, *377*, 552–557.
268. Quelle, D.E.; Ashmun, R.A.; Shurtleff, S.A.; Kato, J.-Y.; Bar-Sagi, D.; Roussel, M.F.; Sherr, C.J. Overexpression of mouse D-type cyclins accelerates phase in rodent fibroblasts. *Genes Dev.* **1993**, *7*, 1559–1571.
269. Dou, Q.-P.; Levin, A.H.; Zhao, S.; Pardee, A.B. Cyclin E and Cyclin A as Candidates for the Restriction Point Protein1. *Cancer Res.* **1993**, *53*, 1493–1497.

270. Waga, S.; Hannon, G.J.; Beach, D.; Stillman, B. The p21 inhibitor of cyclin-dependent kinases controls DNA replication by interaction with PCNA. *Nature* **1994**, *369*, 574–578.
271. Kim, E.M.; Kim, J.; Park, J.K.; Hwang, S.-G.; Kim, W.-J.; Lee, W.-J.; Kang, S.W.; Um, H.-D. Bcl-w promotes cell invasion by blocking the invasion-suppressing action of Bax. *Cell. Signal.* **2012**, *24*, 1163–1172.
272. Dotto, G.P. p21 WAF1aCip1 : More than a break to the cell cycle? *Biochim. Biophysica Acta* **2000**, *1471*, 43–56.
273. Roninson, I.B. Oncogenic functions of tumour suppressor p21 Waf1/Cip1/Sdi1 : Association with cell senescence and tumour-promoting activities of stromal fibroblasts. *Cancer Lett.* **2002**, *179*, 1–14.
274. Gartel, A.L.; Tyner, A.L. The Role of the Cyclin-dependent Kinase Inhibitor p21 in Apoptosis 1. *Mol. Cancer Ther.* **2002**, *1*, 349–639.
275. Georgakilas, A.G.; Martin, O.A.; Bonner, W.M. p21: A Two-Faced Genome Guardian. *Trends Mol. Med.* **2017**, *23*, doi:10.1016/j.molmed.2017.02.001.
276. Kim, E.M.; Jung, C.H.; Kim, J.; Hwang, S.G.; Park, J.K.; Um, H.D. The p53/p21 complex regulates cancer cell invasion and apoptosis by targeting Bcl-2 family proteins. *Cancer Res.* **2017**, *77*, 3092–3100, doi:10.1158/0008-5472.CAN-16-2098.
277. Chang, B.-D.; Watanabe, K.; Broude, E.V.; Fang, J.; Poole, J.C.; Kalinichenko, T.V.; Roninson, I.B. Effects of p21 Waf1/Cip1/Sdi1 on cellular gene expression: Implications for carcinogenesis, senescence, and age-related diseases. *PNAS* **2000**, *97*, 4291–4296.
278. Lukas, J.; Bártková, J.; Rohde, M.; Strauss, M.; Bartek, J. Cyclin D1 Is Dispensable for G 1 Control in Retinoblastoma Gene-Deficient Cells Independently of cdk4 Activity. *Mol. Cell. Biol.* **1995**, *15*, 2600–2611.
279. Ren, B.; Cam, H.; Takahashi, Y.; Volkert, T.; Terragni, J.; Young, R.A.; Dynlacht, B.D. E2F integrates cell cycle progression with DNA repair, replication, and G 2 /M checkpoints. *Genes Dev.* **2002**, *16*, 245–256, doi:10.1101/gad.949802.
280. Shiohara, M.; El-Deiry, W.S.; Wada, M.; Nakamaki, T.; Takeuchi, S.; Yang, rong; Chen, D.-L.; Vogelstein, B.; Koeffler, H.P. Absence of WAF1 Mutations in a Variety of Human Malignancies. *Blood* **1994**, *84*, 3782–3784.
281. Deng, C.; Zhang, P.; Harper, J.W.; Elledge, S.J.; Leder, P. Mice Lacking p21 CIP1/WAF1 Undergo Normal Development, but Are Defective in G1 Checkpoint Control. *Cell* **1995**, *82*, 675–684.
282. Martín-Caballero, J.; Flores, J.M.; García-Palencia, P.; Serrano, M. Tumor Susceptibility of p21 Waf1/Cip1-deficient Mice 1. *Cancer Res.* **2001**, *61*, 6234–6238.
283. Quereda, V.; Martinalbo, J.; Dubus, P.; Carnero, A.; Malumbres, M. Genetic cooperation between p21 Cip1 and INK4 inhibitors in cellular senescence and tumor suppression. *Oncogene* **2007**, *26*, 7665–7674, doi:10.1038/sj.onc.1210578.
284. Adnane, J.; Jackson, R.J.; Nicosia, S.V.; Cantor, A.B.; Jack Pledger, W.; Sebt, S.M.M. Loss of p21 WAF1/CIP1 accelerates Ras oncogenesis in a transgenic/knockout mammary cancer model. *Oncogene* **2000**, *19*, 5338–5347.
285. Duan, Z.; Zarebski, A.; Montoya-Durango, D.; Leighton Grimes, H.; Horwitz, M. Gfi1 Coordinates Epigenetic Repression of p21 Cip/WAF1 by Recruitment of Histone Lysine Methyltransferase G9a and Histone Deacetylase 1. *Mol. Cell. Biol.* **2005**, *25*, 10338–10351, doi:10.1128/MCB.25.23.10338-10351.2005.
286. Schmidt, T.; Karsunky, H.; Gau, E.; Zevnik, B.; Elsässer, H.-P.; Mörröy, Y.T. Zinc finger protein GFI-1 has low oncogenic potential but cooperates strongly with pim and myc genes in T-cell lymphomagenesis. *Oncogene* **1998**, *17*, 2661–2667.

287. Kazanjian, A.; Wallis, D.; Au, N.; Nigam, R.; Venken, K.J.T.; Cagle, P.T.; Dickey, B.F.; Bellen, H.J.; Gilks, C.B.; Grimes, H.L. Growth Factor Independence-1 Is Expressed in Primary Human Neuroendocrine Lung Carcinomas and Mediates the Differentiation of Murine Pulmonary Neuroendocrine Cells. *Cancer Res.* **2004**, *64*, 6874–6882.
288. Wang, Y.A.; Elson, A.; Leder, P. Loss of p21 increases sensitivity to ionizing radiation and delays the onset of lymphoma in atm-deficient mice. *PNAS* **1997**, *94*, 14590–14595.
289. Gartel, A.L. Is p21 an oncogene? *Mol. Cancer Ther.* **2006**, *5*, doi:10.1158/1535-7163.MCT-06-0163.
290. Missero, C.; Cunto, F. Di; Kiyokawa, H.; Koff, A.; Dotto, G.P. The absence of p21Cipl/wAF1 alters keratinocyte growth and differentiation and promotes ras-tumor progression. *Genes Dev.* **1996**, *10*, 3065–3075.
291. Evangelou, K.; Galanos, P.; Gorgoulis, V.G. The Janus face of p21. *Mol. Cell. Oncol.* **2016**, *3*, doi:10.1080/23723556.2016.1215776.
292. Pomerantz, J.; Schreiber-Agus, N.; Liégeois, N.J.; Silverman, A.; Alland, L.; Chin, L.; Potes, J.; Chen, K.; Orlow, I.; Lee, H.W.; et al. The Ink4a tumor suppressor gene product, p19(Arf), interacts with MDM2 and neutralizes MDM2's inhibition of p53. *Cell* **1998**, *92*, 713–723, doi:10.1016/S0092-8674(00)81400-2.
293. Quelle, D.E.; Zindy, F.; Ashmun, R.A.; Sherr, C.J. Alternative reading frames of the INK4a tumor suppressor gene encode two unrelated proteins capable of inducing cell cycle arrest. *Cell* **1995**, *83*, 993–1000, doi:10.1016/0092-8674(95)90214-7.
294. Mao, L.; Merlo, A.; Bedi, G.; Shapiro, G.I.; Edwards, C.D.; Rollins, B.J.; Sidransky, D. A Novel p16INK4A Transcript. *Cancer Res.* **1995**, *55*, 2995–2997.
295. Zhang, Y.; Xiong, Y.; Yarbrough, W.G. ARF Promotes MDM2 Degradation and Stabilizes p53: ARF-INK4a Locus Deletion Impairs Both the Rb and p53 Tumor Suppression Pathways. *Cell* **1998**, *92*, 725–734.
296. Kamijo, T.; Zindy, F.; Roussel, M.F.; Quelle, D.E.; Downing, J.R.; Ashmun, R.A.; Grosveld, G.; Sherr, C.J. Tumor suppression at the mouse INK4a locus mediated by the alternative reading frame product p19(ARF). *Cell* **1997**, *91*, 649–659, doi:10.1016/S0092-8674(00)80452-3.
297. Zhang, Y.; Xiong, Y. Mutations in Human ARF Exon 2 Disrupt Its Nucleolar Localization and Impair Its Ability to Block Nuclear Export of MDM2 and p53. *Mol. Cell* **1999**, *3*, 579–591.
298. Weber, H.O.; Samuel, T.; Rauch, P.; Funk, J.O. Human p14 ARF-mediated cell cycle arrest strictly depends on intact p53 signaling pathways. *Oncogene* **2002**, *21*, 3207–3212, doi:10.1038/sj/onc/1205429.
299. Honda, R.; Yasuda, H. Association of p19 ARF with Mdm2 inhibits ubiquitin ligase activity of Mdm2 for tumor suppressor p53. *EMBO J.* **1999**, *18*, 22–27.
300. Weber, J.D.; Jeffers, J.R.; Rehg, J.E.; Randle, D.H.; Lozano, G.; Roussel, M.F.; Sherr, C.J.; Zambetti, G.P. p53-independent functions of the p19 ARF tumor suppressor. *Genes Dev.* **2000**, *14*, 2358–2365, doi:10.1101/gad.827300.
301. Eischen, C.M.; Weber, J.D.; Roussel, M.F.; Sherr, C.J.; Cleveland, J.L. Disruption of the ARF-Mdm2-p53 tumor suppressor pathway in Myc-induced lymphomagenesis. *Genes Dev.* **1999**, *13*, 2658–2669.
302. Tompkins, V.; Hagen, J.; Zediak, V.P.; Quelle, D.E. Identification of novel ARF binding proteins by two-hybrid screening. *Cell Cycle* **2006**, *5*, 641–646.
303. Britigan, E.M.C.; Wan, J.; Zasadil, L.M.; Ryan, S.D.; Weaver, B.A. The ARF tumor suppressor prevents chromosomal instability and ensures mitotic checkpoint fidelity through regulation of Aurora B. *Mol. Biol. Cell* **2014**, *25*, doi:10.1091/mbc.E14-05-0966.

304. Churchman, M.L.; Roig, I.; Jasin, M.; Keeney, S.; Sherr, C.J. Expression of Arf Tumor Suppressor in Spermatogonia Facilitates Meiotic Progression in Male Germ Cells. *PLoS Genet.* **2011**, *7*, 1002157, doi:10.1371/journal.pgen.1002157.
305. Gromley, A.; Churchman, M.L.; Zindy, F.; Sherr, C.J. Transient expression of the Arf tumor suppressor during male germ cell and eye development in Arf-Cre reporter mice. *PNAS* **2009**, *106*, 6285–6290.
306. Fulci, G.; Labuhn, M.; Maier, D.; Lachat, Y.; Hausmann, O.; Hegi, M.E.; Janzer, R.C.; Merlo, A.; Van Meir, E.G. p53 gene mutation and ink4a-arf deletion appear to be two mutually exclusive events in human glioblastoma. *Oncogene* **2000**, *19*, 3816–3822.
307. Hegi, M.E.; Zur Hausen, A.; Rüedi, D.; Malin, G.; Kleihues, P. Hemizygous or homozygous deletion of the chromosomal region containing the p16INK4a gene is associated with amplification of the EGF receptor gene in glioblastomas. *J. Cancer* **1997**, *73*, 57–63.
308. Esteller, M.; Tortola, S.; Toyota, M.; Capella, G.; Peinado, M.A.; Baylin, S.B.; Herman, J.G. Hypermethylation-associated inactivation of p14(ARF) is independent of p16(INK4a) methylation and p53 mutational status. *Cancer Res.* **2000**, *60*, 129–133.
309. Ren, Y.; Xiao, L.; Weng, G.; Shi, B. Clinical significance of p16 INK4A and p14 ARF promoter methylation in renal cell carcinoma: A meta-analysis. *Oncotarget* **2017**, *8*, 64385–64394.
310. Burri, N.; Shaw, P.; Bouzourene, H.; Sordat, I.; Sordat, B.; Gillet, M.; Schorderet, D.; Bosman, F.T.; Chaubert, P. Methylation Silencing and Mutations of the p14 ARF and p16 INK4a Genes in Colon Cancer. *Lab. Investig.* **2001**, *81*, 271.
311. Fotouhi, O.; Fahmideh, M.A.; Kjellman, M.; Sulaiman, L.; Höög, A.; Zedenius, J.; Hashemi, J.; Larsson, C. Global hypomethylation and promotor methylation in small intestinal neuroendocrine tumors. *Epigenetics* **2014**, *9*, 987–997, doi:10.4161/epi.28936.
312. Esteller, M.; Cordon-Cardo, C.; Corn, P.G.; Meltzer, S.J.; Pohar, K.S.; Watkins, D.N.; Capella, G.; Peinado, M.A.; Matias-Guiu, X.; Prat, J.; et al. p14 ARF Silencing by Promoter Hypermethylation Mediates Abnormal Intracellular Localization of MDM2. *Cancer Res.* **2001**, *61*, 2816–2821.
313. Budina-Kolomets, A.; Hontz, R.D.; Pimkina, J.; Murphy, M.E. A conserved domain in exon 2 coding for the human and murine ARF tumor suppressor protein is required for autophagy induction. *Autophagy* **2013**, *9*, 1553–1565, doi:10.4161/auto.25831.
314. Xie, Y.; Liu, S.; Lu, W.; Yang, Q.; Williams, K.D.; Binhazim, A.A.; Carver, B.S.; Matusik, R.J.; Chen, Z. Slug regulates E-cadherin repression via p19Arf in prostate tumorigenesis. *Mol. Oncol.* **2014**, *8*, 1355–1364, doi:10.1016/j.molonc.2014.05.006.
315. Xie, Y.; Lu, W.; Liu, S.; Yang, Q.; Shawn Goodwin, J.; Sathyanarayana, S.A.; Pratap, S.; Chen, Z. MMP7 interacts with ARF in nucleus to potentiate tumor microenvironments for prostate cancer progression in vivo. *Oncotarget* **2016**, *7*, 47609–47619, doi:10.18632/oncotarget.10251.
316. Owczarek, T.B.; Kobayashi, T.; Ramirez, R.; Rong, L.; Puzio-Kuter, A.M.; Teo, M.Y.; Sánchez-Vega, F.; Wang, J.; Schultz, N.; Zheng, T.; et al. ARF confers a context-dependent response to chemotherapy in muscle invasive bladder cancer. *Cancer Res.* **2017**, *77*, 1035–1046, doi:10.1158/0008-5472.CAN-16-2621.
317. Harland, M.; Taylor, C.F.; Chambers, P.A.; Kukulicz, K.; Randerson-Moor, J.A.; Gruis, N.A.; De Snoo, F.A.; Ac Ter Huurne, J.; Goldstein, A.M.; Tucker, M.A.; et al. A mutation hotspot at the p14ARF splice site. *Oncogene* **2005**, *24*, 4604–4608, doi:10.1038/sj.onc.1208678.
318. Reddy, B.A.; Etkin, L.D.; Freemont, P.S. A novel zinc finger coiled-coil domain in a family of nuclear proteins. *Trends Biochem. Sci.* **1992**, *17*, 443–453.

319. Reymond, A.; Meroni, G.; Fantozzi, A.; Merla, G.; Cairo, S.; Luzi, L.; Riganelli, D.; Zanaria, E.; Messali, S.; Cainarca, S.; et al. The tripartite motif family identifies cell compartments. *EMBO J.* **2001**, *20*, 2140–2151.
320. Li, Y.; Wu, H.; Wu, W.; Zhuo, W.; Liu, W.; Zhang, Y.; Cheng, M.; Chen, Y.-G.; Gao, N.; Yu, H.; et al. Structural insights into the TRIM family of ubiquitin E3 ligases. *Cell Res.* **2014**, *24*, doi:10.1038/cr.2014.46.
321. Zhou, Z.; Ji, Z.; Wang, Y.; Li, J.; Cao, H.; Zhu, H.H.; Gao, W.-Q. TRIM59 Is Up-regulated in Gastric Tumors, Promoting Ubiquitination and Degradation of p53. *Gastroenterology* **2014**, *147*, 1043–1054, doi:10.1053/j.gastro.2014.07.021.
322. Han, Y.; Tan, Y.; Zhao, Y.; Zhang, Y.; He, X.; Yu, L.; Jiang, H.; Lu, H.; Tian, H. TRIM23 overexpression is a poor prognostic factor and contributes to carcinogenesis in colorectal cancer. *J. Cell. Mol. Med.* **2020**, *24*, 5491–5500, doi:10.1111/jcmm.15203.
323. Zhang, Y.; Du, H.; Li, Y.; Yuan, Y.; Chen, B.; Sun, S. Elevated TRIM23 expression predicts cisplatin resistance in lung adenocarcinoma. *Cancer Sci.* **2020**, *111*, 637–646, doi:10.1111/cas.14226.
324. Yin, H.; Li, Z.; Chen, J.; Jia, H.; X. Expression and the potential functions of TRIM32 in lung cancer tumorigenesis. *J. Cell. Biochem.* **2018**, *120*, doi:10.1002/jcb.27798.
325. Liu, J.; Zhang, C.; Wang, X.L.; Ly, P.; Belyi, V.; Xu-Monette, Z.Y.; Young, K.H.; Hu, W.; Feng, Z. E3 ubiquitin ligase TRIM32 negatively regulates tumor suppressor p53 to promote tumorigenesis. *Cell Death Differ.* **2014**, *21*, 1792–1804, doi:10.1038/cdd.2014.121.
326. Zhan, W.; Han, T.; Zhang, C.; Xie, C.; Gan, M.; Deng, K.; Fu, M.; Wang, J.-B. TRIM59 Promotes the Proliferation and Migration of Non-Small Cell Lung Cancer Cells by Upregulating Cell Cycle Related Proteins. *PLoS ONE* **2015**, *10*, doi:10.1371/journal.pone.0142596.
327. Sun, Y.; Ji, B.; Feng, Y.; Zhang, Y.; Ji, D.; Zhu, C.; Wang, S.; Zhang, C.; Zhang, D.; Sun, Y. TRIM59 facilitates the proliferation of colorectal cancer and promotes metastasis via the PI3K/AKT pathway. *Oncol. Rep.* **2017**, *38*, 43–52, doi:10.3892/or.2017.5654.
328. Liang, J.; Xing, D.; Li, Z.; Shen, J.; Zhao, H.; Li, S. TRIM59 is upregulated and promotes cell proliferation and migration in human osteosarcoma. *Mol. Med. Rep.* **2016**, *13*, 5200–5206.
329. Shen, H.; Zhang, J.; Zhang, Y.; Feng, Q.; Wang, H.; Li, G.; Jiang, W.; Li, X. Knockdown of tripartite motif 59 (TRIM59) inhibits proliferation in cholangiocarcinoma via the PI3K/AKT/mTOR signalling pathway. *Gene* **2019**, *698*, 50–60, doi:10.1016/j.gene.2019.02.044.
330. Frankish, A.; Diekhans, M.; Ferreira, A.-M.; Johnson, R.; Jungreis, I.; Loveland, J.; Mudge, J.M.; Sisu, C.; Wright, J.; Armstrong, J.; et al. GENCODE reference annotation for the human and mouse genomes. *Nucleic Acids Res.* **2019**, *47*, 767, doi:10.1093/nar/gky955.
331. Guttman, M.; Amit, I.; Garber, M.; French, C.; Lin, M.F.; Feldser, D.; Huarte, M.; Zuk, O.; Carey, B.W.; Cassady, J.P.; et al. Chromatin signature reveals over a thousand highly conserved large non-coding RNAs in mammals. *Nature* **2009**, *458*, 223–227, doi:10.1038/nature07672.
332. Derrien, T.; Johnson, R.; Bussotti, G.; Tanzer, A.; Djebali, S.; Tilgner, H.; Guernec, G.; Martin, D.; Merkel, A.; Knowles, D.G.; et al. The GENCODE v7 catalog of human long noncoding RNAs: Analysis of their gene structure, evolution, and expression. *Genome Res.* **2012**, *22*, 1775–1789, doi:10.1101/gr.132159.111.
333. Congrains, A.; Kamide, K.; Ohishi, M.; Rakugi, H. ANRIL: Molecular Mechanisms and Implications in Human Health. *Int. J. Mol. Sci.* **2013**, *14*, 1278–1292, doi:10.3390/ijms14011278.

334. Gordon, F.E.; Nutt, C.L.; Cheunsuchon, P.; Nakayama, Y.; Provencher, K.A.; Rice, K.A.; Zhou, Y.; Zhang, X.; Klibanski, A. Increased Expression of Angiogenic Genes in the Brains of Mouse Meg3-Null Embryos. *Endocrinology* **2010**, *151*, 2443–2452, doi:10.1210/en.2009-1151.
335. Brown, C.J.; Balabio, A.; Rupert, J.L.; Lafreniere, R.G.; Grompe, M.; Tonlorenzi, R.; Willard, H.F. A gene from the region of the human X inactivation centre is expressed exclusively from the inactive X chromosome. *Nature* **1991**, *349*, 38–44.
336. Guttman, M.; Donaghey, J.; Carey, B.W.; Garber, M.; Grenier, J.K.; Munson, G.; Young, G.; Lucas, A.B.; Ach, R.; Bruhn, L.; et al. lincRNAs act in the circuitry controlling pluripotency and differentiation. *Nature* **2012**, *477*, 295–300, doi:10.1038/nature10398.
337. Yap, K.L.; Li, S.; Muñoz-Cabello, A.M.; Raguz, S.; Zeng, L.; Mujtaba, S.; Gil, J.; Walsh, M.J.; Zhou, M.-M. Molecular Interplay of the Non-coding RNA ANRIL and Methylated Histone H3 Lysine 27 by Polycomb CBX7 in Transcriptional Silencing of INK4a. *Mol. Cell* **2010**, *38*, 662–674, doi:10.1016/j.molcel.2010.03.021.
338. Pasmant, E.; Laurendeau, I.; Héron, D.; Vidaud, M.; Vidaud, D.; Bièche, I. Characterization of a Germ-Line Deletion, Including the Entire INK4/ARF Locus, in a Melanoma-Neural System Tumor Family: Identification of ANRIL, an Antisense Noncoding RNA Whose Expression Coclusters with ARF. *Cancer Res.* **2007**, *67*, doi:10.1158/0008-5472.CAN-06-2004.
339. Cunnington, M.S.; Koref, M.S.; Mayosi, B.M.; Burn, J.; Keavney, B. Chromosome 9p21 SNPs Associated with Multiple Disease Phenotypes Correlate with ANRIL Expression. *PLoS Genet.* **2010**, *6*, doi:10.1371/journal.pgen.1000899.
340. Pal, S.; Datta, K.; Mukhopadhyay, D. Central Role of p53 on Regulation of Vascular Permeability Factor/ Vascular Endothelial Growth Factor (VPF/VEGF) Expression in Mammary Carcinoma 1. *Cancer Res.* **2001**, *61*, 6952–6957.
341. Lee, Y.; Ahn, C.; Han, J.; Choi, H.; Kim, J.; Yim, J.; Lee, J.; Provost, P.; Rådmark, O.; Kim, S.; et al. The nuclear RNase III Drosha initiates microRNA processing. *Nature* **2003**, *425*, 415–419.
342. Hutvagner, G.; Mclachlan, J.; Pasquinelli, A.E.; Bálint, É.; Tuschl, T.; Zamore, P.D. A Cellular Function for the RNA-Interference Enzyme Dicer in the Maturation of the let-7 Small Temporal RNA. *Science* **2001**, *293*, 834–838.
343. Bernstein, E.; Kim, S.Y.; Carmell, M.A.; Murchison, E.P.; Alcorn, H.; Li, M.Z.; Mills, A.A.; Elledge, S.J.; Anderson, K.V.; Hannon, G.J. Dicer is essential for mouse development. *Nat. Genet.* **2003**, *35*, doi:10.1038/ng1253.
344. Doench, J.G.; Sharp, P.A. Specificity of microRNA target selection in translational repression. *Genes Dev.* **2004**, *18*, 504–511, doi:10.1101/gad.1184404.
345. Hammond, S.M.; Bernstein, E.; Beach, D.; Hannon, G.J. An RNA-directed nuclease mediates post-transcriptional gene silencing in Drosophila cells. *Nature* **2000**, *404*, 293–296, doi:10.1038/35005107.
346. Le, M.T.N.; Teh, C.; Shyh-Chang, N.; Xie, H.; Zhou, B.; Korzh, V.; Lodish, H.F.; Lim, B. MicroRNA-125b is a novel negative regulator of p53. *Genes Dev.* **2009**, *23*, 862–876, doi:10.1101/gad.1767609.
347. Shi, X.-B.; Xue, L.; Yang, J.; Ma, A.-H.; Zhao, J.; Xu, M.; Tepper, C.G.; Evans, C.P.; Kung, H.-J.; deVere White, R.W. An androgen-regulated miRNA suppresses Bak1 expression and induces androgen-independent growth of prostate cancer cells. *PNAS* **2007**, *104*, 19983–19988.
348. Bousquet, M.; Quelen, C.; Rosati, R.; Mas, V.M. De; Starza, R. La; Bastard, C.; Lippert, E.; Talmant, P.; Lafage-Pochitaloff, M.; Leroux, D.; et al. Myeloid cell differentiation arrest by miR-125b-1 in myelodysplastic syndrome and acute myeloid leukemia with the t(2;11)(p21;q23) translocation. *J. Exp. Med.* **2008**, *205*, 2499–2506, doi:10.1084/jem.20080285.

349. Chen, L.; Luo, L.; Chen, W.; Xu, H.-X.; Chen, F.; Chen, L.-Z.; Zeng, W.-T.; Chen, J.-S.; Huang, X.-H. MicroRNA-24 increases hepatocellular carcinoma cell metastasis and invasion by targeting p53: miR-24 targeted p53. *Biomed. Pharmacother.* **2016**, *84*, 1113–1118, doi:10.1016/j.biopha.2016.10.051.
350. Zhang, C.; Liu, J.; Wang, X.; Wu, R.; Lin, M.; Laddha, S.V.; Yang, Q.; Chan, C.S.; Feng, Z. MicroRNA-339-5p inhibits colorectal tumorigenesis through regulation of the MDM2/p53 signaling. *Oncotarget* **2014**, *15*, 9106–9117.
351. Zhang, C.; Liu, J.; Tan, C.; Yue, X.; Zhao, Y.; Peng, J.; Wang, X.; Laddha, S.V.; Chan, C.S.; Zheng, S.; et al. microRNA-1827 represses MDM2 to positively regulate tumor suppressor p53 and suppress tumorigenesis. *Oncotarget* **2016**, *7*, 8783–8796.
352. Zhou, C.; Liu, G.; Wang, L.; Lu, Y.; Yuan, L.; Zheng, L.; Chen, F.; Peng, F.; Li, X. MiR-339-5p Regulates the Growth, Colony Formation and Metastasis of Colorectal Cancer Cells by Targeting PRL-1. *PLoS ONE* **2013**, *8*, doi:10.1371/journal.pone.0063142.
353. Wu, Z.-S.; Wu, Q.; Wang, C.-Q.; Wang, X.-N.; Wang, Y.; Zhao, J.-J.; Mao, S.-S.; Zhang, G.-H.; Zhang, N.; Xu, X.-C. MiR-339-5p inhibits breast cancer cell migration and invasion in vitro and may be a potential biomarker for breast cancer prognosis. *BMC Cancer* **2010**, *10*, doi:10.1186/1471-2407-10-542.
354. Bae, Y.U.; Son, Y.; Kim, C.H.; Kim, K.S.; Hyun, S.H.; Woo, H.G.; Jee, B.A.; Choi, J.H.; Sung, H.K.; Choi, H.C.; et al. Embryonic Stem Cell-Derived mmu-miR-291a-3p Inhibits Cellular Senescence in Human Dermal Fibroblasts Through the TGF- β Receptor 2 Pathway. *J. Gerontol. A Biol. Sci. Med. Sci.* **2019**, *74*, 1359–1367, doi:10.1093/gerona/gly208.
355. Rasko, J.E.J.; Klenova, E.M.; Leon, J.; Filippova, G.N.; Loukinov, D.I.; Vatolin, S.; Robinson, A.F.; Hu, Y.J.; Ulmer, J.; Ward, M.D.; et al. Cell Growth Inhibition by the Multifunctional Multivalent Zinc-Finger Factor CTCF. *Cancer Res.* **2001**, *61*, 6002–6007.
356. Lobanekov, V.V.; Nicolas, R.H.; Adler, V.V.; Paterson, H.; Klenova, E.M.; Polotskaja, A.V.; Goodwin, G.H. A novel sequence-specific DNA binding protein which interacts with three regularly spaced direct repeats of the CCCTC-motif in the 5'-flanking sequence of the chicken c-myc gene. *Oncogene* **1990**, *5*, 1743–1753.
357. Filippova, G.N.; Fagerlie, S.; Klenova, E.M.; Myers, C.; Dehner, Y.; Goodwin, G.; Neiman, P.E.; Collins, S.J.; Lobanekov, V. V An Exceptionally Conserved Transcriptional Repressor, CTCF, Employs Different Combinations of Zinc Fingers To Bind Diverged Promoter Sequences of Avian and Mammalian c-myc Oncogenes. *Mol. Cell. Biol.* **1996**, *16*, 2802–2813.
358. Klenova, E.M.; Nicolas, R.H.; Paterson, H.F.; Carne, A.F.; Heath, C.M.; Goodwin, G.H.; Neiman, P.E.; Lobanekov3, V.V.; Lobanekov, V.V.; Nicolas, R.H.; et al. CTCF, a Conserved Nuclear Factor Required for Optimal Transcriptional Activity of the Chicken c-myc Gene, Is an 11-Zn-Finger Protein Differentially Expressed in Multiple Forms. *Mol. Cell. Biol.* **1993**, *13*, 7612–7624.
359. Kanduri, C.; Pant, V.; Loukinov, D.; Pugacheva, E.; Qi, C.-F.; Wolffe, A.; Ohlsson, R.; Lobanekov, V. V Functional association of CTCF with the insulator upstream of the H19 gene is parent of origin-specific and methylation-sensitive. *Curr. Biol.* **2000**, *10*, 853–856.
360. Quitschke, W.W.; Taheny, M.J.; Fochtman, L.J.; Vostrov, A.A. Differential effect of zinc finger deletions on the binding of CTCF to the promoter of the amyloid precursor protein gene. *Nucleic Acids Res.* **2000**, *28*, 3370–3378.
361. Chen, H.; Tian, Y.; Shu, W.; Bo, X.; Wang, S. Comprehensive Identification and Annotation of Cell Type-Specific and Ubiquitous CTCF-Binding Sites in the Human Genome. *PLoS ONE* **2012**, *7*, 41374, doi:10.1371/journal.pone.0041374.

362. Moore, J.M.; Rabaia, N.A.; Smith, L.E.; Fagerlie, S.; Gurley, K. Loss of Maternal CTCF Is Associated with Peri-Implantation Lethality of Ctfc Null Embryos. *PLoS ONE* **2012**, *7*, 34915, doi:10.1371/journal.pone.0034915.
363. Macpherson, M.J.; Beatty, L.G.; Zhou, W.; Du, M.; Sadowski, P.D. The CTCF Insulator Protein Is Posttranslationally Modified by SUMO. *Mol. Cell. Biol.* **2009**, *29*, 714–725, doi:10.1128/MCB.00825-08.
364. Yu, W.; Ginjala, V.; Pant, V.; Chernukhin, I.; Whitehead, J.; Docquier, F.; Farrar, D.; Tavoosidana, G.; Mukhopadhyay, R.; Kanduri, C.; et al. Poly(ADP-ribosyl)ation regulates CTCF-dependent chromatin insulation. *Nat. Genet.* **2004**, *36*, doi:10.1038/ng1426.
365. Kemp, C.J.; Moore, J.M.; Moser, R.; Bernard, B.; Teater, M.; Smith, L.E.; Rabaia, N.A.; Gurley, K.E.; Guinney, J.; Busch, S.E.; et al. CTCF haploinsufficiency destabilizes DNA methylation and predisposes to cancer. *Cell Rep.* **2014**, *7*, 1020–1029, doi:10.1016/j.celrep.2014.04.004.
366. Filippova, G.N.; Lindblom, A.; Meincke, L.J.; Klenova, E.M.; Neiman, P.E.; Collins, S.J.; Doggett, N.A.; Lobanenko, V. V A Widely Expressed Transcription Factor With Multiple DNA Sequence Specificity, CTCF, Is Localized at Chromosome Segment 16q22.1 Within One of the Smallest Regions of Overlap for Common Deletions in Breast and Prostate Cancers. *Genes. Chromosomes Cancer* **1998**, *22*, 26–36.
367. Soto-Reyes, E.; Recillas-Targa, F. Epigenetic regulation of the human p53 gene promoter by the CTCF transcription factor in transformed cell lines. *Oncogene* **2010**, *29*, 2217–2227, doi:10.1038/onc.2009.509.
368. Witcher, M.; Emerson, B.M. Epigenetic Silencing of the p16 INK4a Tumor Suppressor is Associated with Loss of CTCF Binding and a Chromatin Boundary. *Mol. Cell* **2009**, *34*, 271–284, doi:10.1016/j.molcel.2009.04.001.
369. Docquier, F.; Farrar, D.; Arcy, V.D.; Chernukhin, I.; Robinson, A.F.; Loukinov, D.; Vatolin, S.; Pack, S.; Mackay, A.; Harris, R.A.; et al. Heightened Expression of CTCF in Breast Cancer Cells Is Associated with Resistance to Apoptosis. *Cancer Res.* **2005**, *65*, 5112–5122.
370. Méndez-Catalá, C.F.; Gretton, S.; Vostrov, A.; Pugacheva, E.; Farrar, D.; Ito, Y.; Docquier, F.; Kita, G.-X.; Murrell, A.; Lobanenko, V.; et al. A novel mechanism for CTCF in the epigenetic regulation of Bax in breast cancer cells. *Neoplasia* **2013**, *15*, 912, doi:10.1593/neo.121948.
371. Lee, J.-Y.; Mustafa, M.; Yuri Kim, C.; Hee Kim, M. Depletion of CTCF in Breast Cancer Cells Selectively Induces Cancer Cell Death via p53. *J. Cancer* **2017**, *8*, 2124–2131, doi:10.7150/jca.18818.
372. Basu, S.; Murphy, M.E. Genetic modifiers of the p53 pathway. *Cold Spring Harb. Perspect. Med.* **2016**, *6*, a026302, doi:10.1101/cshperspect.a026302.
373. Ruggero, D.; Grisendi, S.; Piazza, F.; Rego, E.; Mari, F.; Rao, P.H.; Cordon-Cardo, C.; Pandolfi, P.P. Dyskeratosis Congenita and Cancer in Mice Deficient in Ribosomal RNA Modification. *Science* **2003**, *299*, 259–262.
374. Wang, D.; Wengrod, J.; Gardner, L.B. Overexpression of the c-myc Oncogene Inhibits Nonsense-mediated RNA Decay in B Lymphocytes. *J. Biol. Chem.* **2011**, *286*, 40038–40043, doi:10.1074/jbc.M111.266361.
375. Kalkat, M.; De Melo, J.; Hickman, K.A.; Lourenco, C.; Redel, C.; Resetca, D.; Tamachi, A.; Tu, W.B.; Penn, L.Z. MYC Deregulation in Primary Human Cancers. *Genes* **2017**, *8*, doi:10.3390/genes8060151.
376. He, X.; Zhang, P. Serine/arginine-rich splicing factor 3 (SRSF3) regulates homologous recombination-mediated DNA repair. *Mol. Cancer* **2015**, *14*, doi:10.1186/s12943-015-0422-1.
377. Jia, R.; Li, C.; Mccoy, J.P.; Deng, C.-X.; Zheng, Z.-M. SRp20 is a proto-oncogene critical for cell proliferation and tumor induction and maintenance. *Int. J. Biol. Sci.* **2010**, *6*, 806–826.

378. Mitsuuchi, Y.; Johnson, S.W.; Selvakumaran, M.; Williams, S.J.; Hamilton, T.C.; Testa, J.R. The Phosphatidylinositol 3-Kinase/AKT Signal Transduction Pathway Plays a Critical Role in the Expression of p21 WAF1/CIP1/SDI1 Induced by Cisplatin and Paclitaxel. *Cancer Res.* **2000**, *60*, 5390–5394.
379. Sun, L.; Li, Y.; Yang, B. Downregulated long non-coding RNA MEG3 in breast cancer regulates proliferation, migration and invasion by depending on p53's transcriptional activity. *Biochem. Biophys. Res. Commun.* **2016**, *478*, 323–329, doi:10.1016/j.bbrc.2016.05.031.
380. Chernukhin, I.; Shamsuddin, S.; Kang, S.Y.; Bergström, R.; Kwon, Y.-W.; Yu, W.; Whitehead, J.; Mukhopadhyay, R.; Docquier, F.; Farrar, D.; et al. CTCF Interacts with and Recruits the Largest Subunit of RNA Polymerase II to CTCF Target Sites Genome-Wide. *Mol. Cell. Biol.* **2007**, *27*, 1631–1648, doi:10.1128/MCB.01993-06.
381. Zhang, C.; Yu, M.; Li, X.; Zhang, Z.; Han, C.; Yan, B. Overexpression of long non-coding RNA MEG3 suppresses breast cancer cell proliferation, invasion, and angiogenesis through AKT pathway. *Tumor Biol.* **2017**, 1–12, doi:10.1177/1010428317701311.
382. Lee, J.; Go, Y.; Kang, I.; Han, Y.-M.; Kim, J. Oct-4 controls cell-cycle progression of embryonic stem cells. *Biochem. J.* **2010**, *426*, 171–181, doi:10.1042/BJ20091439.
383. Gutekunst, M.; Mueller, T.; Weilbacher, A.; Dengler, M.A.; Bedke, J.; Kruck, S.; Oren, M.; Aulitzky, W.E.; Van Der Kuip, H. Cisplatin Hypersensitivity of Testicular Germ Cell Tumors Is Determined by High Constitutive Noxa Levels Mediated by Oct-4. *Cancer Res.* **2013**, *73*, doi:10.1158/0008-5472.CAN-12-2876.
384. Oing, C.; Winfried; Alsdorf, H.; Gunhild Von Amsberg; Oechsle, K. Carsten Bokemeyer, Platinum-refractory germ cell tumors: An update on current treatment options and developments. *World J. Urol* **2017**, *35*, 1167–1175, doi:10.1007/s00345-016-1898-z.
385. Tisato, V.; Voltan, R.; Gonelli, A.; Secchiero, P.; Zauli, G. MDM2/X inhibitors under clinical evaluation: Perspectives for the management of hematological malignancies and pediatric cancer. *J. Hematol. Oncol.* **2017**, *10*, doi:10.1186/s13045-017-0500-5.

Chapter



3

Chapter 3

The Role of *TP53* in Cisplatin Resistance in Mediastinal and Testicular Germ Cell Tumors

Dennis M. Timmerman, Thomas F. Eleveld, Ad J. M. Gillis, Carlijn C. Friedrichs, Sanne Hillenius, Tessa L. Remmers, Sruthi Sriram and Leendert H. J. Looijenga *

Princess Máxima Center for Pediatric Oncology, Heidelberglaan 25, 3584 CS Utrecht, The Netherlands; D.M.Timmerman-6@prinsesmaximacentrum.nl (D.M.T.); t.f.eleveld@prinsesmaximacentrum.nl (T.F.E.); A.J.M.Gillis@prinsesmaximacentrum.nl (A.J.M.G.); c.c.friedrichs-2@prinsesmaximacentrum.nl (C.C.F.); hillenius.sanne@gmail.com (S.H.); tessa.l.remmers@gmail.com (T.L.R.); s.s.sriram@prinsesmaximacentrum.nl (S.S.)

* Correspondence: l.looijenga@prinsesmaximacentrum.nl; Tel.: +31-88-972-5211;

ABSTRACT

Germ cell tumors (GCTs) are considered to be highly curable; however, there are major differences in the outcomes related to histology and anatomical localization. GCTs originating from the testis are, overall, sensitive to platinum-based chemotherapy, whereas GCTs originating from the mediastinum show a worse response, which remains largely unexplained. Here, we address the differences among GCTs from two different anatomical locations (testicular versus mediastinal/extragonadal), with a specific focus on the role of the P53 pathway. It was recently shown that GCTs with *TP53* mutations most often localize to the mediastinum. To elucidate the underlying mechanism, *TP53* knock-out lines were generated in cisplatin-sensitive and -resistant clones of the representative 2102Ep cell line (wild-type *TP53* testicular GCT) and NCCIT cell line (hemizygously mutated *TP53*, mutant *TP53* mediastinal GCT). The full knock-out of *TP53* in 2102Ep and resistant NCCIT resulted in an increase in cisplatin resistance, suggesting a contributing role for P53, even in NCCIT, in which P53 had been reported to be non-functional. In conclusion, these results suggest that *TP53* mutations contribute to the cisplatin-resistant phenotype of mediastinal GCTs and, therefore, are a potential candidate for targeted treatment. This knowledge provides a novel model system to elucidate the underlying mechanism of clinical behavior and possible alternative treatment of the *TP53* mutant and mediastinal GCTs.

Keywords: human malignant germ cell tumors; mediastinal germ cell tumors; testicular germ cell tumors; cisplatin resistance; *TP53*; NCCIT; 2102Ep; stratification

INTRODUCTION

Germ cell tumors (GCTs) are the most common solid malignancies in young men [1,2]. Despite the high frequency of these cancers within this defined age group, the discovery of the exceptional sensitivity of these tumors to the platinum DNA crosslinking compound cisplatin has led to the survival of most patients, with the current five-year survival rate exceeding 95% [3–5]. As GCTs are derived from embryonic germ cells, closely resembling embryonic stem cells, their hypersensitivity to DNA-damaging agents is often traced back to their early embryonic phenotype [6–8]; for instance, similarly to embryonic stem cells, GCTs often display a low/inefficient DNA damage response and, as opposed to most solid malignancies, GCTs that are naïve to systemic treatment rarely harbor *TP53* mutations, irrespective of histology [9,10]. Moreover, the wild-type *TP53* status of GCTs, combined with a pluripotent phenotype, high levels of PUMA and NOXA, and, often, low expression levels of *CDKN1A* (P21), result in a cellular disbalance and a favor towards apoptosis over DNA repair [11–15]. Furthermore, a physiological antagonist of P53, mouse double minute 2 homologue (MDM2), has been illustrated to be especially important in P53 regulation in GCTs, as it has been shown to hamper the apoptotic response via binding to P53 and can be a putative important clinical target [8,16–19]. It has already been shown that the inhibition of MDM2 and disruption of the MDM2–P53 interaction can potentiate apoptosis and sensitize GCT cells to cisplatin [16,17]. On the other hand, no correlation has been identified between the levels of MDM2 and the treatment response [10]. Furthermore, the existence of many MDM2 binding partners, and the reported synergy between MDM2 antagonists and (targeted) therapy, both in GCTs and other cancers, make this an interesting and relevant target as well [16,17,20,21]. Histologically and clinically, GCTs can be divided into two main subtypes, referring partly to their pluripotent potential, namely, seminomas and non-seminomas [6,7]. While patients presenting with seminomas have an excellent prognosis, patients harboring non-seminomas have a mixed prognosis, based on tumor histology (e.g., embryonal carcinoma (EC), yolk sac tumor (YST), choriocarcinoma (CC), or teratoma (TE)), therapy naivety or chemotherapeutic resistance, and anatomical location, mainly focusing on extra-cranial GCTs of the mediastinum versus the testis [6,7,9,14,22]. Apart from tumor histology and origin, the P53 pathway and deregulation thereof has been studied in light of GCT treatment resistance [8–10,13,14,16,17,19,23]. Even though P53's have many implications in resistance, no clear-cut result has been obtained that displays their role in clinical resistance, especially related to informative in vitro models [10,23]. In this study, we focused on the latter (i.e., mediastinal GCTs vs. testicular GCTs) and developed a novel approach to shed light on the difference in treatment resistance between testicular and mediastinal GCTs. This is an important issue, as it is currently unclear whether mediastinal GCTs are more resistant to treatment because of their *TP53* mutations, or whether these mutations simply occur more in these tumors as these tumors harbor different intrinsic resistance mechanisms. To this end, we wanted to elucidate

whether the removal of *TP53* in a testicular GCT cell line can convey cisplatin resistance, and, thus, (partly) explain mediastinal GCT aggressiveness and treatment resistance. Firstly, we used the online cBioPortal tool to analyze an extensive GCT patient data set containing detailed clinical information, including treatment, tumor resistance, tumor stage, anatomical location, histology, and genetic mutations [9]. Furthermore, two well-established GCT cell lines, originating from different anatomical locations and harboring a different *TP53* background (*TP53* mutant/loss in NCCIT from the mediastinum and *TP53* wild-type in 2102Ep from the testis), were modified using a CRISPR/Cas9-mediated *TP53* knock-out model system. We subsequently investigated the difference in cisplatin resistance in these testicular and mediastinal GCT cell lines. Using both GCT patient data characteristics and functional mechanistic cell line investigations, we show a role of P53 in GCT cisplatin resistance related to the anatomical location of the tumor.

RESULTS

Presence of TP53 Mutations in Refractory Cisplatin-Resistant GCTs with a Specificity towards Mediastinal Localization

To elucidate the function of P53 in (resistant) GCTs, we initially used the cBioPortal online tool. We investigated the MSKCC data set on refractory GCTs previously reported by Bagrodia and colleagues in 2016 [9]. The rationale for investigating this data set was based on the abundant presence of detailed clinical data, including anatomical location, treatment, number of chemotherapy cycles, patient survival and outcome, and tumor histology. Supplemental Figure S1A illustrates the presence of *TP53* (and *MDM2*) alterations in cisplatin-sensitive and -resistant GCTs. Strikingly, while GCTs rarely harbor *TP53* mutations, in line with their embryonic phenotype [8], alterations in *TP53* are detected in cisplatin-resistant patients. Furthermore, we observe that *MDM2* amplifications become increasingly abundant in patients with cisplatin-resistant GCTs. Note that, as expected, alterations regarding *TP53* are often missense mutations or deep deletions. When comparing the disease-free survival of patients with alterations in the *TP53* gene to patients with wild-type *TP53* (unaltered group), we observed a highly significant (logrank test p -value of 1.991×10^{-6}) decrease in disease-free survival in patients harboring *TP53* alterations (Supplemental Figure S1B). As previously reported, there could be a bias in this analysis, associated with the type of genetic aberration in relation to the anatomic location of GCTs [9]. The tumors of patients harboring *TP53* mutations often localize to the mediastinum, whereas the tumors of patients harboring *MDM2* amplifications primarily localize to the testis (Supplemental Figure S1C,D). Interestingly, *TP53* or *MDM2* aberrations occur significantly more frequently in patients with chemotherapy-resistant tumors (Figure 1A,B).

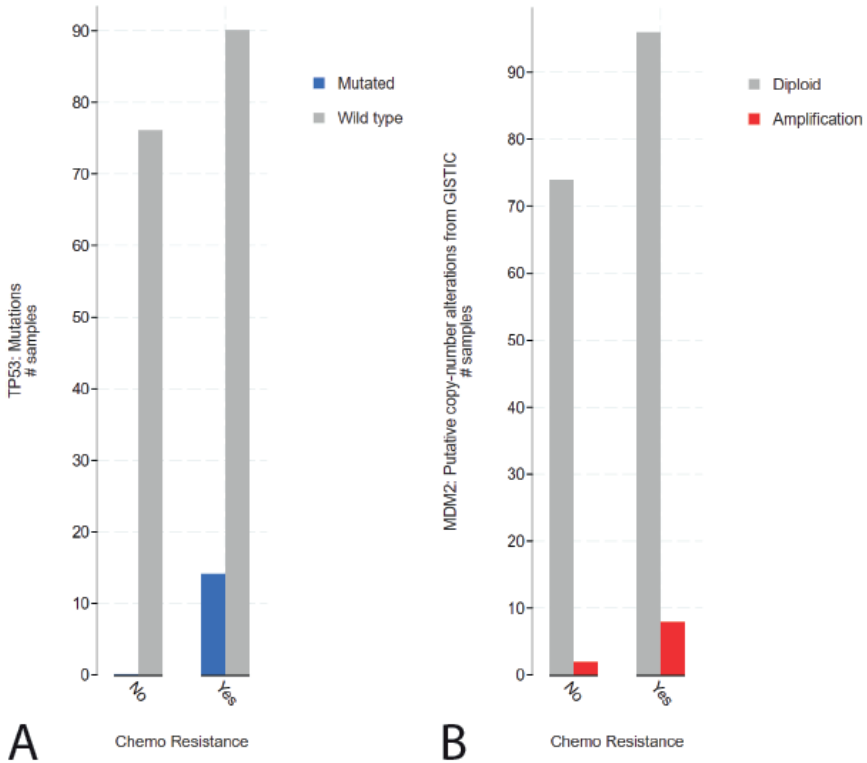


Figure 1. cBioPortal analysis of the tumor resistance in TP53- or MDM2-altered patients in the MSKCC, J Clin Oncol 2016 data set. **(A)** Bar graph displaying the number of patients with sensitive or resistant cisplatin, patients harboring wild-type (grey) or mutated (blue) TP53 are plotted. **(B)** Bar graph displaying the number of patients with sensitive or resistant cisplatin, patients harboring wild-type (grey) or amplified (red) MDM2 are plotted. [9,24,25].

Mediastinal GCT Cell Line NCCIT Harbors Low Levels of MDM2 and Mutant TP53 whereas Testicular GCT Cell Line 2102Ep Harbors Wild-Type TP53 and High Levels of MDM2

To study the difference between mediastinal and testicular GCTs, we used the well-established and -characterized NCCIT and 2102Ep GCT (EC) cell lines. While 2102Ep originates from the testis, NCCIT originates from the mediastinum, with a similar differentiation state [26]. Furthermore, similarly to most GCTs, 2120Ep has a wild-type *TP53* status, whereas NCCIT carries a hemizygous one-base-pair deletion at nucleotide 949 (codon 272), resulting in a frameshift and a premature STOP codon at codon 347 (Figure 2A). This observation is in line with the finding of *TP53* mutations in mediastinal GCTs (see above).

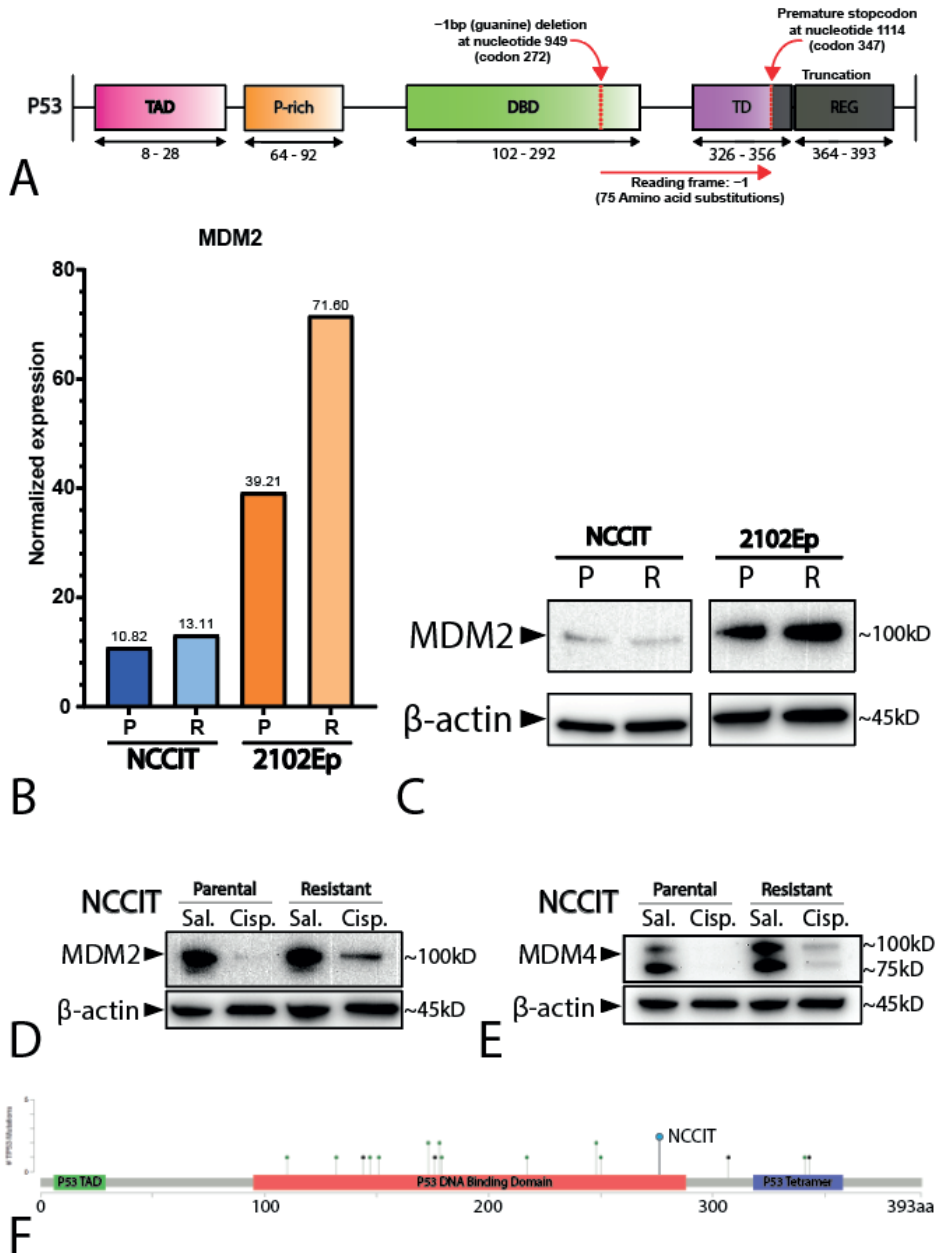


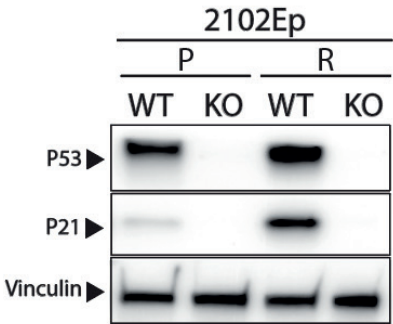
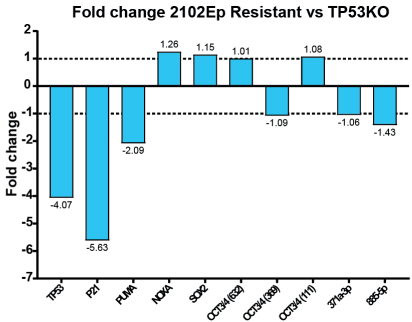
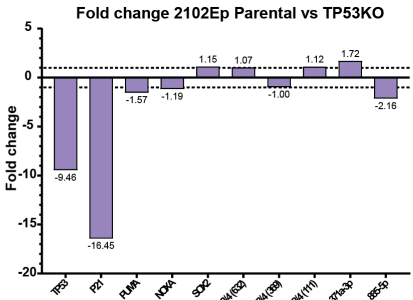
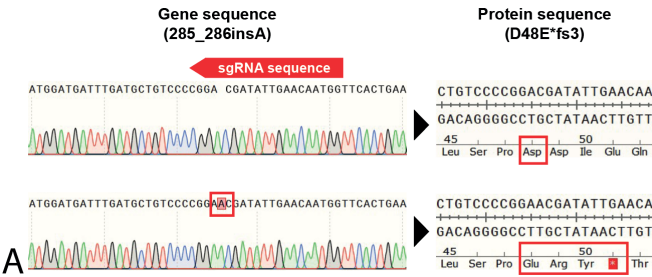
Figure 2. Characterization of the cell lines NCCIT and 2102Ep. **(A)** Schematic overview of the hemizygous mutation present in the NCCIT cell line. **(B)** Bar graph displaying the normalized expression (RNA-seq) of MDM2 in the NCCIT and 2102Ep parental and resistant cell lines. **(C)** Western blot showing the protein levels of MDM2 in the NCCIT and 2102Ep parental and resistant cell lines. **(D,E)** Western blot displaying the MDM2 **(D)** and MDM4 **(E)** protein levels after treatment with sublethal cisplatin doses (1 μ M) or saline vehicle control. **(F)** Mutational position of TP53 mutations in patients in the MSKCC, J Clin Oncol 2016 data set. The mutation found in NCCIT is highlighted with a blue dot.

Additionally, we employed matched isogenic clones of both NCCIT and 2102Ep that have acquired a cisplatin resistance phenotype through long-term sublethal exposure to cisplatin (see Materials and Methods section for details). RNA sequencing (RNA-seq) analysis showed that both the parental and resistant NCCIT cell lines had lower normalized *MDM2* expression than both the 2102Ep cell lines, with 2102Ep resistance displaying the highest levels of *MDM2* (Figure 2B), supported by Western blotting showing that the resistant 2102Ep subclone had higher levels of *MDM2* (Figure 2C). In contrast, the expression levels of *MDM4* were similar between all the cell lines (Supplemental Figure S2). Principal component analysis of the matched parental and resistant cell lines showed no major differences and demonstrated close similarities between the matched subclones (data not shown). To determine whether NCCIT had an active DNA damage response and possible P53 pathway activation, despite a low *MDM2* level, we treated NCCIT cells with sublethal (1 μ M) levels of cisplatin for 24 h prior to protein analysis via Western blotting. Both the NCCIT parental and resistant cell lines showed a clear decrease in *MDM2* and *MDM4* after exposure to cisplatin, an effect that was not visible in the saline vehicle control condition (Figure 2D,E). This indicates a functional DNA-damage sensing pathway upstream of *MDM2* and *MDM4*, and, therefore, suggests an intact regulation of P53 downstream of *MDM2* and *MDM4*, despite the suggested null status of *TP53* as described in the literature [13,16,23,27].

P53 Is Involved in Cisplatin Resistance in Both Wild-Type (Testicular) and Mutant (Mediastinal) GCT Cell Lines

It is largely accepted that the chemotherapeutic hypersensitivity of GCTs is partly due to their wild-type *TP53* status [8,14,28–30]. However, despite its *TP53* mutant status, the NCCIT cell line is considered to be inherently sensitive to cisplatin. Thus, we further compared the mutational status of the NCCIT cell line to the mutations found in refractory GCT patients (Figure 2F). When comparing the intrinsic *TP53* mutation in the NCCIT cell line to the *TP53* mutations present in refractory GCT patients, we observed that most mutations found in patients disrupt the DNA-binding domain of *TP53*, a well-known mutational hotspot [9,31]. In contrast, the intrinsic *TP53* mutation of NCCIT appears to largely spare the DNA-binding domain and is, therefore, more C-terminally located than most mutations found in refractory patients, suggesting the possibility for residual protein activity. Furthermore, the enrichment of mutations in *TP53* in refractory patients, together with a bias towards mediastinal anatomical localization (and, hence, a more resistant phenotype), suggests that *TP53* mutations could add additively to inherent cisplatin resistance mechanisms [9,14,22]. Based on these observations, we decided to further test the involvement of *TP53* in cisplatin resistance in the approach described. Therefore, we generated isogenic CRISPR/Cas9-mediated *TP53* knock-out clones of both

2102Ep and NCCIT, as well as their resistant counterparts. Sanger sequencing, after mono-clonal picking and expansion, revealed mono-clonal sequence traces and a one-base-pair insertion at amino acid 48, resulting in a premature STOP codon at amino acid 51 (Figure 3A). We were able to obtain clones harboring this mutation for all the investigated cell lines. No major copy number changes between the original and *TP53* knock-out NCCIT and 2102Ep subclones were identified based on Infinium Global Screening Array-24 v3.0 BeadChipGSA (GSA) profiling (Supplemental Figure S3). Gene expression analysis using RT-qPCR indicated a clear reduction in both *TP53* and *CDKN1A* (P21) expression in both 2102Ep parental *TP53* knock-out lines (~9.46 and ~16.45, respectively) and 2102Ep-resistant *TP53* knock-out lines (~4.07 and 5.63, respectively), which was also confirmed by Western blot (Figure 3B–D). No differences were observed in P53 target gene expression (PUMA/NOXA) or differentiation marker expression (SOX2, OCT3/4, miR371a-3p, or miR885-5p); the latter indicates that the loss of *TP53* expression had no effect on the differentiation status. The miR371a-3p expression levels were checked because of its many implications in GCTs (mostly as a biomarker and marker of pluripotency in these tumors), together with the implications of P53 pathway regulation [7,20,32–38]. Strikingly, after treating 2102Ep parental and resistant cells, as well as their isogenic *TP53* knock-out clones, with cisplatin, we identified a clear significant (parental $p = 0.0049$, resistant $p \leq 0.0001$) shift in cisplatin resistance when comparing the *TP53* knock-out clone to its wild-type counterpart, with the 2102Ep-resistant *TP53* knock-out clone demonstrating the highest cisplatin resistance (Figure 3E–G). When we performed this approach with the NCCIT cell line, we obtained clones with the same one-base-pair insertion mutation (A) found in the 2102Ep cell lines (Figure 3A). However, we found no strong reduction in either *TP53* or *CDKN1A* expression, P53 target gene expression, or differentiation marker expression (Figure 4A,B). Interestingly, however, we did observe a reduction in miR371a-3p expression (3.37-fold) in the parental *TP53* knock-out clone compared to its parental counterpart, while we observed an increase in miR371a-3p expression (6.91-fold) in the NCCIT-resistant *TP53* knock-out clone compared to its NCCIT-resistant counterpart (Figure 4A,B). Western blotting confirmed that the *TP53* knock-out lines had lost P53 protein expression; however, strikingly, the levels of P21 were increased in the NCCIT-resistant *TP53* knock-out line compared to its NCCIT-resistant counterpart (and both other lines; Figure 4C). Moreover, *TP53* knock-out in the NCCIT clones resulted in no shift in cisplatin resistance in the NCCIT parental clone, and a major significant ($p = 0.0005$) shift in cisplatin resistance in the NCCIT-resistant *TP53* knock-out clone compared to its NCCIT-resistant counterpart (Figure 4D,E).



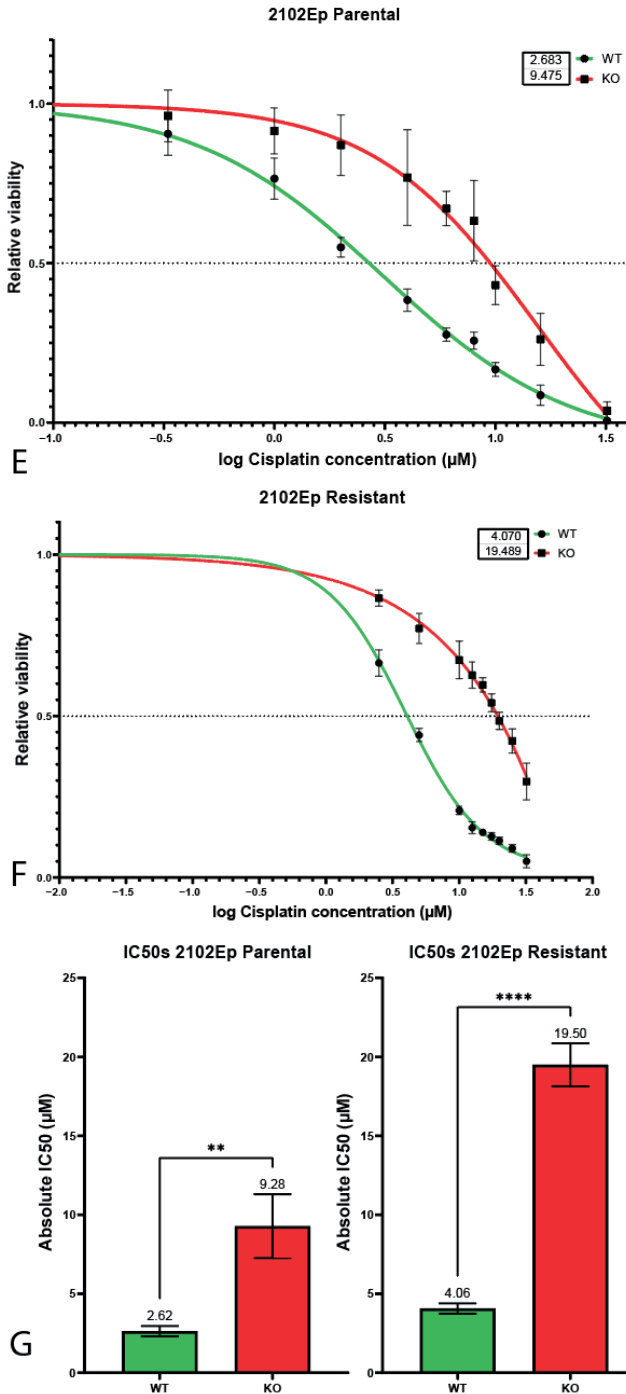


Figure 3. Characterization of 2102Ep TP53 knock-out cell lines. (A) SnapGene genome sequence alignments of the CRISPR/Cas9 target site of the TP53 gene. The knock-out cell line (bottom sequence) shows a one-base-pair insertion (A) at amino acid 49, resulting in a premature STOP codon at amino acid 51. (B,C) Bar graphs showing the fold change in expression between 2102Ep parental cell line and its isogenic TP53 knock-out clone (B) or 2102Ep-resistant cell line and its isogenic TP53 knock-out clone (C). (D) Western blots showing the protein levels of P53, P21 and vinculin (as loading control) in 2102Ep parental and resistant cell lines and their isogenic TP53 knock-out clones. (E,F) S-curves showing the viability of the parental (E) and resistant (F) 2102Ep cell lines and their corresponding knock-out when treated with cisplatin for 72 h. Graphs represent three biological replicates with three technical replicates each. (G) Bar plots displaying IC50 values of all 2102Ep cell lines. Both cell line pairs show significant differences in IC50 values after knock-out (parental $p = 0.0049$, resistant $p \leq 0.0001$, unpaired Student's t-test). Mean \pm SD: 2102Ep parental 2.62 ± 0.33 , 2102Ep parental TP53 KO 9.28 ± 2.02 , 2102Ep resistant 4.06 ± 0.32 , and 2102Ep resistant TP53 KO 19.50 ± 1.36 . Graphs represent three biological replicates with three technical replicates each. ** $p \leq 0.01$, **** $p \leq 0.0001$.

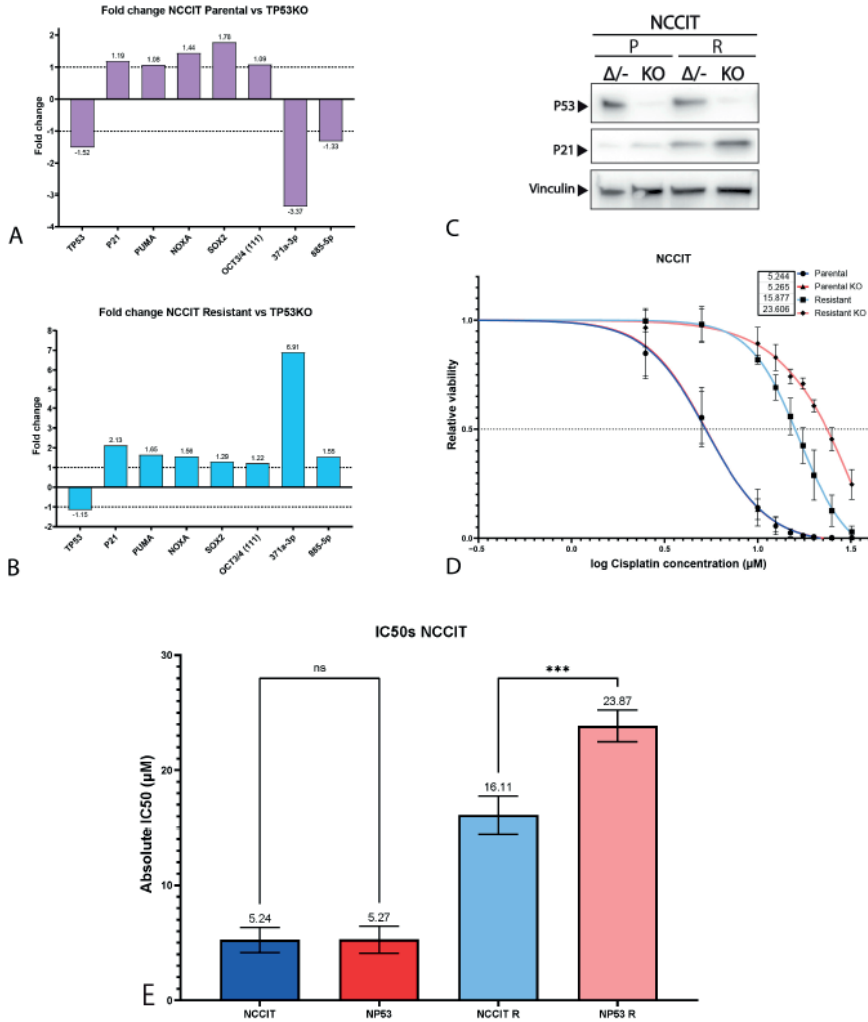


Figure 4. Characterization of NCCIT TP53 knock-out cell lines. **(A,B)** Bar graphs showing the fold change in expression between NCCIT parental cell line and its isogenic TP53 knock-out clone **(A)** or NCCIT-resistant cell line and its isogenic TP53 knock-out clone **(B)**. **(C)** Western blots showing the protein levels of P53, P21 and vinculin (as loading control) in NCCIT parental and resistant cell lines and their isogenic TP53 knock-out clones. **(D)** S-curves showing the viability of the NCCIT cell lines (parental and resistant and TP53 knock-out lines) when treated with cisplatin for 72 h. Graphs represent three biological replicates with three technical replicates each. **(E)** Bar plots displaying IC50 values of all NCCIT cell lines. The NCCIT-resistant cell line shows a significant difference in IC50 values after knock-out ($p = 0.0005$, one-way ANOVA, Tukey's multiple comparisons post hoc test). Mean \pm SD: NCCIT parental 5.24 ± 1.09 , NCCIT parental TP53 KO 5.27 ± 1.18 , NCCIT resistant 16.11 ± 1.67 , and NCCIT resistant TP53 KO 23.87 ± 1.38 . ns = $p > 0.05$, *** $p \leq 0.001$

DISCUSSION

Here, we present a study on the effect of the loss of *TP53* in two well-studied GCT cell lines, representative of a mediastinal and testicular origin, as a starting point to further investigate the role of *TP53* in cisplatin resistance in GCTs, in relation to their anatomical localization. Based on the initial analysis of refractory GCT patients, we observed an overrepresentation of *TP53* mutations and *MDM2* amplification in proven cisplatin-resistant tumors [9]. Of note, only one patient harbored a *MDM4* alteration (missense mutation of unknown significance) [9]. This low frequency of *MDM4* alterations is not fully unexpected, as *MDM4* is not able to directly ubiquitinate P53 and target it for proteasomal degradation; this is in stark contrast to *MDM2*, which is able to directly downregulate P53 through proteasomal degradation [8,21,39]. Subsequent analysis showed that tumors harboring *MDM2* amplifications were mostly testicular in origin, whereas *TP53*-mutated tumors were primarily mediastinal [9]. As reported previously and as part of the International Germ Cell Cancer Collaborative Group (IGCCCG) risk stratification, patients harboring a primary mediastinal GCT have the worst prognosis [40]. One could speculate that the bias for *TP53* mutations in mediastinal GCTs could be due to a less favorable niche and more strict selection for these tumors [41]. As mentioned before, the embryonal origin of these tumors is still in favor of genome protection and an intact *TP53* signaling pathway [8]. It could well be that mediastinal GCTs are on the cross-roads between unfavorable niche selection and, thus, a bias towards *TP53* mutations, and, thereby, a more treatment-resistant phenotype. In this study, we tried to elucidate if there was a causal link between the poor prognosis for mediastinal GCTs and their bias towards *TP53* mutations. In line with cBioPortal analysis, both the Western blot and RNA-seq data indicated higher *MDM2* protein levels and a higher *MDM2* expression in the testicular 2102Ep GCT cell line compared to the mediastinal NCCIT GCT cell line, despite the lack of *MDM2* amplifications in 2102Ep. This suggests a mechanism for treatment resistance within wild-type *TP53* GCTs via *MDM2* [16]. This is even more interesting in light of the many *MDM2* interacting proteins and implications for *MDM2* antagonists as anti-cancer therapies, working synergistically with both chemotherapeutics and targeted therapies [16,21,42]. We demonstrate that there are no differences in the RNA expression of *MDM4* between the mediastinal and testicular cell lines. Finally, as P53 is known to regulate *MDM2* and *MDM4*, and could, therefore, interfere with DNA-damage sensing, we studied the upstream activity of the DNA-damage signaling pathway in the *TP53*-mutated NCCIT cell line [8,27]. Cells were treated with a sublethal dose of cisplatin (1 μ M), and we observed a strong reduction in both *MDM2* and *MDM4* levels in both the parental and resistant cell lines. This indicates a functioning DNA-damage sensing response in the NCCIT cell line [27,43–45]. Of note, we identified a stronger reduction in *MDM2* and *MDM4* after cisplatin treatment in the parental cell line, most likely related to the already higher cisplatin resistance in the NCCIT-resistant cell line that functions upstream of the

DNA-damage sensing response [27,43–45]. When comparing the *TP53* mutation present in the NCCIT cell line to the mutational profile of *TP53* mutations in refractory GCT patients, we noticed that the NCCIT mutant was located more distally within the protein and was unlikely to fully disrupt the function of the DNA-binding domain [9]. To test the function of *TP53* in GCT cisplatin resistance and to interrogate the functionality of the mutant *TP53* in the NCCIT cell line, we generated CRISPR/Cas9-mediated *TP53* knock-out cell lines. As the loss of *TP53* can contribute to chromosomal instability and, therefore, cisplatin resistance, we used GSA analysis to verify the genomic changes between the original and knock-out clones. No major copy number changes were identified related to the *TP53* knock-out procedure and subsequent selection. However, small copy number alterations could be observed, possibly related to clonal selection and expansion. Interestingly, although rarely observed in testicular GCT patients, full knock-out of *TP53* in the testicular EC cell line 2102Ep resulted in a significant increase in cisplatin resistance in both a parental and resistant background. This coincided with both the reduced expression levels of *TP53* and *CDKN1A* (P21), as well as the reduced protein levels of P53 and P21, suggesting a strong dependency on intact *TP53* for *CDKN1A* expression in this cell line. Strikingly, when we knocked out *TP53* in the *TP53* mutant mediastinal EC cell line NCCIT, we also observed an increase in cisplatin resistance in the resistant cell line only. The knock-out of *TP53* resulted in a full loss of P53 at the protein level and a minor reduction at the mRNA level. Interestingly, the parental *TP53* knock-out cell line showed reduced expression of microRNA371a-3p, while the resistant *TP53* knock-out line showed an increase. It remains to be elucidated whether this NCCIT observation is a passenger effect or is possibly related to previous findings regarding the negative regulatory effect of this microRNA cluster on *TP53* expression [32]. The absence of a lack of expression in the case of *TP53* knock-out is relevant in the context of the informativity of this molecular biomarker for GCTs, as recently reviewed by Leão and colleagues, as well as in the case of refractory disease [38]. In contrast, no effect on differentiation status was identified, demonstrating that the knock-out of *TP53* does not induce differentiation, excluding the possibility of increased resistance due to a differentiated phenotype [46]. It is important to note that despite the *TP53* status of these cell lines, being wild-type, hemizygous mutant, or full knock-out, it did not interfere with the detection of the microRNA cluster 371a-3. In other words, the miR371a-3 cluster appears to retain its suitability as a GCT biomarker irrespective of the tumor's *TP53* status and, thus, also partially the level of cisplatin resistance [20,32–38,47–49]. The knock-out of *TP53* in the NCCIT-resistant (but not 2102Ep) cell line resulted in increased protein levels of P21, an effect not readily observed at the mRNA level, suggesting a negative effect on the P21 levels of the mutant *TP53* present in the resistant NCCIT subclone. This is interesting in light of previous studies indicating increased tumor resistance, malignancy, and aggressiveness caused by the P53-independent upregulation of P21 in *TP53* mutant tumors [50–54].

MATERIALS AND METHODS

Cell Culture

The parental (T)GCT cell lines used were previously reported and further characterized by us [26]. NCCIT (RRID:CVCL_1451) was cultured in Roswell Park Memorial Institute (RPMI) 1640 medium with GlutamaxTM-I (Gibco; Thermo Fischer Scientific, Bleiswijk, the Netherlands) and 2102Ep (RRID:CVCL_C522) was cultured in Dulbecco's modified Eagle's medium (DMEM) with 4.5 g/L D-glucose with L-glutamine (Gibco; Thermo Fischer Scientific, Bleiswijk, the Netherlands) [55,56]. Media were supplemented with 10% fetal bovine serum and 1% penicillin–streptomycin (Gibco; Thermo Fischer Scientific, Bleiswijk, the Netherlands). The cell lines were cultured at 37 °C and 5% CO₂. The resistant isogenic clones were generated by the group of Christoph Oing and Friedemann Honecker, University of Hamburg, Germany. These resistant cell lines were obtained by exposing the parental cell lines to cisplatin over a period of 6–9 months to increase the sublethal concentrations of these cells to cisplatin. Cisplatin dose was kept the same for two subsequent treatments and stepwise increased by 30–50%. Each cisplatin treatment was applied for 24 h in 80% confluent cells, followed by a medium change. Cells were allowed to rest with regular medium change over a period of 5–7 days until re-growth was detectable, and cells were re-plated afterwards. After one passage to regenerate, the next treatment was applied as mentioned above. Cells were passaged for a maximum of 7 cycles, followed by intermittent cryopreservation to prevent differentiation. For experimental use, obtained resistant subclones were cultured similarly to their sensitive parental lines without continuous cisplatin supplementation. The resistant subclones were maintained similarly to the parental cells (i.e., without cisplatin).

cBioPortal

Patient data were analyzed by using cBioPortal [24,25] by visiting cBioportal for Cancer Genomics. Available online: <https://www.cbioportal.org/> (accessed on 28 September 2021) and selecting the germ cell tumors (MSKCC, J. Clin. Oncol. 2016) data set under testis tumors [9]. We queried for *TP53* and *MDM2* in the gene query section. Subsequent analysis was performed using the tools provided by cBioPortal.

RNA-seq

STAR (v2.5.3a) was used as aligner for RNA-seq data, using 2-pass mapping for each sample separately. Mapping quality plots were generated and checked based on sambamba flagstat (v0.6.7) statistics. Count files, with the number of RNA-seq reads for

each gene were created with subread FeatureCounts (v1.5.2) and normalized for library size to counts per million (CPM).

Western Blot

Cell lysates were made using RIPA buffer, followed by measuring protein concentrations according to Pierce BCA Protein Assay Kit (Gibco; Thermo Fischer Scientific, Bleiswijk, the Netherlands). A total of 25 µg protein was loaded onto a 4–15% Mini-Protean TGX Stain-Free Protein Gel (Bio-Rad Laboratories, Lunteren, The Netherlands). After separation, the proteins were transferred to a 0.2 µm PVDF membrane with the Turbo Trans-Blot system (Bio-Rad Laboratories, Lunteren, The Netherlands). The following primary antibodies were added to the membranes: mouse anti-MDM2 (IF2) (1:1000; Gibco; Thermo Fischer Scientific, Bleiswijk, the Netherlands; #33-7100), mouse anti-MDMX (1:1000; Merck KGaA, Darmstadt, Germany; #04-1555), anti-β-actin antibody (1:10,000; Thermo Fischer Scientific, Bleiswijk, the Netherlands; #MA5-15739), mouse anti-human p53 (1:1000; Dako Denmark A/S, Hilden, Germany; #M7001), rabbit anti-human p21 Waf1/Cip1 (1:1000; Cell Signaling Technology, Leiden, The Netherlands; #2947) and mouse anti-vinculin (1:4000; Merck KGaA, Darmstadt, Germany; #V9131), as a loading control. After incubating the membranes overnight at 4 °C, either goat anti-mouse IgG(H+L) cross-absorbed, HRP (1:2000; Invitrogen; Thermo Fischer Scientific, Bleiswijk, the Netherlands; #G-21040) or goat anti-rabbit IgG (H+L) cross-absorbed, HRP (1:2000; Invitrogen; #G-21234) were added as secondary antibodies and the membranes were incubated for 2 h at RT. To detect the proteins, Clarity Western ECL substrate (Bio-Rad Laboratories, Lunteren, The Netherlands) was added to the membranes.

CRISPR-Mediated Knock-Out Cell Lines

Both parental and resistant cells of NCCIT and 2102Ep were exposed to a ribonucleoprotein complex made of resuspension buffer R, 61 µM Cas9 protein and 100 µM gRNA duplex consisting of crRNA and tracrRNA, which was designed to target the gene of interest, *TP53* (Hs.Cas9.*TP53*.1.AA: CCATTGTTCAATATCGTTCCGGGG; Integrated DNA Technologies, Leuven, Belgium), using the Neon Transfection System (Thermo Fischer Scientific, Bleiswijk, the Netherlands). To confirm a successful *TP53* knock-out and to determine introduced mutations, of all the different cell lines, DNA was isolated using QuickExtract according to manufacturer's protocol, followed by PCR with the following primers: forward: CAGTCAGATCCTAGCGTCTGA and reverse: CACTGACAGGAAGCCAAAGG. Sequencing was performed by MacroGen Europe and knock-out efficiency was determined with the online ICE analysis tool by Synthego ICE analysis. Available online: <https://ice.synthego.com/#/> (accessed on 15 September 2021).

Real-Time Quantitative Polymerase Chain Reaction (RT-qPCR)

RNA Isolation

High-quality total RNA was extracted from the above-mentioned cell lines using TRIzol reagent (Life Technologies; Thermo Fischer Scientific, Bleiswijk, the Netherlandscat. nr. 15596018) according to the manufacturer's instructions. Quantity and quality were assessed on Nanodrop One (Isogen Lifescience B.V., de Meern, the Netherlands/ Thermo Fischer Scientific, Bleiswijk, the Netherlands) and with Qubit 4 fluorometer (Invitrogen; Thermo Fischer Scientific, Bleiswijk, the Netherlands).

miRNA Profiling

Targeted miRNA profiling was performed on diluted RNA (5 ng) using TaqMan MicroRNA Reverse Transcription Kit (Thermo Fischer Scientific, Bleiswijk, the Netherlandscat.nr 4366597) and TaqMan Assays RNU48 (001006), hsa-miR371-3p (002124), and hsa-miR885-5p (002296) as described before [49]. RNU48 was used as for normalization and relative miRNA levels were computed as $2^{-\Delta\Delta Ct}$.

mRNA Gene Expression

Diluted RNA (50 ng) was reverse transcribed using SuperScript IV reverse transcriptase (Thermo Fischer Scientific, Bleiswijk, the Netherlandscat.nr. 18090050). RT-QPCR was run using the following TaqMan gene expression assays: *HPRT* (hs02800695_m1), *TP53* (hs01034249_m1), *TP73* (hs01056231_m1), *CDKN1A/P21* (hs99999142_m1), *BBC3/PUMA* (hs00248075_m1), *PMAIP1/NOXA* (hs00560402_m1), *SOX2* (hs01053049_s1), *POU5F1* (hs00999632_g1), *POU5F1* (hs04195369_s1), *POU5F1* (hs03005111_g1). The 2× TaqMan Advanced PCR Master Mix (Thermo Fischer Scientific, Bleiswijk, the Netherlandscat. nr. 4444556) was used and reactions were run in 96-well plates on QuantStudio 12K Flex System (Thermo Fischer Scientific, Bleiswijk, the Netherlands). *HPRT* was used as a housekeeping gene for normalization purposes and relative gene expression levels were computed as $2^{-\Delta\Delta Ct}$. Fold change between parental and knock-out clones was plotted.

Viability Assays

The sensitivity of the cells (both NCCIT and 2102Ep) to cisplatin was determined using a viability assay. To test the sensitivity of the cells to cisplatin, 10.000 NCCIT and 2102Ep parental cells and 4.000 2102Ep-resistant cells (based on performed seeding density assays; data not shown) were seeded in 100 μ L RPMI or DMEM (respectively) medium per well in a 96-well plate. The plate was incubated at 37 °C and 5% CO₂ overnight. Then, the following concentrations of cisplatin were made from 1 mg/mL cisplatin stock (Accord

Healthcare B.V., Utrecht, the Netherlands) diluted in fresh medium enriched with 0.9% NaCl: 32 μ M, 16 μ M, 10 μ M, 8 μ M, 6 μ M, 4 μ M, 2 μ M, 1 μ M and 0.33 μ M, or, 32 μ M, 25 μ M, 20 μ M, 17.5 μ M, 15 μ M, 12.5 μ M, 10 μ M, 5 μ M and 2.5 μ M, dependent on expected IC50. The medium in the wells was replaced with 100 μ L of the corresponding cisplatin medium. The plate was incubated at 37 °C and 5% CO₂ for 72 h.

After incubation of either 2102Ep cells or NCCIT cells with cisplatin concentrations, CellTiter-Glo® 2.0 Luminescent Cell Viability Assay kit (Promega, Leiden, the Netherlands) was used to lyse the cells to be able to measure the viability. Afterwards, 100 μ L of the lysate was transferred to a Pierce white opaque 96-well plate (Thermo Fisher). The luminescence was measured on an ID3 Spectramax (Molecular Devices, San Jose, the United States) or a FLUOstar Omega (BMG Labtech, Ortenberg, Germany).

The viability assays were performed with three technical replicates and at least on three separate occasions (biological replicates). Data were visualized and interpreted using GraphPad Prism 9. To extract IC50 values, concentrations were transformed to logarithms, non-linear S-curves were fit through the data set using a GraphPad algorithm to extract absolute IC50s and the S-curves were interpolated with $y = 0.5$ to derive the absolute IC50s. Statistic differences were calculated using either an unpaired Student's *t*-test or one-way ANOVA with a Tukey's multiple comparisons post hoc test.

Genotyping with GSA Arrays

Genomic changes between original and knock-out subclones were identified after monoclonal expansion and a minimum of ~3 months of separate cell culture using Infinium Global Screening Array-24 v3.0 BeadChipGSA (GSA) profiling. Array data were obtained from the HUGE-F as a Genome Studio vs. 2.0.4 (Illumina, Eindhoven, the Netherlands) project using the hg38 reference genome.

Data Visualization

Data were visualized using cBioPortal (v3.7.12), Adobe Illustrator (2020), SnapGene® 5.3.2 and GraphPad Prism 9.

CONCLUSIONS

In conclusion, this study, combining GCT patient data characteristics and functional mechanistic cell line investigations, illustrates the role of *TP53* status in cisplatin resistance in GCTs, related to the anatomical location associated with molecular constitution. The results obtained show that the investigated cell lines, independent of intrinsic resistance,

demonstrate a beneficial effect of the loss of *TP53* regarding cisplatin resistance, as schematically represented in Figure 5. Furthermore, it is interesting to note that the hemizygous mutant *TP53*, originally present in the commonly used NCCIT, is functional in the context of cisplatin sensitivity, as the knock-out of this mutant resulted in increased cisplatin resistance. The isogenic generated cell lines provide a novel informative model system to study the involvement of *TP53* in the original cellular background (of NCCIT ad 2102Ep), and provide insight into the clinical behavior of GCTs. Moreover, we provide, to our knowledge, for the first time, insights into the functionality of the hemizygous *TP53* mutant present in NCCIT, and, additionally, we developed a cell line harboring a bona fide *TP53* null status. More GCT cell lines originating from both tumor sites (i.e., mediastinum and testis), or even tumor-derived organoids from these sites, could provide more insights into the role of *TP53* in the clinical behavior and chemotherapy response of these tumors. These data can aid in patient stratification for optimal clinical decision making, especially for mediastinal tumors in which *TP53* mutations are more common. Patients could benefit from screening for intrinsic *TP53* mutations in the primary tumor or acquired *TP53* mutations in the refractory malignancies. This study illustrates the contribution of *TP53* not only to known cisplatin sensitivity, but also as a potential target for acquired cisplatin resistance.

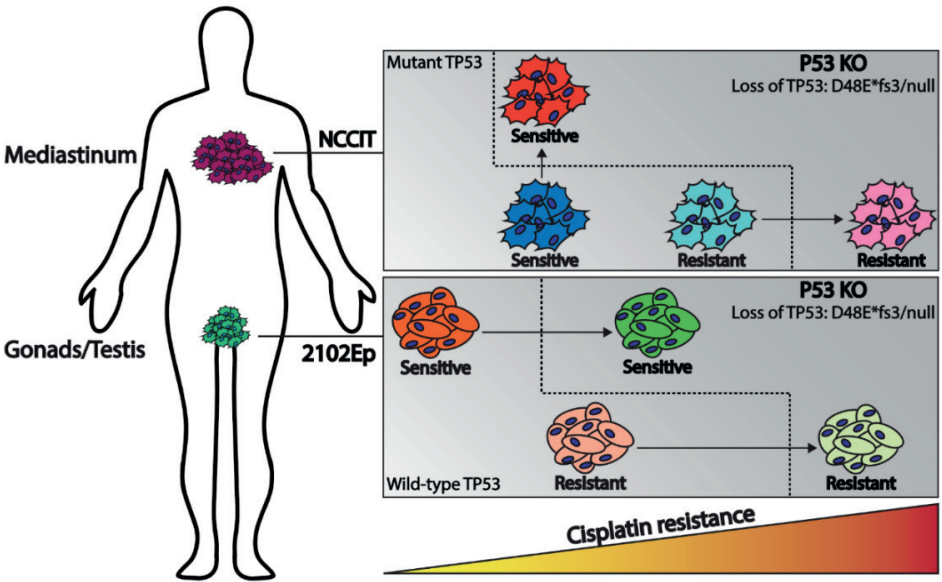


Figure 5. Schematic overview illustrating the model of this study. Mediastinal GCTs (NCCIT cell line) have a bias towards *TP53* mutations where testicular GCTs (2102Ep cell line) usually harbor wild-type *TP53*. In both cases knock-out of *TP53* results in increased cisplatin resistance.

Supplementary Materials: The following are available online at www.mdpi.com/xxx/s1.

Author Contributions: Conceptualization, D.M.T., T.F.E. and L.H.J.L.; methodology, D.M.T., T.F.E. and L.H.J.L.; software, D.M.T. and T.F.E.; validation, D.M.T., A.J.M.G., C.C.F., S.H. and S.S.; formal analysis, D.M.T., T.F.E. and C.C.F.; investigation, D.M.T., T.F.E., C.C.F., S.H., T.L.R. and L.H.J.L.; resources, L.H.J.L.; data curation, D.M.T., T.F.E., C.C.F. and L.H.J.L.; writing—original draft preparation, D.M.T. and L.H.J.L.; writing—review and editing, D.M.T., T.F.E., C.C.F., S.H., T.L.R., S.S. and L.H.J.L.; visualization, D.M.T.; supervision, L.H.J.L.; project administration, D.M.T. and L.H.J.L.; funding acquisition, L.H.J.L. All authors have read and agreed to the published version of the manuscript.

Funding: The work has been financially supported by the Princess Maxima Center for Pediatric Oncology and the Bergh in het Zadel Foundation.

Institutional Review Board Statement: Not applicable.

Informed Consent Statement: Not applicable.

Data Availability Statement: The data presented in this study are available on request from the corresponding author.

Acknowledgments: Financially supported by the Princess M^axima Center for Pediatric Oncology (D.M.T.).

Conflicts of Interest: A patent application has been filed covering the finding of using miR-885-5p and miR-448 as molecular markers for teratoma (and contradicting effect of miR-885-5p on the P53 pathway compared to miR371a-3p).

REFERENCES

1. Cheng, L.; Albers, P.; Berney, D.M.; Feldman, D.R.; Daugaard, G.; Gilligan, T.; Looijenga, L. Testicular cancer. *Nat. Rev. Dis. Prim.* **2018**, *4*, 29, <https://doi.org/10.1038/s41572-018-0029-0>.
2. Palumbo, C.; Mistretta, F.A.; Mazzone, E.; Knipper, S.; Tian, Z.; Perrotte, P.; Antonelli, A.; Montorsi, F.; Shariat, S.F.; Saad, F.; et al. Contemporary Incidence and Mortality Rates in Patients with Testicular Germ Cell Tumors. *Clin. Genitourin. Cancer* **2019**, *17*, e1026–e1035, <https://doi.org/10.1016/j.clgc.2019.06.003>.
3. Einhorn, L.H. Cis-Diamminedichloroplatinum, Vinblastine, and Bleomycin Combination Chemotherapy in Disseminated Testicular Cancer. *Ann. Intern. Med.* **1977**, *87*, 293–298, <https://doi.org/10.7326/0003-4819-87-3-293>.
4. Allen, J.C.; Kirschner, A.; Scarpato, K.R.; Morgans, A.K. Current Management of Refractory Germ Cell Tumors and Future Directions. *Curr. Oncol. Rep.* **2017**, *19*, 8, <https://doi.org/10.1007/s11912-017-0572-y>.
5. Siegel, R.L.; Mph, K.D.M.; Jemal, A. Cancer Statistics, 2019. *CA A Cancer J. Clin.* **2019**, *69*, 7–34, <https://doi.org/10.3322/caac.21551>.
6. Oosterhuis, J.W.; Looijenga, L. Testicular Germ-Cell Tumours in a Broader Perspective. *Nat. Rev. Cancer* **2005**, *5*, 210–222, <https://doi.org/10.1038/nrc1568>.
7. Oosterhuis, J.W.; Looijenga, L.H.J. Human Germ Cell Tumours from a Developmental Perspective. *Nat. Rev. Cancer* **2019**, *19*, 522–537, <https://doi.org/10.1038/s41568-019-0178-9>.
8. Timmerman, D.; Remmers, T.; Hillenius, S.; Looijenga, L. Mechanisms of *TP53* Pathway Inactivation in Embryonic and Somatic Cells—Relevance for Understanding (Germ Cell) Tumorigenesis. *Int. J. Mol. Sci.* **2021**, *22*, 5377, <https://doi.org/10.3390/ijms22105377>.
9. Bagrodia, A.; Lee, B.; Lee, W.; Cha, E.K.; Sfakianos, J.P.; Iyer, G.; Pietzak, E.J.; Gao, S.P.; Zabor, E.C.; Ostrovskaya, I.; et al. Genetic Determinants of Cisplatin Resistance in Patients with Advanced Germ Cell Tumors. *J. Clin. Oncol.* **2016**, *34*, 4000–4007, <https://doi.org/10.1200/jco.2016.68.7798>.
10. Kersemaekers, A.-M.F.; Mayer, F.; Molier, M.; Van Weeren, P.C.; Oosterhuis, J.W.; Bokemeyer, C.; Looijenga, L.H. Role of P53 and MDM2 in Treatment Response of Human Germ Cell Tumors. *J. Clin. Oncol.* **2002**, *20*, 1551–1561, <https://doi.org/10.1200/jco.2002.20.6.1551>.
11. Ulbright, T.M.; Orazi, A.; De Riese, W.; De Riese, C.; Messmer, E.J.; Foster, R.S.; Donohue, J.P.; Eble, J.N. The Correlation of P53 Protein Expression with Proliferative Activity and Occult Metastases in Clinical Stage I Non-Seminomatous Germ Cell Tumors of the Testis. *Mod. Pathol.* **1994**, *7*, 64–68.
12. Fillion, T.M.; Qiao, M.; Ghule, P.N.; Mandeville, M.; van Wijnen, A.J.; Stein, J.L.; Lian, J.B.; Altieri, D.C.; Stein, G.S. Survival Responses of Human Embryonic Stem Cells to DNA Damage. *J. Cell. Physiol.* **2009**, *220*, 586–592, <https://doi.org/10.1002/jcp.21735>.
13. Gutekunst, M.; Oren, M.; Weillbacher, A.; Dengler, M.A.; Markwardt, C.; Thomale, J.; Aulitzky, W.E.; Van Der Kuip, H. p53 Hypersensitivity is the Predominant Mechanism of the Unique Responsiveness of Testicular Germ Cell Tumor (TGCT) Cells to Cisplatin. *PLoS ONE* **2011**, *6*, e19198, <https://doi.org/10.1371/journal.pone.0019198>.
14. Jacobsen, C.; Honecker, F. Cisplatin Resistance in Germ Cell Tumours: Models and Mechanisms. *Andrology* **2015**, *3*, 111–121, <https://doi.org/10.1111/andr.299>.
15. Bloom, J.C.; Loehr, A.R.; Schimenti, J.C.; Weiss, R.S. Germline Genome Protection: Implications for Gamete Quality and Germ Cell Tumorigenesis. *Andrology* **2019**, *7*, 516–526, <https://doi.org/10.1111/andr.12651>.

16. Bauer, S.; Mühlenberg, T.; Leahy, M.; Hoiczky, M.; Gauler, T.; Schuler, M.; Looijenga, L. Therapeutic Potential of Mdm2 Inhibition in Malignant Germ Cell Tumours. *Eur. Urol.* **2010**, *57*, 679–687, <https://doi.org/10.1016/j.eururo.2009.06.014>.
17. Koster, R.; Timmer-Bosscha, H.; Bischoff, R.; Gietema, J.; De Jong, S. Disruption of the MDM2–p53 Interaction Strongly Potentiates p53-Dependent Apoptosis in Cisplatin-Resistant Human Testicular Carcinoma Cells via the Fas/FasL Pathway. *Cell Death Dis.* **2011**, *2*, e148–e148, <https://doi.org/10.1038/cddis.2011.33>.
18. Gutekunst, M.; Mueller, T.; Weilbacher, A.; Dengler, M.A.; Bedke, J.; Kruck, S.; Oren, M.; Aulitzky, W.E.; Van Der Kuip, H. Cisplatin Hypersensitivity of Testicular Germ Cell Tumors Is Determined by High Constitutive Noxa Levels Mediated by Oct-4. *Cancer Res.* **2013**, *73*, 1460–1469, <https://doi.org/10.1158/0008-5472.can-12-2876>.
19. Lobo, J.; Jerónimo, C.; Henrique, R. Cisplatin Resistance in Testicular Germ Cell Tumors: Current Challenges from Various Perspectives. *Cancers* **2020**, *12*, 1601, <https://doi.org/10.3390/cancers12061601>.
20. Mego, M.; Van Agthoven, T.; Gronesova, P.; Chovanec, M.; Miskovska, V.; Madiak, J.; Looijenga, L.H.J. Clinical Utility of Plasma miR-371a-3p in Germ Cell Tumors. *J. Cell. Mol. Med.* **2019**, *23*, 1128–1136, <https://doi.org/10.1111/jcmm.14013>.
21. Fähræus, R.; Olivares-Illana, V. MDM2's Social Network. *Oncogene* **2013**, *33*, 4365–4376, <https://doi.org/10.1038/onc.2013.410>.
22. Zhou, Z.-T.; Wang, J.-W.; Yang, L.; Wang, J.; Zhang, W. Primary Germ Cell Tumor in the Mediastinum-Report of 47 Cases. *Zhonghua Zhong Liu Za Zhi* **2006**, *28*, 863–866.
23. Burger, H.; Nooter, K.; Boersma, A.W.; Kortland, C.J.; Stoter, G. Lack of Correlation Between Cisplatin-Induced Apoptosis, p53 Status and Expression of Bcl-2 Family Proteins in Testicular Germ Cell Tumour Cell Lines. *Int. J. Cancer* **1997**, *73*, 592–599, [https://doi.org/10.1002/\(sici\)1097-0215\(19971114\)73:4<592::aid-ijc22>3.0.co;2-a](https://doi.org/10.1002/(sici)1097-0215(19971114)73:4<592::aid-ijc22>3.0.co;2-a).
24. Cerami, E.; Gao, J.; Dogrusoz, U.; Gross, B.E.; Sumer, S.O.; Aksoy, B.A.; Jacobsen, A.; Byrne, C.J.; Heuer, M.L.; Larsson, E.; et al. The cBio Cancer Genomics Portal: An Open Platform for Exploring Multidimensional Cancer Genomics Data: Figure 1. *Cancer Discov.* **2012**, *2*, 401–404, <https://doi.org/10.1158/2159-8290.cd-12-0095>.
25. Gao, J., Aksoy, B. A., Dogrusoz, U., Dresdner, G., Gross, B., Sumer, S. O., Sun, Y., Jacobsen, A., Sinha, R., Larsson, E., Cerami, E., Sander, C., & Schultz, N. (2013). Integrative analysis of complex cancer genomics and clinical profiles using the cBioPortal. *Science signaling*, 6(269), p11. <https://doi.org/10.1126/scisignal.2004088>
26. de Jong, J.; Stoop, H.; Gillis, A.J.M.; Hersmus, R.; van Gurp, R.J.H.L.M.; van de Geijn, G.-J.M.; van Drunen, E.; Beverloo, H.B.; Schneider, D.T.; Sherlock, J.K.; et al. Further Characterization of the First Seminoma Cell Line TCam-2. *Genes Chromosom. Cancer* **2008**, *47*, 185–196, <https://doi.org/10.1002/gcc.20520>.
27. Li, J.; Kurokawa, M. Regulation of MDM2 Stability After DNA Damage. *J. Cell. Physiol.* **2015**, *230*, 2318–2327, <https://doi.org/10.1002/jcp.24994>.
28. Spierings, D.; De Vries, E.E.G.; Vellenga, E.; De Jong, S. The Attractive Achilles Heel of Germ Cell Tumours: An Inherent Sensitivity to Apoptosis-Inducing Stimuli. *J. Pathol.* **2003**, *200*, 137–148, <https://doi.org/10.1002/path.1373>.
29. Kerley-Hamilton, J.S.; Pike, A.M.; Li, N.; DiRenzo, J.; Spinella, M.J. A p53-Dominant Transcriptional Response to Cisplatin in Testicular Germ Cell Tumor-Derived Human Embryonal Carcinoma. *Oncogene* **2005**, *24*, 6090–6100, <https://doi.org/10.1038/sj.onc.1208755>.

30. Romano, F.J.; Rossetti, S.; Conteduca, V.; Schepisi, G.; Cavaliere, C.; Di Franco, R.; La Mantia, E.; Castaldo, L.; Nocerino, F.; Ametrano, G.; et al. Role of DNA Repair Machinery and P53 in the Testicular Germ Cell Cancer: A Review. *Oncotarget* **2016**, *7*, 85641–85649, <https://doi.org/10.18632/oncotarget.13063>.
31. Baugh, E.H.; Ke, H.; Levine, A.J.; Bonneau, A.R.; Chan, C.S. Why are there Hotspot Mutations in the *TP53* Gene in Human Cancers? *Cell Death Differ.* **2018**, *25*, 154–160, <https://doi.org/10.1038/cdd.2017.180>.
32. Voorhoeve, P.M.; le Sage, C.; Schrier, M.; Gillis, A.J.; Stoop, H.; Nagel, R.; Liu, Y.-P.; van Duijse, J.; Drost, J.; Griekspoor, A.; et al. A Genetic Screen Implicates miRNA-372 and miRNA-373 as Oncogenes in Testicular Germ Cell Tumors. *Cell* **2006**, *124*, 1169–1181, <https://doi.org/10.1016/j.cell.2006.02.037>.
33. Lobo, J.; Gillis, A.J.; Berg, A.V.D.; Dorssers, L.C.J.; Belge, G.; Dieckmann, K.-P.; Roest, H.P.; Van Der Laan, L.J.W.; Gietema, J.; Hamilton, R.J.; et al. Identification and Validation Model for Informative Liquid Biopsy-Based microRNA Biomarkers: Insights from Germ Cell Tumor In Vitro, In Vivo and Patient-Derived Data. *Cells* **2019**, *8*, 1637, <https://doi.org/10.3390/cells8121637>.
34. Almstrup, K.; Lobo, J.; Mørup, N.; Belge, G.; Meyts, E.R.-D.; Looijenga, L.H.J.; Dieckmann, K.-P. Application of miRNAs in the Diagnosis and Monitoring of Testicular Germ Cell Tumours. *Nat. Rev. Urol.* **2020**, *17*, 201–213, <https://doi.org/10.1038/s41585-020-0296-x>.
35. Murray, M.J.; Bell, E.; Raby, K.L.; Rijlaarsdam, M.; Gillis, A.J.M.; Looijenga, L.; Brown, H.; Destenaves, B.; Nicholson, J.C.; Coleman, N.S. A pipeline to Quantify Serum and Cerebrospinal Fluid Micrnas for Diagnosis and Detection of Relapse in Paediatric Malignant Germ-Cell Tumours. *Br. J. Cancer* **2016**, *114*, 151–162, <https://doi.org/10.1038/bjc.2015.429>.
36. Murray, M.J.; Halsall, D.J.; Hook, C.E.; Williams, D.M.; Nicholson, J.C.; Coleman, N.; Sweet, W.; Duh, Y.-J.; Greenfield, L.; Tarco, E.; et al. Identification of MicroRNAs From the miR-371-373 and miR-302 Clusters as Potential Serum Biomarkers of Malignant Germ Cell Tumors. *Am. J. Clin. Pathol.* **2011**, *135*, 119–125, <https://doi.org/10.1309/ajcpoe11keyzcjht>.
37. Syring, I.; Bartels, J.; Holdenrieder, S.; Kristiansen, G.; Müller, S.C.; Ellinger, J. Circulating Serum miRNA (miR-367-3p, miR-371a-3p, miR-372-3p and miR-373-3p) as Biomarkers in Patients with Testicular Germ Cell Cancer. *J. Urol.* **2015**, *193*, 331–337, <https://doi.org/10.1016/j.juro.2014.07.010>.
38. Leão, R.; Albersen, M.; Looijenga, L.H.; Tandstad, T.; Kollmannsberger, C.; Murray, M.J.; Culine, S.; Coleman, N.; Belge, G.; Hamilton, R.J.; et al. Circulating MicroRNAs, the Next-Generation Serum Biomarkers in Testicular Germ Cell Tumours: A Systematic Review. *Eur. Urol.* **2021**, *80*, 456–466, <https://doi.org/10.1016/j.eururo.2021.06.006>.
39. Toledo, F.; Wahl, G.M. MDM2 and MDM4: p53 Regulators as Targets in Anticancer Therapy. *Int. J. Biochem. Cell Biol.* **2007**, *39*, 1476–1482, <https://doi.org/10.1016/j.biocel.2007.03.022>.
40. Kollmannsberger, C.; Nichols, C.; Meisner, C.; Mayer, F.; Kanz, L.; Bokemeyer, C. Identification of Prognostic Subgroups Among Patients with Metastatic 'IGCCCG Poor-Prognosis' Germ-Cell Cancer: An Explorative Analysis Using Cart Modeling. *Ann. Oncol.* **2000**, *11*, 1115–1120, <https://doi.org/10.1023/a:1008333229936>.
41. Oosterhuis, J.W.; Looijenga, L.H. Mediastinal Germ Cell Tumors: Many Questions and Perhaps an Answer. *J. Clin. Investig.* **2020**, *130*, 6238–6241, <https://doi.org/10.1172/jci143884>.
42. Saiki, A.Y.; Caenepeel, S.; Yu, D.; Lofgren, J.A.; Osgood, T.; Robertson, R.; Canon, J.; Su, C.; Jones, A.; Zhao, X.; et al. MDM2 Antagonists Synergize Broadly and Robustly with Compounds Targeting Fundamental Oncogenic Signaling Pathways. *Oncotarget* **2014**, *5*, 2030–2043.
43. Zhang, X.-P.; Liu, F.; Wang, W. Two-Phase Dynamics of p53 in the DNA Damage Response. *Proc. Natl. Acad. Sci. USA* **2011**, *108*, 8990–8995, <https://doi.org/10.1073/pnas.1100600108>.

44. Beishline, K.; Azizkhan-Clifford, J. Interplay between the Cell Cycle and Double-Strand Break Response in Mammalian Cells. 2014, 1170, 41–59, https://doi.org/10.1007/978-1-4939-0888-2_3.
45. Aubrey, B.; Kelly, G.L.; Janic, A.; Herold, M.; Strasser, A. How does p53 Induce Apoptosis and how does this Relate to P53-Mediated Tumour Suppression? *Cell Death Differ.* 2018, 25, 104–113, <https://doi.org/10.1038/cdd.2017.169>.
46. Mayer, F.; Stoop, H.; Scheffer, G.L.; Scheper, R.; Oosterhuis, J.W.; Looijenga, L.; Bokemeyer, C. Molecular Determinants of Treatment Response in Human Germ Cell Tumors. *Clin. Cancer Res.* 2003, 9, 767–773.
47. Dieckmann, K.-P.; Spiekermann, M.; Balks, T.; Flor, I.; Löning, T.; Bullerdiek, J.; Belge, G. MicroRNAs miR-371-3 in Serum as Diagnostic Tools in the Management of Testicular Germ Cell Tumours. *Br. J. Cancer* 2012, 107, 1754–1760, <https://doi.org/10.1038/bjc.2012.469>.
48. Dieckmann, K.-P.; Radtke, A.; Spiekermann, M.; Balks, T.; Matthies, C.; Becker, P.; Ruf, C.; Oing, C.; Oechsle, K.; Bokemeyer, C.; et al. Serum Levels of MicroRNA miR-371a-3p: A Sensitive and Specific New Biomarker for Germ Cell Tumours. *Eur. Urol.* 2017, 71, 213–220, <https://doi.org/10.1016/j.eururo.2016.07.029>.
49. Dieckmann, K.-P.; Radtke, A.; Geczi, L.; Matthies, C.; Anheuser, P.; Eckardt, U.; Sommer, J.; Zengerling, F.; Trenti, E.; Pichler, R.; et al. Serum Levels of MicroRNA-371a-3p (M371 Test) as a New Biomarker of Testicular Germ Cell Tumors: Results of a Prospective Multicentric Study. *J. Clin. Oncol.* 2019, 37, 1412–1423, <https://doi.org/10.1200/jco.18.01480>.
50. Koster, R.; Di Pietro, A.; Timmer-Bosscha, H.; Gibcus, J.H.; Berg, A.V.D.; Suurmeijer, A.; Bischoff, R.; Gietema, J.; De Jong, S. Cytoplasmic p21 Expression Levels Determine Cisplatin Resistance in Human Testicular Cancer. *J. Clin. Investig.* 2010, 120, 3594–3605, <https://doi.org/10.1172/jci41939>.
51. Galanos, P.; Vougas, K.; Walter, D.; Polyzos, A.; Maya-Mendoza, A.; Haagensen, E.J.; Kokkalis, A.; Roumelioti, F.-M.; Gagos, S.; Tzetis, M.; et al. Chronic p53-Independent p21 Expression Causes Genomic Instability by Deregulating Replication Licensing. *Nat. Cell Biol.* 2016, 18, 777–789, <https://doi.org/10.1038/ncb3378>.
52. Georgakilas, A.G.; Martin, O.A.; Bonner, W.M. p21: A Two-Faced Genome Guardian. *Trends Mol. Med.* 2017, 23, 310–319, <https://doi.org/10.1016/j.molmed.2017.02.001>.
53. Galanos, P.; Pappas, G.; Polyzos, A.; Kotsinas, A.; Svolaki, I.; Giakoumakis, N.N.; Glytsou, C.; Pateras, I.S.; Swain, U.; Souliotis, V.L.; et al. Mutational Signatures Reveal the role of RAD52 in p53-Independent p21-Driven Genomic Instability. *Genome Biol.* 2018, 19, 37, <https://doi.org/10.1186/s13059-018-1401-9>.
54. Kreis, N.-N.; Louwen, F.; Yuan, J. The Multifaceted p21 (Cip1/Waf1/CDKN1A) in Cell Differentiation, Migration and Cancer Therapy. *Cancers* 2019, 11, 1220, <https://doi.org/10.3390/cancers11091220>.
55. Teshima S, Shimosato Y, Hirohashi S, Tome Y, Hayashi I, Kanazawa H, Kakizoe T. Four new human germ cell tumor cell lines. *Lab Invest.* 1988 Sep;59(3):328-36. PMID: 2842544.
56. Wang N, Trend B, Bronson DL, Fraley EE. Nonrandom abnormalities in chromosome 1 in human testicular cancers. *Cancer Res.* 1980 Mar;40(3):796-802. PMID: 7471097.

Chapter



4

Chapter 4

Chromosome 3p25.3 gain is associated with cisplatin resistance and is an independent predictor of poor outcome in male malignant germ cell tumors

Dennis M. Timmerman^{1*}, Thomas F. Eleveld^{1*}, Sruthi Sriram¹, Lambert C.J. Dorssers², Ad J.M. Gillis¹, Silvia Schmidtova^{3,4}, Katarina Kalavska^{3,4,5}, Harmen J.G. van de Werken⁶, Christoph Oing^{7,8}, Friedemann Honecker^{7,9}, Michal Mego^{3,4,5}, Leendert H.J. Looijenga^{1#}

¹ Princess Máxima Center for Pediatric Oncology, Heidelberglaan 25, 3584 CS Utrecht, The Netherlands

² Department of Pathology, Lab. for Exp. Patho-Oncology (LEPO), Erasmus MC-University Medical Center Rotterdam, Cancer Institute, The Netherlands

³ Cancer Research Institute, Biomedical Research Center, Slovak Academy of Sciences, Dubravska Cesta 9, 845 05 Bratislava, Slovakia

⁴ Translational Research Unit, Faculty of Medicine, Comenius University, Klenova 1, 833 10 Bratislava, Slovakia

⁵ 2nd Department of Oncology, Faculty of Medicine, Comenius University and National Cancer Institute, Klenova 1, 833 10 Bratislava, Slovakia

⁶ Cancer Computational Biology Center & Department of Urology & Department of Immunology, Erasmus MC Cancer Institute, University Medical Center, Rotterdam, the Netherlands

⁷ Department of Oncology, Hematology and Bone Marrow Transplantation with Division of Pneumology, University Medical Center Eppendorf, Hamburg, Germany

⁸ Mildred Scheel Cancer Career Center HaTriCs4, University Cancer Center Hamburg, University Medical Center Eppendorf, Hamburg, Germany

⁹ Tumor- and Breast Center ZeTuP, Sankt Gallen, Switzerland

* Equal contribution

PURPOSE

Cisplatin is the main systemic treatment modality for male type II Germ Cell Tumors (GCTs). Although generally very effective, 5-10% of patients suffer from cisplatin-resistant disease. Identification of the driving mechanisms of resistance will enable improved risk stratification and development of alternative treatments.

METHODS

We developed and characterized cisplatin resistant GCT cell line models and compared their molecular characteristics to patient samples with cisplatin resistance and/or a poor clinical outcome. Subsequently, the association between the overlapping genetic features and clinical data were assessed. Finally, we used Cox regression to determine the prognostic relevance of these features within the currently used risk classification.

RESULTS

Gain of chromosome 3p25.3 was detected in all cisplatin resistant cell lines and copy number of this region correlated with the level of resistance ($R=0.96$, $p=1.5e-04$). Gain of this region was detected at low frequencies in primary tumors and at higher frequencies in relapsed and/or cisplatin-resistant tumors. Chromosome 3p25.3 gain was associated with shorter progression-free and overall survival, with the strongest association observed in non-seminomas excluding pure teratomas. 3p25.3 gain was more frequently observed in tumors with yolk sac tumor histology and predicted adverse outcome independent of the IGCCCG risk classification and the presence of *TP53*/*MDM2* alterations.

CONCLUSION

Based on both *in vitro* analyses and clinical data, we found 3p25.3 to be strongly associated with cisplatin resistance and poor clinical outcome in male type II GCTs. Using genomic profiling, 3p25.3 status could help to improve risk stratification in male type II GCT patients. Further characterization of this locus and underlying mechanisms of resistance is warranted to guide development of novel treatment approaches for cisplatin resistant disease.

CONTEXT SUMMARY

Key Objective

Cisplatin is highly effective in treatment of type II male germ cell tumors (GCTs); however, resistance occurs in 5-10% of patients. Understanding of this clinically relevant observation has been hampered by scarcity of suitable material and tools for evaluation. We aim to identify biomarkers of cisplatin resistance through a unique integrated analysis of experimental data and publicly available GCT patient datasets.

Knowledge Generated

Copy number gain of chromosome 3 cytoband p25.3 was identified in laboratory cell line models as a possible driver of cisplatin resistance. In multiple GCT cohorts it was associated with cisplatin resistance, yolk sac tumor histology and significantly poorer PFS and OS. Finally, 3p25.3 gain was demonstrated to be a predictor of poor outcome, independent of the IGCCCG model currently used for GCT risk classification.

Relevance

Incorporating chromosome 3p25.3 copy number status in GCT risk classification can help to identify patients who will respond poorly to cisplatin-based therapy.

INTRODUCTION

Germ cell tumors (GCTs) comprise a heterogeneous group of neoplasms derived from the germ cell lineage, with multiple subtypes mirroring different cells of origin. The most common subtype are the malignant GCTs of the adult testis (Type II), which are the most frequent solid malignancy in men until the age of 34 years¹. Despite an increasing incidence across the globe, mortality rates have decreased remarkably since the introduction of cisplatin-based combination chemotherapies², leading to current five-year survival rates exceeding 90%³. Despite its association with significant long-term side effects, cisplatin yet remains the most effective cytotoxic drug in GCTs and therefor is considered the cornerstone of standard chemotherapy regimens used in the clinic.^{4,5} However, resistance to cisplatin emerges in a small but clinically meaningful number of patients and, apart from high-dose chemotherapy, no alternative treatment options are available⁶.

Cisplatin resistance is known to be associated with histological composition in male type II GCTs. Tumors can consist of seminoma and non-seminoma histologies, with non-seminomas being further subdivided into embryonal carcinoma, yolk sac tumor (YST), choriocarcinoma and teratoma^{7,8}. Seminomas are less likely to develop cisplatin resistance than non-seminomas⁹, while teratomas are inherently cisplatin resistant due to their benign nature¹⁰. Another determinant of cisplatin resistance is anatomical localization of the tumor, with mediastinal tumors showing resistance more frequently. Interestingly, these tumors show frequent *TP53* mutations, implicating this pathway in cisplatin resistance in GCTs¹¹.

It is currently impossible to reliably predict which tumors will respond poorly to cisplatin. The International Germ Cell Cancer Collaborative Group (IGCCCG) classification is a risk staging system that takes into account levels of marker proteins, histology and location, and classifies patients in good, intermediate and poor prognosis¹². Although this classification is the reference for assessing expected outcome, there is still considerable heterogeneity in response to treatment, even within the patients belonging to the poor prognosis subgroup. Consequently, a deeper understanding of cisplatin resistance mechanisms of male type II GCTs may impact upfront patient stratification and would also help development of alternative targeted therapies in this challenging clinical setting.

METHODS

Patient inclusion

Use of patient samples was approved for research by the Medical Ethical Committee of the Erasmus Medical Center (the Netherlands), permit no. 02.981. Samples were used according to the “Code for Proper Secondary Use of Human Tissue in The Netherlands” developed by the Dutch Federation of Medical Scientific Societies (FMWV, version, 2002; update 2011).

Methylation and copy number alteration (CNA) profiling

Analyses were performed as previously described^{13,14}. In brief, copy number analyses were done using the conumee package (Hovestadt V, Zapatka M. conumee: Enhanced copy-number variation analysis using Illumina DNA methylation arrays. R package version 1.9.0, <http://bioconductor.org/packages/conumee>). Data were generated for bins with at least 25 probes. Other settings were default. The reference set was composed of 64 normal male samples from an in-house set (n=14) and from the German Cancer Research Center (n=50, DKFZ, Heidelberg, obtained from Dr. Martin Sill).

Public datasets

Processed data from the TCGA, MSKCC-2016 and MSKCC-2017 cohorts^{11,15,16} were downloaded from cBioportal (February 2021). Copy number data from the MSKCC-2008 cohort¹⁷ was downloaded from NCBI GEO (GSE8614) and subjected to segmentation using the DNACopy R-package (version 1.64.0) using standard settings. MSKCC-2008 contains more than one tumor per patients for some patients. If either of these contains a 3p25.3 gain the respective patient was classified as positive.

Data analysis

Tumors were scored as positive for 3p25.3 gain if any segment that falls within this region (chr3:870000-11800000, HG19) had a higher log2ratio CN than 0.1 (0.2 for TCGA). Using these cut-offs, ~90% of tumors showed gain of chromosome 12p in every dataset, in line with previously reported frequencies of isochromosome 12 presence in type II GCTs^{18,19}. Relationship between categorical variables was determined using Fisher’s exact test or Chi-square test, while the relationship between numerical variables was determined using Pearson correlation coefficient. Cox regression was used to determine multivariable relationships with PFS and OS. Analysis and visualization were performed in R (v4.0.2) and the R2 bioinformatics analysis platform (R2.amc.nl) was used for visualization.

Data availability

Sequencing data ENA PRJEB121669 (WGS, accession numbers ERX4136458-61; RNAseq, accession numbers ERX4136722-30). Methylation data, Array Express, accession number E-MTAB-9114 and GSA data, Array Express, accession number E-MTAB-9266. The primary datasets are available via the various repositories.

Conflict of interest statement

A patent application has been filed covering the finding of using the presence of 3p amplification as a molecular marker to predict cisplatin resistance in germ cell tumors, and the possibility of alternative treatment options.

RESULTS

This study includes a unique set of matched sensitive (i.e. parental) and cisplatin-resistant male type II GCT non-seminoma cell lines generated in two laboratories independently (Supplementary Table I). Cisplatin concentrations at which cell growth was inhibited by 50% (IC50s) were significantly higher in the resistant subclones of NCCIT, 2102Ep, and NT2 than in their parental counterparts (Figure 1A). No chemo-naïve subclone was available for Tera-1, however its IC50 is higher than all sensitive subclones and in the same order of magnitude as found in the resistant cell lines.

To determine the mechanism behind the observed resistance, parental and resistant cell lines were subjected to complete molecular characterization. Cisplatin resistance has been shown to be associated with differentiation in GCTs²⁰, however, no changes were identified in microRNAs 371-3p, 373-3p and 885-5p, which are associated with the differentiation status in GCTs²¹ (Figure 1B). Concordantly, no major consistent changes in RNA expression and methylation status were identified in the resistant lines (Supplementary Figure 1A and B), which would be expected if resistant lines underwent differentiation. Overall, this demonstrated that the observed acquired resistance was not driven by differentiation, which has been identified as a major mechanism of intrinsic treatment resistance in teratomas. Moreover, no clearly enriched processes were identified in the differentially expressed/methylated genes (data not shown).

Analysis of DNA copy number variation by Whole Genome Sequencing identified a recurrent copy number gain involving chromosome 3p, cytoband 25.3 in all the resistant lines compared to their parental counterparts (Figure 1C), suggesting that this aberration could be associated with cisplatin resistance in male type II GCTs. Copy number of this region showed a strong correlation with the IC50 in the corresponding cell lines, suggesting that there is a dose dependent effect (Supplementary Figure 2). The two

resistant clones for NCCIT and NT2 that were independently generated showed different breakpoints for the 3p25.3 region, precluding the selection of an existing subclone, therefore indicating a *de novo* event likely promoted through repeated cisplatin exposure (Supplementary Figure 3).

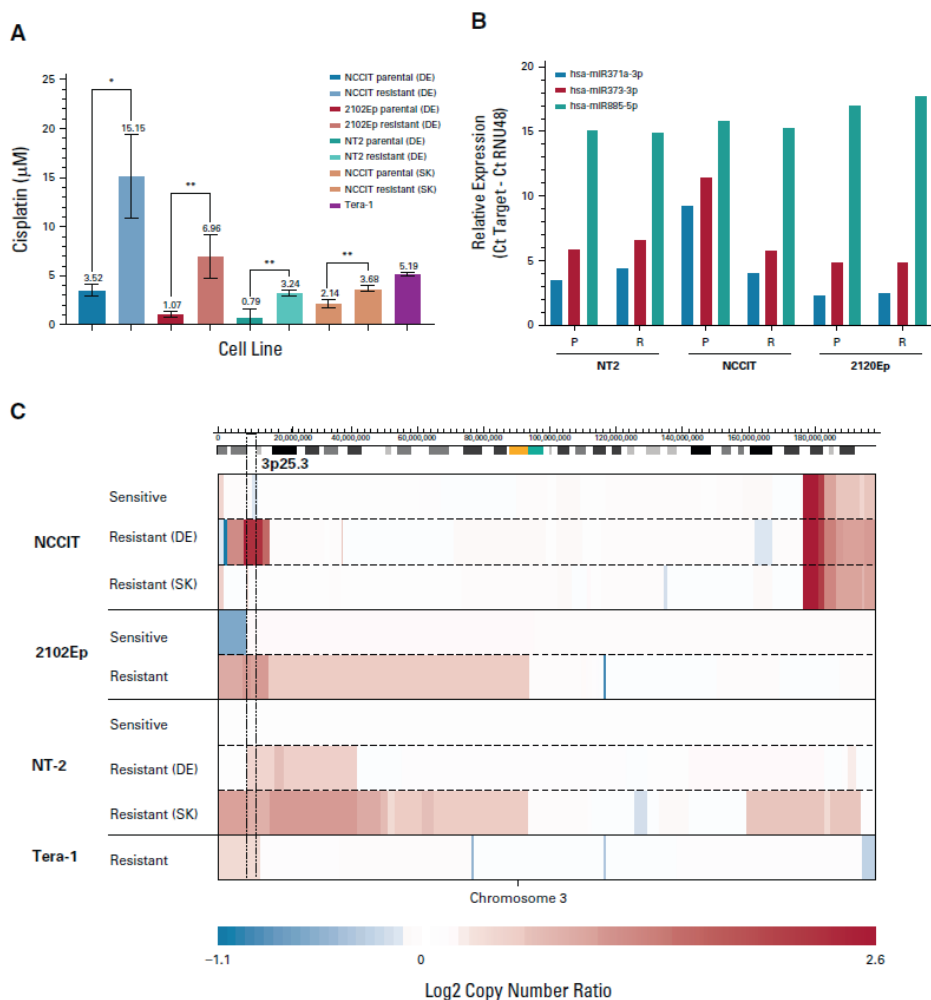


FIG 1. Characterization of cisplatin-resistant cell lines indicates 3p25.3 gain as a potential driver of cisplatin resistance in GCTs. **(A)** IC50s of cisplatin sensitive lines and resistant counterparts. Bars represent the means and standard deviations of triplicate experiments. * $P \leq .05$, ** $P \leq .01$. **(B)** Expression of selected microRNAs in cell lines as determined by using RT-qPCR. Bars represent expression relative to the RNU48 snoRNA. **(C)** Copy number plots of selected cell lines on chromosome 3. Copy numbers were determined using WGS. Blue indicates loss and red indicates gain of the respective region, with color intensity reflecting the extent which is indicated in the scale bar below. The 3p25.3 region is indicated with dashed lines. DE, Germany; GCT, germ cell tumor; IC50, half maximal inhibitory concentration; P, parental; R, resistant; RT-qPCR, quantitative reverse transcription PCR; SK, Slovakia; WGS, whole-genome sequencing.

To assess whether copy number gain of chromosome 3p25.3 also occurred in GCT tissue samples, unselected primary type II male GCTs were screened for the presence of this aberration. Copy number gain on chromosome 3p25.3 (defined as a log2 copy number ratio >0.1) was identified in 15/221 tumors (6.8%), indicating that it is a rare event in primary GCTs. Both segmental gains as well as whole chromosome gains were observed (Figure 2A). In metastasized and/or cisplatin resistant GCTs the frequency of 3p25.3 gain was higher (29%, 2/7), although the number of cases was limited. In addition, 3p25.3 gain was present in several relapses/metastases, while it was not detectable or present at lower copy number in the matched primary tumor (Figure 2B and C). This suggests that 3p25.3 gain might either occur as a *de novo* event, as we observed in our resistant cell lines, or could already be present at diagnosis, possibly at lower frequencies, providing a selective advantage during treatment and progression.

To determine whether the observed frequencies are representative, several publicly available male type II GCT cohorts were analyzed (Supplementary Table 2). The cohort from the TCGA contains untreated primary male type II GCTs and yields a somewhat higher frequency of 3p25.3 gain than our cohort (13/133, 9.7%). The tumors in the MSKCC-2016 cohort are classified as cisplatin sensitive or cisplatin resistant based on their treatment response. A frequency of 17.1% (13/76) was found in the chemotherapy sensitive tumors and 33.7% (35/104) in the chemo resistant tumors (Figure 3A, $p=0.02$ as determined by Fisher's exact test). In the MSKCC-2008 cohort, which contains primary GCTs, treated samples and metastases, 3p25.3 gain was identified in 12.2% of tumors (9/74). In summary, 3p25.3 gain is relatively rare in primary, untreated GCTs, while this frequency increases in metastasized and/or cisplatin resistant tumors.

In line with a proposed role for 3p25.3 gain in cisplatin resistance, patients with a 3p copy number gain have a significantly poorer prognosis than patients without this aberration, as determined in the MSKCC-2016 patient series (Supplementary Figure 4). Seminomas generally respond better to chemotherapy and are less likely to develop resistance than non-seminomas⁹ and therefore the occurrence of 3p25.3 gain was analyzed separately in both histologic subgroups. Gain of 3p25.3 was less frequent in seminomas, where it was observed in similar frequencies in resistant and non-resistant tumors, while in non-seminomas, it was significantly more frequent in resistant tumors (Figure 3B, $p=0.003$ Fisher's exact test). This suggests that 3p25.3 gain contributes to cisplatin resistance only in non-seminomas. Concordantly, in non-seminomas there was a highly significant correlation between gain of 3p25.3 and shorter Progression Free Survival (PFS) (Figure 3C), while no such association was found in seminomas (Supplementary Figure 5A). In the MSKCC-2008 cohort, which consists of only non-seminomas, there is a strong association between 3p25.3 gain and shorter Overall Survival (OS) (Figure 3D). Teratomas are known to be intrinsically cisplatin resistant, and that is why they were excluded from the MSKCC-2016 cohort. If excluded from the MSKCC-2008

cohort, the relationship between 3p25.3 gain and shorter OS became even more apparent (Supplementary Figure 6). Finally, a GCT dataset from the pan-cancer MSK-Impact series¹⁶ was assembled, focusing only on male tumors. This set has a large overlap with the MSKCC-2016 dataset; however, for this set, the OS instead of PFS was reported for 124 tumors. In this set (MSKCC-2017) there also was a significant association between 3p25.3 gain and shorter OS, specifically in non-seminomas (Figure 3E, Supplementary Figure 5B). The GCTs that were previously reported in the MSKCC-2016 showed a similar effect on OS as the other tumors from the GCT MSKCC-2017 cohort, excluding the possibility that the observed OS effect is solely driven by the observed PFS effect shown in Figure 3C (Supplementary Figure 7). This reinforces the presumed role of 3p25.3 gain in cisplatin resistance and the poor prognosis that is associated with it, especially in non-seminomas.

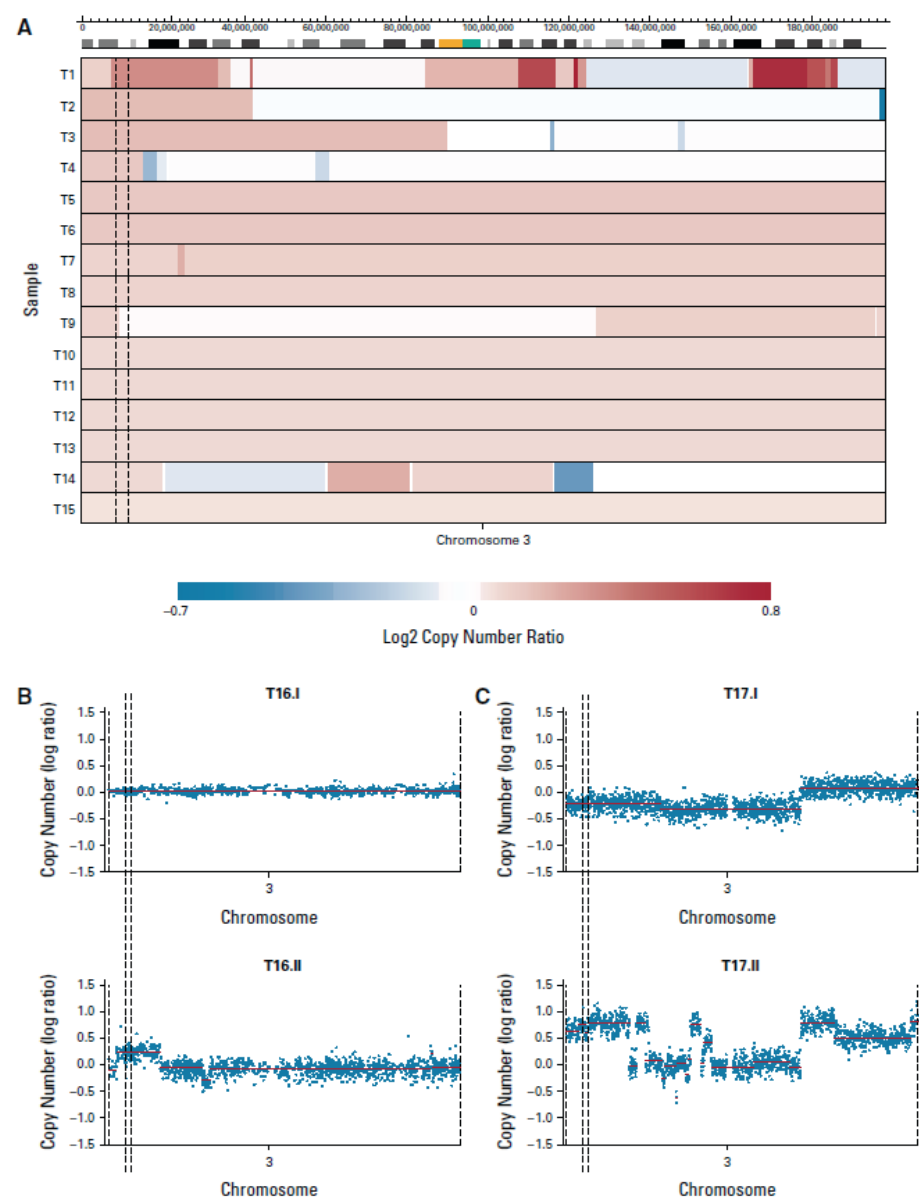


FIG 2. (Continued). 3p25.3 gain is rare in primary tumors and more frequent in resistant and/or metastasized tumors. **(A)** Copy number plots of all tumors in our cohort that show 3p25.3 gain. Copy numbers were determined using methylation profiling. Blue indicates loss and red indicates gain of the respective region, with color intensity reflecting the extent which is indicated in the scale bar below. The 3p25.3 region is indicated with dashed lines. **(B)** Copy number plots of a primary metastasis pair that has a 3p25.3 gain in the metastasis (lower) and not in the primary tumor (upper). Blue dots represent bins and red lines represent copy number segments. The 3p25.3 region is indicated with dashed lines. **(C)** Copy number plots of a pre-post treatment tumor pair that has a 3p25.3 gain in the pretreatment tumor (upper), which shows an increase in copy number in the post-treatment tumor (lower). Blue dots represent bins and red lines represent copy number segments. The 3p25.3 region is indicated with dashed lines.

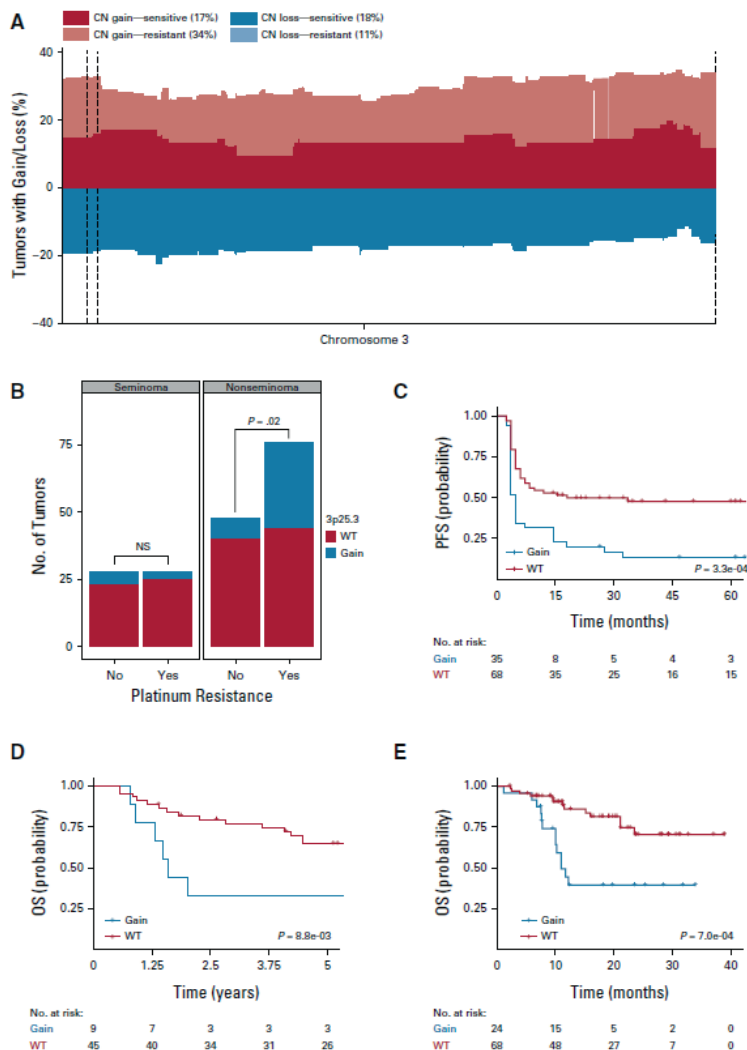


FIG 3. 3p25.3 gain is more frequent in cisplatin-resistant tumors and is associated with poor prognosis, especially in nonseminoma tumors. **(A)** Frequency plot of gain and loss on chromosome 3 in the MSKCC-2016 cohort. Gain/loss in the cisplatin-sensitive tumors is plotted in deep red/blue while gain/loss in the cisplatin-resistant tumors is superimposed in a lighter color. The 3p25.3 region is indicated by dashed lines. Frequencies at which 3p25.3 gain/loss is identified in the sensitive/resistant tumors are shown in the legend within parentheses. Note that the light blue bars are not visible in the figure since the cisplatin-resistant tumors consistently show lower frequencies of chromosome 3 loss than sensitive tumors. **(B)** Bar graph showing the number of tumors with 3p25.3 gain in seminomas and nonseminomas, respectively. Lines show the significance of the ratio 3p gained versus nongained in the sensitive and resistant tumors in each subtype as determined by using Fisher's exact test. **(C)** Kaplan-Meier plot of PFS in nonseminoma tumors in the MSKCC-2016 cohort on the basis of the presence of 3p25.3 gain. The P value was generated using the log-rank test. **(D)** Kaplan-Meier plot of OS in nonseminomas in the MSKCC-2008 cohort on the basis of the presence of 3p25.3 gain. The P value was generated using the log-rank test. **(E)** Kaplan-Meier plot of OS in nonseminomas in the MSKCC-2017 cohort on the basis of the presence of 3p25.3 gain. The P value was generated using the log-rank test. CN, copy number; OS, overall survival; PFS, progression-free survival; WT, wild-type.

Correlating clinical data with gain of 3p25.3 in non-seminomas revealed a strong association with YST histology (Figure 4A, $p\text{-val}=7.5\text{e-}0,3$ Fisher's exact test). The same association was observed in the other cohorts (Supplementary Figure 8). Hypothetically, YST histology is the main determinant of poor survival, which may determine the association between 3p25.3 and poorer survival outcomes. However, in the MSKCC-impact dataset there was no clear association between histology and PFS in general, while within the YSTs 3p25.3 gain was borderline associated with a poor prognosis. Moreover, within the non-seminomas 3p25.3 gain was still strongly associated with poor prognosis if YSTs were excluded from the analysis (Supplementary Figure 9). This suggests that 3p25.3 gain occurs preferentially but not exclusively in YSTs and may serve as a biomarker of treatment resistance and poor prognosis for all non-teratomatous non-seminomas.

Genetic aberrations in *TP53* and *MDM2* have previously been suggested to be involved in cisplatin resistance in male type II GCTs¹¹. To determine how the presence of these aberrations relates to 3p25.3 gain and survival, *TP53/MDM2* and 3p25.3 status were analyzed together. Aberrations in *TP53* and gain of 3p25.3 co-occurred more frequently than expected by chance alone (Figure 4A, $p=0.02$, Fisher's exact test), while there was no association with an *MDM2* amplification ($p=1$, Fisher's exact test). In line with the observation that *TP53* mutations are frequently seen in mediastinal tumors, there was also an enrichment of 3p25.3 gain in mediastinal tumors ($p=0.01$, Fisher's exact test). GCTs that had both 3p25.3 gain and aberrations in *TP53* or *MDM2* had a poorer prognosis than tumors with a single aberration, while there was no difference in survival between patients that harbored only 3p25.3 gain and no *TP53/MDM2* aberrations, and patients that showed the inverse pattern (Figure 4B). This suggests that P53 pathway inactivation and 3p25.3 gain are two separate mechanisms leading to cisplatin resistance in GCTs. If they co-occur in the same tumor, the prognosis seems to be even worse.

The main predictor for the prognosis of primarily advanced GCTs is currently the IGCCCG risk classification¹², however, there was no significant association between IGCCCG poor risk stage and 3p25.3 gain ($p=0.167$, Chi-square test). To determine how IGCCCG stage and 3p25.3 status relate to prognosis and whether 3p25.3 status could add to GCT risk classification, a multivariable Cox regression analysis was performed. This showed that 3p25.3 gain was a strong predictor of poor PFS, independent of IGCCCG risk category, in this cohort of non-seminomas (Supplementary Figure 10). Moreover, if *TP53/MDM2* status was added to the model, 3p25.3 gain remained a strong independent predictor of PFS, while *TP53/MDM2* status was not significant anymore (Figure 4C). Within the MSKCC-2008 set, 3p25.3 gain showed a similar effect as an independent predictor of OS when analyzed together with the IGCCCG risk classification, although it does not reach significance, possibly due to the low number of cases (Supplementary Figure 11). Overall, this indicates that 3p25.3 status may aid in risk classification of male type II GCTs.

Chromosome 3p25.3 gain is associated with cisplatin resistance and is an independent predictor of poor outcome in male malignant germ cell tumors

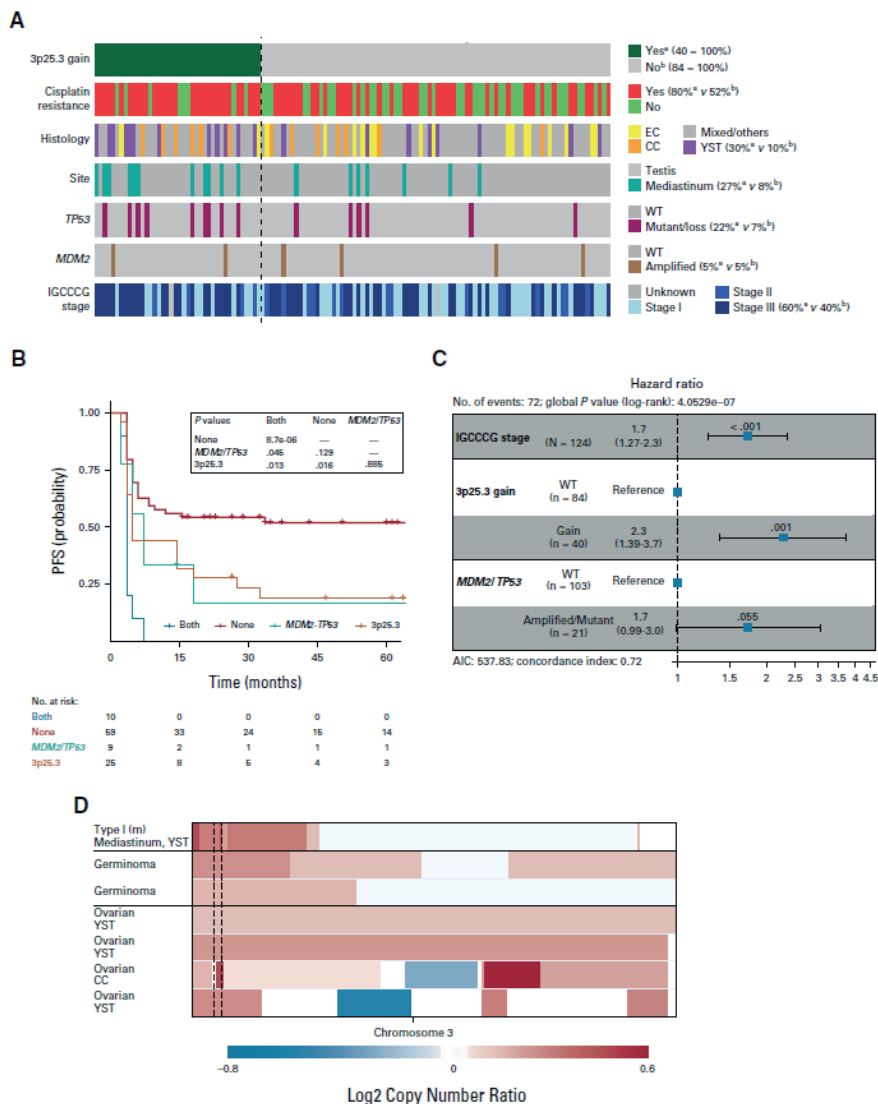


FIG 4. 3p25.3 gain is an independent predictor for poor prognosis in male type II nonseminomas. **(A)** OncoPrint of 3p25.3 gain and various other genetic and clinical parameters of the 124 nonseminomas in the MSKCC-2016 cohort. Columns represent tumors with colors representing the various characteristics per tumor. The dashed line separates the tumors with 3p gain from the tumors without. Numbers to the right of the legend represent the percentage of tumors with the indicated characteristic in the ^a3p25.3 gained and ^bWT tumors, respectively. **(B)** Kaplan-Meier analysis of the MSKCC-2016 nonseminoma cohort separated by TP53/MDM2 and 3p25.3 gain status. The table shows P values for between-group comparisons which were generated using the log-rank test with Benjamini-Hochberg multiple testing correction. **(C)** Forest plot of the hazard ratios calculated by Cox regression survival analysis on the MSKCC-2016 nonseminoma cohort. **(D)** Copy number plots of selected GCTs on chromosome 3. Copy numbers were generated using methylation profiling/next-generation sequencing. Blue indicates loss and red indicates gain of the respective region, with color intensity reflecting the extent which is indicated in the scale bar below. The 3p25.3 region is indicated with dashed lines. AIC, Akaike's information criterion; CC, choriocarcinoma; EC, embryonal carcinoma; GCT, germ cell tumor; PFS, progression-free survival; TE, teratoma; WT, wild-type; YST, yolk sac tumor.

Although the post-pubertal type II male GCTs are the most frequent manifestation of GCTs, they can also occur in pediatric patients (type I) and in post-pubertal girls (type II ovarian), as well as in the brain (i.e. germinoma or dysgerminoma)⁷. Our data and the MSKCC-Impact data were screened and gain of 3p25.3 was identified in one male pediatric type I tumor, two germinomas, and four ovarian type II GCTs (Figure 4D). Interestingly, four of these seven tumors contained a YST histology, suggesting that 3p25.3 could be associated with YST histology also in other GCTs.

DISCUSSION

Despite the excellent overall five-year survival rates of male type II GCTs since the introduction of cisplatin-based combination chemotherapy, intrinsic or acquired cisplatin resistance remains a major clinical challenge with unfavorable prognostic impact. Understanding the biology of this phenomenon is paramount to identify (i) biomarkers to predict treatment resistance, (ii) ways to prevent it from developing, and (iii) novel effective targeted therapies for relapsed and refractory disease. Research on this topic is hampered by the overall low availability of metastatic cisplatin resistant tumors, especially with histologically proven, viable non-teratomatous disease.

Therefore, we initially used several independent sets of male type II GCT-derived cell lines to screen for general mechanisms of cisplatin resistance. The cisplatin-resistant cell line subclones showed different magnitudes of cisplatin resistance and were generated using different methodologies, however, they all showed *de novo* gain of chromosome 3p25.3. No other recurrent molecular changes were identified, even though the lines were extensively investigated. Moreover, copy number on chromosome 3p25.3 showed a strong dose-dependent relationship with cisplatin sensitivity in our cell line models.

The subsequent analysis of patient samples demonstrated that the observed 3p25.3 gain can

be found in patient samples and is not an *in vitro* artefact. It was identified at low frequencies in untreated primary GCTs and at significantly higher frequencies in metastasized, pre-treated and / or cisplatin resistant tumors, which highlights a possible role in cisplatin resistance. There was considerable heterogeneity in the frequencies at which 3p25.3 gain was identified in the different datasets; however, we propose that this is at least partially driven by heterogeneity in the patient composition of the individual datasets investigated. Especially the various MSKCC datasets are heavily enriched for metastasized and pre-treated tumors and are not a representative sampling of all male type II GCTs^{11,17}. Gain of 3p25.3, however, remains strongly associated with both PFS and OS independently of dataset composition, indicating that this gain in chromosomal material may possibly serve as a stable predictive and prognostic biomarker of cisplatin

resistant disease. The fact that 3p25.3 gain is associated with worse PFS as well as OS suggests that cisplatin resistance through 3p25.3 gain is not readily overcome by high-dose chemotherapy.

The preferential presence of the 3p25.3-amplification in YSTs was identified before¹⁷ and is in keeping with identification of 3p25.3 gain in a cisplatin-resistant ovarian YST cell line²². In addition, about 20% of ovarian YSTs showed increased copy numbers of 3p25.3²³. While this predominance of 3p25.3-amplification in YSTs remains to be explained, it might be related to a higher vulnerability of this histological element to develop copy number aberrations because of less stringent DNA maintenance mechanisms due to the limited life span of this tissue type under physiological circumstances⁸. Interestingly, the presence of 3p25.3 gain remains associated with poor prognosis, even within the YSTs, indicating that it is not a bystander but a driving event in cisplatin resistance.

Gain of 3p25.3 was observed across all histological GCT subtypes; however, it is not associated with a worse prognosis in seminomas. Furthermore, if teratomas are excluded, the relationship with poor outcome becomes stronger. Consequently, we propose that 3p25.3 gain should only be considered as a marker for poor prognosis in non-seminomas excluding pure teratomas. Most observed male type II GCTs contain mixed histologies at diagnosis²⁴. Our data does indicate that 3p25.3 gain promises to be a useful prognostic marker for this group as well. However, more research is needed to identify whether the histological composition is associated with the prognostic power of 3p25.3 gain.

The fact that 3p25.3 gain was found in both pediatric (type I) and adult (type II) GCTs, as well as in testicular, mediastinal, and ovarian primaries, suggests that it could represent a more general, possibly universal type of mechanism of cisplatin resistance in GCTs. Whether there is an association with survival, and whether this is specific to certain histological subtypes, remains to be determined. Interestingly, loss of chromosome 3p is generally much more common than gain of this region, especially in squamous cell tumors²⁵. Further research should indicate whether 3p25.3 gain as a proposed mechanism of cisplatin resistance is specific to GCTs or is a more general mechanism that has not been identified so far in other tumor types.

We detect a positive correlation between the presence of 3p25.3 gain and *TP53* mutations, but the background and functional impact of this remains to be determined. Hypothetically, this could be caused by a higher tolerance/propensity for acquiring genetic aberrations in specific tumors, or that presence of one aberration increases the chances of acquiring the other. The survival analyses showed that tumors with both 3p25.3 and *TP53/MDM2* aberrations had an even poorer prognosis than tumors harboring only one alteration. This suggests that 3p25.3 gain and aberrations in the *TP53/MDM2* axis are independent mechanisms of cisplatin resistance, in line with a recently described independent functional role of P53 in GCT treatment resistance²⁶.

The IGCCCG risk staging is an established tool for risk classification and treatment-decision making in male type II GCTs. Our analyses suggests that 3p25.3 gain could be a strong independent predictor of poor prognosis, even when accounting for the IGCCCG risk categories. It has recently been described that the presence of *TP53/MDM2* mutations could also add to patient stratification in male type II GCTs¹¹, but even when this information was added to the regression model, gain of 3p25.3 remains a strong independent risk factor for poor outcome. Although this finding awaits validation using more clinical datasets, we believe that gain of 3p25.3 could be a valuable diagnostic tool and prognostic biomarker for the identification of cisplatin-resistant tumors. Identification of a genomically defined "high risk" group of patients which is already clinical routine in many other malignancies, e.g. leukemias or myeloma^{27,28}, could improve risk stratification and potentially guide treatment decisions in GCT patients, too. Finally, further research on the mechanism(s) through which 3p25.3 gain drives cisplatin-resistance could open new therapeutic avenues to treat refractory patients for whom currently little curative treatment options are available.

Funding

This study received funding from the Princess Máxima Center for Pediatric Oncology and the Bergh in het Zadel Foundation.

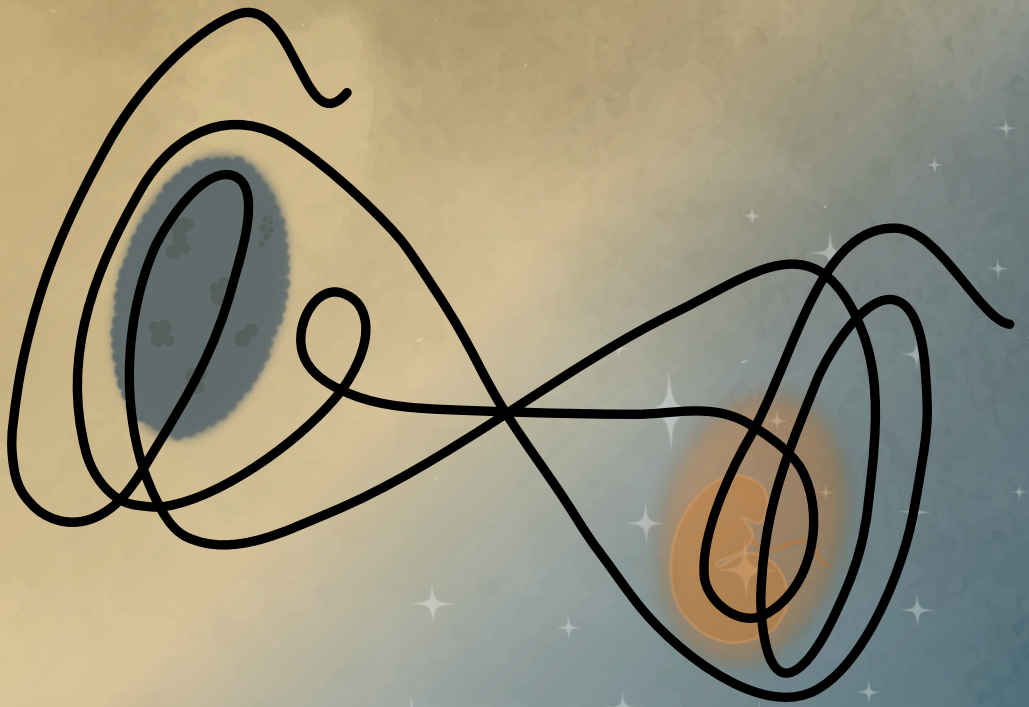
REFERENCES

1. Bray F, Richiardi L, Ekbom A, et al: Trends in testicular cancer incidence and mortality in 22 European countries: continuing increases in incidence and declines in mortality. *Int J Cancer* 118:3099-111, 2006
2. Einhorn LH, Donohue J: Cis-diamminedichloroplatinum, vinblastine, and bleomycin combination chemotherapy in disseminated testicular cancer. *Ann Intern Med* 87:293-8, 1977
3. Siegel RL, Miller KD, Fuchs HE, et al: Cancer Statistics, 2021. *CA Cancer J Clin* 71:7-33, 2021
4. Chovanec M, Abu Zaid M, Hanna N, et al: Long-term toxicity of cisplatin in germ-cell tumor survivors. *Ann Oncol* 28:2670-2679, 2017
5. Curreri SA, Fung C, Beard CJ: Secondary malignant neoplasms in testicular cancer survivors. *Urol Oncol* 33:392-8, 2015
6. Jacobsen C, Honecker F: Cisplatin resistance in germ cell tumours: models and mechanisms. *Andrology* 3:111-21, 2015
7. Oosterhuis JW, Looijenga LH: Testicular germ-cell tumours in a broader perspective. *Nat Rev Cancer* 5:210-22, 2005
8. Oosterhuis JW, Looijenga LHJ: Germ cell tumors from a developmental perspective. *Nat. Rev. Cancer*. 19(9):522-537., 2019
9. Adra N, Einhorn LH: Testicular cancer update. *Clin Adv Hematol Oncol* 15:386-396, 2017
10. Korkola JE, Houldsworth J, Bosl GJ, et al: Molecular events in germ cell tumours: linking chromosome-12 gain, acquisition of pluripotency and response to cisplatin. *BJU Int* 104:1334-8, 2009
11. Bagrodia A, Lee BH, Lee W, et al: Genetic Determinants of Cisplatin Resistance in Patients With Advanced Germ Cell Tumors. *J Clin Oncol* 34:4000-4007, 2016
12. Gillissen S, Sauv   N, Collette L, et al: Predicting Outcomes in Men With Metastatic Nonseminomatous Germ Cell Tumors (NSGCT): Results From the IGCCCG Update Consortium. *J Clin Oncol* 39:1563-1574, 2021
13. Dorssers LCJ, Gillis AJM, Stoop H, et al: Molecular heterogeneity and early metastatic clone selection in testicular germ cell cancer development. *Br J Cancer* 120:444-452, 2019
14. Rijlaarsdam MA, Tax DM, Gillis AJ, et al: Genome wide DNA methylation profiles provide clues to the origin and pathogenesis of germ cell tumors. *PLoS One* 10:e0122146, 2015
15. Shen H, Shih J, Hollern DP, et al: Integrated Molecular Characterization of Testicular Germ Cell Tumors. *Cell Rep* 23:3392-3406, 2018
16. Zehir A, Benayed R, Shah RH, et al: Mutational landscape of metastatic cancer revealed from prospective clinical sequencing of 10,000 patients. *Nat Med* 23:703-713, 2017
17. Korkola JE, Heck S, Olshen AB, et al: In vivo differentiation and genomic evolution in adult male germ cell tumors. *Genes Chromosomes Cancer* 47:43-55, 2008
18. Kraggerud SM, Skotheim RI, Szymanska J, et al: Genome profiles of familial/bilateral and sporadic testicular germ cell tumors. *Genes Chromosomes Cancer* 34:168-74, 2002
19. Mostert MM, van de Pol M, Olde Weghuis D, et al: Comparative genomic hybridization of germ cell tumors of the adult testis: confirmation of karyotypic findings and identification of a 12p-amplicon. *Cancer Genet Cytogenet* 89:146-52, 1996

20. Abada PB, Howell SB: Cisplatin induces resistance by triggering differentiation of testicular embryonal carcinoma cells. *PLoS One* 9:e87444, 2014
21. Lobo J, Gillis AJM, van den Berg A, et al: Identification and Validation Model for Informative Liquid Biopsy-Based microRNA Biomarkers: Insights from Germ Cell Tumor In Vitro, In Vivo and Patient-Derived Data. *Cells* 8, 2019
22. Schmidtova S, Dorssers LCJ, Kalavska K, et al: Napabucasin overcomes cisplatin resistance in ovarian germ cell tumor-derived cell line by inhibiting cancer stemness. *Cancer cell international* 20:364-364, 2020
23. Kraggerud SM, Hoei-Hansen CE, Alagaratnam S, et al: Molecular characteristics of malignant ovarian germ cell tumors and comparison with testicular counterparts: implications for pathogenesis. *Endocr Rev* 34:339-76, 2013
24. Mostofi FK, Sesterhenn IA: Pathology of germ cell tumors of testes. *Prog Clin Biol Res* 203:1-34, 1985
25. Taylor AM, Shih J, Ha G, et al: Genomic and Functional Approaches to Understanding Cancer Aneuploidy. *Cancer Cell* 33:676-689.e3, 2018
26. Timmerman DM, Eleveld TF, Gillis AJM, et al: The Role of TP53 in Cisplatin Resistance in Mediastinal and Testicular Germ Cell Tumors. *Int J Mol Sci* 22, 2021
27. Perrot A, Corre J, Avet-Loiseau H: Risk Stratification and Targets in Multiple Myeloma: From Genomics to the Bedside. *American Society of Clinical Oncology Educational Book*:675-680, 2018
28. Papaemmanuil E, Gerstung M, Bullinger L, et al: Genomic Classification and Prognosis in Acute Myeloid Leukemia. *New England Journal of Medicine* 374:2209-2221, 2016

Chromosome 3p25.3 gain is associated with cisplatin resistance and is an independent predictor of poor outcome in male malignant germ cell tumors

Chapter



5

Chapter 5

Comparative Analyses of Liquid-Biopsy MicroRNA371a-3p Isolation Protocols for Serum and Plasma

Dennis M. Timmerman¹, Ad J.M. Gillis ¹, Michal Mego ² and Leendert H.J. Looijenga ^{1,*}

Princess Máxima Center for Pediatric Oncology, 3584 CSUtrecht, The Netherlands;
D.M.Timmerman-6@prinsesmaximacentrum.nl (D.M.T.);
A.J.M.Gillis@prinsesmaximacentrum.nl (A.J.M.G.)

² Translational Research Unit and 2nd Department of Oncology, Faculty of Medicine, Comenius University and National Cancer Institute, 84505 Bratislava, Slovakia; misomego@gmail.com

* Correspondence: L.Looijenga@prinsesmaximacentrum.nl; Tel.: +31-88-972-5211

SIMPLE SUMMARY

The active disease status of patients with a malignant germ cell tumor can be evaluated using detection of specific body-circulating microRNAs. However, various methods are reported to isolate and detect microRNAs from blood, possibly influencing the score as positive or negative. Here, we investigated two frequently used techniques for microRNA isolation from blood, either serum or plasma, to evaluate possible differences. These data are required to compare published studies and to select the best methods in the future. No effect of either starting with plasma or serum was found, indicating that both blood products can be used. The bead-based method was more stable and applicable on small blood volumes, whereas the total RNA method exhibited a higher sensitivity due to a larger starting volume. These results are important to develop the optimal method for the detection of microRNAs in blood to monitor malignant germ cell tumor patients in clinic practice.

ABSTRACT

MicroRNAs (miRNAs) are short, non-coding RNAs involved in translation regulation. Dysregulation has been identified in cancer cells. miRNAs can be secreted and detectable in body fluids; therefore, they are potential liquid-biopsy biomarkers. The miR-371a-3 cluster members are an example, monitoring the presence of malignant germ cell tumors based on patient serum/plasma analyses. However, a large variety of isolation techniques on sample types (serum vs. plasma) are reported, hampering interstudy comparisons. Therefore, we analyzed the impact of using the miRNeasy Serum/Plasma Kit (cell-free total RNA purification) Qiagen extraction kit and the TaqMan anti-miRNA bead-capture procedure of ThermoFisher for miRNA isolation. Ten normal male matched serum and plasma samples and seventeen testicular germ cell tumor patient serum samples were investigated. The Qiagen kit requires a higher input volume (200 μ L vs. 50 μ L), resulting in higher sensitivity. Serum and plasma comparison demonstrated high similarity in miRNA levels. Titration experiments showed that the bead-capture procedure is superior in cases of lower starting volumes (<100 μ L). This study highlights the strengths and limitations of two different isolation protocols, relevant for in vivo analysis with small starting volumes. In summary, miRNA detection levels results varied little between plasma and serum, whereas for low volumes the bead capture isolation method is preferable.

Keywords: cancer; clinical investigation; molecular diagnostics; real-time PCR; quantitative analysis of nucleic acids.

INTRODUCTION

Biomarkers are known to be a strong clinical tool to detect, diagnose and stratify cancer patients as well as aid in the development of new treatments by predicting patient responses and outcomes [1]. In this context, microRNAs (miRNAs) are potentially highly useful as molecular biomarkers because they can be disease-specific, are often secreted into bodily fluids, are stable with a short half-life, and are relatively easy to extract and detect [2]. Secreted miRNAs are therefore extremely interesting as clinical liquid-biopsy biomarkers because they can mark the cells of (tumor) origin and can be used as clinical tools for disease monitoring (e.g., whole blood, serum or plasma and cerebrospinal fluid) [3]. However, various isolation and determination techniques are characterized by different sensitivity and specificities; therefore, determining a precise cut-off between the different methods has been challenging the field of liquid-biopsy-based biomarker applications [4,5].

Liquid-biopsy-based miRNA biomarkers have, for example, been demonstrated to be particularly useful in (testicular) germ cell tumors ((T)GCTs) [6–11]. The levels of the miRNA cluster 371a-373 (normally specifically present during embryonal development) are elevated in 87% in seminomas and in more than 90% of non-seminomatous (T)GCT patients (teratomas excluded), while hardly detected in healthy individuals [11], excluding false positive findings. However, the detection limit, precision and specificity of various extraction methods and isolation protocols have not yet been compared extensively, thereby increasing the risk of identifying false positive and negative cases. We exploit the already proven high specificity and sensitivity of hsa-miRNA371a and 373 to demonstrate a clean comparison between isolation protocols and starting material [11].

To shed light on these aspects, we performed a relatively simple, although highly informative, comparative study using matched serum and plasma samples from 10 healthy male donors (age 18–40 years) and 17 serum samples from diagnosed TGCT patients. The miRNeasy Serum/Plasma Advanced Kit Qiagen extraction kit (cell-free total RNA purification) was compared to the TaqMan anti-miRNA bead-capture procedure (~370 miRNAs) from ThermoFisher. This comparison was specifically investigated because of the various methods used in the field possibly relating to variations in results [7,8,12–14] or conditions [4,5,15–21]. Together with the use of various isolation methods, differences between serum and plasma samples have been suggested to explain results between studies [8,12–14,18]. Our results demonstrate a lower detection limit for the cell-free total RNA purification of the Qiagen kit compared to the bead-based method, whereby the latter generally showed a lower variation in isolation efficiency. Furthermore, using hsa-miR371a-3p, we demonstrate that the bead-based method is more sensitive to low levels of this specific miR target. We conclude that both serum and plasma samples can be used as liquid-biopsy starting material to detect hsa-miR371a-3p as molecular biomarker for TGCTs, whereas the Qiagen kit generally has a lower detection limit in

exchange for lower precision. Furthermore, the bead-capture procedure is superior even in cases of small starting voluminal amounts of the sample. These data are relevant in the context of development of the most stable, sensitive and specific method for final clinical applications of hsa-miR371a-3p in liquid biopsies.

MATERIALS AND METHODS

Patient and Control Serum/Plasma Samples

Use of patient samples remaining after diagnosis was approved for research by the Medical Ethical Committee of the EMC (The Netherlands), permit no. 02.981. This included permission to use the secondary samples without further consent. Samples were used according to the “Code for Proper Secondary Use of Human Tissue in The Netherlands” developed by the Dutch Federation of Medical Scientific Societies (FMWV, version, 2002;update 2011). The use of patient samples provided by Dr. Michal Mego was approved according to institutional board review (2020). This retrospective translational study was approved by the Institutional Review Board (IRB) of the National Cancer Institute.

miRNA Purification

miRNAs were isolated from 50 µl serum and plasma using target-specific anti-miR magnetic beads, as reported before (OncoTarget 2016). In short, a KingFisher Flex robot with TaqMan® miRNA ABC Purification Kit Human Panel A (ThermoFisher PN 4473087, Waltham, MA, USA) was used to isolate miRNAs. All reagents are provided in the kit. These panels consist of superparamagnetic Dynabeads covalently bound to a unique set of ~380 anti-miR oligonucleotides. Briefly, 100 µl of lysis buffer (containing spike-in) was added to 50 µl of serum/plasma, followed by the addition of 80 µl of beads (10^6 beads/µl). Samples were incubated at 30°C for 40 min, then washed three times with wash buffer. The bound miRNAs were eluted from the beads with 100 µl elution buffer.

RNA from 200 µl of thawed serum and plasma was isolated using the miRNeasy Serum/Plasma Advanced Kit from Qiagen (PN 217204), according to the manufacturer's instructions. In order to increase RNA yield, MS2 carrier RNA (Roche PN 10165948001) was added to a final concentration of 1.25 µg/ml. Total RNA was eluted from columns with 50 µl of nuclease-free water. During the lyses of the samples, a non-human spike-in Cel-miR39 (5.6×10^8 copies) external control was added to each sample, in both isolation-techniques, to monitor the RNA recovery.

Quality Control Assessment

To check the RNA recovery and suitability for use in subsequent RT-PCR, 1 μ l of the purified miRNA/RNA was reverse-transcribed using a TaqMan miRNA RT Kit (PN 4366597) and TaqMan miRNA assays for Cel-miR39-3p (000200) and hsa-miR30b-5p (000602). miRNA levels were detected on a QuantStudio 12K Flex machine.

Hemolysis Assessment

Hemolysis levels were evaluated according to the “miR-32a/451a” ratio, as previously reported [22]. Furthermore, it was assessed by visual inspection as previously reported by Lobo et al. [7]. No samples were discarded after both assessments.

Target-Specific Real-Time PCR

For miRNA profiling, 5 μ l of the purified miRNA/RNA was reverse-transcribed using TaqMan miRNA RT Kit (PN 4366597) and an equal mixture of the RT-primers of Cel-miR39-3p (000200), hsa-miR30b-5p (000602), hsa-miR371a-3p (002124), hsa-miR373-3p (000561), and hsa-miR375 (000564). The final volume of 15 μ l for each reaction underwent RT using a BioRad T100 Thermal Cycler at 16 °C for 30 min, 42 °C for 30 min, followed by a final step of 85 °C for 5 min. To increase sensitivity and specificity, a 12-cycle pre-amplification step was included. Briefly, an equal mix of all 20 \times TaqMan miRNA assay probes was prepared for each reaction and diluted to 0.2 \times with 1 \times Tris-EDTA Buffer (pH 8.0). Each sample contained 12.5 μ l 2 \times TaqMan PreAmp Master Mix (PN 4488593), 7.5 μ l of diluted TaqMan assay probe mix, and 5 μ l of multiplexed cDNA product. After heating to 95 °C for 10 min, 12 cycles of 95 °C for 15 s and 60 °C for 4 min were run on a thermal cycler (BioRad). The resulting reaction products were diluted 1:4 with nuclease-free water to a final volume of 100 μ l. For the final singleplex PCR, 1.5 μ l of the diluted pre-amplification product was added to 10 μ l 2 \times TaqMan Advanced PCR Master Mix (PN 4444964), and 1 μ l of each individual 20 \times TaqMan primer/probe assay. All reactions were performed in duplicate. miRNA levels were determined on a QuantStudio 12K Flex machine. All kits were purchased from Thermo Fisher Scientific, Bleiswijk, The Netherlands.

Data Normalization and Analysis

For normalization, endogenous reference hsa-miR30b-5p was used as described previously [24]. miRNA levels were relatively quantified according to the $2^{-\Delta\Delta C_t}$ method after normalization to housekeeping hsa-miR30b-5p. Targets were corrected for hsa-miR30b-5p values corrected for average hsa-miR30b-5p levels in the total population to correct for deviations in the endogenous levels of hsa-miR30b-5p. Data were processed

using Excel, and data were visualized using GraphPad Prism 9.3. Statistical significance was determined using an unpaired two-tailed Student's *t*-test.

RESULTS

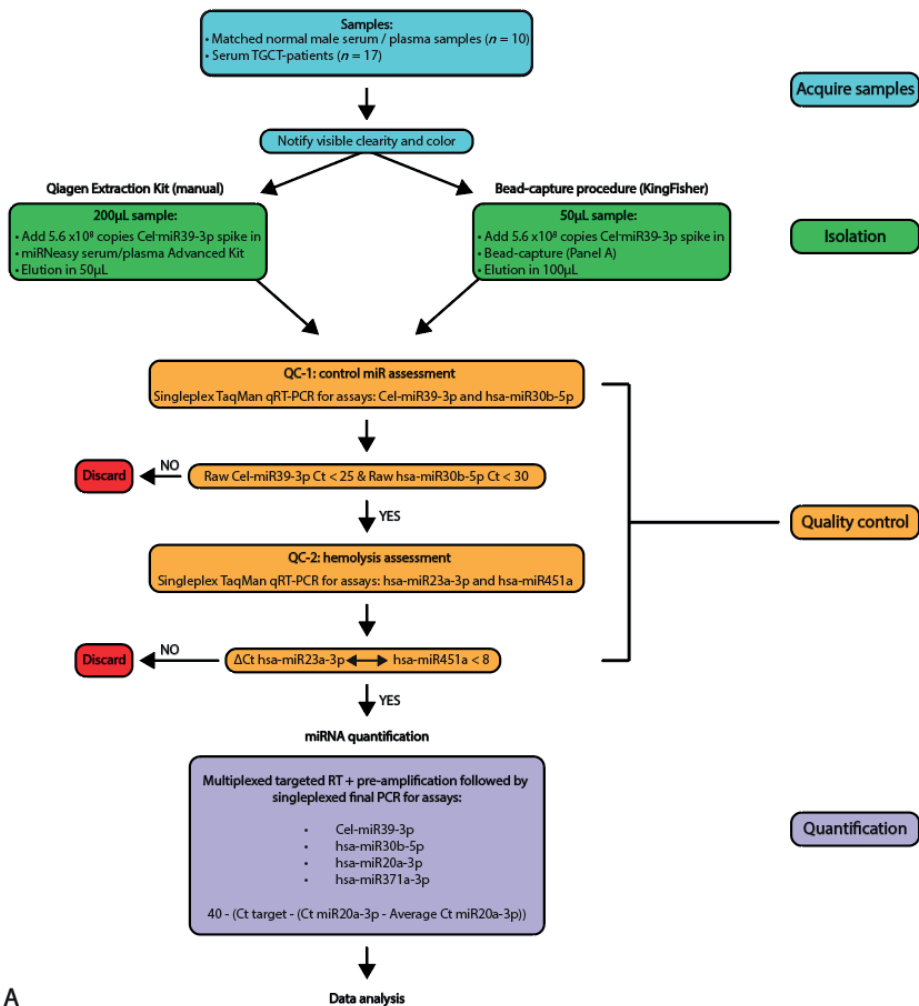
Sample Preparation and Quality Control.

miRNAs from 10 unrelated matched serum and plasma samples originating from control males and 17 serum samples from independent TGCT patients were isolated using the two different methods and qualitatively analyzed and quantified using qRT-PCR (full study set-up and workflow are displayed in Figure 1 A and B, sample names are presented in Table 1). The samples were first subjected to multiple quality control experiments before being analyzed quantitatively for miRNA levels. Figure 2A and 2B display box-plotted Ct values for the spike-in Cel-miR39-3p (Median Ct Beads: 23.81 ± 1.3 , Median Ct Qiagen 28.84 ± 5.25) and endogenous hsa-miR30b-5p (Median Ct Beads: 30.33 ± 7.59 , Median Ct Qiagen 27.62 ± 7.56) (Quality control 1), measured by singleplex TaqMan qRT-PCR (individual values plotted in Figure S1A and B). Consistency of RNA extraction efficiency between samples was as expected, as measured by Cel-miR39-3p (Median Ct Beads: 23.81 ± 1.30 , Median Ct Qiagen: 24.84 ± 5.25 , Figure 2A). Serum/plasma levels of internal control hsa-miR30b-5p were also within the expected range (Median Ct Beads: 30.33 ± 7.59 , Median Ct Qiagen: 27.62 ± 7.56 , Figure 2B). The bead capture procedure displayed little variation with the spike-in control, whereas the Qiagen kit showed a consistent difference (~ 2 Ct) between control serum and plasma samples (Figure 2A). In the TGCT patient serum samples, again, the bead-based protocol resulted in little variation with the spike-in, where the Qiagen kit showed more differences in isolation efficiency (up to ~ 5 Ct). Both methods showed little variation (or differences) relating to the endogenous hsa-miR30b-5p levels (Figure 2B). Due to differences in inputs (200 μ L for Qiagen and 50 μ L for beads) and elutions (50 μ L Qiagen and 100 μ L beads), a difference of 1Ct, in favor of the Qiagen kit, was expected. However, when comparing the Ct values for hsa-miR30b-5p for the Qiagen isolation and bead capture, the Qiagen kit overall showed a more efficient recovery of hsa-miR30b-5p ($p < 0.0001$), where the bead-capture showed a more efficient recovery of Cel-miR39-3p ($p = 0.0002$). In summary, little difference was observed in isolation efficiency between serum and plasma when using a bead-capture isolation protocol, where the Qiagen kit probably had a slightly better detection limit (Figure 2C).

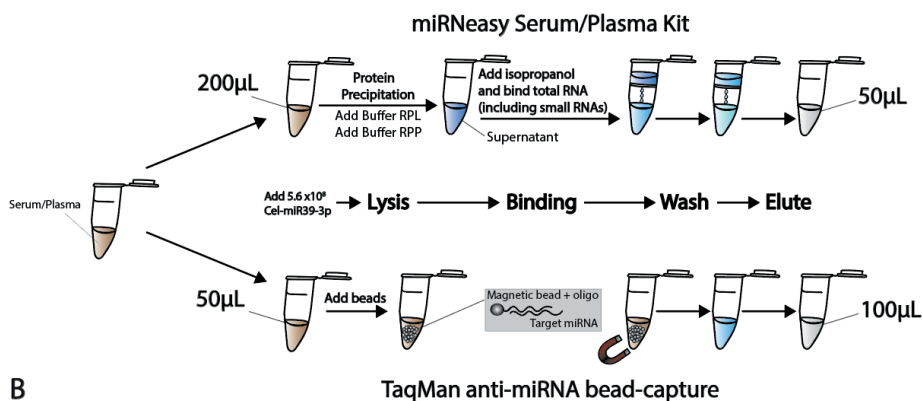
Table 1. Sample codes. Corresponding samples linked to codes used in figures.

#	Code	Serum/Plasma	Graph Annotation
1	S-267	normal serum	S1
2	P-299	normal plasma	P1
3	S-306	normal serum	S2
4	P-326	normal plasma	P2
5	S-254	normal serum	S3
6	P-279	normal plasma	P3
7	S-255	normal serum	S4
8	P-289	normal plasma	P4
9	S-310	normal serum	S5
10	P-331	normal plasma	P5
11	S-261	normal serum	S6
12	P-277	normal plasma	P6
13	S-263	normal serum	S7
14	P-293	normal plasma	P7
15	S-270	normal serum	S8
16	P-285	normal plasma	P8
17	S-265	normal serum	S9
18	P-280	normal plasma	P9
19	S-268	normal serum	S10
20	P-300	normal plasma	P10
21	L10-156	serum TGCT (YST)	TGCTS1
22	L11-107	serum TGCT (YST)	TGCTS2
23	L11-160	serum TGCT (mixed NS)	TGCTS3
24	L12-360	serum TGCT (mixed NS)	TGCTS4
25	L12-067	serum TGCT (mixed NS)	TGCTS5
26	L13-035	serum TGCT (EC)	TGCTS6
27	L13-109	serum TGCT (mixed NS)	TGCTS7
28	L13-121	serum TGCT (mixed NS)	TGCTS8
29	L13-138	serum TGCT (EC)	TGCTS9
30	L12-187	serum TGCT (mixed NS)	TGCTS10
31	L12-026	serum TGCT (mixed NS)	TGCTS11
32	L17-220	serum TGCT (mixed NS)	TGCTS12
33	L18-141	serum TGCT (SE)	TGCTS13
34	L14-254	serum TGCT (mixed NS)	TGCTS14
35	L15-193	serum TGCT (SE)	TGCTS15
36	L15-402	serum TGCT (SE)	TGCTS16
37	L18-137	serum TGCT (mixed NS)	TGCTS17

Abbreviations: SE: seminoma, NS: non-seminoma, EC: embryonal carcinoma, YST: yolk-sac tumor.



A



B

Figure 1. Schematic overview of the study set-up and workflow. **(A)** A schematic overview of the study setup used, depicting the acquiring of the samples, isolation, quality control and quantification techniques used. **(B)** Schematic overview of the workflow used with the two isolation protocols (Qiagen kit and bead-capture).

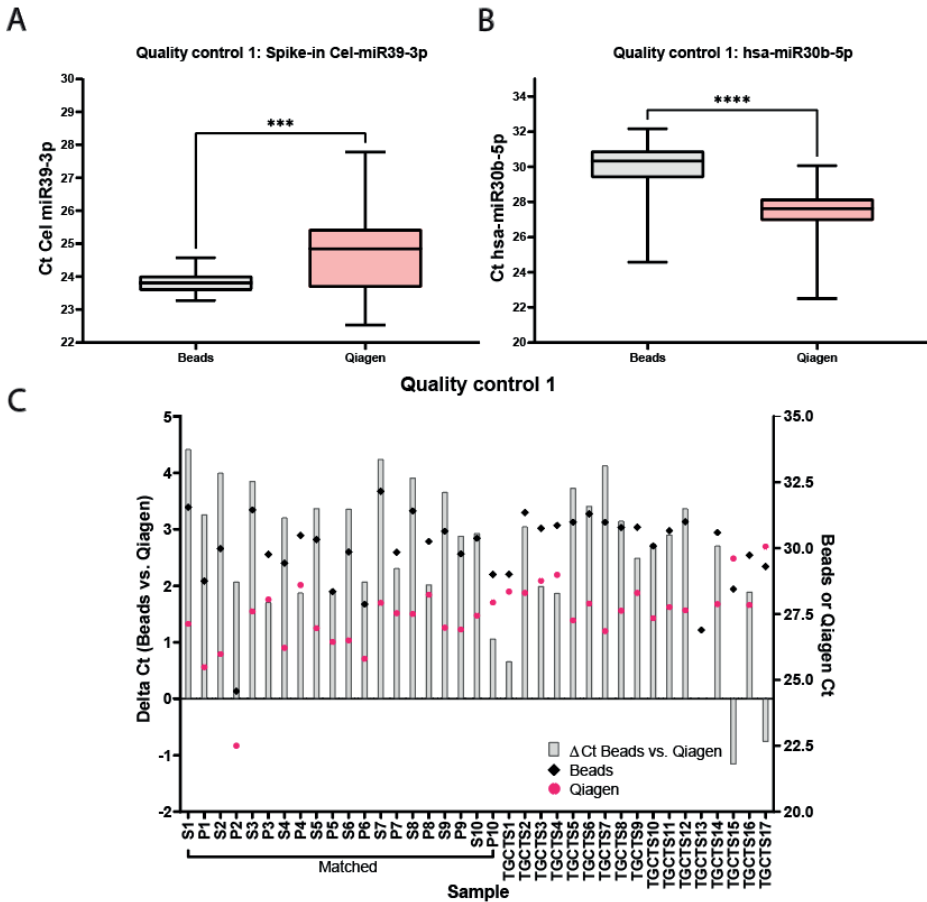


Figure 2. Quality control for bead-capture and Qiagen kit isolation. **(A)** Cts for Cel-miR39-3p spike-in quality control isolated with beads (black) or Qiagen (pink). Average Ct Beads: 23.81 ± 0.33 , Average Ct Qiagen 24.68 ± 1.32 , *** $p < 0.005$. **(B)** Cts for hsa-miR30b-5p endogenous quality control isolated with beads (black) or Qiagen (pink). Average Ct Beads: 29.98 ± 1.45 , Average Ct Qiagen 27.45 ± 1.30 , **** $p < 0.0001$. **(C)** Delta Cts of hsa-miR30b-5p between the bead-capture and Qiagen kit isolation (grey bars). Raw Cts obtained with the bead (black) or Qiagen (pink) isolation protocol are plotted on the right y-axis.

Qiagen Kit MiRNA Isolation Has a Higher Detection, Whereas Both Kit and Bead Isolation Display Similar Results between Serum- and Plasma-Isolated Samples.

Next, we profiled the serum and plasma samples for hsa-miR371a-3p, normalized for hsa-miR30b-5p and displayed as 40 – normalized Ct. The results are displayed for the Qiagen kit and bead-capture in Figure 3A and B, respectively (p values in Table 2, raw data and correction in Table S1 and S2). Black bars represent samples that were corrected for the average hsa-miR30b-5p Cts among combined serum and plasma samples, whereas pink bars represent data corrected for the average Ct of only serum samples (because TGCTS samples were only serum-derived, these were only corrected for serum averages). The Qiagen kit resulted in less low-level detection and showed comparable results between serum and plasma samples, except for S3 and S10, showing some low-levels of the GCT miRNA (Ct of ~33 and 35, respectively) Furthermore, hsa-miR371a-3p could be detected in all TGCT sera, except in the case of TGCTS13, being excluded from the analysis due to high viscosity after protein precipitation (Qiagen kit only), and TGCTS 15–17, which were pure seminomas known to express low levels of hsa-miR371a-3p. Notably, TGCTS 15, 16 and 17 were derived from patients that had normal levels of the standard biomarkers AFP, bHCG and LDH and had tumors <2 mm (Table 3). The bead-capture procedure showed more low-level detection, e.g., the control sera displayed some levels (Ct of ~30–35) of the TGCT-specific miRNA. All tested TGCTS samples were positive for hsa-miR371a-3p, albeit lower levels were detected in TGCTS 15–17, again, due to these samples being known to have low levels of biomarkers (Table 2). Correction for endogenous control hsa-miR20a-5p produced similar results (Figure S2 and Table S3 and S4). Finally, we also measured the levels of hsa-miR375 in 10 matched serum and plasma samples of healthy control samples and corrected for endogenous hsa-miR30b-3p (Ct hsa-miR375–Ct hsa-miR30b-5p, Figure 3C and Table S5). We present no differences between the Qiagen kit or bead-capture-based miRNA isolation (Δ Ct Qiagen vs. Beads 0.65 ± 0.50 , $p = 0.16$). Furthermore, we did not find differences between serum or plasma samples (Δ Ct serum vs. plasma Qiagen 0.83 ± 0.40 , $p = 0.64$, Δ Ct serum vs. plasma Beads 0.63 ± 0.43 , $p = 0.22$, Raw data presented in Table S5).

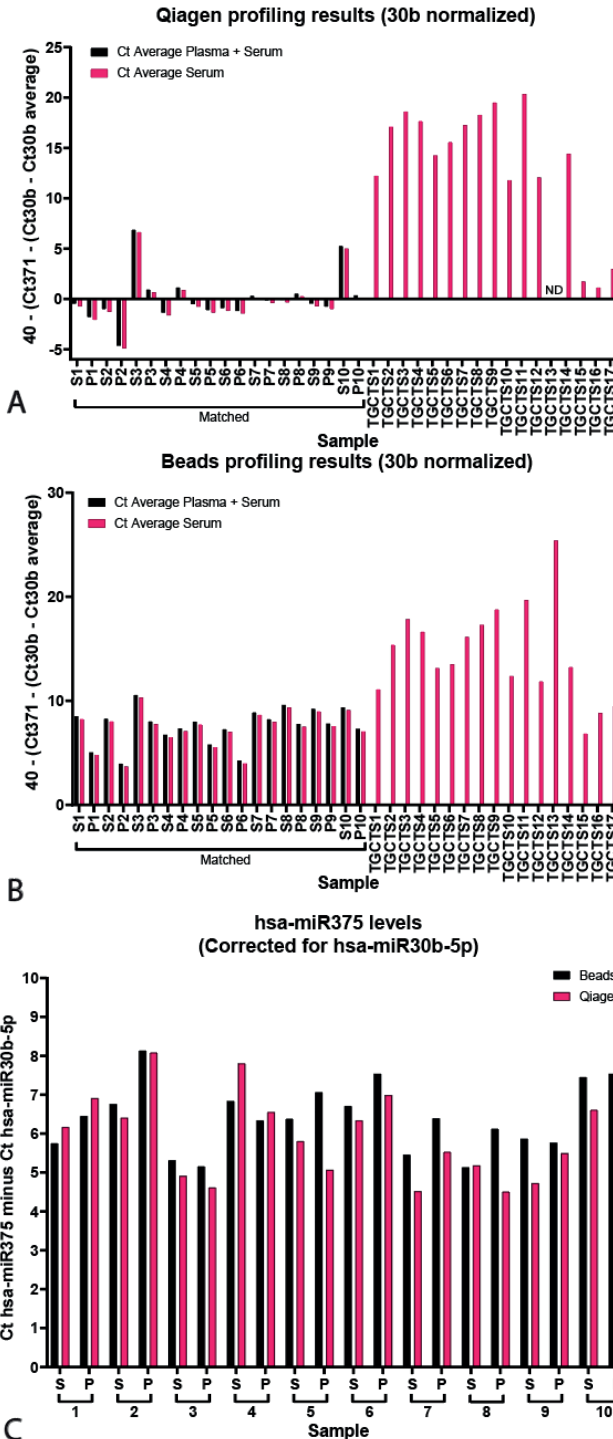


Table 2. p-values of hsa-miR371a-3p detection in healthy control and TGCT patient samples corrected for hsa-miR30b-5p.

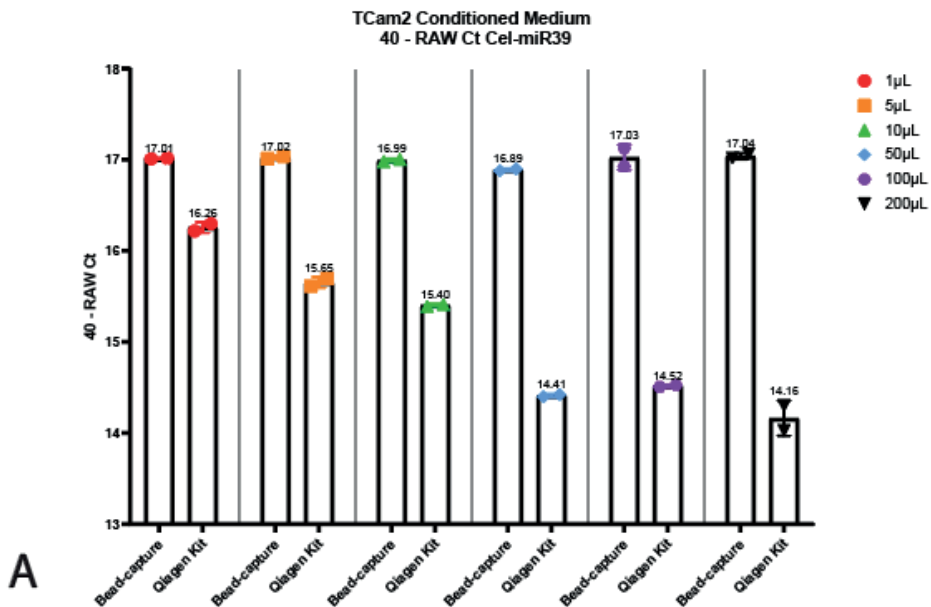
Comparison	p-Value
Qiagen kit healthy donor serum vs. plasma	0.18
Qiagen kit healthy serum vs. TGCT serum	<0.0001
Bead-capture healthy donor serum vs. plasma	0.0039
Bead-capture healthy serum vs. TGCT serum	0.0003
Healthy serum + plasma samples Qiagen vs. Beads	<0.0001
Healthy serum samples Qiagen vs. Beads	<0.0001
Healthy plasma samples Qiagen vs. Beads	<0.0001
TGCT serum Qiagen vs. Beads	0.56

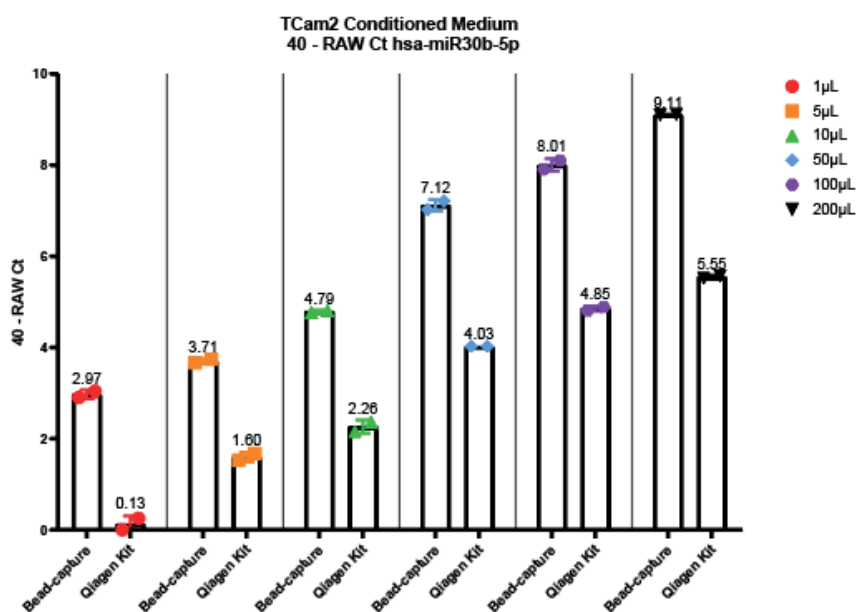
Table 3. Serum marker TGCT patients. Serum marker levels of classical GCT serum markers AFP, b-HCG and LDH. Cells marked with red indicate clinically elevated (above threshold) serum levels of these markers.

		Pre-	Orchiectomy	Markers
Sample-nr.		AFP ug/L	b-HCG IU/L	LDH U/L
1	21	856	< 0.1	190
2	22	1349	< 0.1	237
3	23	669	829	275
4	24	2123	2698	583
5	25	90	< 0.2	98
6	26	1	6	354
7	27	40	400	166
8	28	175	4,5	195
9	29	35	65	275
10	30	29	1268	365
11	31	1.3	0.1	712
12	32	465	210	167
13	33	1	< 1.0	1610
14	34	24	33	219
15	35	0.9	0.8	255
16	36	1.4	0.3	237
17	37	5	4.3	181

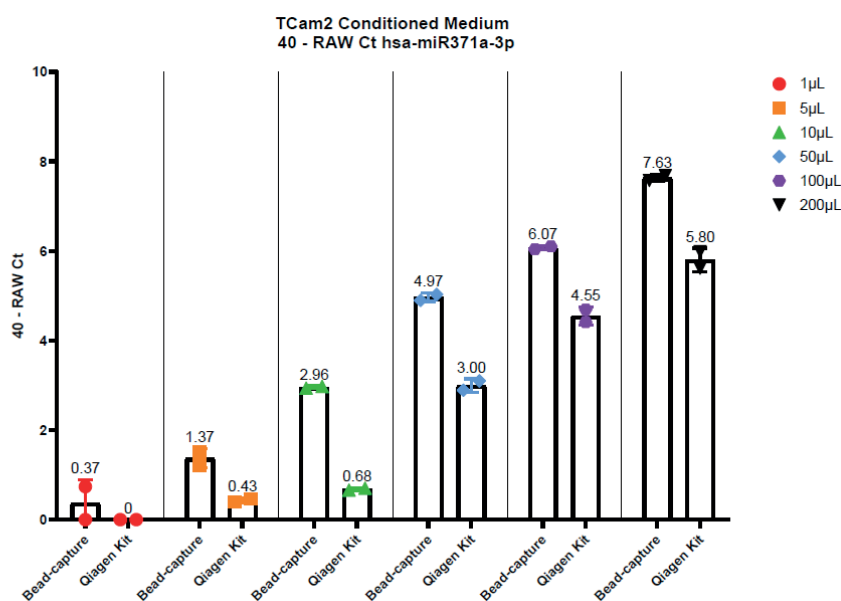
Input Titration Suggests Bead-Capture to Be Superior in Low-Volume Ranges.

The Qiagen kit and the beads required different input volumes (200 μ L vs. 50 μ L, respectively, see above); therefore, we wanted to interrogate whether this had any influence on the quantitative output or detected miRNA levels. To test this, we titrated TCam-2 (TGCT cell line) conditioned medium into various volumes ranging from 1 μ L to 200 μ L, all diluted in PBS up to 200 μ L (Figure 4). Note that conditioned medium does not give a full representation of serum and/or plasma; it can, however, faithfully demonstrate the reproducibility of the technique. Surprisingly, the 40 minus RAW Cts for the Cel-miR39 for the Qiagen kit decreased as the input increased (Figure 4A). However, when using bead-capture isolation, no differences in miRNA detection could be observed when using different input volumes. When using different input volumes to detect endogenous miRNA levels (hsa-miR30b, 371a-3p and 373), the bead-based method was shown to be superior (Figure 3B–D). Even when using 1 μ L (instead of the recommended 50 μ L) for bead-capture isolation, we were able to isolate detectable levels of all three miRNAs (Figure 4). As expected, increasing the amount of input also increased detection levels. Using a 1 μ L starting volume resulted in low (hsa-miR30b-5p) or undetectable miRNA (hsa-miR371a-3p and 373) levels when using the Qiagen kit, increasing the detection levels as the input volume increased.

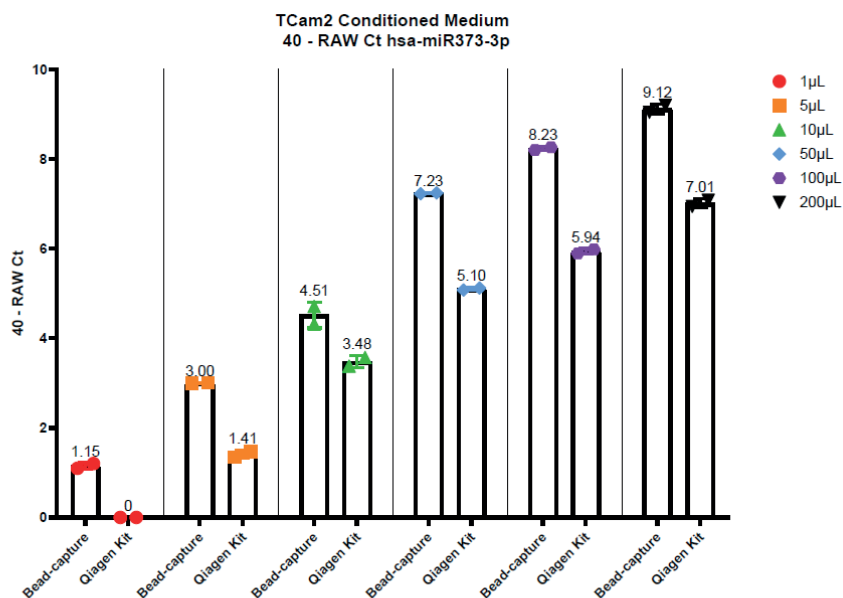




B



C



D

Figure 4. Titration using TCam2 conditioned medium. Displayed are the 40 – Raw Ct values isolated using the bead-capture or Qiagen kit for Cel-miR39 (A), hsa-miR30b-5p (B), hsa-miR371a-3p (C) and hsa-miR373-3p (D). A 40 minus transformation was performed to improve the visual interpretation of data (high bars mean more target detected).

DISCUSSION

Ever since the study published by Lawrie and colleagues in 2008, miRNAs in bodily fluids have been an interesting target for oncogenic biomarker detection [24]. With the discovery of the miR371a-3 cluster and its specific expression in (T)GCTs [25,26], miRNAs have become a suggested cornerstone in (T)GCT detection and monitoring [6,7,9–11]. Many studies have investigated the effects of sample handling on the outcome of biomarker identification studies [4,5, 15–21]. Not only have these studies reported (minor) differences in sample handling, but different groups all over the world use various techniques, protocols (i.e., Bead-capture vs. Qiagen kit) and starting materials (i.e., serum vs. plasma). Where most groups report similar results, especially regarding the fidelity of the miR371a-3 cluster in (T)GCT detection [6,7,9–11], some discrepancies have arisen in the field regarding biomarkers to specifically detect residual teratoma [8, 12–14]. These discrepancies have been suggested by several authors [12,14] to be linked to differences between starting material, i.e., serum vs. plasma, and isolation protocol, i.e.,

Qiagen kit vs. bead-capture. Here, we report a comprehensive analysis of two relevant aspects in the field: (1) the isolation technique: ThermoFisher's TaqMan anti-miRNA bead-capture procedure (~370 miRNAs) vs. the miRNeasy Serum/Plasma Advanced Kit Qiagen extraction kit (cell-free total RNA purification), two of the most commonly used isolation methods; and (2) serum vs. plasma as starting materials [27]. For this study, we used ThermoFisher's RT-primers and assays (Materials and Methods) to detect the miRNAs because these assays have been used by many groups in the field, allowing us to faithfully compare the isolation method and starting material independent of detection [27]. First, we used spike-in Cel-miR39-3p spike-in and endogenous hsa-miR30b-5p as controls to validate to isolation efficiency. We identified an overall lower variation in detection levels and better recovery with the bead-based method (Median Ct Beads: 23.81 ± 1.30 , Median Ct Qiagen: 24.84 ± 5.25 , $p = 0.0002$) for Cel-miR39-3p. Furthermore, we found an overall lower detection limit but equal variation for endogenous miR30b-5p using the Qiagen kit isolation (Median Ct Beads: 30.33 ± 7.59 , Median Ct Qiagen: 27.62 ± 7.56 , $p < 0.0001$), partly accounting for the difference in input volume and total vs. targeted RNA isolation. We compared the differences between serum and plasma using both the Qiagen and bead-based (mi)RNA isolation (results normalized for both endogenous hsa-miR30b and 20a). We observed no differences between serum and plasma in hsa-miR371a-3p levels when isolating miRNAs using the Qiagen kit, whereas the bead-capture performed better when using serum samples ($p = 0.0039$). There was no difference in the detection of hsa-miR371a-3p in TGCT patient serum samples between the Qiagen kit isolation of the bead-capture ($p = 0.56$), whereas bead-capture did detect significantly higher levels of hsa-miR371a-3p in healthy donors ($p < 0.0001$). Both the Qiagen kit and the bead-capture isolation resulted in the detection of significantly higher levels of hsa-miR371a-3p ($p < 0.0001$ and $p = 0.0003$, respectively). The majority of miR371a-3p-related studies are performed on serum samples. However, as concluded in the recent systematic review on the use of this microRNA as a biomarker for TGCT [27], similar overall results have been obtained when serum or plasma were used as starting materials. This is amongst other analyses based on the matched serum and plasma samples of 50 healthy males, showing similar results using the ampTSMiR assay [7,28]. These results show consistent differences between the normalizer (hsa-miR30b-5p) and the target hsa-miR371a-3p, being higher and lower in plasma versus serum, respectively. Therefore, it was concluded that mixed series of both serum as well as plasma will be problematic regarding normalization, and as a result, interpretation. The consistent differences between plasma and serum samples reported is confirmed independently in the study presented here, being independent of the isolation technique applied. Moreover, 25% of the studies included in the forementioned systematic review [27] were based on the bead-capture-based method, whereas the others used a total RNA isolation method, demonstrating the relevance of this comparative analysis. Even when we compared the levels of hsa-miR375 between

the serum and plasma of healthy males, we found no difference between serum and plasma (ΔCt serum vs. plasma Qiagen 0.83 ± 0.40 , $p = 0.64$, ΔCt serum vs. plasma Beads 0.63 ± 0.43 , $p = 0.22$). Furthermore, because we observed clear detectable levels of hsa-miR375 in 10 healthy males (both serum and plasma), we support the findings of Lafin and colleagues, showing that hsa-miR375 is not suitable as a teratoma biomarker at present [13]. Thirdly, because we did not observe any differences between serum and plasma with either hsa-miR371a-3p or hsa-miR375 when using the Qiagen kit ($p = 0.18$), we conclude that this therefore cannot explain reported inconsistencies regarding hsa-miR375 as a teratoma marker as well, also supported by findings in a recent systematic review [12–14,27]. Finally, because the Qiagen kit and bead-capture require different input volumes, we used TCam-2 conditioned medium to detect the differences in miRNA levels between different input volumes. We report an overall lower detection limit for the Qiagen kit, possibly related to total RNA extraction versus targeted extraction. However, when using increasing volumes of Cel-miR39-3p, we found lower levels with the Qiagen kit. In other words, adding more input with the same amount of spike-in detected less of the miRNA when isolating the samples using the Qiagen kit. This is likely explained by the loss of spike-in miRNA during the precipitation step.

CONCLUSIONS

We conclude that in low volume ranges, the bead-capture method is therefore superior and more useful for studies with young patients or mice where less starting volume is available. In summary, the Qiagen kit is the preference compared to the bead-based approach for expected low-expressed miRNAs. However, when limited sample volume is available, the bead-capture method outperforms the Qiagen kit. These results will aid future studies to determine the optimal isolation method for miRNA detection both using serum and plasma.

Supplementary Materials: The following are available online at www.mdpi.com/xxx/s1, Figure S1: Quality control values of Spike-in Cel-miR39-3p (A) and has-miR30b-5p (B). Figure S2: Qiagen kit (A) and bead-capture (B) isolated levels of hsa-miR371a-3p plotted as $40 - (Ct371 - (Ct20a - Ct20a \text{ average}))$. Table S1: Raw data and corrections for hsa-miR371a-3p corrected for hsa-miR30b-5p, extracted using the bead-capture technique. Table S2: Raw data and corrections for hsa-miR371a-3p corrected for hsa-miR30b-5p extracted using the Qiagen kit. Table S3: Raw data and corrections for hsa-miR371a-3p corrected for hsa-miR20a-5p extracted using the bead-capture technique. Table S4: Raw data and corrections for hsa-miR371a-3p corrected for hsa-miR20a-5p extracted using the Qiagen kit. Table S5: Raw Ct values for hsa-miR375.

Author Contributions: Conceptualization, D.M.T., A.J.M.G., M.M. and L.H.J.L.; methodology, A.J.M.G.; software, D.M.T.; validation, D.M.T., A.J.M.G. and L.H.J.L.; formal analysis, D.M.T. and A.J.M.G.; investigation, D.M.T., A.J.M.G. and L.H.J.L.; resources, M.M. and L.H.J.L.; data curation, D.M.T. and A.J.M.G.; writing—original draft preparation, D.M.T.; writing—review and editing, D.M.T., A.J.M.G., M.M. and L.H.J.L.; visualization, D.M.T.; supervision, L.H.J.L.; project administration, M.M. and L.H.J.L.; funding acquisition, L.H.J.L. All authors have read and agreed to the published version of the manuscript.

Funding: This research received no external funding.

Institutional Review Board Statement: This study was conducted according to the guidelines of the Declaration of Helsinki. Use of patient samples remaining after diagnosis was approved for research by the Medical Ethical Committee of the EMC (The Netherlands), permit no. 02.981. This included permission to use the secondary samples without further consent. Samples were used according to the “Code for Proper Secondary Use of Human Tissue in The Netherlands” developed by the Dutch Federation of Medical Scientific Societies (FMWV, version, 2002; update 2011). The use of patient samples provided by Dr. Michal Mego was approved according to institutional board review (2020). This retrospective translational study was approved by the Institutional Review Board (IRB) of the National Cancer Institute.

Informed Consent Statement: Informed consent was obtained from all subjects involved in the study.

Data Availability Statement: The data presented in this study are available on request from the corresponding author. The data are not publicly available due to presence of patient data from different institutes and the pending of a patent.

Acknowledgments: Financially supported by the Princess Maxima Center for Pediatric Oncology (to D.M.T.).

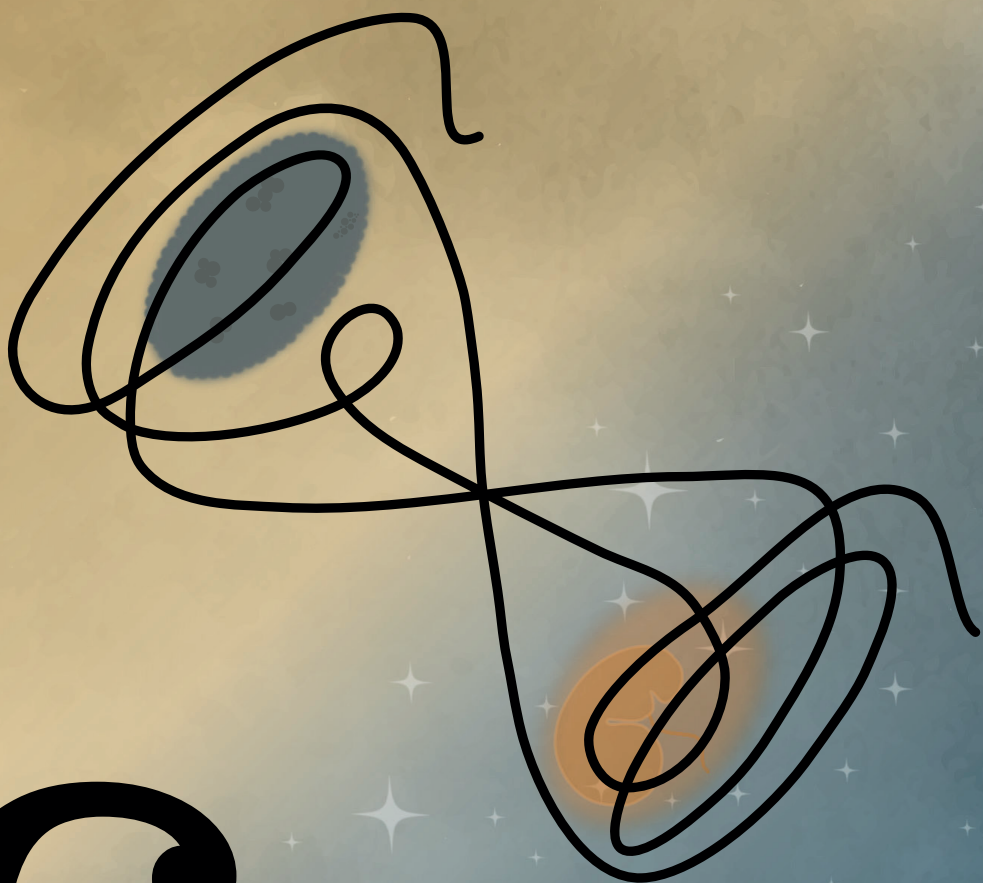
Conflicts of Interest: A patent application has been filed covering the finding of using miR-885-5p and miR-448 as molecular markers for teratoma (and contradicting effect of miR-885-5p on the P53 pathway compared to miR371a-3p).

REFERENCES

1. Lopes, G.; Parker, J.L.; Willan, A.; Shah, S.; Weerasinghe, A.; Rubinger, D.; Falconi, A. The role of biomarkers in improving clinical trial success: A study of 1079 oncology drugs. *J. Clin. Oncol.* 2015, 33, e17804. [CrossRef]
2. Wang, K. The Ubiquitous Existence of MicroRNA in Body Fluids. *Clin. Chem.* 2017, 63, 784–785. [CrossRef] [PubMed]
3. Alix-Panabieres, C.; Pantel, K. Liquid Biopsy: From Discovery to Clinical Application. *Cancer Discov.* 2021, 11, 858–873. [CrossRef] [PubMed]
4. Zhao, H.; Shen, J.; Hu, Q.; Davis, W.; Medico, L.; Wang, D.; Yan, L.; Guo, Y.; Liu, B.; Qin, M.; et al. Effects of preanalytic variables on circulating microRNAs in whole blood. *Cancer Epidemiol. Biomark. Prev.* 2014, 23, 2643–2648. [CrossRef]
5. Matias-Garcia, P.R.; Wilson, R.; Mussack, V.; Reischl, E.; Waldenberger, M.; Gieger, C.; Anton, G.; Peters, A.; Kuehn-Steven, A. Impact of long-term storage and freeze-thawing on eight circulating microRNAs in plasma samples. *PLoS ONE* 2020, 15, e0227648. [CrossRef] [PubMed]
6. Rijlaarsdam, M.A.; van Agthoven, T.; Gillis, A.J.; Patel, S.; Hayashibara, K.; Lee, K.Y.; Looijenga, L.H. Identification of known and novel germ cell cancer-specific (embryonic) miRs in serum by high-throughput profiling. *Andrology* 2015, 3, 85–91. [CrossRef] [PubMed]
7. Lobo, J.; Gillis, A.J.; van den Berg, A.; Dorssers, L.C.; Belge, G.; Dieckmann, K.P.; Roest, H.P.; van der Laan, L.J.; Gietema, J.; Hamilton, R.J.; et al. Identification and Validation Model for Informative Liquid Biopsy-Based microRNA Biomarkers: Insights from Germ Cell Tumor In Vitro, In Vivo and Patient-Derived Data. *Cells* 2019, 8, 1637. [CrossRef]
8. Nappi, L.; Thi, M.; Adra, N.; Hamilton, R.J.; Leao, R.; Lavoie, J.M.; Soleimani, M.; Eigl, B.J.; Chi, K.; Gleave, M.; et al. Integrated Expression of Circulating miR375 and miR371 to Identify Teratoma and Active Germ Cell Malignancy Components in Malignant Germ Cell Tumors. *Eur. Urol.* 2021, 79, 16–19. [CrossRef] [PubMed]
9. Lafin, J.T.; Singla, N.; Woldu, S.L.; Lotan, Y.; Lewis, C.M.; Majmudar, K.; Savelyeva, A.; Kapur, P.; Margulis, V.; Strand, D.W.; et al. Serum MicroRNA-371a-3p Levels Predict Viable Germ Cell Tumor in Chemotherapy-naïve Patients Undergoing Retroperitoneal Lymph Node Dissection. *Eur. Urol.* 2020, 77, 290–292. [CrossRef]
10. Liu, Q.; Lian, Q.; Lv, H.; Zhang, X.; Zhou, F. The Diagnostic Accuracy of miR-371a-3p for Testicular Germ Cell Tumors: A Systematic Review and Meta-Analysis. *Mol. Diagn.* 2021, 1–9. [CrossRef]
11. Almstrup, K.; Lobo, J.; Morup, N.; Belge, G.; Rajpert-De Meyts, E.; Looijenga, L.H.J.; Dieckmann, K.P. Application of miRNAs in the diagnosis and monitoring of testicular germ cell tumours. *Nat. Rev. Urol.* 2020, 17, 201–213. [CrossRef]
12. Lafin, J.T.; Bagrodia, A. Re: Lucia Nappi, Marisa Thi, Nabil Adra, et al. Integrated Expression of Circulating miR375 and miR371 to Identify Teratoma and Active Germ Cell Malignancy Components in Malignant Germ Cell Tumors. *Eur. Urol.* 2021; 79: 16–9. *Eur. Urol.* 2021, 79, e96–e97. [CrossRef]
13. Lafin, J.T.; Kenigsberg, A.P.; Meng, X.; Abe, D.; Savelyeva, A.; Singla, N.; Woldu, S.L.; Lotan, Y.; Mauck, R.J.; Lewis, C.M.; et al. Serum Small RNA Sequencing and miR-375 Assay Do Not Identify the Presence of Pure Teratoma at Postchemotherapy Retroperitoneal Lymph Node Dissection. *Eur. Urol. Open Sci.* 2021, 26, 83–87. [CrossRef]

14. Nappi, L.; Nichols, C.; Kollmannsberger, C. Reply to John T. Lafin, Aditya Bagrodia's Letter to the Editor Re: Lucia Nappi, Marisa Thi, Nabil Adra; et al. Integrated Expression of Circulating miR375 and miR371 to Identify Teratoma and Active Germ Cell Malignancy Components in Malignant Germ Cell Tumors. *Eur. Urol.* 2021, 79, e85–e86. [CrossRef] [PubMed]
15. El Messaoudi, S.; Rolet, F.; Mouliere, F.; Thierry, A.R. Circulating cell free DNA: Preanalytical considerations. *Clin. Chim. Acta* 2013, 424, 222–230. [CrossRef]
16. Weber, D.G.; Casjens, S.; Rozynek, P.; Lehnert, M.; Zilch-Schöneweis, S.; Bryk, O.; Taeger, D.; Gomolka, M.; Kreuzer, M.; Otten, H.; et al. Assessment of mRNA and microRNA Stabilization in Peripheral Human Blood for Multicenter Studies and Biobanks. *Biomark Insights* 2010, 5, 95–102. [CrossRef]
17. Faraldi, M.; Sansoni, V.; Perego, S.; Gomasasca, M.; Kortas, J.; Ziemann, E.; Banfi, G.; Lombardi, G. Study of the preanalytical variables affecting the measurement of clinically relevant free-circulating microRNAs: Focus on sample matrix, platelet depletion, and storage conditions. *Biochem. Med.* 2020, 30, 010703. [CrossRef] [PubMed]
18. McDonald, J.S.; Milosevic, D.; Reddi, H.V.; Grebe, S.K.; Algeciras-Schimmich, A. Analysis of circulating microRNA: Preanalytical and analytical challenges. *Clin. Chem.* 2011, 57, 833–840. [CrossRef] [PubMed]
19. Shiotsu, H.; Okada, K.; Shibuta, T.; Kobayashi, Y.; Shirahama, S.; Kuroki, C.; Ueda, S.; Ohkuma, M.; Ikeda, K.; Ando, Y.; et al. The Influence of Pre-Analytical Factors on the Analysis of Circulating MicroRNA. *Microna* 2018, 7, 195–203. [CrossRef] [PubMed]
20. Binderup, H.G.; Madsen, J.S.; Brasen, C.L.; Houliand, K.; Andersen, R.F. Quantification of microRNA in plasma using probe based TaqMan assays: Is microRNA purification required? *BMC Res. Notes* 2019, 12, 261. [CrossRef]
21. Drula, R.; Ott, L.F.; Berindan-Neagoe, I.; Pantel, K.; Calin, G.A. MicroRNAs from Liquid Biopsy Derived Extracellular Vesicles: Recent Advances in Detection and Characterization Methods. *Cancers* 2020, 12, 2009. [CrossRef]
22. Shah, J.S.; Soon, P.S.; Marsh, D.J. Comparison of Methodologies to Detect Low Levels of Hemolysis in Serum for Accurate Assessment of Serum microRNAs. *PloS ONE* 2016, 11, e0153200. [CrossRef]
23. Murray, M.J.; Bell, E.; Raby, K.L.; Rijlaarsdam, M.A.; Gillis, A.J.; Looijenga, L.H.; Brown, H.; Destenaves, B.; Nicholson, J.C.; Coleman, N. A pipeline to quantify serum and cerebrospinal fluid microRNAs for diagnosis and detection of relapse in paediatric malignant germ-cell tumours. *Br. J. Cancer* 2016, 114, 151–162. [CrossRef] [PubMed]
24. Lawrie, C.H.; Gal, S.; Dunlop, H.M.; Pushkaran, B.; Liggins, A.P.; Pulford, K.; Banham, A.H.; Pezzella, F.; Boulwood, J.; Wainscoat, J.S.; et al. Detection of elevated levels of tumour-associated microRNAs in serum of patients with diffuse large B-cell lymphoma. *Br. J. Haematol.* 2008, 141, 672–675. [CrossRef]
25. Murray, M.J.; Halsall, D.J.; Hook, C.E.; Williams, D.M.; Nicholson, J.C.; Coleman, N. Identification of microRNAs From the miR-371~373 and miR-302 clusters as potential serum biomarkers of malignant germ cell tumors. *Am. J. Clin. Pathol.* 2011, 135, 119–125. [CrossRef] [PubMed]
26. Syring, I.; Bartels, J.; Holdenrieder, S.; Kristiansen, G.; Muller, S.C.; Ellinger, J. Circulating serum miRNA (miR-367-3p, miR-371a-3p, miR-372-3p and miR-373-3p) as biomarkers in patients with testicular germ cell cancer. *J. Urol.* 2015, 193, 331–337. [CrossRef] [PubMed]
27. Leão, R.; Albersen, M.; Looijenga, L.H.; Tandstad, T.; Kollmannsberger, C.; Murray, M.J.; Culine, S.; Coleman, N.; Belge, G.; Hamilton, R.J.; et al. Circulating MicroRNAs, the Next-Generation Serum Biomarkers in Testicular Germ Cell Tumours: A Systematic Review. *Eur. Urol.* 2021. [CrossRef] [PubMed]
28. Mego, M.; van Agthoven, T.; Gronesova, P.; Chovanec, M.; Miskovska, V.; Mardiak, J.; Looijenga, L.H.J. Clinical utility of plasma miR-371a-3p in germ cell tumors. *J. Cell Mol. Med.* 2019, 23, 1128–1136. [CrossRef] [PubMed]

Chapter



6

Chapter 6

miR371a-3 cluster functionality in germ cell tumor cell lines

D. M. Timmerman¹, M. T. Buiting^{1,*}, A. J. M. Gillis^{1,*}, T. F. Eleveld¹, S. Sriram¹, L. Kucerova^{2,3,4}, K. Hainova^{2,3,4}, M. Mego^{2,3,4}, L. H. J. Looijenga¹

¹ Princess Maxima Center for Pediatric Oncology, Heidelberglaan 25, 3584 CS Utrecht, The Netherlands

² Cancer Research Institute, Biomedical Research Center, Slovak Academy of Sciences, Dubravska Cesta 9, 845 05 Bratislava, Slovakia

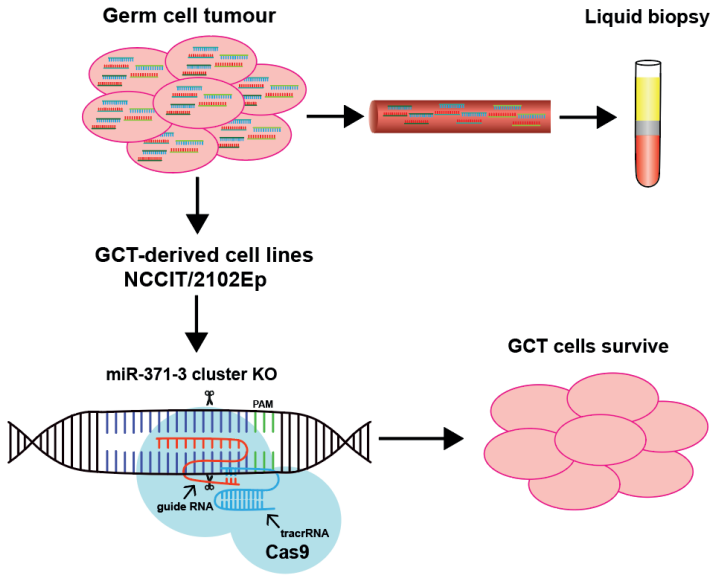
³ Translational Research Unit, Faculty of Medicine, Comenius University, Klenova 1, 833 10 Bratislava, Slovakia

⁴ 2nd Department of Oncology, Faculty of Medicine, Comenius University and National Cancer Institute, Klenova 1, 833 10 Bratislava, Slovakia

* Equal contribution

ABSTRACT

Germ cell tumors (GCTs) are malignancies derived from primordial germ cells, of which the latter are formed in the yolk-sac during early embryogenesis. Like primordial germ cells and embryonic stem cells, specific histologies of GCTs display high levels of the miR371a-3 cluster, a relatively recently discovered liquid biopsy-based marker for these cancers. Expression of this cluster is predominantly a characteristic of embryonal stem cells where it is suggested to be involved in the maintenance of pluripotency. Considering that virtually all malignant GCT patients harbor elevated blood levels of these miRs (teratomas excluded), this study aims to elucidate whether these miRs have a functional oncogenic role in the tumor cell or are a mere passenger effect. To investigate this, CRISPR Cas9-mediated knockouts were generated, introducing mutations in the miR371a-3 cluster in embryonal carcinoma GCT cell lines NCCIT and 2102Ep. The results show that absence of miR-371 has no impact on differentiation, cell growth, or cisplatin response. Knockout of both miR-372 and miR-373 showed an (slight) increase in LATS2, verifying this as a target of miR-372 and miR-373, but not miR-371. In addition, these clones developed xenografts in nude mice, while the miR could not be detected in the blood. Finally, for the first time, we were able to generate viable clones with a knockout of the entire miR-371-3 cluster in GCT cells. This suggests that the miR-371-3 cluster is not involved in tumor maintenance, the increase in cluster levels may be a remnant from the primordial germ / embryonal stem cell origin combined with a lack of selection pressure on loss of this cluster.



INTRODUCTION

Germ cell tumours (GCTs) are neoplasms originating from primordial germ cells (PGCs), which are the stem cell of the germ line (Bosl & Motzer, 1997; Oosterhuis & Looijenga, 2019). These cells are formed during early embryogenesis and migrate from the yolk sac along the midline of the body and eventually only reside in the genital ridge to form the future gonads under physiological conditions (Nikolic et al., 2016; Oosterhuis & Looijenga, 2019). If PGCs do not differentiate and remain in a toti- or pluripotent state, GCTs can develop (Oosterhuis & Looijenga, 2019). GCTs can originate anywhere in the migratory route of the PGCs along the midline of the body, however, they are most common in the gonads and less commonly found in extragonadal sites such as, the retroperitoneum, mediastinum, as well as intracranially (Oosterhuis & Looijenga, 2019).

GCTs can be divided into various types, depending on histology, type of precursor lesion, pathogenesis, status of genomic imprinting and their developmental potency (Oosterhuis & Looijenga, 2005, 2019). Most common are Type I and Type II GCTs, which occur in both males and females. Type I are the non-germ cell neoplasia *in situ* (GCNIS)-related tumours and are mostly diagnosed at paediatric age, consisting of, either or both, teratomas and yolk sac tumours (Looijenga, 2014; Oosterhuis & Looijenga, 2005). Type II are the GCNIS-related tumours, where GCNIS lesions precede Type II GCTs (Skakkebaek et al., 1982). Depending on histology, the Type II GCTs include non-seminomatous and seminomatous GCTs (seminoma in males and dysgerminoma in females). Non-seminomatous tumours can be further divided into embryonal carcinomas, choriocarcinomas, yolk sac tumors, and teratomas (Müller et al., 2021; Nauman & Leslie, 2022). In males, pure testicular seminomas are the most common Type II GCT comprising approximately half of the cases, with a median age of diagnosis at 35 years old (Radtko et al., 2018; Stang et al., 2023). The non-seminomas, which can be a mix of the non-seminomatous elements, develop earlier at around 25 years of age and present about 30% of the cases. The remaining cases are a combination of seminomatous and non-seminomatous tumors (Dieckmann et al., 2018; Oosterhuis & Looijenga, 2005).

Type II testicular GCTs (TGCTs) account for 60% of the malignancies found in young adult males ranging from 15 to 44 years of age (Cheng et al., 2018; Oosterhuis & Looijenga, 2005, 2019; Palumbo et al., 2019). Each year, over 9000 males are diagnosed with TGCT in the United States (Siegel et al., 2022). This makes TGCTs the most prevalent solid malignancy found in men within this age group. Furthermore, in Caucasian populations, the incidence of TGCTs is increasing annually with up to 3-6% (Baade et al., 2008; Nigam et al., 2015; Walschaerts et al., 2008). Risk factors for GCNIS lesions, and therefore TGCTs, are related to testicular dysgenesis syndrome comprising of cryptorchidism, hypospadias, and poor quality of semen (Müller et al., 2021; Skakkebaek et al., 2001).

Other than a similar transcription profile including the pluripotency factors *NANOG*, *POU5F1* (OCT3/4), and *SOX2*, PGCs and embryonic stem cells share a low mutation rate

compared to somatic cells (Looijenga et al., 2003; Bloom et al., 2019). Upon DNA damage, embryonic stem cells and PGCs are more prone to become apoptotic due to a lack of G1 checkpoint in the cell cycle and high expression levels of wildtype *TP53* (Hong et al., 2007; Ottaviano et al., 2021). This makes TGCTs remarkably sensitive to DNA-damaging chemotherapy, such as cisplatin (Bloom et al., 2019; Lobo et al., 2020). Consequently, if treated, patients with TGCTs have a high overall survival rate of over 95% after 5 years (Gillesen et al., 2019; Mele et al., 2021). Treatment of TGCTs consists of orchiectomy often combined with adjuvant platinum-based chemotherapy or radiotherapy. Up to 30% of the patients with metastatic TGCTs are not cured after the initial treatment (Lobo et al., 2020). Furthermore, 10-15% of the patients show intrinsic or acquired cisplatin resistance (Lorch et al., 2010; Országhová et al., 2022). Of these patients, 50% will eventually die as a result of the tumour since the treatment options are limited (Lobo et al., 2020). This drastically increases the years of life lost in these young patients hence why TGCTs are the highest-ranking cancer regarding premature years of life lost per death (Song et al., 2020). Up to 40% of surviving patients that have undergone chemotherapy experience impaired hearing and approximately 25% must cope with fertility complications (Brydøy et al., 2009; Hartmann et al., 1999). Additionally, chemotherapy can cause cardiovascular disease and other secondary malignancies, thereby increasing noncancer mortality (Fosså et al., 2007; Kvammen et al., 2016). Because there are limited alternative therapies, it is important to focus on improving the current treatment strategies.

Currently, serum tumour markers (STMs) are used to diagnose and monitor GCTs (Gilligan et al., 2010). Clinical management and risk stratification of patients with GCTs depends on the measures of three STMs: α -fetoprotein (AFP), β -human chorionic gonadotropin (β -hCG), and lactate dehydrogenase (LDH) (Gilligan et al., 2010; Leão et al., 2021; Mead, 1997). However, seminomatous cells do not produce AFP and the levels of β -hCG and LDH are normal in half of the patients with seminomas (Almstrup et al., 2020; Gilligan et al., 2010; Sidi et al., 1984; Smith et al., 2018). The STM levels for patients with non-seminomas are higher and show elevated levels of AFP, β -hCG, and LDH in up to 60%, 40%, and 60% of the patients with advanced disease, respectively (Almstrup et al., 2020; Gilligan et al., 2010). The expression of these markers differs for the distinct non-seminomatous GCTs (Kinkade, 1999; Smith et al., 2018). Other than low sensitivity, these STMs also show low specificity (Almstrup et al., 2020; Gilligan et al., 2010). Elevated levels of AFP are also seen in liver disease, gastrointestinal malignancies, and other tumours, the latter causes an increase in β -hCG levels as well, while an elevation in LDH levels can be caused by anything causing cellular lysis (Gilligan et al., 2010; Lange & Winfield, 1987). Because these markers also decay slowly, 3 days for β -hCG and 5 to 7 days for AFP, the period of monitoring before diagnosis becomes several weeks (Leão et al., 2021; Stevens et al., 2016; Willemse et al., 1981).

Other biomarkers that have been proven to have high sensitivity and specificity preclinically but are not used in the clinic for GCTs yet, are certain microRNAs (miRNA) (Condrat et al., 2020; Gillis et al., 2007; Murray et al., 2011). To fully understand the set-up and results presented in this study, it is important to understand the fundamentals of miRNA biosynthesis. miRNAs are small non-coding RNAs that post-transcriptionally regulate gene expression (Ghildiyal & Zamore, 2009; Green et al., 2016). Following the canonical pathway of biogenesis, the miRNA gene is transcribed after which the primary miRNA (pri-miRNA) is cleaved by DROSHA resulting in a precursor miRNA (pre-miRNA) hairpin that is exported out of the nucleus by XPO5 (Figure 1; Filipowicz et al., 2008). In the cytoplasm, the pre-miRNA is further processed by DICER to produce a mature miRNA duplex of approximately 22 nucleotides long (Filipowicz et al., 2008; Lu & Rothenberg, 2018). Often only one strand will function as the mature miRNA and is loaded into the RNA-induced silencing complex (RISC), while the other strand is degraded (Filipowicz et al., 2008). The strands are specified as either the 3p or 5p strand. RISC searches for mRNA that is mostly complementary to the miRNA and silences the gene either via degradation or the prevention of mRNA translation (Filipowicz et al., 2008). Binding of the miRNA is reliant on the seed sequence; the first 2-8 nucleotides on the 5' end of the mature miRNA strand will bind to the 3' untranslated region of the target mRNA (Chipman & Pasquinelli, 2019). One of the miRNA clusters that is expressed uniquely in embryonic stem cells is the miRNA-371/372/373 (miR-371-3) cluster located on chromosome 19 (Suh et al., 2004).

About two decades ago it was found that this cluster is also expressed in all Type I and II gonadal and extragonadal GCTs, except for teratomas (Eini et al., 2013; Gillis et al., 2007; Looijenga et al., 2007; Murray et al., 2011; Voorhoeve et al., 2006). The miRNAs are secreted into the bloodstream by the tumor cells, where they are highly stable (Eini et al., 2013; Murray et al., 2011). Additionally, the miRNAs have a short half-life of less than 12 hours (Radtke et al., 2018). Taken together this makes them excellent potential biomarkers according to the Lange-Winfield criteria (Lange & Winfield, 1987; Leão et al., 2021). A study measuring the miR-371a-3p serum levels of GCT patients compared to healthy controls showed that miR-371a-3p has a sensitivity of 90% and a specificity of 94% with positive predictive values over 97% (Almstrup et al., 2020; Dieckmann et al., 2019). The short half-life of the marker also makes it possible to closely monitor treatment response (Spiekermann et al., 2015). The miR-371a-3p levels significantly lowered after orchiectomy as well as during chemotherapy, while levels increased in patients with relapsed disease (Dieckmann et al., 2019; Murray et al., 2011; van Agthoven et al., 2017). Pre-treatment levels of miR-371a-3p can also be used for prognostic value, indicating the progress-free survival and overall survival of patients with Type II GCTs (Mego et al., 2019). The inability of miR-371a-3p to detect teratoma is a limitation (Looijenga et al., 2007; Mego et al., 2019).

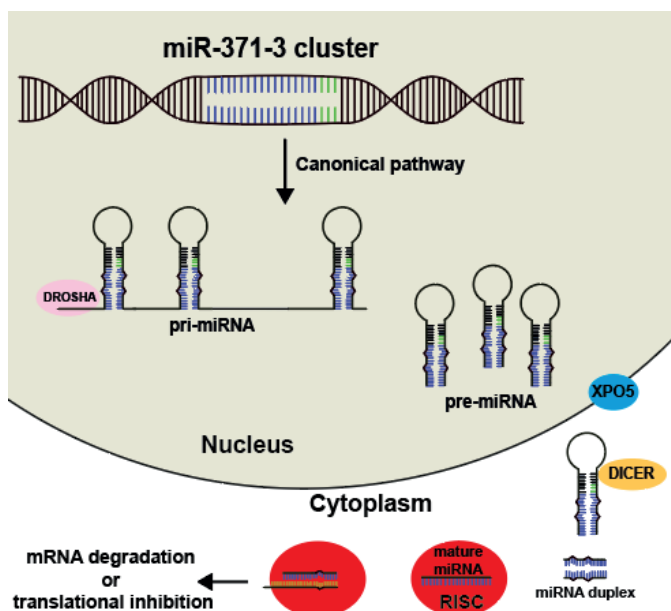


Figure 1: microRNA biogenesis. miRNA (cluster) gene is transcribed to produce primary miRNA (pri-miRNA). Pri-miRNA is cleaved by DROSHA into precursor miRNA (pre-miRNA), which is transported out of the nucleus by XPO5. Pre-miRNA is processed by DICER to produce a miRNA duplex. One strand of the miRNA duplex is incorporated into the RNA-induced silencing complex (RISC) and used as a template for finding complementary mRNA. Translation of this (partially) complementary mRNA is then silenced either by degradation of mRNA or inhibition of translation.

The function of the miR-371-3 cluster has not been fully elucidated yet. However, suppression of the murine homolog miR-290-5 cluster causes partially penetrant embryonic lethality and a reduced number of germ cells in the gonads (Medeiros et al., 2011). Due to the high expression of the miR-371-3 cluster in embryonic stem cells and the hypothesis that this cluster is under regulation of OCT3/4 and SOX2, it is suggested the cluster functions as a regulator of stem cell maintenance (Tiscornia & Carlos Izpisua Belmonte, 2010; Wu et al., 2014). Overexpression of the cluster has been shown to promote proliferation in cancer cells via the Wnt/ β -catenin signalling pathway to enhance stem cell renewal (Zhou et al., 2011). Cell proliferation also increased after overexpression of the miR-371-3 cluster because of P53 inactivation (Voorhoeve et al., 2006). The cluster is hypothesized to target Large Tumour Suppressor homolog 2 (LATS2), consequently increasing the level of active P53-inhibitory protein MDM2 (Aylon et al., 2006; Lee et al., 2009; Voorhoeve et al., 2006).

This raises the question of whether overexpression of the miR-371-3 cluster is an oncogenic driver or a passenger effect in GCT development and maintenance, as well as whether the expression of miR-371-3 influences the tumour response to cisplatin. To investigate this, two GCT cell lines were used, the NCCIT cell line and 2102Ep cell line (Andrews et al., 1980; Teshima et al., 1988). The NCCIT cell line is derived from a mediastinal embryonal carcinoma and carries a heterozygous *TP53* mutation with loss of heterozygosity of the wildtype allele (hemizygous *TP53* mutation) (Teshima et al.,

1988). 2102Ep cells are testicular embryonal carcinoma-derived containing wildtype *TP53* (Andrews et al., 1980; Wang et al., 1980). Using CRISPR/Cas9, the cell lines were modified to generate knockouts (Kos) for either miR-371a, miR-372, and/or miR-373. After obtaining valid KO clones, the cells were characterized by investigating cell growth and cisplatin response was measured, in addition to analysis of expression profiles of the miR-371-3 cluster and mRNA of pluripotency factors *OCT3/4* and *SOX2* and several P53 pathway-related transcripts. Cell growth, differentiation status and morphology were not reliant on the expression of the miR-371-3 cluster, neither was cisplatin response. We propose that the high levels of the miR-371-3 cluster found in GCTs is a remnant of their precursor cells, either PGCs or embryonal stem cells. Furthermore, we postulate that these high levels are only present due to a lack of selective pressure on loss of the cluster, without fulfilling an (important) function in oncogenic maintenance.

MATERIALS AND METHODS

Cell culture

The 2102EP cell line (RRID:CVCL_C522) was cultured in DMEM with 4.5 g/L D-glucose and L-glutamine (Gibco, Thermo Fisher Scientific, Bleiswijk, The Netherlands). The NCCIT cell line (RRID:CVCL_1451) was cultured in RPMI with GlutamaxTM-I (Gibco, Thermo Fisher Scientific, Bleiswijk, The Netherlands). Media was supplemented with 10% foetal bovine serum and 1% penicillin-streptomycin. Cells were passaged by trypsinization twice every week and incubated at 37°C and 5% CO₂.

Generating knockout using CRISPR-Cas9

1 µL of 100 µM crRNA (guide for hsa-mir-371a-3p: TCTTTTGAGTGTTACCGCTT; hsa-mir-372: CACCCTGTGGGCTCAAATG; or hsa-mir-373: TCATACTGGGATACTCAAAA) was added to 1 µL of 100 µM tracrRNA for the single CRISPR Kos. 0.5 µL of 100 µM crRNA guide 372, 0.5 µL of 100 µM crRNA guide 373, and 1 µL of tracrRNA were combined. This was heated for 5 minutes at 95°C and left at room temperature for an hour to allow duplex formation. Ribonucleoprotein complexes were made by combining 1.5 µL buffer R with 0.25 µL Cas9, 1.75 µL guide RNA duplex, and 1.75 µL buffer R. The complexes were incubated for 10 minutes at room temperature. Cells were trypsinized and resuspended in medium without Pen/Strep. Approximately 300.000 cells were centrifuged, medium was removed and 8 µL of buffer R was added. 4 µL of component mixture was added and electroporated at 1200V for 20ms three times using the Neon Transfection system (Thermo Fisher Scientific, Bleiswijk, The Netherlands). On day 0, cells were cultured in medium without Pen/Strep.

For the monoclonal expansion of KO cells, 1000 cells/10 mL were plated from the bulk. Monoclonal colonies were picked and expanded for characterization.

DNA extraction

For characterization of the clones, DNA was extracted. 1 mL of cell suspension was centrifuged at 2000 rpm for 5 minutes. Supernatant was removed, after which QuickExtract™ DNA Extraction Solution (Lucigen, Biosearch Technologies, Halle-Zoersei, Belgium) was used according to manufacturer's instruction. The samples were run at 65°C for 10 minutes and another 5 minutes at 98°C in a PCR machine. Samples were stored in 1:2 MilliQ dilution at -20°C.

DNA extraction for Real Time quantitative PCR analysis was done according to manufacturer's instruction using the Dneasy® Blood & Tissue kit (Qiagen, Venlo, The Netherlands, cat.nr.69504).

Polymerase Chain Reaction (PCR)

20 µL total volume consisting of 10 µL GoTaq® G2 Hot Start Green Master Mix (Promega, Leiden, The Netherlands), 6 µL MilliQ, 2 µL gDNA, and 2 µL primer mix (1:1 forward and reverse primer). Using a Bio-Rad T100 Thermal Cycler samples were incubated at 95°C for 5 minutes, followed by 34 cycles of: 1) 95°C for 30 seconds; 2) 58°C for 30 seconds; 3) and 72°C for 30 seconds, and a final extension step of 7 minutes. The following primer sequences were used to target hsa-miR-371, hsa-miR-372, and hsa-miR-373: forward primer hsa-miR-371 (CCTCACACGTGTCCTTCCT), reverse primer hsa-miR-371 (CTGCGGGTATAGTTGCCTAC), forward primer hsa-miR-372 (TCTGATGGGTAAGTGCTTCCA), reverse primer hsa-miR-372 (CCGAGAGTGGACTGTGTTGA or ATACAGCCCCTTGGTCACAG), forward primer hsa-miR-373 (AGCAGCTGTGACCAAGGG), and reverse primer hsa-miR-373 (TTCCGAACCTTCAACCAAACC).

Viability assay

Viability assays were performed in three technical and two or three biological replicates. Cells were cultured in aforementioned conditions in increasing densities of 0, 500, 1.000, 2.000, 4.000, 6.000, 8.000, and 10.000 cells in 100 µL per well in a 96 well plate. After 4 days, the CellTiter-Glo® 2.0 Luminescent Cell Viability Assay kit (Promega, Leiden, The Netherlands) was used to analyse cell viability. 1:1 CellTiter-Glo® was added and mixed for 5 minutes. After 10 minutes of incubation at room temperature, cells were transferred to a Pierce white opaque 96-well plate (Thermo Fisher Scientific, Bleiswijk, The Netherlands,

cat.nr. 15042) and luminescence was measured on the ID3 Spectramax (Molecular Devices, San Jose, CA, USA).

Cisplatin viability assay

On day 0, 1000 E371 cells or 2000 NCCIT clone cells in 50 μ L were plated per well in a 96 wells plate. On day 1, 50 μ L of 0.66 μ M, 2 μ M, 4 μ M, 8 μ M, 12 μ M, 16 μ M, 20 μ M, 32 μ M, and 64 μ M was added in RPMI or DMEM with 0.9% NaCl. On day 4, 1:1 CellTiter-Glo® was added for luminescence measuring as described above.

RNA isolation

Total RNA was isolated using TRIzol reagent (Thermo Fisher Scientific, Bleiswijk, The Netherlands), according to manufacturer's instruction. To measure the quality and quantity, the NanoDrop One (Thermo Fisher Scientific, Bleiswijk, The Netherlands) and Qubit 4 Fluorometer (Invitrogen™, Thermo Fisher Scientific, Bleiswijk, The Netherlands) were used. RNA was stored at -80°C.

Real Time quantitative PCR (RT-qPCR) miRNA

The TaqMan microRNA Reverse Transcription kit (Thermo Fisher Scientific, Bleiswijk, The Netherlands, cat.nr 4366597) was used to synthesize cDNA of the purified (mi)RNA. RT primers and assays used were: housekeeper RNU48 (001006), and hsa-mir-371a-3p (002124), hsa-mir-372 (000560), hsa-mir-373-3p (000561), and hsa-mir-885-5p (002296). TaqMan Real Time qPCR was performed in duplo using 2X TaqMan Advanced Master Mix and 20X TaqMan Advanced miRNA assays for RNU48, miR-371a-3p, miR-372, miR-373-3p, and miR-885-5p. PCR was run in the MicroAmp Fast Optical 96-Well Reaction Plate (Thermo Fisher Scientific, Bleiswijk, The Netherlands, cat.nr. 4346906) on the QuantStudio™ (Thermo Fisher Scientific, Bleiswijk, The Netherlands) 12k Flex. CRISPR/Cas9-edited clones were normalized against their respective parental cell line.

RT-qPCR miRNA Advanced

Isolated RNA was used to synthesize cDNA using the TaqMan Advanced miRNA cDNA Synthesis kit (Thermo Fisher Scientific, Bleiswijk, The Netherlands, cat.nr. A28007) following manufacturer's instructions. TaqMan Advanced assays used were: housekeepers hsa-miR-20a-5p (478007_miR) and hsa-miR-30b-5p (478586_miR), and targeted assays for hsa-miR-371a-3p (478070_miR), hsa-miR-371a-5p (478851_miR), hsa-miR-371b-3p (478852_miR), hsa-miR-371b-5p (478853_miR), hsa-miR-372-3p (478071_miR), hsa-miR-

372-5p (478854_miR), hsa-miR-373-3p (478363_miR), hsa-miR-373-5p (478073_miR). PCR was run in the MicroAmp Fast Optical 96-Well Reaction Plate (Thermo Fisher Scientific, Bleiswijk, The Netherlands, cat.nr. 4346906) on the QuantStudio™ (Thermo Fisher Scientific, Bleiswijk, The Netherlands) 12k Flex. CRISPR/Cas9-edited clones were normalized against their respective parental cell line.

RT-qPCR miRNA in Conditioned Medium

Medium was extracted from cultured cells and stored at -20°C. miRNAs were isolated from the conditioned medium using the miRNeasy Serum/Plasma Advanced kit (Qiagen, Venlo, The Netherlands, cat.nr. 217204) following manufacturer's instruction or by bead-capturing using the TaqMan miRNA ABC Purification kit – Human panel A (Thermo Fisher Scientific, Bleiswijk, the Netherlands). For purification using bead-capturing, the KingFisher Flex with 96 KF Head, KingFisher 96 KF microplate, KingFisher 96-Tip combs for KF Magnets and the Ultrasonic Waterbath M2800H-E were used.

Non-human spike-in control ath-miR-159a (000338) and cel-miR-39-3p (000200) was used. cDNA was synthesized using the TaqMan miRNA Reverse Transcription kit, following manufacturer's instruction. The RT primers used were: ath-miR-159a, housekeepers hsa-miR-20a-5p (000580) and hsa-miR-30b-5p (000602), targeted RT primers were for hsa-miR-371a-3p (002124), hsa-miR-372 (000560), and hsa-miR-373-3p (000561). PCR was performed using 2X TaqMan Advanced Master Mix and 20X TaqMan Advanced miRNA assays in a MicroAmp Fast Optical 96-Well Reaction Plate on the QuantStudio™ 12k Flex. CRISPR/Cas9-edited clones were normalized against their respective parental cell line.

RT-qPCR mRNA

cDNA was synthesised according to manufacturer's instruction using total RNA, oligod(T)₁₈ and random hexamers. For PCR, 2X TaqMan Advanced Master Mix was used together with 20X TaqMan Advanced gene expression assays: housekeeper *HPRT* (hs02800695_m1), *POU5F1* (hs04195369_s1), *SOX2* (hs01053049_s1), *TP53* (hs01034249_m1), *CDKN1A* (hs99999142_m1), *BBC3* (hs00248075_m1), *PMAIP1* (hs00560402_m1), *BAX* (hs99999001_m1), and *LATS2* (hs00324396_m1/hs01059009_m1) in duplo. PCR was run using MicroAmp Fast Optical 96-Well Reaction Plate (Thermo Fisher Scientific, cat.nr. 4346906) in a MicroAmp Fast Optical 96-Well Reaction Plate on the QuantStudio™ 12k Flex. CRISPR/Cas9-edited clones were normalized against their respective parental cell line.

RT-qPCR 3p amplification

For chromosome 3p amplification analysis, purified total DNA was used. 2X Power SYBR Green Master Mix with primers p48+p49 (control 100bp), p50+p51 (control 200 bp), p57+p58 (3p amp 100bp), or p59+p60 (3p amp 200bp) were run as a standard run on a MicroAmp Fast Optical 96-Well Reaction Plate on the QuantStudio™ 12k Flex. The used primer sequences were for p48 (GCCCCACATTCTGCAAGTCC), p49 (GGTGTGCGCGGAAGGGTT), p50 (TGTTGACTCGATCCACCCCA), p51 (TGAGCTGCAAGTTTGCTGAA), p57 (TGCATGAAAAGCTCTCTCCCA), p58 (AGCTGCTGAGTAGGGGTGTA), p59 (TGGAGTGGTGTACTAGCGGA), p60 (GAAGTGGGAGTCCACGGAAC). CRISPR/Cas9-edited clones were normalized against their respective parental cell line.

Western Blot

Cells were harvested by cell scraping and lysed using Laemmli buffer. Samples were incubated at 70°C for 10 minutes. Protein concentrations were measured using the Pierce Micro BCA Protein Assay Kit (Thermo Fisher Scientific, Bleiswijk, The Netherlands, cat.nr. 23235). 1:4 Laemmli sample buffer containing 10% β -mercaptoethanol was incubated with the desired amount of protein at 95°C for 5 minutes. 54 μ g of protein was loaded into a 4-15% Mini-Protean TGX Stain-Free precast gel (Bio-Rad Laboratories, Lunteren, The Netherlands). The proteins were transferred to 0.2 μ m PVDF membrane blotting paper using the Turbo Trans-Blot system (Bio-Rad Laboratories, Lunteren, The Netherlands). The membrane was incubated overnight at 4°C with mouse anti-LATS2 primary antibody (1:2500, Thermo Fisher Scientific, Bleiswijk, The Netherlands; #CF804435) or mouse anti- β -actin primary antibody (1:5000, Thermo Fisher Scientific, Bleiswijk, The Netherlands; #MA5-15739). After washing three times for 5 minutes with PBS-Tween 0.1%, the samples were incubated with goat anti-mouse IgG (H+L) horseradish peroxidase conjugated (1:5000, Thermo Fisher Scientific, Bleiswijk, The Netherlands; #G21040) as secondary antibody and washed again. Proteins were visualized using Clarity Western ECL substrate (Bio-Rad Laboratories, Lunteren, The Netherlands) and the ChemiDoc (Bio-Rad Laboratories, Lunteren, The Netherlands).

Imaging

Brightfield images were obtained using the Leica Dmi1 (Leica Microsystems, Amsterdam, The Netherlands).

Data visualization and analysis

Data was analyzed and visualized using Synthego ICE, Graphpad Prism 9, SnapGene 6.2.1., miRTargetLink2.0, and Adobe Illustrator 27.5

RESULTS

Generation of NCCIT miR-371a knockout lines

NCCIT clones with a miR-371a KO were generated using CRISPR/Cas9. The guide was designed to modify the sequence surrounding miR-371a-3p (**Figure 2A**). Sanger sequencing analyzed by Synthego ICE or SnapGene (InDels over 40 base pairs) showed four suitable NCCIT miR-371 KO (N371) clones that had deletions of up to 25 nucleotides surrounding the Cas9 cut site (**Figure 2B**). Using RT-qPCR, miRNA levels were measured. The miR-371a-3p profile of the N371 clones showed that KO clones N371-3, -5, -11, and -12 had lower to no levels of miR-371a-3p, while the wildtype miR-371 clones harbored unchanged (N371-1) or even increased levels of miR-371 (N371-10) (**Figure 3A**). The levels of miR-372 and miR-373 remained unaltered for all clones, except for clone N371-10. This clone demonstrated substantially increased levels of miR-372 and miR-373, in line with the elevated expression of miR-371a, likely due to clonal effects (**Figure 3B**). The putative molecular marker of teratomas, miR-885-5p (Lobo et al., 2019), was unaffected in all clones (**Figure 3C**). As the CRISPR/Cas9 guide was designed to cut in miR-371a-3p, it was predicted that miR-371b(-5p) on the reverse strand of miR-371a was also negatively affected. Further downstream analysis of the expression profile of the miR-3p and miR-5p arms with advanced RT-qPCR illustrated that both the 3p and 5p arm of miR-371a had decreased levels in the KO clones (**Figure 3D**). Coincidentally, miR-371b levels of both the miR-3p and miR-5p arm were also decreased in the KO clones while remaining relatively unchanged in the wildtype clones. Analysis of the secretion of the miR-371-3 cluster into conditioned medium confirmed the reduction of miR-371a-3p in the KO clones and showed again slightly increased levels of the whole cluster in clone N371-10 (**Figure 3E**).

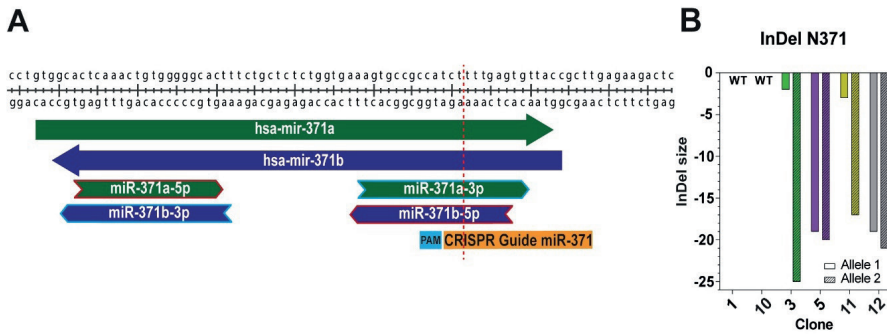


Figure 2: Knockout of miR-371. A) The CRISPR/Cas9 cut site (red dashed line) of the CRISPR Guide (orange) lies in the sequence of hsa-mir-371a/b and mature miR-371a-3p and miR-371b-5p. **B)** InDel size of N371 clones as indicated by analysis of Sanger sequencing data using ICE Syntheso.

N371 clones display no difference in mRNA expression or growth

To investigate the differentiation state of the various miR-371 KO clones, RT-qPCR was performed to look at the expression of pluripotency markers *OCT3/4* (*POU5F1*) and *SOX2*. The expression of *OCT3/4* and *SOX2* were similar to NCCIT parental in all clones (**Figure 4A**). Due to the putative involvement of the miR-371-3 cluster in the P53 pathway, expression of various genes in this pathway were studied. KO of miR-371 caused no major difference of the P53 pathway-related transcripts, *TP53*, *P21* (*CDKN1A*), *BAX*, *PUMA* (*BBC3*), and *NOXA* (*PMAIP1*) (**Figure 4B**). The mRNA levels of the hypothesized direct target of the miR-371-3 cluster, *LATS2*, was unaffected as well (**Figure 4C**). Cell growth was investigated by seed density assays. The clones displayed similar growth rates as well as morphology, indicating no effect of miR-371 KO on cell growth and survival (**Figure 4D** and **4E**).

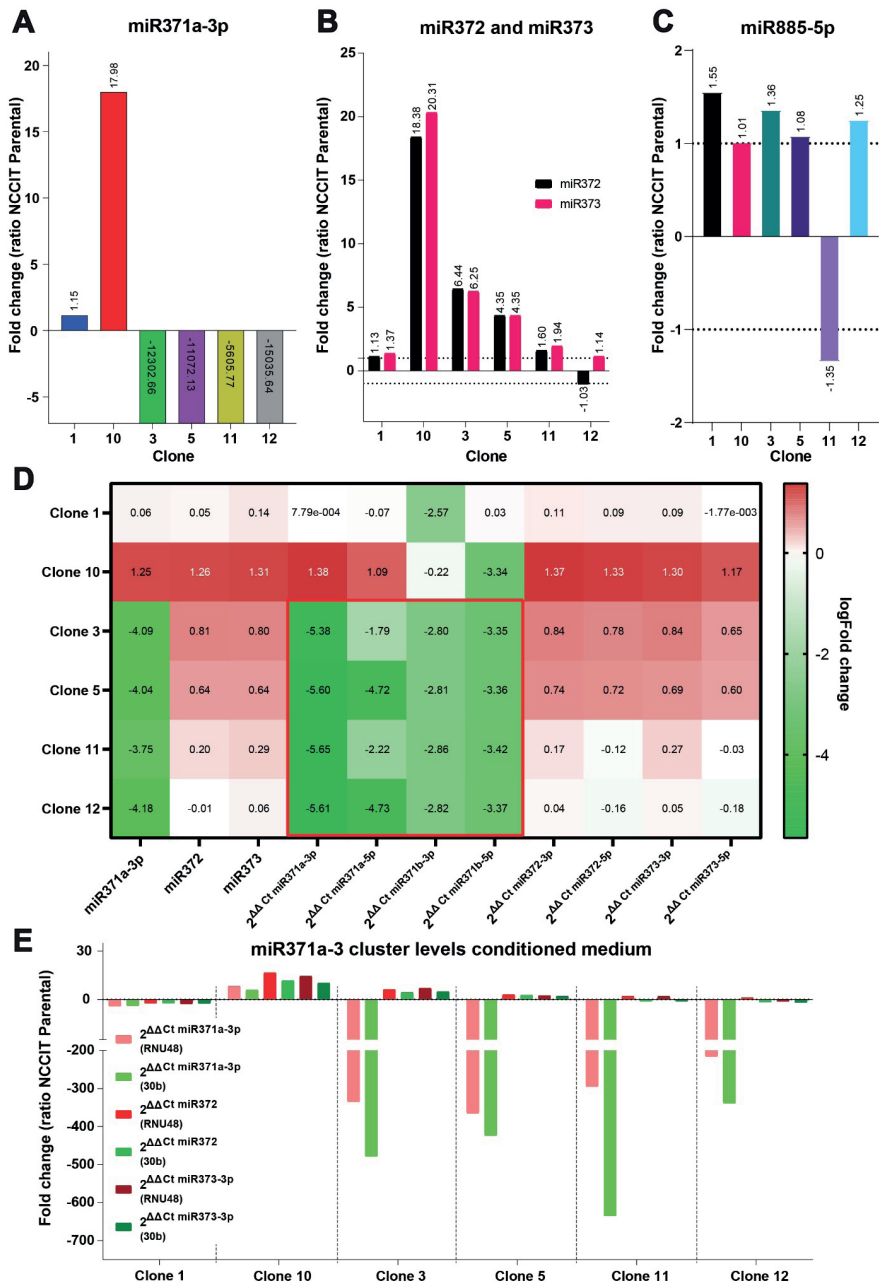


Figure 3: Expression profile of miR-371-3 cluster in NCCIT miR-371 (N371) knockout clones. **A)** Fold change of the level of miR-371a-3p in the N371 clones compared to NCCIT parental. **B)** Fold change levels of miR-372 and miR-373-3p in N371 clones compared to NCCIT parental. **C)** Level of miR-885-5p in N371 clones. **D)** Advanced logFold change levels of miR-371-3 cluster including the miR-3p and miR-5p arms of the miRNAs in the cells of N371 clones. **E)** Level of secreted miR-371-3 cluster in the conditioned medium of N371 clones, normalized to either RNU48 (red) or hsa-mir-30b (green).

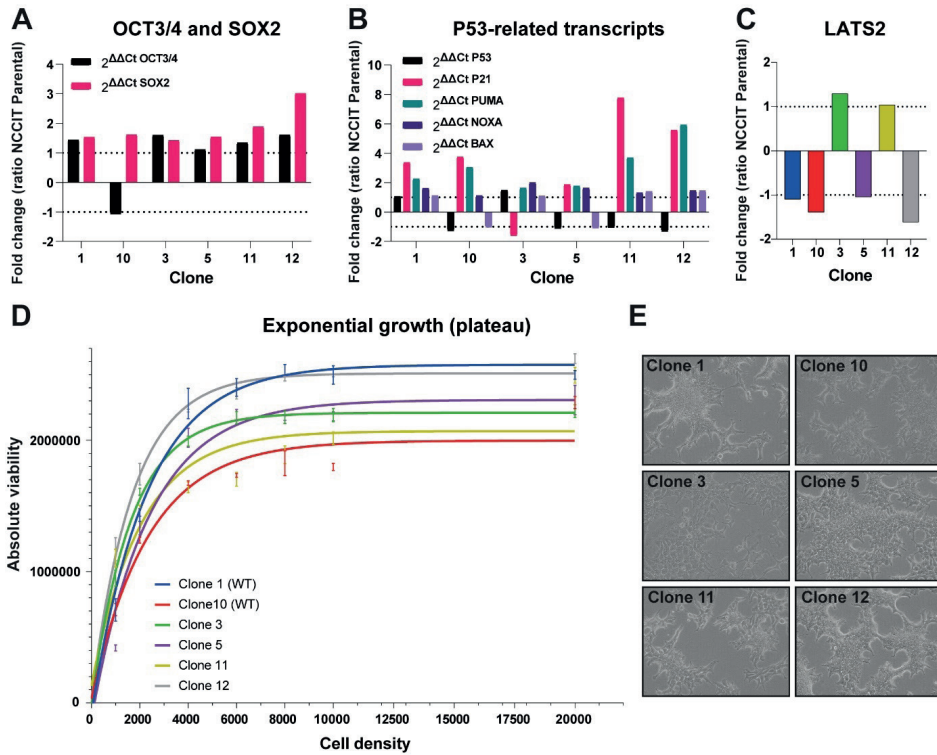


Figure 4: Expression of pluripotency markers, P53-pathway targets, and cell growth and morphology of N371 clones. **A)** Fold change expression of the pluripotency markers: OCT3/4 (POU5F1) and SOX2. **B)** Fold change expression of P53-related transcripts: TP53, P21 (CDKN1A), BAX, PUMA (BBC3), NOXA (PMAIP1). **C)** Fold change level of LATS2 expression. **D)** Exponential growth curve defined by absolute viability of increasing cell densities. N=3. **E)** Morphology of the six clones. Magnification: 300x.

Because cisplatin is the standard treatment for GCTs, the cisplatin response was measured in N371 KO clones by exposing the clones to increasing cisplatin concentrations (**Figure S1A**). The derived IC50s showed that some N371, but not all, clones carrying miR-371 KO mutations were more sensitive to cisplatin (**Figure S1B**). These results indicate that miR-371 is not necessary for NCCIT cell growth nor cisplatin response. Moreover, it does not affect mRNA levels of the measured pluripotency markers and P53-related targets.

Generation of 2102Ep miR-371a knockout lines

Since NCCIT cells have a hemizygotously mutated *TP53* (Teshima et al., 1988), the response to miR-371 KO may differ in GCT cells harboring wildtype *TP53*. To further investigate the function of miR-371 in GCT cells with wildtype *TP53*, miR-371 KO clones (E371) were generated in 2102Ep cells using CRISPR/Cas9 with the previously discussed guide (**Figure 2A**). Sanger sequencing and subsequent ICE analysis demonstrated that two clones had deletions surrounding the expected Cas9 cut site; clone E371-B harboured deletions of 2 and 46 nucleotides, while clone E371-G harboured two relatively large deletions of 19 and 23 nucleotides (**Figure 5**). Of the clones, four had an one base pair insertion on each allele (**Figures 5** and **S2A**). Analysis of the expression profile of the miR-371-3 cluster indicated that these four clones indeed did not have significantly altered miR-371a-3p levels compared to 2102Ep parental (**Figure S2B**). Clone E371-C demonstrated closest similarity to 2102Ep parental regarding miR-371-3 cluster levels (**Figure 6A**). The miR-371a-3p levels in E371 KO clones B and G were significantly lower or undetermined. The levels of the other miRNAs of the miR-371-3 cluster remained unchanged compared to 2102Ep parental (**Figure 6B**), as were the levels of miR-885-5p (**Figure 6C**). Similar to N371, both the 3p and 5p arm of miR-371a were negatively affected by KO of miR-371a-3p in E371 (**Figure 6D**). The secretion of the miR-371-3 cluster by the E371 clones was measured by RT-qPCR after two different methods of miRNA isolation of conditioned medium. Both methods show a similar trend among the E371 KO clones, E371-B and E371-G secrete lower levels of miR-371a-3p compared to E371-C when normalized to the parental control (**Figure 6E**).

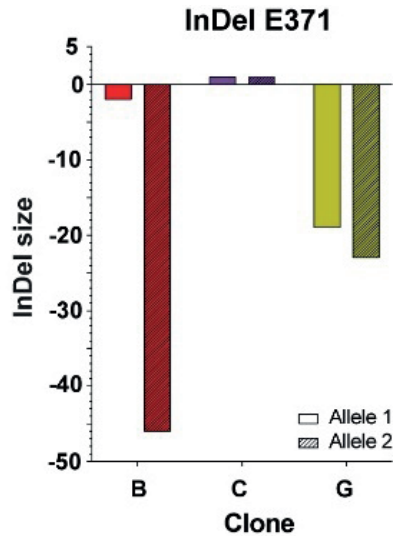


Figure 5: InDel size of 2102Ep miR-371a knockout (E371) clones. InDel size of E371 clones as indicated by analysis of Sanger sequencing.

E371 clones display no difference in mRNA expression or growth

To verify the results obtained in the N371 clones, expression levels of the pluripotency markers and P53 pathway-related transcripts were measured via RT-qPCR in the E371 clones. Expression of *OCT3/4* and *SOX2* were unchanged compared to 2102Ep parental (**Figure 7A**). mRNA of genes involved in the P53 pathway were unaffected by KO of miR-371 (**Figure 7B**). The levels of *TP53*, *BAX*, *PUMA* (*BBC3*), *NOXA* (*PMAIP1*), and *LATS2* were increased in clone E371-C (**Figures 7B and 7C**), accompanied by a worse performance in cell growth (**Figure 7D**). Results of the exponential cell growth curve indicate clonal differences independent of miR-371 KO with clone E371-B and -G outperforming clone E371-C (**Figure S3**). The morphology of the clones did not demonstrate any discrepancies (**Figure 7E**). Next, cisplatin response was measured in the same manner as for the N371 clones. Unlike the N371 KO clones, the E371 clones did not acquire cisplatin sensitivity after miR-371 KO (**Figure S4**). Previous research illustrated that CRISPR/Cas9 editing and clonal expansion can cause amplification of chromosome 3p25.3, associated with cisplatin resistance (Timmerman et al., 2022). No gain of chromosome 3p25.3 seen in the E371 clones (**Figure S5**). These results suggest that the differences in cisplatin response are clonal, unrelated to miR-371 KO status.

Generation of CRISPR/Cas9 NCCIT miR-372 and/or miR-373 knockout clones

Analysis of the strongly validated targets of the cluster using miRTargetLink2.0, illustrated that miR-372 and miR-373 are the miRNAs with the broadest network of targets (**Figure S6**). Therefore, to investigate if the increase of miR-371a in GCTs is due to a passenger effect or oncogenicity of the other miRNAs in the miR-371-3 cluster, we generated NCCIT clones with either a miR-372 (N372), miR-373 (N373), or combination (N23c) KO mutation (**Figure 8A**). A total of eight clones were characterized beyond Sanger sequencing, of each line a CRISPR-edited wildtype was taken as a control. Sanger sequencing analysis showed that one of the N372 KO clones harboured an allele with a relatively shorter deletion of 4 nucleotides and one long deletion of 117 nucleotides surrounding the expected Cas9 cut site in miR-372, the other clone harboured two longer deletions of 27 and 23 nucleotides, respectively (**Figure 8B**). The N373 KO clone had deletions of 10 and 13 nucleotides in miR-373. Sanger sequencing of clone N23c-3 showed one allele with an inversion of the 5' \diamond 3' strand sequence into the 3' \diamond 5' strand between the cut sites of Cas9 in miR-372 and miR-373, causing double KO of miR-372 and miR-373 (**Figure 8C**). The other allele of clone N23c-3 harboured a 2-base pair insertion in miR-373, we were unsuccessful in elucidating the miR-372 sequence of this allele. Clone N23c-10 had two large deletions in miR-372, yet harboured wildtype alleles for miR-373.

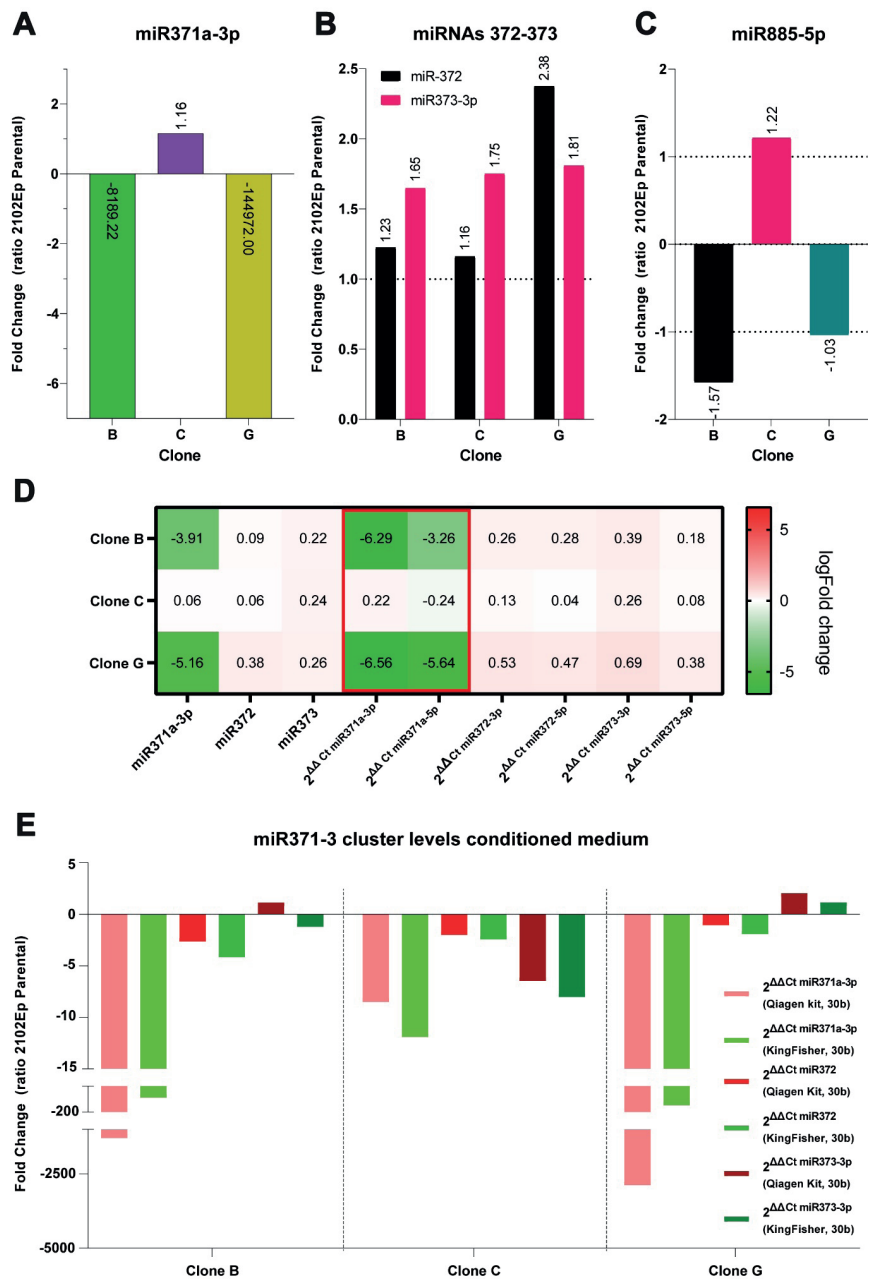


Figure 6: Profile of miR-371-3 cluster in 2102Ep miR-371 knockout (E371) clones. **A)** Fold change level of miR-371a-3p in E371 clones compared to 2102Ep. **B/C)** Fold change levels of **B)** miR-372 and miR-373 and **C)** miR-885-5p are unchanged after knockout of miR-371. **D)** logFold change of both miR-3p and -5p arm of the miRNAs of miR-371-3 cluster, miR-371a-3p and miR-371a-5p (outlined in red) measured by advanced RT-qPCR. **E)** Fold change levels of secreted miR-371-3 cluster isolated from conditioned medium either by total miRNA isolation (red) or using the magnetic bead-capture method (green).

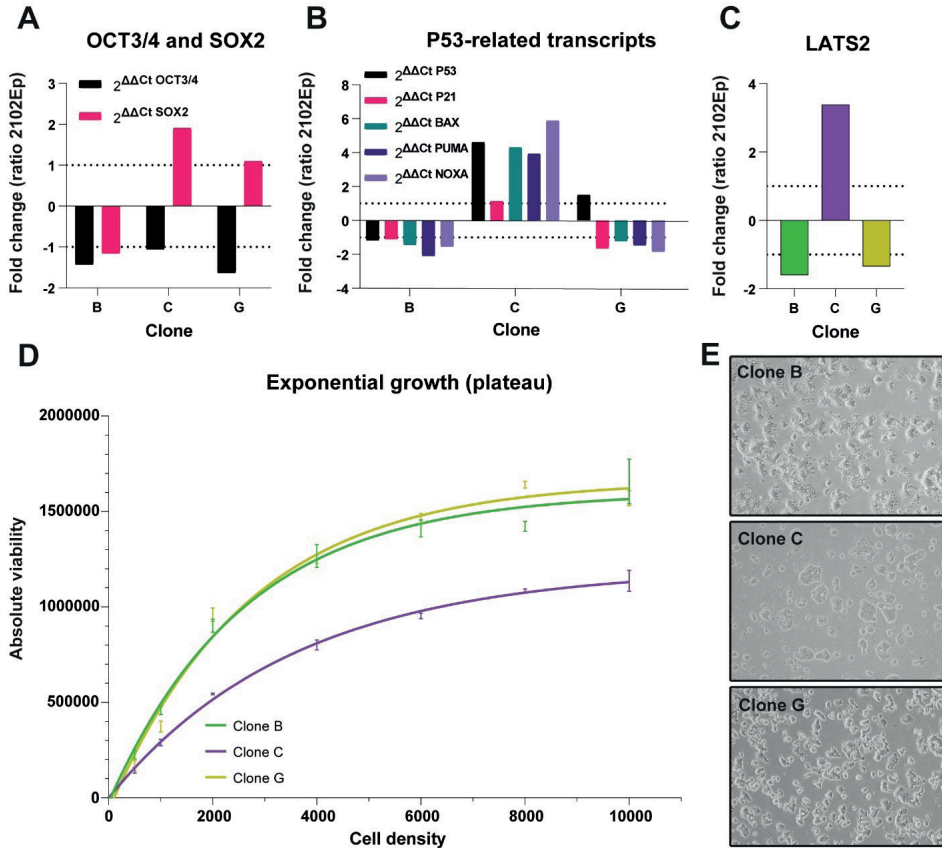


Figure 7: Expression of mRNA and cell growth of E371 clones. **A)** Fold change of pluripotency markers mRNA expression OCT3/4 (POU5F1) and SOX2 compared to 2102Ep parental. **B)** Fold change of mRNA of TP53 and its pathway related genes, P21 (CDKN1A), BAX, PUMA (BBC3), NOXA (PMAIP1). **C)** Fold change of LATS2 expression in E371 clones normalized to 2102Ep parental. **D)** Cell growth as defined by the absolute viability of different cell densities. N=3. **E)** Morphology of the E371 clones. Magnification: 50x.

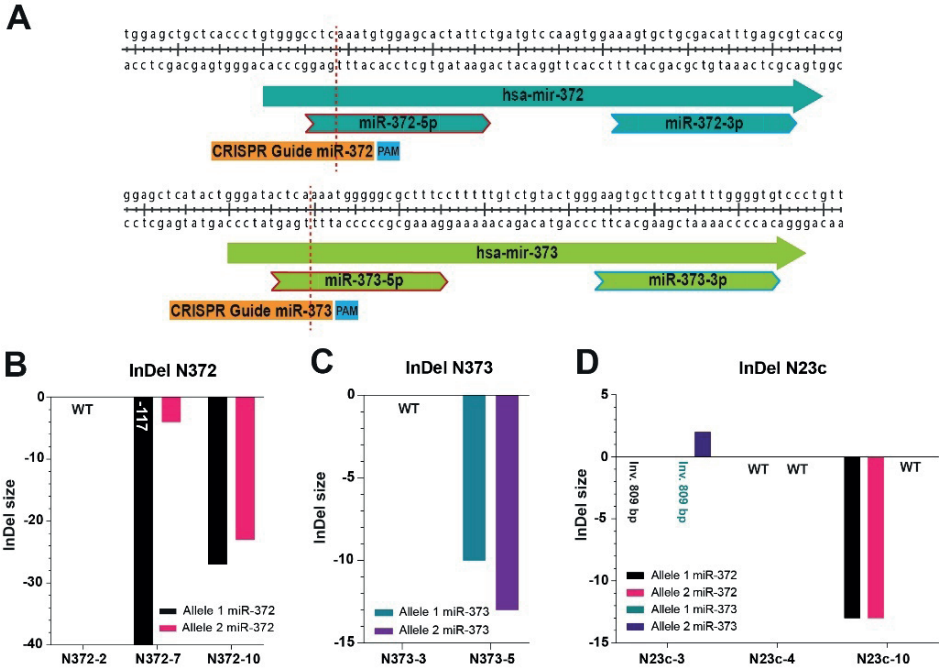


Figure 8: Knockout of miR-372 and miR-373. A) The cut site (red dashed line) of CRISPR/Cas9 lies in the sequence of mature miR-372-5p or miR-373-5p using the CRISPR guides (orange). **B)** Three miR-372 CRISPR-edited clones (N372) were continued to characterize: wildtype N372-2, and miR-372 knockout clones N372-7 and N372-10. **C)** Two miR-373 CRISPR-edited clones (N373) were characterized: wildtype N373-3 and knockout clone N373-5. **D)** Three miR-372 and miR-373 CRISPR-edited clones (N23c) were characterized: double-knockout clone N23c-3, wildtype N23c-4, and miR-372 knockout N23c-10.

The other allele of clone N23c-3 harboured a 2-base pair insertion in miR-373, we were unsuccessful in elucidating the miR-372 sequence of this allele. Clone N23c-10 had two large deletions in miR-372, yet harboured wildtype alleles for miR-373. The miR-371-3 cluster profile showed that miR-371a-3p levels were similar in the cells of all clones, while a steep decrease could be seen in miR-372 levels in the miR-372 KO clones N372-2, N372-10, N23c-3, and N23c-10 compared to NCCIT parental (**Figure 9A**). Clones N373-5 and N23c-3 had lower levels of miR-373 compared to NCCIT parental. Similar results were obtained when measuring the levels of secreted miR-371-3 cluster in conditioned medium (**Figure 9B**), indicating that the miRNAs were absent in the generated KO clones.

Increase in LATS2 mRNA levels after knockout of both miR-372 and miR-373

The expression of the pluripotency markers and P53-related transcripts were measured in the N372, N373, and N23c clones using RT-qPCR. KO of either miR-372 or miR-373 gave similar levels of *OCT3/4* and *SOX2* as NCCIT parental (**Figure 10A**). For the double-KO clone N23c-3, the levels of the pluripotency markers decreased by a fold change of near three. Expression levels of the P53-related genes in the clones did not differ from NCCIT parental, except for a decrease of *CDNK1A* (P21) in clone N372-10 (**Figure 10B**). This clone had a significantly higher absolute IC50 than all clones but N373-3 and N23c-3 (**Figure S7**). Nonetheless, no miR-371-3 cluster-related differences could be demonstrated in cisplatin response of the clones. Remarkably, clone N23c-3 had a more than 3.5-fold increase in *LATS2* expression, despite similar levels of other P53-related transcripts compared NCCIT parental, indicating an effect of miR-372 and miR-373 (**Figure 10C**). Analysis of the cell growth of the clones, illustrates similar growth curves for most clones (**Figure 10D**). Double-KO clone N23c-3 had a more levelled growth curve. However, clonal differences could also be seen for the clones with wildtype miR-371-3 cluster. The morphology of the clones showed no difference (**Figure 10E**).

Increase in LATS2 in double-knockout clone

To get more insight into the increase in *LATS2* expression in clone N23c-3, Western blot was performed. Western blot showed a relatively higher intensity of *LATS2* in the double-KO clone N23c-3 compared to its CRISPR-edited wildtype counterpart clone N23c-4 (**Figure 11A**). *LATS2* protein intensity was not increased in the N372 clones, however clone N373-5 appears to have higher intensity of *LATS2* as well (**Figure 11B**). This indicates a positive effect of miR-373 KO on *LATS2* protein levels.

Double-knockout cells are able to form tumors in vivo

To test the hypothesis on whether miR372 and miR373 are responsible for oncogenic features, we subcutaneously xenografted double-knockout clone N23c-3 and wildtype control N23c-4 into both sides of mice (two tumors per animal, three animals per cell line). Tumors were harvested, formalin fixed, paraffin embedded and stained for histology using H&E at endpoints (data not shown). All animals developed tumors and no differences in histology was identified, i.e., all cases were embryonal carcinomas. To confirm, plasma of the the xenografted mice was analysed using the respective miR levels (**Figure 12**). Indeed, plasma of the animals injected with the double knock-out cell line showed only presence of miR371a, with low to absent levels of miR372/373. In contrast, the wildtype injected animals, serving as controls, all three miRs were detected.

GCT cells survive knockout of miR-371-3 cluster

To confirm the passenger effect of miR-371a on the transcription of the miR-371-3 cluster, we generated miR-371 KO clones in the miR-372 and miR-373 double-KO clone N23c-3 (NT) using CRISPR/Cas9. Six triple KO clones were further characterized (**Figure S8**). Analysis of the miR371-3 cluster profile confirmed the decreased levels of miR-371a-3p, and consequently the entire cluster, in all clones (**Figure 13A**). Noticeable is how some clones had even lower levels of miR-372 and miR-373 than their precursor clone N23c-3 while no CRISPR/Cas9-editing was performed on these miRNAs at that time. The secreted miR-371-3 cluster levels in the conditioned medium of the clones showed similar decreases in the miR-371-3 cluster levels (**Figure 13B**). mRNA expression of *OCT3/4* and *SOX2* was unchanged in response to miR-371-3 cluster KO compared to NCCIT parental (**Figure S9A**). Clone NT-9 displayed lower levels of the pluripotency marker as well as higher levels of *P21*, expectedly due to clonal differences. Surprisingly, *LATS2* expression was only increased in half of the clones (**Figure S9C**). The morphology and cell growth rates of the NT clones were indistinguishable (**Figure S9D and E**).

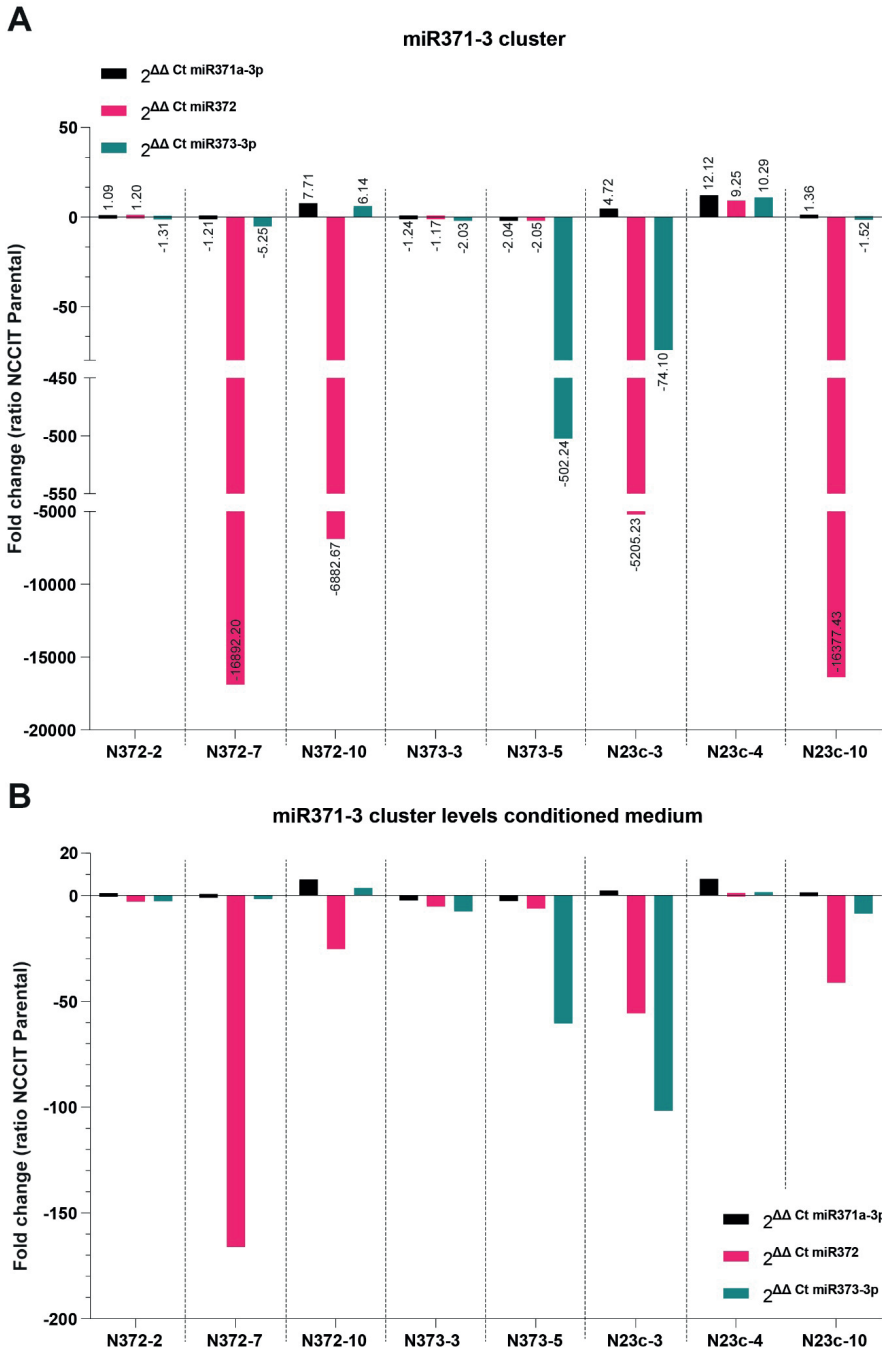


Figure 9: miR-371-3 profile of N372, N373, and N23c clones. A) Profile of fold change of miR-371-3 cluster in cells of miR-372, miR-373, or combination knockout clones compared to NCCIT parental. B) Profile of fold change of secreted miR-371-3 cluster by N372, N373, and N23c clones compared to NCCIT parental.

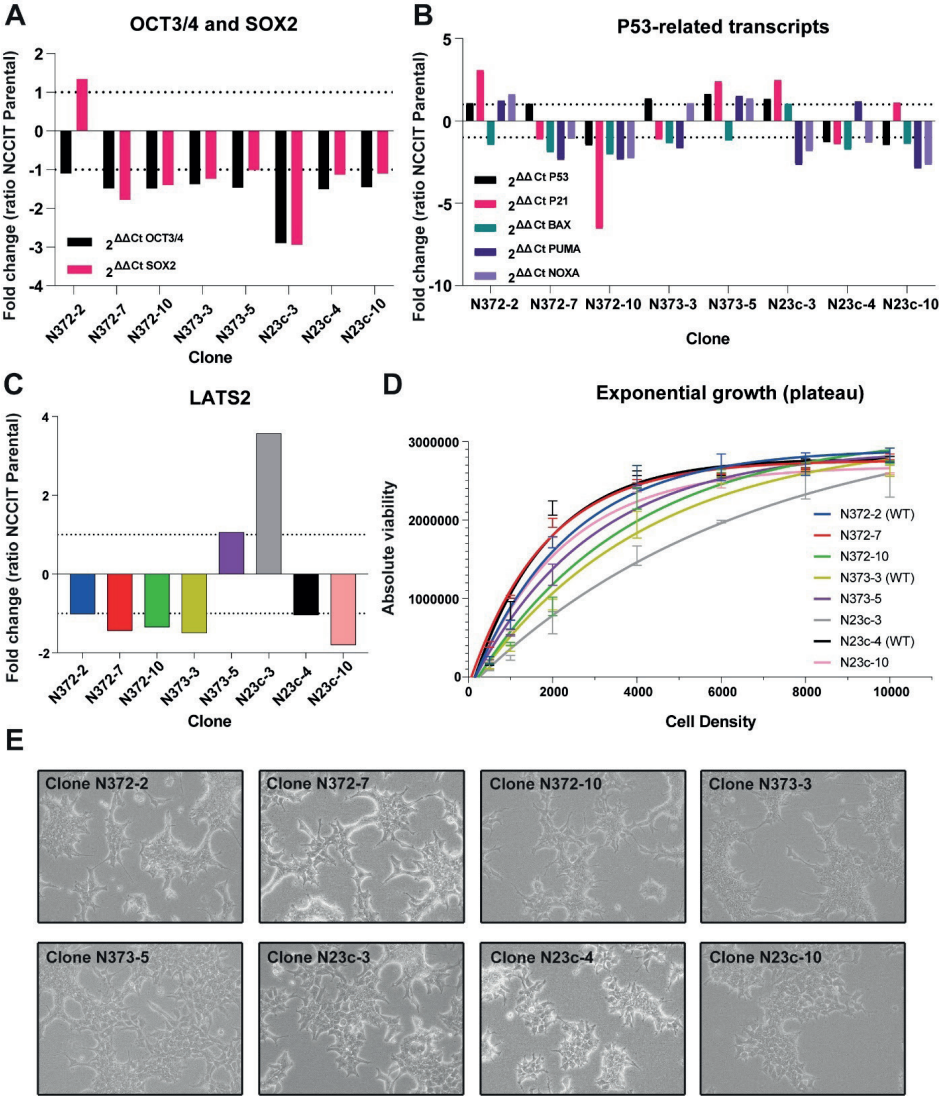


Figure 10: Expression of mRNA and cell growth of N372, N373, and N23c clones. **A)** Fold change of OCT3/4 (POU5F1) and SOX2 compared to NCCIT parental. **B)** Expression level of mRNA of P53-related transcripts: TP53, P21 (CDKN1A), BAX, PUMA (BBC3), and NOXA (PMAIP1). **C)** Fold change of LATS2 expression compared to NCCIT parental. **D)** Cell growth as defined by the absolute viability of increasing cell densities. N=2. **E)** Morphology of the clones in culture. Magnification: 300x.

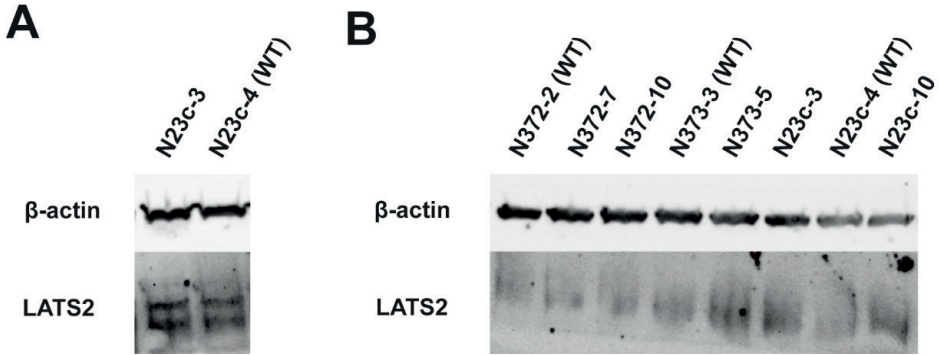


Figure 11: Western blot of β -actin and LATS2. **A)** Protein signal intensity of β -actin (housekeeper) and LATS2 (red arrow) in double-knockout clone N23c-3 and CRISPR-edited wildtype clone N23c-4. **B)** Protein signal intensity of β -actin (housekeeper) and LATS2 in N372, N373, and N23c clones.

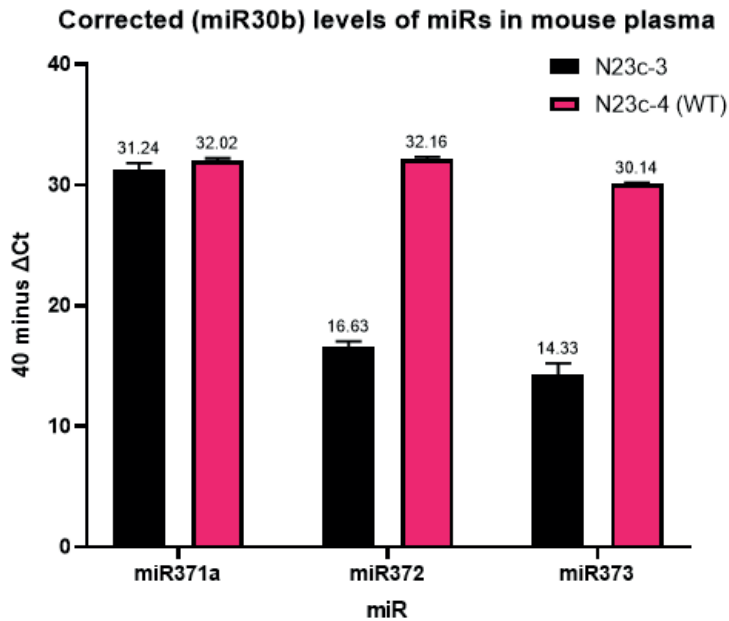


Figure 12: miR-371-3 cluster levels in mouse plasma after xenografting N23c-3 or wildtype N23c-4. miR levels measured in the plasma from separate animals depicted as 40 minus the deltaCt (high values indicate high miR levels). Only plasma coming from animals injected with the N23c-3 (KO) show strong reduced levels of the miR372 and 373, indicating that indeed these tumors are coming from double-knockout cells.

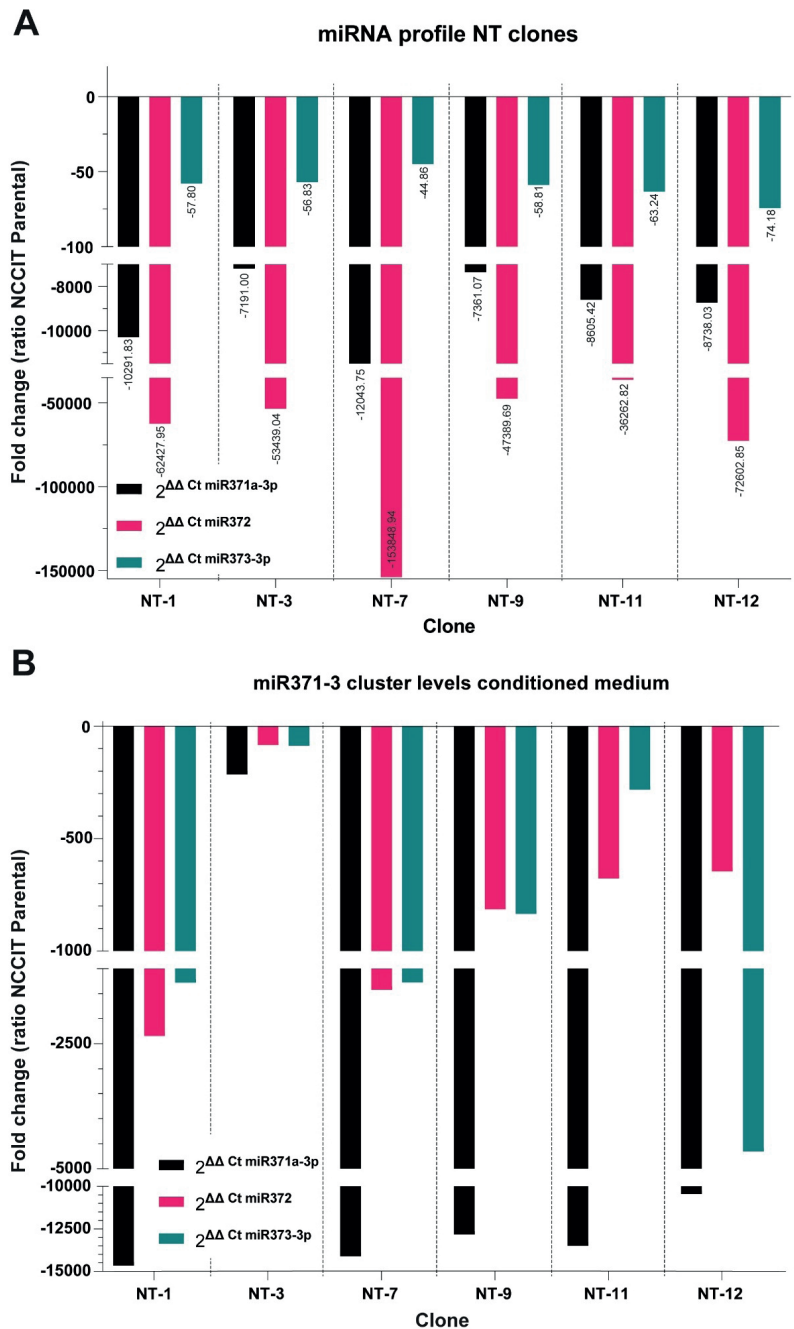


Figure 13: miR-371-3 cluster profile NT clones. A) Fold change of miR-371-3 cluster levels in cells of NT clones compared to NCCIT parental. **B)** Fold change of secreted miR-371-3 cluster levels in conditioned medium of NT clones compared to NCCIT parental.

DISCUSSION

For over a decade it has been known that the miR-371-3 cluster is expressed and secreted by all malignant GCT cells (Eini et al., 2013; Gillis et al., 2007; Looijenga et al., 2007; Murray et al., 2011; Voorhoeve et al., 2006). Of this cluster, miR-371a-3p is most studied in the serum of (T)GCT patients (Syring et al., 2015). Therefore, we tried to elucidate if this miRNA had oncogenic properties, if its presence is a passenger effect of the transcription of the miR-371-3 cluster and miR-372 and/or miR-373 are the oncogenic drivers, or if transcription of the entire miR-371-3 cluster is a passenger effect in GCTs, or more precise, a remaining phenotype from their precursor cells. In this study, for the first time, CRISPR/Cas9-edited GCT cell clones were generated harbouring both individual KO mutations of the miR-371-3 cluster miRNAs and various combinations.

Investigation of the N371 and E371 KO clones showed a decrease not only in miR-371a-3p levels, but also in miR-371a-5p levels (**Figures 3D** and **6D**). This indicates that a mutation in miR-371a-3p causes a defect in the formation of the miR-371a hairpin, therefore impairing the maturation of both miRNAs (**Figure 14**). Along with the expression of the miR-371-3 cluster, miR-885-5p expression was measured as this miRNA is a putative molecular marker for teratoma; the only GCT histology that does not secrete the miR-371-3 cluster. The unchanged levels of miR-885-5p compared to their parental cell line (**Figure 3C** and **6C**) was in concordance with results obtained from mouse xenografts. Xenografting of N371 KO clones in mice showed no histological differentiation and similar tumour growth between wildtype and KO clones (data not shown). This indicates that miR-371 is not required for maintenance of pluripotency in the embryonal carcinoma phenotype. mRNA data of the pluripotency markers *OCT3/4* and *SOX2* and cell morphology demonstrate this as well (**Figures 4A/E** and **7A/E**). mRNA expression of transcripts involved in the P53 pathway, especially the miR-371-3 target *LATS2*, did not differ significantly from NCCIT/2102Ep parental and are thus likely not a target of miR-371. This is substantiated by earlier research indicating miR-372 and miR-373 to be responsible for regulation of *LATS2* (Voorhoeve et al., 2006). Clonal differences were observed in cell growth and cisplatin response; however these could not be designated to the loss of miR-371 as results varied between miR-371 KO clones (**Figure S1** and **S4**). We therefore concluded that the increased levels of miR-371a-3p in GCT cells are not involved in cell survival after tumour establishment.

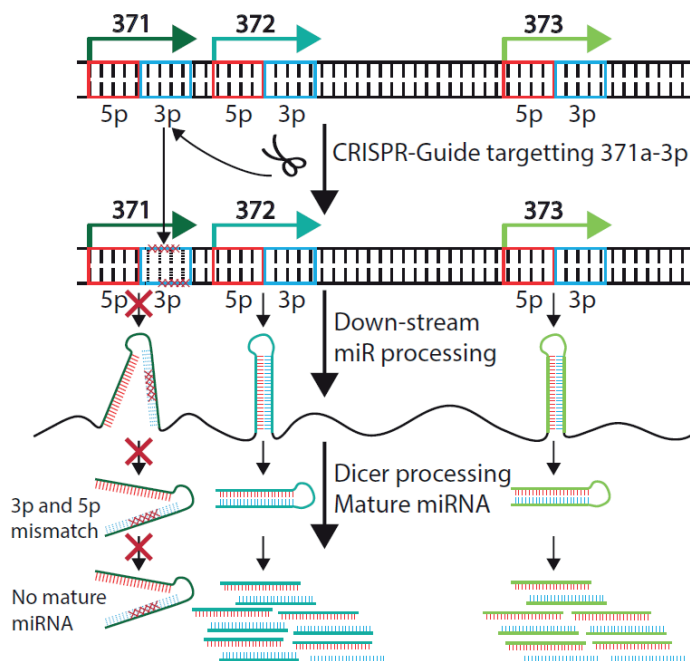


Figure 14: Expected miRNA biogenesis after CRISPR/Cas9 editing. Proposed model of impairment of miRNA biogenesis after InDel in one arm of the miRNA. miR371 is used as an example of an edited miR while miR372 and 373 serve as wildtype controls.

This conclusion was followed by the investigation of the possibility that the increase in miR-371a-3p is due to tumor dependency on miR-372 and/or miR-373, and because the cluster is transcribed to form one pri-miRNA the increase in miR-371 is merely a passenger effect of the transcription of the full cluster. Most interesting were the results obtained from the miR-372 and miR-373 double-KO clone. While KO of either miR-372 or miR-373 did not affect *LATS2* expression, the combination KO of both increased *LATS2* levels (**Figure 10C**). To verify the increase and study the possibility that the miRNAs silence the gene by preventing mRNA translation and not only mRNA degradation, Western blot was performed. The increase in *LATS2* was confirmed, showing a higher protein signal intensity in the double-KO clone (**Figure 11**). The increase in *LATS2* after KO of miR-372 and miR-373 is consistent with our earlier findings of Voorhoeve et al., (2006), showing that increasing miR-372 and miR-373 expression decreased *LATS2* mRNA levels 2-fold and protein levels 4- to 5-fold, indicating a combination of mRNA degradation and translational inhibition of the miRNAs. The increase in cell proliferation demonstrated by the researchers after transduction with a miR-371&2 or miR-373 vector was seen by us as a slight decrease in cell proliferation in the double-KO clone. However, it is difficult to confirm if this decrease in cell proliferation was due to the loss of miR-372/373 in

the generated clones. Mostly because clones harbouring similar or no mutations did not always demonstrate comparable growth, indicating clonal differences. Considering that NCCIT cells carry hemizygotously mutated *TP53*, no effect was seen in the mRNA levels of *TP53* in our clones. Nonetheless, the increase in the miR-371-3 cluster in GCTs with wildtype *TP53* may be advantageous to the tumour by suppressing P53-regulated apoptosis via *LATS2* (Aylon et al., 2006; Voorhoeve et al., 2006). Interestingly, clones that grew slower had increased levels of *LATS2*. This is in line with the findings of Voorhoeve et al., (2006), however, we also observed this effect in clones with mutations in miR-371 (**Figure S3B**) and not only in miR-372 or miR-373-mutated clones. This may indicate an off-target effect of editing in the miR-371-3 cluster or an effect independent of the cluster. Interestingly, both wildtype and double-knockout cells were able to form tumors *in vivo*. Strikingly, no impact on histology was identified resulting from the double-knockout compared to the wildtype cells (embryonal carcinoma, and absence of differentiated elements). Due to the known levels of these miRs during embryonal development we expected that loss of these miRs would, if there would be tumor formation at all, at least have an impact on viability or histology (i.e., differentiation into teratoma). The explanation could be related to residual functionality of miR371 in the double-knockout cells. *In vivo* xenografting of triple-knockout clones would be a logical next step to further study this.

Using miRTargetLink 2.0 targets of the miR-371-3 cluster can be analysed as weak and/or strong validated (Kern et al., 2021). This shows that miR-372(-3p) and miR-373(-3p) are the strongest representatives of the cluster regarding strongly validated targets (**Figure S6**). This corresponds with RNAseq data of the N371 clones, which indicates no significant difference in the miR-371-3 cluster targets with strong validation compared with NCCIT parental (data not shown). It is striking that many targets with strong validation are involved in the regulation of metabolic processes. This was confirmed by RNAseq of the N371 clones, likely due to lower levels of miR-371a-5p, an inhibitor of hypoxia-inducible factor-1 α (Yao et al., 2016). One strong validated target that all three miRNAs of the cluster share is Dickkopf-1 (DKK1), an inhibitor of the Wnt signalling pathway crucial for embryonic development (Semenov et al., 2008). An increase in the miR-371-3 cluster may therefore help induce or maintain pluripotency via Wnt signalling in GCT cells (Zhou et al., 2011).

It is important to note that the miR-371-3 cluster is not the only interactor of its targets, thereby complicating a study into the function of only this cluster. This may clarify why only half the NT KO clones show a slight increase in *LATS2* levels (**Figure S9C**). A luciferase assay using a luciferase expressing vector with a miR (371a/2/3) target sequence in the 3' untranslated region could really verify that the edited miRNAs are non-functional. Furthermore, due to the hemizygous mutation of *TP53* in NCCIT, the results may vary in 2102Ep as this cell line might be more dependent on the expression

of the miR-371-3 cluster, this in line with results indicating that GCTs expressing high miR-371-3 cluster levels did not have *TP53* mutations (Voorhoeve et al., 2006). Therefore, it will be of interest to repeat the experiments in 2102Ep to investigate the dependency of the *TP53* status. There is also a possibility of CRISPR/Cas9 off-target effects. As was seen in N371 clone 10, this clone harboured wildtype miR-371-3 cluster, however the levels of the cluster were slightly but consistently increased (**Figure 3**). This suggests that just binding and cutting by Cas9 in the cluster, followed by correct repair after CRISPR/Cas9 treatment, may influence the clones DNA in a way that allows for higher expression.

The important outcome of this study is that we were able to generate GCT-derived cells with triple KO of the miR-371-3 cluster which would not be possible if the miR-371-3 cluster was essential for survival of GCT cells. One possibility is that an, thus far, unknown oncogenic driver causes the increase in miR-371-3 cluster expression, which is necessary for oncogenic onset of GCT development, yet after the GCT is established, the miRNAs may not have a function anymore. One theory is that the increase in the miR-371-3 cluster could, in part, help developing GCT cells escape P53-mediated apoptosis; as *LATS2* is inhibited and degraded by the cluster, P53 levels will also decline thereby decreasing the amount of apoptosis-inducing BAX (Hemann & Lowe, 2006; Qu et al., 2019; Runyan et al., 2008). To confirm the need for the miR-371-3 cluster during oncogenic onset a study should be performed demonstrating that induced pluripotent stem cells or embryonic stem cells harbouring a miR-371-3 cluster KO mutation are not capable of becoming a GCT. Yet, researchers have not succeeded in inducing undifferentiated GCTs from stem cells. Another, more likely, possibility is that the expression level of the cluster does not get downregulated or lost once a miR-371-3 cluster-expressing PGC, or other GCT precursor cell, transforms into a GCT cell (Bosl & Motzer, 1997; Oosterhuis & Looijenga, 2019; Suh et al., 2004). The latter being more likely especially in the light of GCTs embryonic-like phenotypes, including maintaining DNA integrity and low mutation rate, which makes that GCTs likely harbour a negative selection on genetic rearrangements (Bloom et al., 2019). Therefore, indicating no negative selection in expressing the cluster as well as no positive selection on losing this expression. This would result in the expression of miR-371-3 cluster in undifferentiated GCT cells.

Even though we propose that the miR-371-3 cluster is not required for the maintenance of established GCTs, studies have shown that it is an excellent biomarker that should be incorporated as standard STM for GCTs, together with AFP, β -hCG, and LDH (Almstrup et al., 2020; Dieckmann et al., 2019; Gilligan et al., 2010). Although it is still difficult to say something about aggressiveness of the tumor solely based on these miRs, the levels of miR-371a-3p indicate the presence of a malignant GCT and therefore have prognostic value in the clinic.

REFERENCES

1. Almstrup, K., Lobo, J., Mørup, N., Belge, G., Rajpert-De Meyts, E., Looijenga, L. H. J., & Dieckmann, K. P. (2020). Application of miRNAs in the diagnosis and monitoring of testicular germ cell tumours. *Nature Reviews Urology* 2020 17:4, 17(4), 201–213. <https://doi.org/10.1038/s41585-020-0296-x>
2. Andrews, P. W., Bronson, D. L., Benham, F., Strickland, S., & Knowles, B. B. (1980). A comparative study of eight cell lines derived from human testicular teratocarcinoma. *International Journal of Cancer*, 26(3), 269–280. <https://doi.org/10.1002/IJC.2910260304>
3. Aylon, Y., Michael, D., Shmueli, A., Yabuta, N., Nojima, H., & Oren, M. (2006). A positive feedback loop between the p53 and Lats2 tumor suppressors prevents tetraploidization. *Genes & Development*, 20(19), 2687. <https://doi.org/10.1101/GAD.1447006>
4. Baade, P., Carrière, P., & Fritsch, L. (2008). Trends in testicular germ cell cancer incidence in Australia. *Cancer Causes & Control : CCC*, 19(10), 1043–1049. <https://doi.org/10.1007/S10552-008-9168-Z>
5. Bloom, J. C., Loehr, A. R., Schimenti, J. C., & Weiss, R. S. (2019). Germline Genome Protection: Implications for Gamete Quality and Germ Cell Tumorigenesis. *Andrology*, 7(4), 516. <https://doi.org/10.1111/ANDR.12651>
6. Bosl, G. J., & Motzer, R. J. (1997). Testicular Germ-Cell Cancer. <https://doi.org/10.1056/NEJM199707243370406>, 337(4), 242–254. <https://doi.org/10.1056/NEJM199707243370406>
7. Brydøy, M., Oldenburg, J., Klepp, O., Bremnes, R. M., Wist, E. A., Wentzel-Larsen, T., Hauge, E. R., Dahl, O., & Fosså, S. D. (2009). Observational Study of Prevalence of Long-term Raynaud-Like Phenomena and Neurological Side Effects in Testicular Cancer Survivors. *Articles | JNCI*, 101, 24. <https://doi.org/10.1093/jnci/djp413>
8. Cheng, L., Albers, P., Berney, D. M., Feldman, D. R., Daugaard, G., Gilligan, T., & Looijenga, L. H. J. (2018). Testicular cancer. *Nature Reviews Disease Primers* 2018 4:1, 4(1), 1–24. <https://doi.org/10.1038/s41572-018-0029-0>
9. Chipman, L. B., & Pasquinelli, A. E. (2019). MiRNA Targeting – Growing Beyond the Seed. *Trends in Genetics : TIG*, 35(3), 215. <https://doi.org/10.1016/J.TIG.2018.12.005>
10. Condrat, C. E., Thompson, D. C., Barbu, M. G., Bugnar, O. L., Boboc, A., Cretoiu, D., Suciu, N., Cretoiu, S. M., & Voinea, S. C. (2020). miRNAs as Biomarkers in Disease: Latest Findings Regarding Their Role in Diagnosis and Prognosis. *Cells*, 9(2). <https://doi.org/10.3390/CELLS9020276>
11. Dieckmann, K. P., Radtke, A., Geczi, L., Matthies, C., Anheuser, P., Eckardt, U., Sommer, J., Zengerling, F., Trenti, E., Pichler, R., Belz, H., Zastrow, S., Winter, A., Melchior, S., Hammel, J., Kranz, J., Bolten, M., Kregge, S., Haben, B., ... Belge, G. (2019). Serum Levels of MicroRNA-371a-3p (M371 Test) as a New Biomarker of Testicular Germ Cell Tumors: Results of a Prospective Multicentric Study. *Journal of Clinical Oncology*, 37(16), 1412. <https://doi.org/10.1200/JCO.18.01480>
12. Dieckmann, K. P., Richter-Simonsen, H., Kulejewski, M., Ikogho, R., Zecha, H., Anheuser, P., Pichlmeier, U., & Isbarn, H. (2018). Testicular Germ-Cell Tumours: A Descriptive Analysis of Clinical Characteristics at First Presentation. *Urologia Internationalis*, 100(4), 409. <https://doi.org/10.1159/000488284>
13. Eini, R., Dorssers, L. C. J., & Looijenga, L. H. J. (2013). Role of stem cell proteins and microRNAs in embryogenesis and germ cell cancer. *International Journal of Developmental Biology*, 57(2–4), 319–332. <https://doi.org/10.1387/IJDB.130020RE>
14. Filipowicz, W., Bhattacharyya, S. N., & Sonenberg, N. (2008). Mechanisms of post-transcriptional regulation by microRNAs: are the answers in sight? *Nature Reviews Genetics* 2008 9:2, 9(2), 102–114. <https://doi.org/10.1038/nrg2290>

15. Fosså, S. D., Gilbert, E., Dores, G. M., Chen, J., McGlynn, K. A., Schonfeld, S., Storm, H., Holowaty, E., Andersen, A., Joensuu, H., Andersson, M., Kaijser, M., Gospodarowicz, M., Cohen, R., Pukkala, E., & Travis, L. B. (2007). *Noncancer Causes of Death in Survivors of Testicular Cancer*. <https://doi.org/10.1093/jnci/djk111>
16. Ghildiyal, M., & Zamore, P. D. (2009). Small silencing RNAs: an expanding universe. *Nature Reviews. Genetics*, 10(2), 94–108. <https://doi.org/10.1038/NRG2504>
17. Gillessen, S., Collette, L., Daugaard, G., de Wit, R., Tryakin, A., Albany, C., Stahl, O., Fizazi, K., Gietema, J. A., De Giorgi, U. F. F., Hansen, A. R., Feldman, D., Cafferty, F., Tandstad, T., Garcia del Muro, X., Huddart, R. A., Sweeney, C. J., Heng, D. Y. C., Sauve, N., & Beyer, J. (2019). Redefining the IGCCCG classification in advanced non-seminoma. *Annals of Oncology*, 30, v357–v358. <https://doi.org/10.1093/ANNONC/MDZ249.002>
18. Gilligan, T. D., Seidenfeld, J., Basch, E. M., Einhorn, L. H., Fancher, T., Smith, D. C., Stephenson, A. J., Vaughn, D. J., Cosby, R., & Hayes, D. F. (2010). American Society of Clinical Oncology Clinical Practice Guideline on uses of serum tumor markers in adult males with germ cell tumors. *Journal of Clinical Oncology: Official Journal of the American Society of Clinical Oncology*, 28(20), 3388–3404. <https://doi.org/10.1200/JCO.2009.26.4481>
19. Gillis, A. J. M., Stoop, H. J., Hersmus, R., Oosterhuis, J. W., Sun, Y., Chen, C., Guenther, S., Sherlock, J., Veltman, I., Baeten, J., Van Der Spek, P. J., De Alarcon, P., & Looijenga, L. H. J. (2007). High-throughput microRNAome analysis in human germ cell tumours. *The Journal of Pathology*, 213(3), 319–328. <https://doi.org/10.1002/PATH.2230>
20. Green, D., Dalmay, T., & Chapman, T. (2016). Microguards and micromessengers of the genome. *Heredity*, 116(2), 125. <https://doi.org/10.1038/HDY.2015.84>
21. Hartmann, J. T., Albrecht, C., Schmoll, H. J., Kuczyk, M. A., Kollmannsberger, C., & Bokemeyer, C. (1999). Long-term effects on sexual function and fertility after treatment of testicular cancer. *British Journal of Cancer* 1999 80:5, 80(5), 801–807. <https://doi.org/10.1038/sj.bjc.6690424>
22. Hemann, M. T., & Lowe, S. W. (2006). The p53-Bcl-2 connection. *Cell Death and Differentiation*, 13(8), 1256–1259. <https://doi.org/10.1038/SJ.CDD.4401962>
23. Hong, Y., Cervantes, R. B., Tichy, E., Tischfield, J. A., & Stambrook, P. J. (2007). Protecting genomic integrity in somatic cells and embryonic stem cells. *Mutation Research*, 614(1–2), 48–55. <https://doi.org/10.1016/J.MRFMMM.2006.06.006>
24. Kern, F., Aparicio-Puerta, E., Li, Y., Fehlmann, T., Kehl, T., Wagner, V., Ray, K., Ludwig, N., Lenhof, H. P., Meese, E., & Keller, A. (2021). miRTargetLink 2.0—interactive miRNA target gene and target pathway networks. *Nucleic Acids Research*, 49(W1), W409–W416. <https://doi.org/10.1093/NAR/GKAB297>
25. Kinkade, S. (1999). Testicular Cancer. *American Family Physician*, 59(9), 2539–2544.
26. Kvammen, Ø., Myklebust, T., Solberg, A., Møller, B., Klepp, O. H., Fosså, S. D., & Tandstad, T. (2016). Long-term relative survival after diagnosis of testicular germ cell tumor. *Cancer Epidemiology Biomarkers and Prevention*, 25(5), 773–779. <https://doi.org/10.1158/1055-9965.EPI-15-1153/68747/AM/LONG-TERM-RELATIVE-SURVIVAL-AFTER-DIAGNOSIS-OF>
27. Lange, P. H., & Winfield, H. N. (1987). Biological Markers in Urologic Cancer. *Cancer*, 60, 464–472.
28. Leão, R., Albersen, M., Looijenga, H. J., Tandstad, T., Kollmannsberger, C., Murray, M. J., Culine, S., Coleman, N., Belge, G., Hamilton, R. J., Dieckmann, K.-P., & Novara, G. (2021). Circulating MicroRNAs, the Next-Generation Serum Biomarkers in Testicular Germ Cell Tumours: A Systematic Review. *European Urology*, 80, 456–466. <https://doi.org/10.1016/j.eururo.2021.06.006>

29. Lee, K. H., Goan, Y. G., Hsiao, M., Lee, C. H., Jian, S. H., Lin, J. T., Chen, Y. L., & Lu, P. J. (2009). MicroRNA-373 (miR-373) post-transcriptionally regulates large tumor suppressor, homolog 2 (LATS2) and stimulates proliferation in human esophageal cancer. *Experimental Cell Research*, 315(15), 2529–2538. <https://doi.org/10.1016/J.YEXCR.2009.06.001>
30. Lobo, J., Gillis, A. J. M., van den Berg, A., Dorssers, L. C. J., Belge, G., Dieckmann, K. P., Roest, H. P., van der Laan, L. J. W., Gietema, J., Hamilton, R. J., Jerónimo, C., Henrique, R., Salvatori, D., & Looijenga, L. H. J. (2019). Identification and Validation Model for Informative Liquid Biopsy-Based microRNA Biomarkers: Insights from Germ Cell Tumor In Vitro, In Vivo and Patient-Derived Data. *Cells* 2019, Vol. 8, Page 1637, 8(12), 1637. <https://doi.org/10.3390/CELLS8121637>
31. Lobo, J., Jerónimo, C., & Henrique, R. (2020). Cisplatin Resistance in Testicular Germ Cell Tumors: Current Challenges from Various Perspectives. *Cancers*, 12.
32. Looijenga, L. H. J. (2014). Testicular germ cell tumors. *Pediatric Endocrinology Reviews : PER*, 11 Suppl 2, 251–262.
33. Looijenga, L. H. J., Gillis, A. J. M., Stoop, H., Hersmus, R., & Oosterhuis, J. W. (2007). Relevance of microRNAs in normal and malignant development, including human testicular germ cell tumours. *International Journal of Andrology*, 30(4), 304–315. <https://doi.org/10.1111/J.1365-2605.2007.00765.X>
34. Looijenga, L. H. J., Stoop, H., de Leeuw, H. P. J. C., de Gouveia Brazao, C. A., Gillis, A. J. M., van Roozendaal, Kees E P van Zoelen, E. J. J., Weber, R. F. A., Wolffenbuttel, K. P., van Dekken, H., Honecker, F., Bokemeyer, C., Perlman, E. J., Schneider, D. T., Kononen, J., Sauter, G., & Oosterhuis, J. W. (2003). POU5F1 (OCT3/4) identifies cells with pluripotent potential in human germ cell tumors. *Cancer Research*, 63(9), 2244–2250.
35. Lorch, A., Beyer, J., Kramar, A., Einhorn, L. H., Necchi, A., Massard, C., De Giorgi, U., Flechon, A., Margolin, K. A., Lotz, J. P., Germa, J. R. L., Powles, T., Kollmannsberger, C. K., & Bascoul-Mollevi, C. (2010). Prognostic factors in patients with metastatic germ cell tumors who experienced treatment failure with cisplatin-based first-line chemotherapy. *Journal of Clinical Oncology*, 28(33), 4906–4911. <https://doi.org/10.1200/JCO.2009.26.8128>
36. Lu, T. X., & Rothenberg, M. E. (2018). MicroRNA. *The Journal of Allergy and Clinical Immunology*, 141(4), 1202. <https://doi.org/10.1016/J.JACI.2017.08.034>
37. Mead, G. M. (1997). International Germ Cell Consensus Classification: a prognostic factor-based staging system for metastatic germ cell cancers. International Germ Cell Cancer Collaborative Group. *Journal of Clinical Oncology : Official Journal of the American Society of Clinical Oncology*, 15(2), 594–603. <https://doi.org/10.1200/JCO.1997.15.2.594>
38. Medeiros, L. A., Dennis, L. M., Gill, M. E., Houbaviy, H., Markoulaki, S., Fu, D., White, A. C., Kirak, O., Sharp, P. A., Page, D. C., & Jaenisch, R. (2011). Mir-290-295 deficiency in mice results in partially penetrant embryonic lethality and germ cell defects. *Proceedings of the National Academy of Sciences of the United States of America*, 108(34), 14163–14168. <https://doi.org/10.1073/PNAS.1111241108/-/DCSUPPLEMENTAL>
39. Mego, M., van Agthoven, T., Gronesova, P., Chovanec, M., Miskovska, V., Mardiak, J., & Looijenga, L. H. J. (2019). Clinical utility of plasma miR-371a-3p in germ cell tumors. *Journal of Cellular and Molecular Medicine*, 23(2), 1128. <https://doi.org/10.1111/JCMM.14013>
40. Mele, T., Reid, A., & Huddart, R. (2021). Recent advances in testicular germ cell tumours. *Faculty Reviews*, 10. <https://doi.org/10.12703/R/10-67>
41. Müller, M. R., Skowron, M. A., Albers, P., & Nettersheim, D. (2021). Molecular and epigenetic pathogenesis of germ cell tumors. *Asian Journal of Urology*, 8(2), 144. <https://doi.org/10.1016/J.AJUR.2020.05.009>

42. Murray, M. J., Halsall, D. J., Hook, C. E., Williams, D. M., Nicholson, J. C., & Coleman, N. (2011). Identification of microRNAs From the miR-371~373 and miR-302 clusters as potential serum biomarkers of malignant germ cell tumors. *American Journal of Clinical Pathology*, 135(1), 119–125. <https://doi.org/10.1309/AJCPOE11KEYZCJHT>
43. Nauman, M., & Leslie, S. W. (2022). Nonseminomatous Testicular Tumors. *StatPearls*.
44. Nigam, M., Aschebrook-Kilfoy, B., Shikanov, S., & Eggener, S. (2015). Increasing incidence of testicular cancer in the United States and Europe between 1992 and 2009. *World Journal of Urology*, 33(5), 623–631. <https://doi.org/10.1007/S00345-014-1361-Y>
45. Nikolic, A., Volarevic, V., Armstrong, L., Lako, M., & Stojkovic, M. (2016). Primordial Germ Cells: Current Knowledge and Perspectives. *Stem Cells International*, 2016. <https://doi.org/10.1155/2016/1741072>
46. Oosterhuis, J. W., & Looijenga, L. H. J. (2005). Testicular germ-cell tumours in a broader perspective. *Nature Reviews Cancer* 2005 5:3, 5(3), 210–222. <https://doi.org/10.1038/nrc1568>
47. Oosterhuis, J. W., & Looijenga, L. H. J. (2019). Human germ cell tumours from a developmental perspective. *Nature Reviews Cancer*, 19(9), 522–537. <https://doi.org/10.1038/s41568-019-0178-9>
48. Országhová, Z., Kalavská, K., Mego, M., & Chovanec, M. (2022). Overcoming Chemotherapy Resistance in Germ Cell Tumors. *Biomedicines*, 10(5). <https://doi.org/10.3390/BIMEDICINES10050972>
49. Ottaviano, M., Giunta, E. F., Rescigno, P., Mestre, R. P., Marandino, L., Tortora, M., Riccio, V., Parola, S., Casula, M., Paliogiannis, P., Cossu, A., Vogl, U. M., Bosso, D., Rosanova, M., Mazzola, B., Daniele, B., Palmieri, G., Palmieri, G., Barchi, M., ... Garolla, A. (2021). Molecular Sciences The Enigmatic Role of TP53 in Germ Cell Tumours: Are We Missing Something? *J. Mol. Sci*, 22. <https://doi.org/10.3390/ijms22137160>
50. Palumbo, C., Mistretta, F. A., Mazzone, E., Knipper, S., Tian, Z., Perrotte, P., Antonelli, A., Montorsi, F., Shariat, S. F., Saad, F., Simeone, C., Briganti, A., Lattouf, J. B., & Karakiewicz, P. I. (2019). Contemporary Incidence and Mortality Rates in Patients With Testicular Germ Cell Tumors. *Clinical Genitourinary Cancer*, 17(5), e1026–e1035. <https://doi.org/10.1016/j.clgc.2019.06.003>
51. Qu, D., Jiang, M., Huang, D., Zhang, H., Feng, L., Chen, Y., Zhu, X., Wang, S., & Han, J. (2019). Synergistic Effects of The Enhancements to Mitochondrial ROS, p53 Activation and Apoptosis Generated by Aspartame and Potassium Sorbate in HepG2 Cells. *Molecules* 2019, Vol. 24, Page 457, 24(3), 457. <https://doi.org/10.3390/MOLECULES24030457>
52. Radtke, A., Hennig, F., Ikogho, R., Hammel, J., Anheuser, P., Wülfing, C., Belge, G., & Dieckmann, K. P. (2018). The Novel Biomarker of Germ Cell Tumours, Micro-RNA-371a-3p, Has a Very Rapid Decay in Patients with Clinical Stage 1. *Urologia Internationalis*, 100(4), 470. <https://doi.org/10.1159/000488771>
53. Runyan, C., Gu, Y., Shoemaker, A., Looijenga, L., & Wylie, C. (2008). The distribution and behavior of extragonadal primordial germ cells in Δ Bax Δ mutant mice suggest a novel origin for sacrococcygeal germ cell tumors. *The International Journal of Developmental Biology*, 52(4), 333–344. <https://doi.org/10.1387/IJDB.072486CR>
54. Seměnov, M. V., Zhang, X., & He, X. (2008). DKK1 antagonizes Wnt signaling without promotion of LRP6 internalization and degradation. *Journal of Biological Chemistry*, 283(31), 21427–21432. <https://doi.org/10.1074/jbc.M800014200>
55. Sidi, A. A., Chiou, R.-K., & Lange, P. H. (1984). Recent Reflections on Tumor Markers. *World Journal of Urology*, 2(1), 18–25. <https://doi.org/10.1007/BF00326928>
56. Siegel, R. L., Miller, K. D., Fuchs, H. E., & Jemal, A. (2022). Cancer statistics, 2022. *CA: A Cancer Journal for Clinicians*, 72(1), 7–33. <https://doi.org/10.3322/CAAC.21708>

57. Skakkebaek, N. E., Berthelsen, J. G., & Muller, J. (1982). Carcinoma-In-Situ of the Undescended Testis. *Urologic Clinics of North America*, 9(3), 377–385. [https://doi.org/10.1016/S0094-0143\(21\)01352-5](https://doi.org/10.1016/S0094-0143(21)01352-5)
58. Skakkebaek, N. E., Rajpert-De Meyts, E., & Main, K. M. (2001). Testicular dysgenesis syndrome: an increasingly common developmental disorder with environmental aspects: Opinion. *Human Reproduction*, 16(5), 972–978. <https://doi.org/10.1093/HUMREP/16.5.972>
59. Smith, Z. L., Werntz, R. P., & Eggener, S. E. (2018). Testicular Cancer: Epidemiology, Diagnosis, and Management. *Medical Clinics of North America*, 102(2), 251–264. <https://doi.org/10.1016/J.MCNA.2017.10.003>
60. Song, M., Hildesheim, A., & Shiels, M. S. (2020). Premature Years of Life Lost Due to Cancer in the United States in 2017. *Cancer Epidemiology, Biomarkers & Prevention : A Publication of the American Association for Cancer Research, Cosponsored by the American Society of Preventive Oncology*, 29(12), 2591–2598. <https://doi.org/10.1158/1055-9965.EPI-20-0782>
61. Spiekermann, M., Belge, G., Winter, N., Ikogho, R., Balks, T., Bullerdiek, J., & Dieckmann, K. P. (2015). MicroRNA miR-371a-3p in serum of patients with germ cell tumours: evaluations for establishing a serum biomarker. *Andrology*, 3(1), 78–84. <https://doi.org/10.1111/J.2047-2927.2014.00269.X>
62. Stang, A., Trocchi, P., Kajüter, H., Trabert, B., Oosterhuis, J. W., & McGlynn, K. A. (2023). Age-incidence patterns of seminoma and nonseminoma among males and females in Germany and the United States, 2008–2016. *Andrology*, 11(1), 65–72. <https://doi.org/10.1111/ANDR.13282>
63. Stevens, M. J., Norman, A. R., Dearnaley, D. P., & Horwich, A. (2016). Prognostic significance of early serum tumor marker half-life in metastatic testicular teratoma. <https://doi.org/10.1200/JCO.1995.13.1.87>, 13(1), 87–92. <https://doi.org/10.1200/JCO.1995.13.1.87>
64. Suh, M. R., Lee, Y., Kim, J. Y., Kim, S. K., Moon, S. H., Lee, J. Y., Cha, K. Y., Chung, H. M., Yoon, H. S., Moon, S. Y., Kim, V. N., & Kim, K. S. (2004). Human embryonic stem cells express a unique set of microRNAs. *Developmental Biology*, 270(2), 488–498. <https://doi.org/10.1016/J.YDBIO.2004.02.019>
65. Syring, I., Bartels, J., Holdenrieder, S., Kristiansen, G., Müller, S. C., & Ellinger, J. (2015). Circulating Serum miRNA (miR-367-3p, miR-371a-3p, miR-372-3p and miR-373-3p) as Biomarkers in Patients with Testicular Germ Cell Cancer. *The Journal of Urology*, 193(1), 331–337. <https://doi.org/10.1016/J.JURO.2014.07.010>
66. Teshima, S., Shimosato, Y., Hirohashi, S., Tome, Y., Hayashi, I., Kanazawa, H., & Kakizoe, T. (1988). Four new human germ cell tumor cell lines – PubMed. *Laboratory Investigation*, 59(3), 328–336.
67. Timmerman, D. M., Eleveld, T. F., Sriram, S., Dorssers, L. C., Gillis, A. J., Schmidtova, S., Kalavska, K., van de Werken, H. J., Oing, C., Honecker, F., Mego, M., & Looijenga, L. H. (2022). Chromosome 3p25.3 Gain Is Associated With Cisplatin Resistance and Is an Independent Predictor of Poor Outcome in Male Malignant Germ Cell Tumors. *J Clin Oncol*, 40, 3077–3087.
68. Tiscornia, G., & Carlos Izpisu Belmonte, J. (2010). MicroRNAs in embryonic stem cell function and fate. *Genes & Development*, 24, 2732–2741. <https://doi.org/10.1101/gad.1982910>
69. van Agthoven, T., Eijkenboom, W. M. H., & Looijenga, L. H. J. (2017). microRNA-371a-3p as informative biomarker for the follow-up of testicular germ cell cancer patients. *Cellular Oncology (Dordrecht)*, 40(4), 379–388. <https://doi.org/10.1007/S13402-017-0333-9>
70. Voorhoeve, P. M., le Sage, C., Schrier, M., Gillis, A. J. M., Stoop, H., Nagel, R., Liu, Y. P., van Duijse, J., Drost, J., Griekspoor, A., Zlotorynski, E., Yabuta, N., De Vita, G., Nojima, H., Looijenga, L. H. J., & Agami, R. (2006). A Genetic Screen Implicates miRNA-372 and miRNA-373 As Oncogenes in Testicular Germ Cell Tumors. *Cell*, 124(6), 1169–1181. <https://doi.org/10.1016/j.cell.2006.02.037>

71. Walschaerts, M., Huyghe, E., Muller, A., Bachaud, J. M., Bujan, L., & Thonneau, P. (2008). Doubling of testicular cancer incidence rate over the last 20 years in southern France. *Cancer Causes & Control: CCC*, 19(2), 155–161. <https://doi.org/10.1007/S10552-007-9081-X>
72. Wang, N., Trend, B., Bronson, D. L., & Fraley, E. E. (1980). Nonrandom abnormalities in chromosome 1 in human testicular cancers – PubMed. *Cancer Research*, 40(3), 796–802.
73. Willemse, P. H., Sleijfer, D. T., Koops, H. S., Bruijn, H. W. De, Oosterhuis, J. W., Brouwers, T. M., Ockhuizen, T., & Marrink, J. (1981). The value of AFP and HCG half lives in predicting the efficacy of combination chemotherapy in patients with non-seminomatous germ cell tumors of the testis. *Oncodevelopmental Biology and Medicine*, 2(1–2), 129–134.
74. Wu, S., Aksoy, M., Shi, J., & Houbaviy, H. B. (2014). Evolution of the miR-290-295/miR-371-373 Cluster Family Seed Repertoire. *PLoS ONE*, 9(9), 108519. <https://doi.org/10.1371/journal.pone.0108519>
75. Yao, F., Sun, L., Fang, W., Wang, H., Yao, D., Cui, R., Xu, J., Wang, L., & Wang, X. (2016). Hsa-miR-371-5p inhibits human mesangial cell proliferation and promotes apoptosis in lupus nephritis by directly targeting hypoxia-inducible factor 1 α . *Molecular Medicine Reports*, 14(6), 5693–5698. <https://doi.org/10.3892/MMR.2016.5939/HTML>
76. Zhou, A. D., Diao, L. T., Xu, H., Xiao, Z. D., Li, J. H., Zhou, H., & Qu, L. H. (2011). B-Catenin/LEF1 transactivates the microRNA-371-373 cluster that modulates the Wnt/ β -catenin-signaling pathway. *Oncogene* 2012 31:24, 31(24), 2968–2978. <https://doi.org/10.1038/onc.2011.461>

SUPPLEMENTARY

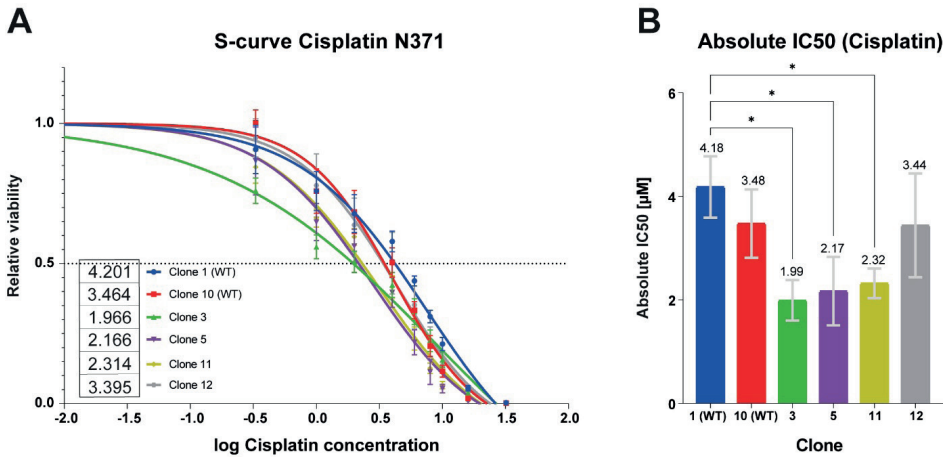


Figure S1: Cisplatin response of N371 clones. **A)** Average S-curve of cisplatin response of N371 clones defined by relative viability of cells exposed to increasing cisplatin concentrations. Graph represents the means of triplicate experiments. **B)** Absolute IC50 of N371 clones. Bars represent the means of triplicate experiments. Statistical analysis by one-way ANOVA. * $P \leq 0.05$.

6

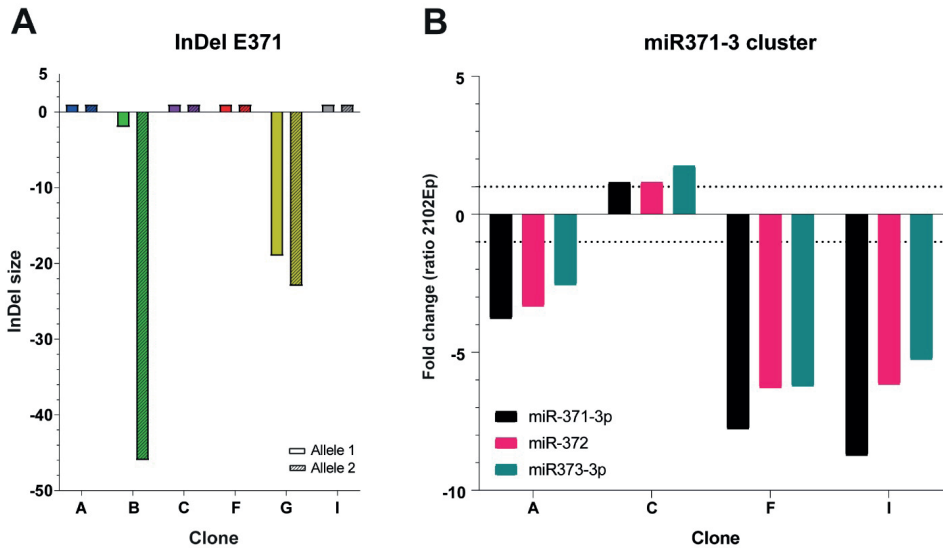


Figure S2: InDel size and miR-371-3 cluster profile E371 clones. **A)** InDel size of all expanded E371 clones. **B)** miR-371-3 cluster profile of E371 clones with insert of 1 nucleotide.

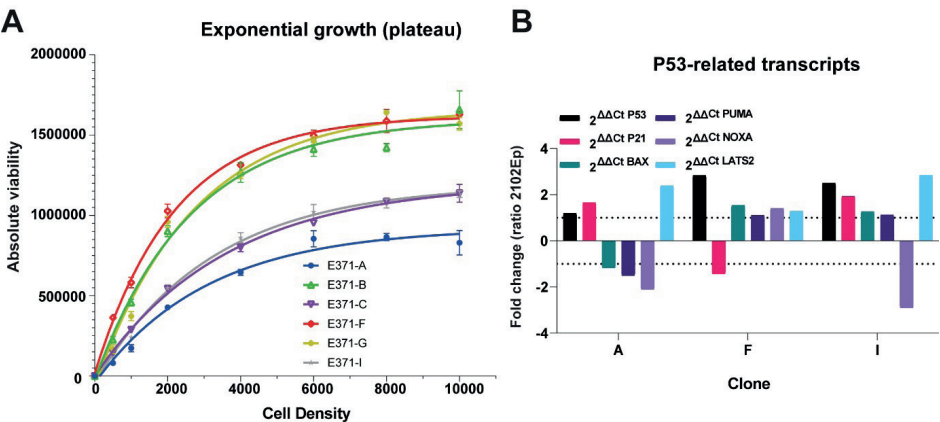


Figure S3: Exponential growth curve of all E371 clones. A) Growth curve defined by the absolute viability of increasing cell densities of the E371 clones including clones with insert of 1 nucleotide. **B)** Fold change levels of P53-related transcripts in other E371 clones with insertion of 1 nucleotide.

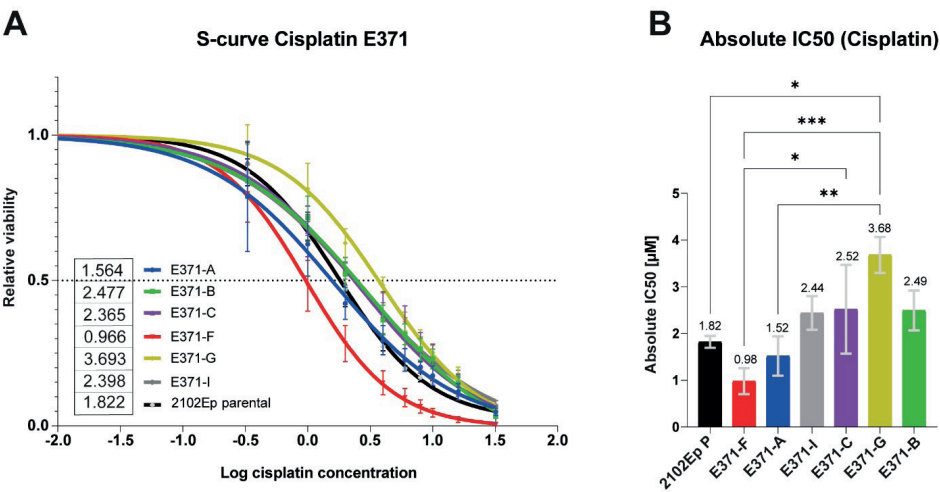
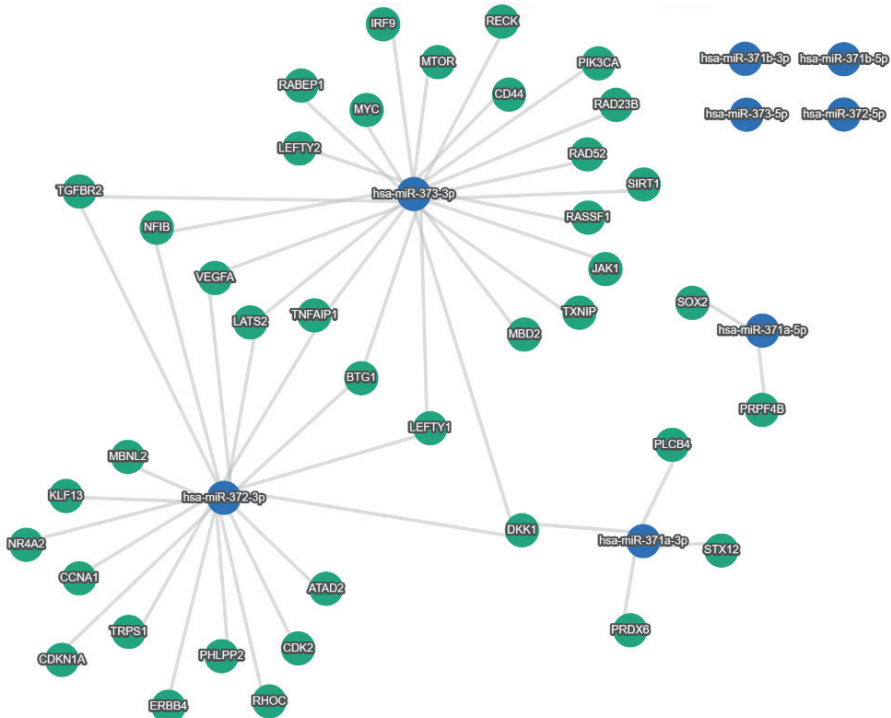
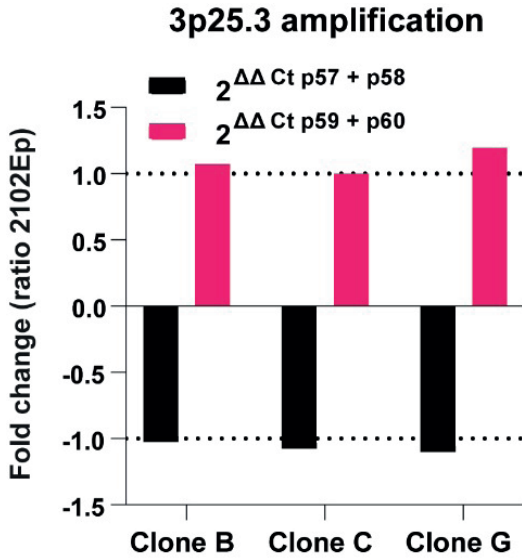


Figure S4: Cisplatin response of E371 clones and 2102Ep parental. A) Average S-curve of cisplatin response of E371 clones defined by relative viability of cells exposed to increasing concentrations of cisplatin. Graph represents the means of triplicate experiments. **B)** Absolute IC50 of E371 clones. Bars represent the means of triplicate experiments. Statistical analysis by one-way ANOVA. * $P \leq 0.05$; ** $P \leq 0.01$; *** $P \leq 0.001$.



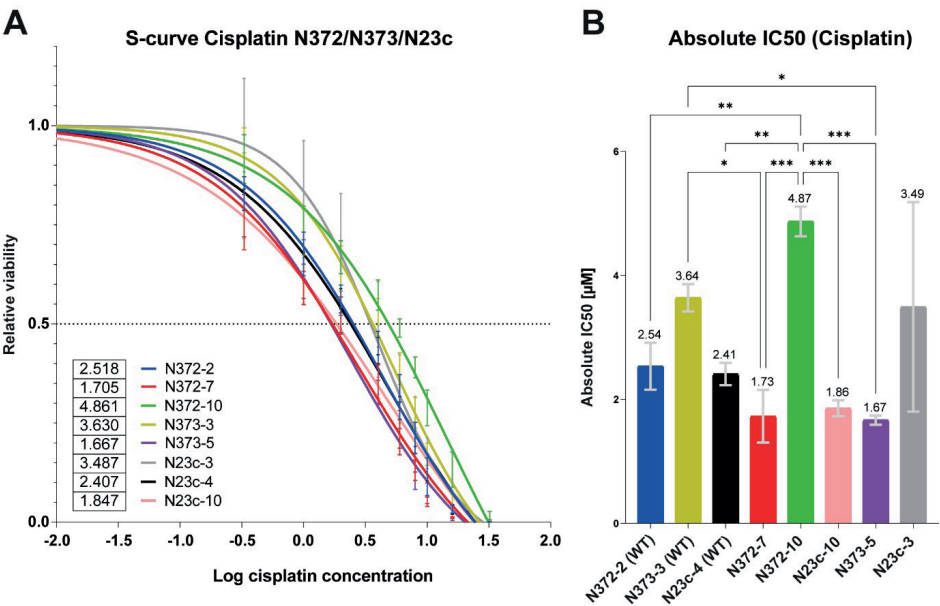


Figure S7: Cisplatin response of N372, N373, and N23c clones. **A)** Average S-curve of cisplatin response of N372, N373, and N23c clones defined by relative viability of cells exposed to increasing concentrations of cisplatin. Graph represents the means of triplicate experiments. **B)** Absolute IC50 of N372, N373, and N23c clones. Bars represent the means of triplicate experiments. Statistical analysis by one-way ANOVA. * $P \leq 0.05$; ** $P \leq 0.01$; *** $P \leq 0.001$.

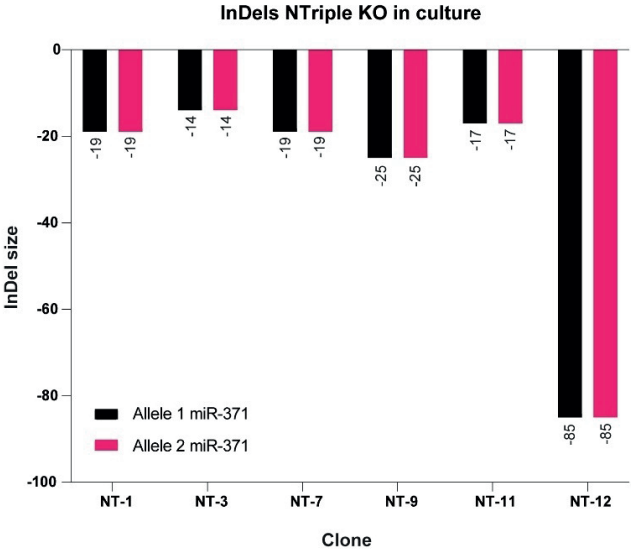


Figure S8: InDel of NT clones. InDel size of NCCIT triple KO (NT) clones as indicated by Sanger sequencing.

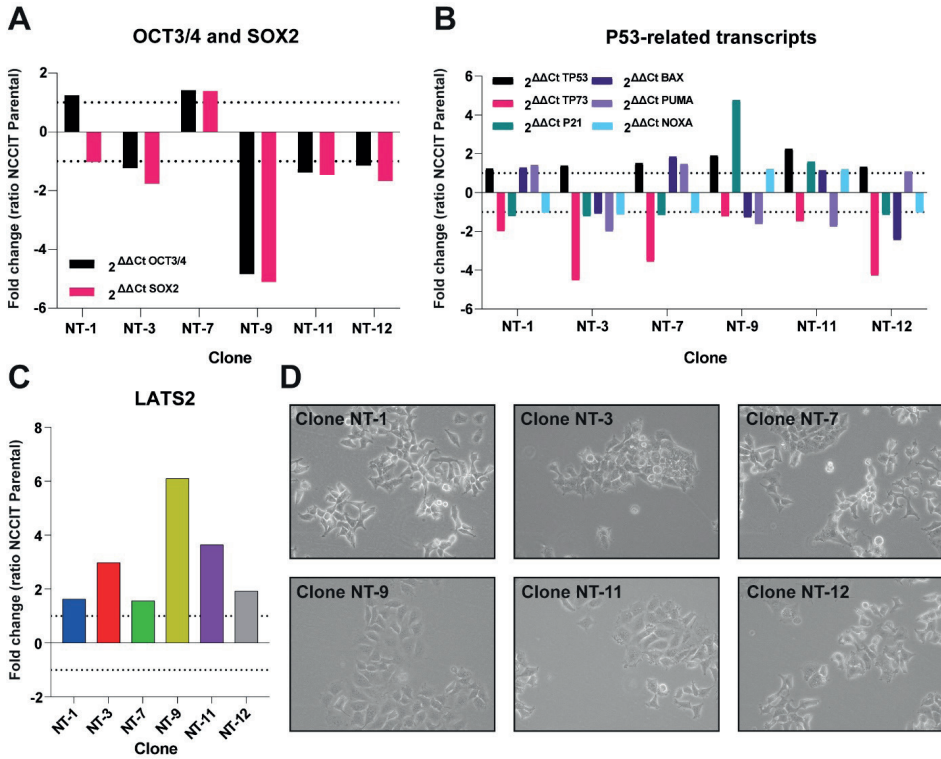


Figure S9: mRNA expression and morphology of NT clones. **A)** Fold change of OCT3/4 (POU5F1) and SOX2 levels in NT clones compared to NCCIT parental. **B)** Fold change of P53-related genes TP53, TP73, P21 (CDKN1A), BAX, PUMA (BBC3), and NOXA (PMAIP1). **C)** Fold change of LATS2 levels in NT clones compared to NCCIT parental. **D)** Morphology of NT clones. Magnification: 300x. **E)** Seeding density assay of NT clones (N=1) indicates no real differences in proliferation rate.

Chapter

7



Chapter 7

Analysis of a mouse germ cell tumor model establishes pluripotency-associated miRNAs (mouse miR-290-295/human miR-371-373) as conserved serum biomarkers for germ cell cancer detection

Amanda R. Loehr¹, **Dennis M. Timmerman**², Michelle Liu¹, Ad J.M. Gillis², Melia Matthews¹, Jordana C. Bloom³, Peter K. Nicholls^{3,‡}, David C. Page^{3,4,5}, Andrew D. Miller¹, Leendert H.J. Looijenga^{2,*}, and Robert S. Weiss^{1,*}

¹ Department of Biomedical Sciences, Cornell University College of Veterinary Medicine, Ithaca, NY

² Princess Máxima Center for Pediatric Oncology, Utrecht, Netherlands

³ Whitehead Institute, Cambridge, MA

⁴ Howard Hughes Medical Institute, Whitehead Institute, Cambridge, MA

⁵ Department of Biology, Massachusetts Institute of Technology, Cambridge, MA

‡ current address: Faculty of Life Sciences, University of Bradford, Bradford, United Kingdom

* corresponding authors (l.looijenga@prinsesmaximacentrum.nl, rsw26@cornell.edu)

to be submitted

ABSTRACT

Malignant testicular germ cells tumors (TGCTs) are the most common solid cancer in young men. Current diagnostics for TGCTs include conventional serum protein markers, but these lack the sensitivity and specificity needed to serve as accurate markers of malignancy across all histologic TGCT subtypes. MicroRNAs (miRNAs) are small non-coding regulatory RNAs and can be informative as biomarkers of many different diseases. In humans, miRNAs of the miR-371-373 cluster are detectable in the serum of patients with malignant TGCTs and outperform existing serum protein markers for both initial diagnosis as well as disease monitoring. We previously developed a genetically engineered mouse model featuring malignant mixed TGCTs consisting of pluripotent embryonal carcinoma (EC) and differentiated teratoma. Like the corresponding human malignancies, these murine cancers originate during embryonic development and are highly sensitive to genotoxic chemotherapy. Here, we report that miRNAs in the mouse miR-290-295 cluster, homologs of the human miR-371-373 cluster, were detectable in the serum of mice with malignant TGCTs but not in serum from mice with benign teratomas or tumor-free control mice. miR-291-293 were expressed and secreted specifically by pluripotent EC cells, and expression was lost following differentiation induced by the drug thioridazine. Notably, miR-291-293 levels were significantly higher in the serum of pregnant dams carrying tumor-bearing fetuses compared to that of control dams. These findings reveal that expression of the miR-290-295 cluster in mice and the miR-371-373 cluster in humans is a conserved feature of malignant TGCTs, further validating the mouse model as representative of the human disease. These data also suggest that serum miR-371-373 assays may contribute to improved patient outcomes by detecting the presence of TGCTs in humans before clinical signs of the disease arise, possibly even prenatally.

INTRODUCTION

Malignant testicular germ cell tumors (TGCT) are the most common cancer diagnosed in adolescent and young adult men 15-39 years old in the US, and incidence has increased almost 40% in the last 50 years.¹ TGCT patients have a 5-year overall survival rate of 95% due to the sensitivity of TGCTs to cisplatin-based chemotherapy. The WHO classifies TGCTs based on their distinct germ cell developmental origins and histological compositions.² Type I TGCTs include teratomas and yolk sac tumors that occur in neonates and children, and Type III TGCTs are spermatocytic tumors that develop in older men. The most common TGCTs are the Type II TGCTs that arise after puberty and develop from germ cell neoplasia *in situ* (GCNIS), which are believed to originate from primordial germ cells (PGCs) that failed to differentiate during embryonic development.³ Of the Type II TGCTs, seminomas resemble embryonic germ cells, like the GCNIS lesions they develop from, while non-seminomas contain one or more other histological components including embryonal carcinoma (EC), yolk sac tumor, choriocarcinoma, and teratoma.² EC consists of malignant pluripotent cells that are capable of self-renewal and differentiation into embryonic and extra-embryonic lineages, thus giving rise to the diverse histogenesis observed in many non-seminomas.⁴⁻⁷

To inform TGCT diagnosis and prognosis, clinicians use a set of imaging techniques and serum protein markers to detect TGCTs and monitor their response to treatment.⁸ Since the 1970s, α -fetoprotein, β -human chorionic gonadotropin, and lactate dehydrogenase have been used as serum biomarkers of TGCTs.^{9,10} However, these traditional biomarkers lack sensitivity and specificity. Only 50% of seminomas and 75% of non-seminomas show elevated levels of any one of the three serum proteins, and they can be elevated due to other disease processes.¹¹ Thus, a better universal biomarker for TGCTs is needed to enable early detection, facilitate accurate diagnosis, and identify disease recurrence.

MicroRNAs (miRNAs) are small, noncoding RNAs that interact with target messenger RNAs (mRNAs) to regulate their stability and translation, and are vital for development and many other biological processes.¹² Over a decade ago, miRNAs from the miR-371-373 cluster were found to be specifically expressed in malignant TGCTs and not in benign teratomas.^{13,14} Since then, these miRNAs have been found to significantly outperform traditional serum biomarkers in sensitivity and specificity for TGCT detection, both in the context of initial diagnosis as well as follow up. A recent study including 616 TGCT patients and 258 controls found that serum miR-371a-3p levels were sufficient to distinguish TGCT patients from male controls with 90.1% sensitivity and 94.0% specificity.¹⁵ Serum miR-371a-3p levels have also been found to correlate with primary tumor size and clinical stage, and they can be used to evaluate response to treatment, with levels decreasing after chemotherapy and orchiectomy.^{15,16} miR-371a-3p is also a good marker for detecting disease relapse. In a cohort of 33 patients with localized disease who underwent

orchiectomy, all 10 patients who relapsed showed elevated miR-371a-3p levels at the time of recurrence, and these recurrences could be detected on average two months earlier using serum miR-371a-3p than with traditional clinical methods.¹⁷ miR-371a-3p expression is specific to malignant GCTs, as miR-371a-3p is undetectable in the serum of patients with testicular cancers of non-germ cell origin as it is in cancer-free controls.¹⁸ One limitation of the miR-371a-3p biomarker is that it is unable to detect pure teratomas, suggesting that it is expressed by undifferentiated cells within TGCTs but not following differentiation.¹⁵

The mouse miR-290-295 cluster is orthologous to the human miR-371-373 cluster, and the miRNAs in these clusters have conserved seed sequences.¹⁹ Additionally, miR-290-295 miRNAs are highly expressed in pluripotent mouse embryonic stem (ES) cells, just as miR-371-373 miRNAs are expressed in pluripotent human ES cells.^{20,21} In mouse ES cells, miR-290-295 have been implicated in pluripotency maintenance, proliferation, and suppression of apoptosis.^{22–24} They are the first miRNAs to be expressed *de novo* in the embryo—as early as the 2-cell stage—and are critical for embryonic development.^{25,26} The miR-290-295 miRNAs are also expressed by PGCs, the cells from which TGCTs originate, and are important for PGC migration during embryogenesis.^{26,27} Therefore, we hypothesized that miR-290-295 would serve as serum biomarkers for the presence of murine malignant GCTs as well.

The germ cell-specific *Pten* and *Kras* mutant (gPAK) mouse is the first genetically engineered mouse model of malignant TGCTs.⁴ These tumors resemble human mixed non-seminomas, containing EC that has tumor propagating and metastatic activity and also differentiates into teratoma components. gPAK tumors are similar to human TGCTs in that they arise from PGCs during embryonic development and are highly responsive to cisplatin-based chemotherapy.⁴ Here, we report that EC cells express and secrete miR-290-295, and serum miR-290-295 levels can be used to detect EC-containing murine TGCTs prior to birth. Additionally, we find that a differentiation-inducing experimental therapeutic, thioridazine (TR)²⁸, can eliminate EC from gPAK tumors and concomitantly reduces miR-290-295 levels. These findings further validate the gPAK mouse as an accurate model of human TGCTs and highlight opportunities for pursuing the use of miR-371-373/miR-290-295 in the early detection of subclinical disease, elucidating the biological roles of these miRNAs in TGCT pathogenesis, and for testing new therapeutics in an animal model in which tumor progression can be easily monitored through serum miRNA levels.

RESULTS

Cultured murine EC cells express and secrete miR-291-293 and lose expression upon differentiation.

We previously characterized three EC cell lines that were derived from *Pten*^{-/-} malignant murine TGCTs with (EC14) or without (EC3, EC11) a *Kras*^{G12D} activating mutation, and reported that these EC cultures can be differentiated with the drugs thioridazine (TR, giving rise to TR3, TR11, and TR14 cell lines) and salinomycin (SAL, giving rise to SAL11 and SAL14 cell lines).²⁸ TR or SAL treatment induces changes in EC cell morphology from an ES cell-like to a fibroblast-like state, accompanied by a loss of pluripotency marker expression and a loss of tumorigenic potential.²⁸ To determine if miR-290-295 cluster miRNAs were expressed by mouse EC cells, we analyzed the expression of miRNAs from this family in the EC cell lines and differentiated counterparts. In particular, levels of miR-291a-3p (homologous to human miR-372-3p and 373-3p) and miR-292-3p and miR-293 (homologous to different isoforms of human miR-371a-3p) were measured as representative miRNAs in this cluster and collectively referred to as miR-291-293 hereafter (Supplemental Figure 1).¹⁹ miR-291-293 miRNAs were highly expressed by all three EC cell lines, and this expression was significantly reduced in the TR and SAL-differentiated derivatives (Figure 1A). As a precursor to determining if miR-291-293 were present in the serum of mice with TGCTs, we next tested if these miRNAs were secreted by cultured EC cells. miR-291-293 were detected in the conditioned media of all three EC cell lines, while very low to no expression was detected in conditioned media from the differentiated cells (Figure 1B). These findings suggest that miR-291-293 expression and secretion is specific to the pluripotent state of EC cells and significantly diminished upon differentiation.

Predicted miR-290-295 targets are enriched in thioridazine-differentiated cells.

To understand if miR-290-295 have a functional role in regulating gene expression in EC cells, we completed RNA sequencing (RNA-Seq) of all three EC cell lines and their TR-differentiated derivatives (part of this RNA-Seq data set was previously published²⁸) and performed Gene Set Enrichment Analysis (GSEA)²⁹ for predicted targets of mouse miRNAs. If miR-290-295 were negatively regulating their target genes, as miRNAs are canonically known to do, then the amount of RNA for their predicted target genes was expected to be enriched in TR-differentiated cells, since these cells lose miR-291-293 expression. The miRDB gene sets deposited in the Molecular Signatures Database consist of a gene set for each mouse miRNA catalogued in miRDB v6.0 containing high-confidence computationally predicted target genes as determined by the MirTarget algorithm.^{30,31} GSEA of the 1,769 miRDB gene sets revealed that the gene set consisting

of predicted targets of miR-291a-3p and miR-294-3p (MIR_291A_3P_MIR_294_3P) was among the most highly enriched gene sets in TR-differentiated cells compared to EC cells for all three cell lines (17th most highly enriched in TR3 cells, 14th in TR11 cells, 26th in TR14 cells) (Figure 2A). In fact, gene sets of predicted targets of many miR-290-295 miRNAs were significantly enriched in all three TR-differentiated cell lines compared to their parental EC cell lines (Figure 2B).

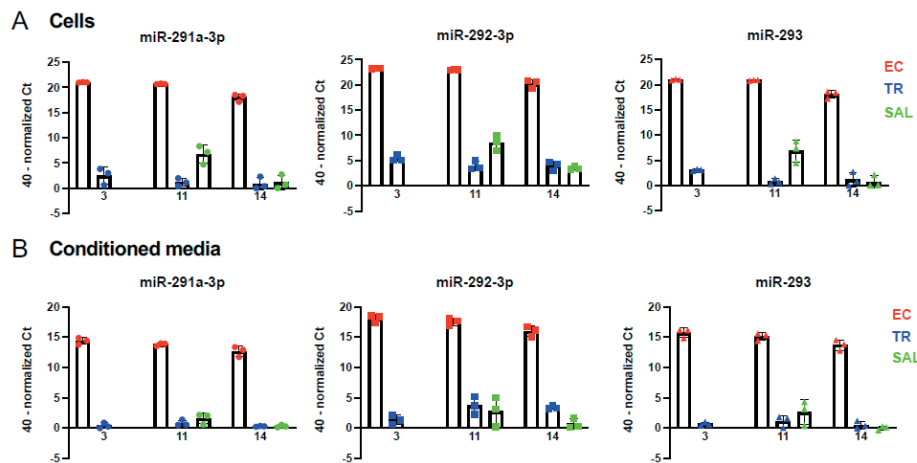


Figure 1. miR-291-293 expression in three independent EC cell lines (3, 11, and 14) is lost following thioridazine (TR)- or salinomycin (SAL)-mediated differentiation. miR-291-293 expression in (A) cells or (B) conditioned media. $n = 3$ independent replicates per group. Data are mean \pm SD. Differences are significant for all comparisons between EC and TR or SAL groups ($p < 0.001$, multiple unpaired t-tests with Holm-Šidák correction for multiple comparisons).

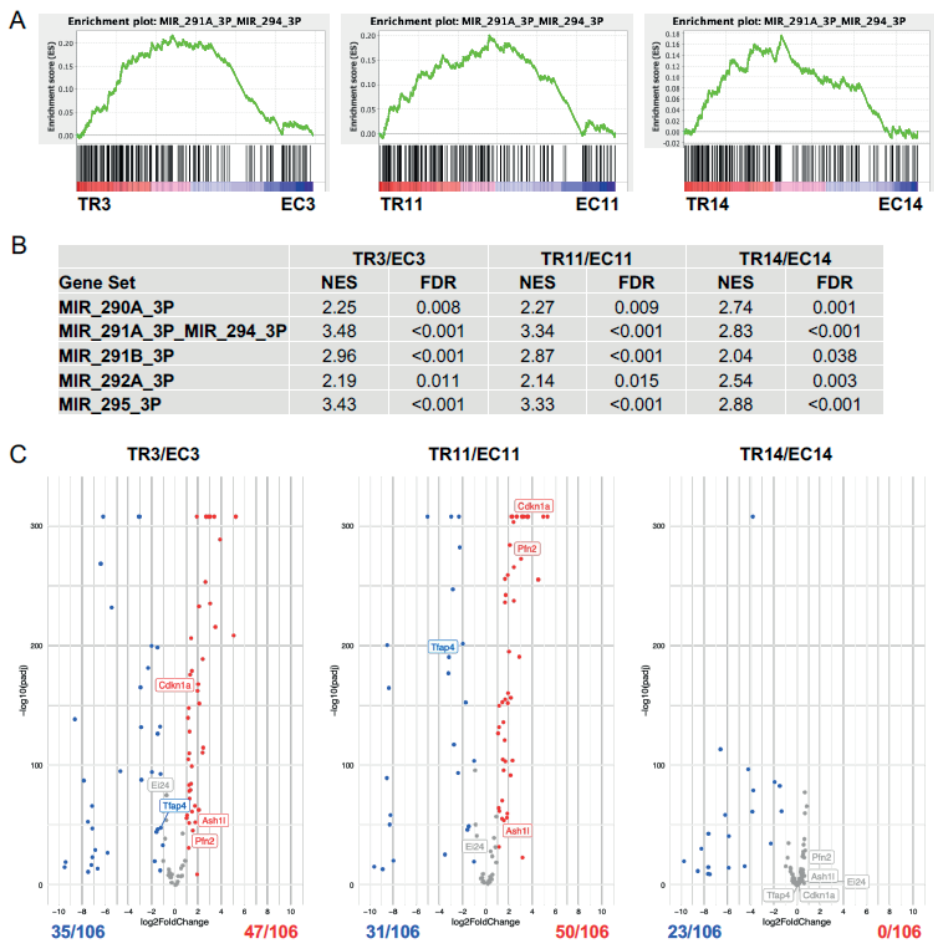


Figure 2. miR-290-295 targets are upregulated in TR-differentiated cells. (A) GSEA enrichment plots for the MIR_291A_3P_MIR_294_3P gene set across pre-ranked gene lists comparing gene expression in TR-differentiated cells to parental EC cell lines. (B) Significantly enriched (FDR < 0.05) mirDB gene sets associated with the miR-290-295 cluster in TR-differentiated cells compared to parental EC cell lines with normalized enrichment scores (NES) as determined by GSEA. (C) Volcano plots showing differential gene expression of the 106 candidate target genes of the miR-290-295 cluster from Schaefer et al.⁴⁰ Gene names of experimentally determined direct targets of the miR-290-295 cluster are labelled. Genes that were significantly upregulated in TR-differentiated cells are in red, genes that were significantly downregulated in TR-differentiated cells are in blue, and genes that were not significantly differentially expressed are in grey. Significance is defined as a p adjusted value (padj) < 0.05.

A literature search was also undertaken to identify experimentally proven direct targets of the miR-290-295 family. In total, 26 target genes were identified from 16 publications, which were focused primarily on ES cells (Supplemental Table 1).^{22–24,32–44} Of these 26 genes, 13 were significantly upregulated and five were significantly downregulated in TR3 cells compared to EC3 cells (Supplemental Figure 2). Similarly,

14 were significantly upregulated and five were significantly downregulated in TR11 cells compared to EC11 cells. This suggests that miR-290-295 downregulate the mRNA levels of their target genes in EC cells, because expression of many target genes was increased following loss of miR-290-295 expression upon differentiation. The decreased RNA levels for some target genes following thioridazine-induced differentiation likely reflects the predominant influence of regulatory mechanisms other than loss of miR-290-295 expression. The limited changes in gene expression observed in EC14 cells after differentiation, with none of the known miR-290-295 target genes being significantly upregulated in TR14 cells, and only two being significantly downregulated, is discussed further below. Of the genes that were significantly upregulated in TR3 and TR11 cells compared to their parental EC cell line, *Cdkn1a*, *Rbl2*, and *Lats2* are all negative regulators of the G₁/S transition that function to slow cell cycle progression.²³

Schaefer *et al.*, recently identified 360 genes predicted to be targets of the mouse miR-290-295 cluster.⁴⁰ The target genes were identified through an integrative analysis of multiple datasets including computationally-predicted miR-290-295 targets in TargetScan, AGO2-miRNA binding and loading data from ES cells, and genes upregulated in global miRNA KO ES cells. 106 of these 360 candidate target genes were found to be upregulated following miR-290-295 KO in ES cells.⁴⁰ Although miRNAs can also act by inhibiting the translation of their mRNA targets,⁴⁵ this target gene set focuses on those mRNAs degraded by the miR-290-295 cluster. We queried the 106 gene targets of miR-290-295 in our RNA-seq data from EC and TR-differentiated cells and found that 47 of them were significantly upregulated and 35 were significantly downregulated in TR3 cells compared to EC3 cells (Figure 2C). Additionally, 50 genes were significantly upregulated and 31 were significantly downregulated in TR11 cells compared to EC11 cells. Together, these data indicate that many miR-290-295 targets are upregulated following EC cell differentiation, although several targets were significantly downregulated, likely because of large-scale reprogramming of gene expression following differentiation that is in part independent of miR-290-295. None of the 106 target genes were significantly upregulated and 23 were significantly downregulated in TR14 cells compared to EC14 cells. This may reflect the fact that, unlike TR3 and TR11, which only harbor a *Pten* inactivating mutation, TR14 cells, which have both *Pten* inactivating and *Kras* activating mutations, remain more highly proliferative and retain some transformed features following differentiation,²⁸ with miR-290-295 target genes perhaps correspondingly less affected than in TR3 and TR11 cells. A greater extent of spontaneous differentiation in EC14 cultures as compared to EC3 or EC11 cultures also may obscure identification of differentially expressed genes following TR treatment of EC14 cells.

Serum miR-291-293 detection is specific to mice with EC-containing tumors.

We previously demonstrated that EC cell tumorigenicity is significantly reduced or fully abrogated after TR or SAL-mediated differentiation.²⁸ Upon subcutaneous injection into immunocompromised host mice, all three EC cell lines formed tumors with EC and teratoma components. By contrast, the differentiated derivatives of EC3 and EC11 did not form tumors, and the differentiated derivatives of EC14 formed small sarcomas that grew much slower than the tumors from the parental EC14 cell line.²⁸ For the present study, we tested whether miR-291-293 could be detected in the serum of mice bearing EC cell-derived tumors. Serum miR-291-293 levels were high in mice that developed tumors from the EC cell lines, but low to undetectable in mice that received differentiated cells (except for two mice that received TR11 cells and had detectable serum miR-291-293 levels despite having no identifiable tumor) (Figure 3A). One mouse that received EC3 cells and had very low levels of serum miR-291-293 formed only one small tumor in which no OCT4 staining was detected, indicating that the tumor may have lacked an EC component. Serum miR-291-293 levels were also low or undetectable in *Dazl*^{-/-} mice with testicular teratomas, as well as in wild-type 129S6 male mice (Figure 3A). These data suggest that it is EC within murine TGCTs that expresses and secretes miR-291-293.

miR-291-293 were also detectable in RNA extracted from EC-cell derived tumor tissue as well as normal adult testis tissue (Figure 3B). Expression in normal testis tissue was expected, as miR-290-295 and miR-371a-3p were previously shown to be expressed in mouse spermatogonia and normal human testis tissue, respectively.^{27,46} To confirm that miR-291-293 expression was specific to germ cells and EC cells, miR-291-293 levels were also measured in *Dazl*^{-/-} testicular teratomas, MMTV-*PyMT* mammary adenocarcinomas, and normal adult mouse spleen. All three of these tissue types had significantly lower levels of miR-291-293 compared to EC-derived tumors (Figure 3B). H&E staining and OCT4 immunohistochemistry confirmed that, as previously reported⁴⁷, the testicular tumors in adult *Dazl*^{-/-} mice were pure teratomas containing tissues derived from all three embryonic germ layers, and unlike gPAK malignant teratocarcinomas, contained no detectable OCT4-positive EC (n = 5) (Figure 3C). These results suggest that miR-291-293 detection is specific to the presence of EC in the mixed TGCTs of gPAK mice. Interestingly, despite comparable levels of miR-291-293 in normal adult testis tissue and EC-containing tumors, the miRNAs were not detected in the serum of wild-type male mice (Figure 3A and B), observations consistent with previous findings in humans⁴⁶. These results suggest that EC, but not adult germ cells, can secrete detectable levels of the pluripotency-associated miRNAs into circulation.

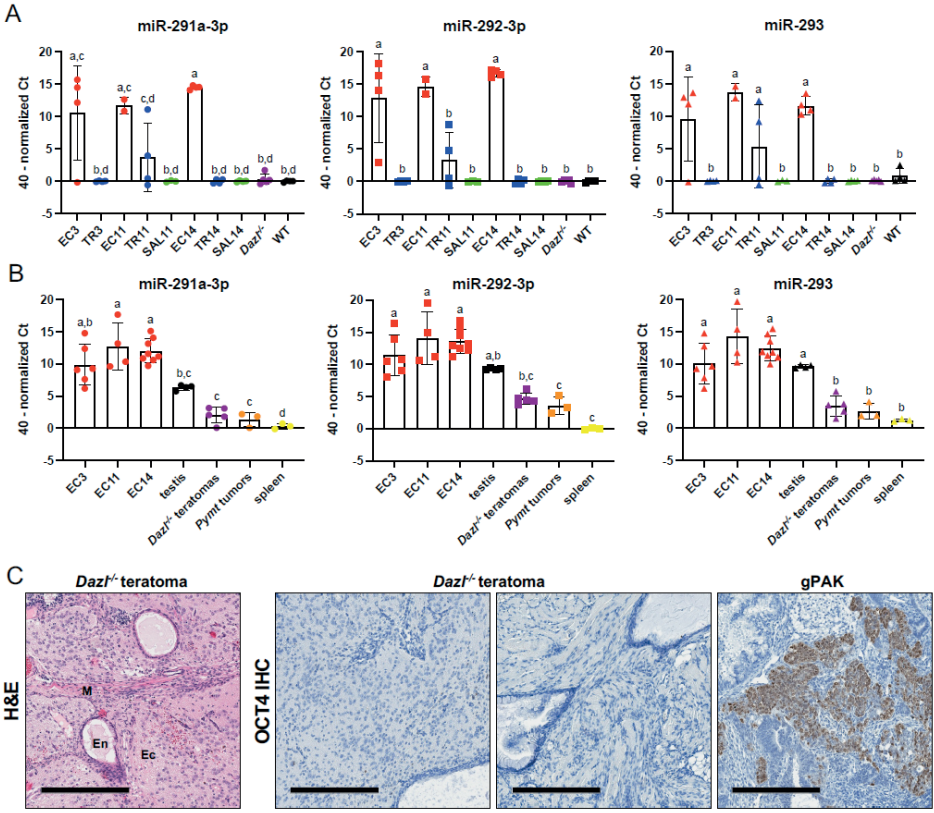


Figure 3. miR-291-293 expression is specific to EC-containing tumors. (A) miR-291-293 expression in serum for mice 2-3 weeks after receiving a subcutaneous injection of EC cells, TR- or SAL-differentiated cells, *Dazl*^{-/-} mice with testicular teratomas, or wild-type 129S6 adult male mice. (B) miR-291-293 expression in EC-derived tumors, normal adult testis from 129S6 mice, teratomas from *Dazl*^{-/-} mice, mammary adenocarcinomas from *Pymt* mice, or spleens from wild-type 129S6 mice. Data represented as mean \pm SD. Significant differences exist between groups that do not share a letter ($p < 0.05$, ordinary one-way ANOVA and Tukey's multiple comparisons test). (C) Representative image of H&E-stained *Dazl*^{-/-} testicular teratomas with tissues derived from endoderm (En), mesoderm (M), and ectoderm (Ec) indicated and representative images of OCT4-IHC stained *Dazl*^{-/-} testicular teratomas ($n = 5$) and a gPAK tumor (positive control). Scale bar = 300 μ m.

Thioridazine treatment eliminates EC cells from gPAK tumors, reducing serum miR-291-293 levels.

We next sought to determine if serum miR-291-293 levels were associated with the presence of EC cells in spontaneously occurring TGCTs in the gPAK mouse model and if expression would be lost following therapy-induced EC ablation *in vivo*. gPAK mice were treated with TR or vehicle control once every three days for three weeks starting at 21 days of age, when testicular tumors often can be first detected by palpation in this model.⁴ We previously found that TR treatment significantly extends the survival of mice

with human EC cell xenografts, and in a transformed induced pluripotent stem (iPS) cell allograft model, TR treatment significantly reduces the percentage of OCT4-positive EC cells within tumors.²⁸ Here, TR extended the survival of gPAK mice, although the effect was not statistically significant (Figure 4A). Of note, two of eight TR-treated mice reached the pre-defined endpoint of 70 days, whereas only one of the nine control mice lived past 42 days and none lived beyond 61 days. To determine EC cell abundance within tumors from control and TR-treated mice, we performed OCT4 immunohistochemistry and quantified the percentage of tumor area that was OCT4-positive. Except for one TR-treated mouse that had two tumors with OCT4-positive cells, tumors from TR-treated mice were depleted of OCT4-positive cells, whereas five of nine control tumors contained OCT4-positive cells (Figure 4B&C).

Knowing that gPAK tumors from TR-treated mice were in most cases depleted of EC, we next assessed miR-291-293 levels in the serum of TR-treated and control mice. Serum miR-291-293 levels were higher in control mice than in TR-treated mice, although the effect was not significant due to the one outlier mouse in the treatment group (Figure 4D). In fact, only the five untreated mice with tumors containing OCT4-positive cells had high levels of miR-291-293 in their serum. There was no significant difference in the levels of miR-291-293 in the tumor tissue from control and TR-treated mice (Figure 4E). These data suggest that elevated serum miR-291-293 levels, but not tumor miR-291-293 levels, indicate the presence of EC within a tumor. Furthermore, plotting the percent OCT4-positive area of a mouse's tumor(s) against the serum miR-291-293 levels from that mouse revealed that miR-291-293 levels were above or below a theoretical threshold based on the presence or absence of EC within a tumor, although they do not perfectly correlate with the abundance of EC within a tumor (Figure 4F). Because there is more variation in tumor miR-291-293 levels, tumors with and without OCT4-positive cells cannot easily be distinguished based on tumor miR-291-293 levels alone (Figure 4G). These data demonstrate that serum miR-291-293 levels can be used to determine whether a mouse carries a tumor that contains pluripotent, malignant cells.

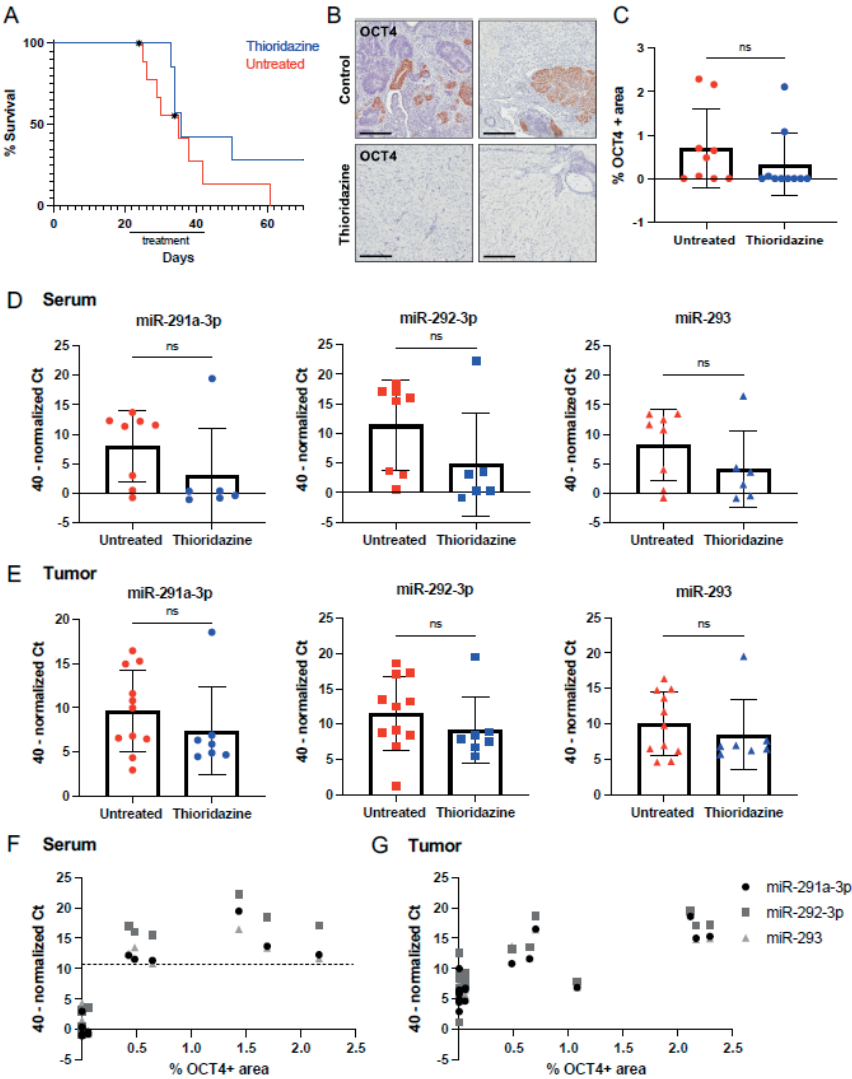


Figure 4. TR treatment reduces OCT4-positive EC cells in gPAK tumors, resulting in decreased serum miR-291-293 levels. (A) gPAK mice were treated with TR or vehicle control once every 3 days for 3 weeks starting at 21 days of age. Kaplan-Meier survival curve depicts the percentage of surviving control (n=9) and TR-treated mice (n=8) mice over time. One control mouse and one TR-treated mouse died during the study for reasons unrelated to the endpoint criteria and were therefore censored (as indicated by an asterisk). $p = 0.2088$ (Log-rank test). (B) Representative images of OCT4 IHC-stained tumors from control and TR treated mice. Scale bar = 200 μ m. (C) Percentage of tumor cross-section (area) that was OCT4-positive as determined by IHC. One section per tumor was stained and quantified. (D) miR-291-293 expression in serum of control or TR-treated gPAK mice. (E) miR-291-293 expression in tumors of control or TR-treated gPAK mice. (F & G) Percent OCT4-positive area (data in C) versus miR-291-293 expression in (F) serum (data in D) or (G) tumor (data in E). In F, the percent OCT4-positive area per mouse for mice with two tumors was determined by calculating a weighted average of the percent OCT4-positive area per tumor section proportional to the whole tumor section area. Data represented as mean \pm SD. ns = not significant (unpaired two-tailed t-test).

Serum miR-291-293 levels can predict the presence of subclinical gPAK TGCTs.

One of the most useful but unsubstantiated applications of the miR-371-373 biomarker is in screening seemingly healthy at-risk young men for the early detection of subclinical TGCTs. We therefore tested if serum miR-291-293 levels could be used to predict the presence of TGCTs in mice prior to clinical signs of the disease. Because TGCTs initiate around embryonic day 12.5 (E12.5) in the gPAK mouse model, we hypothesized that miR-291-293 could be detected in the serum of pregnant dams carrying a fetus with a TGCT. Timed matings were set up between breeders that would generate litters with both gPAK and control pups. Noon of the day on which a copulatory plug was found was defined as E0.5. Blood was collected from the dam at E18.5 and from all pups at 14 to 16-days of age (P14-16), before tumors were detectable by palpation. Mice were monitored for the development of testicular tumors and a terminal blood collection was performed at a humane endpoint or after six weeks of age, which is well beyond initial TGCT detection in gPAK mice (Figure 5A).⁴ Based on the established timing of TGCT development in gPAK mice, mice with testicular tumors at collection were assumed to have had tumors at P14-16 and E18.5.

Analysis of serum from pregnant dams carrying a fetus that developed a TGCT showed significantly higher miR-291a-3p and miR-292-3p levels than that from pregnant dams that did not carry a fetus with a tumor (Figure 5B). Subsequent analysis of serum from individual pups at P14-16 revealed that serum miR-291-293 levels were significantly greater in pups that had a tumor (although at this time the tumor was not detectable by palpation) compared to control male pups without tumors (Figure 5C). Serum miRNA levels in tumor-bearing mice were generally lower at P14-16 than at humane endpoint when the tumor was clinically apparent; nevertheless, the trend shows that serum miR-291-293 levels at P14-16 correlated with serum miR-291-293 levels at endpoint (Figure 5D). Lower miR-291-293 expression at P14-16 may be due in part to much lower serum input volume, since only a small volume of blood could be collected from mice at this age. It is also worth noting that small sample volumes at this timepoint also were associated with lower assay specificity, as a few neonates without tumors showed similar miR-291-293 levels as the tumor-bearing littermates (Figure 5C). Together, these data demonstrate that serum miR-291-293 levels can be used to detect subclinical TGCTs, as early as during fetal development.

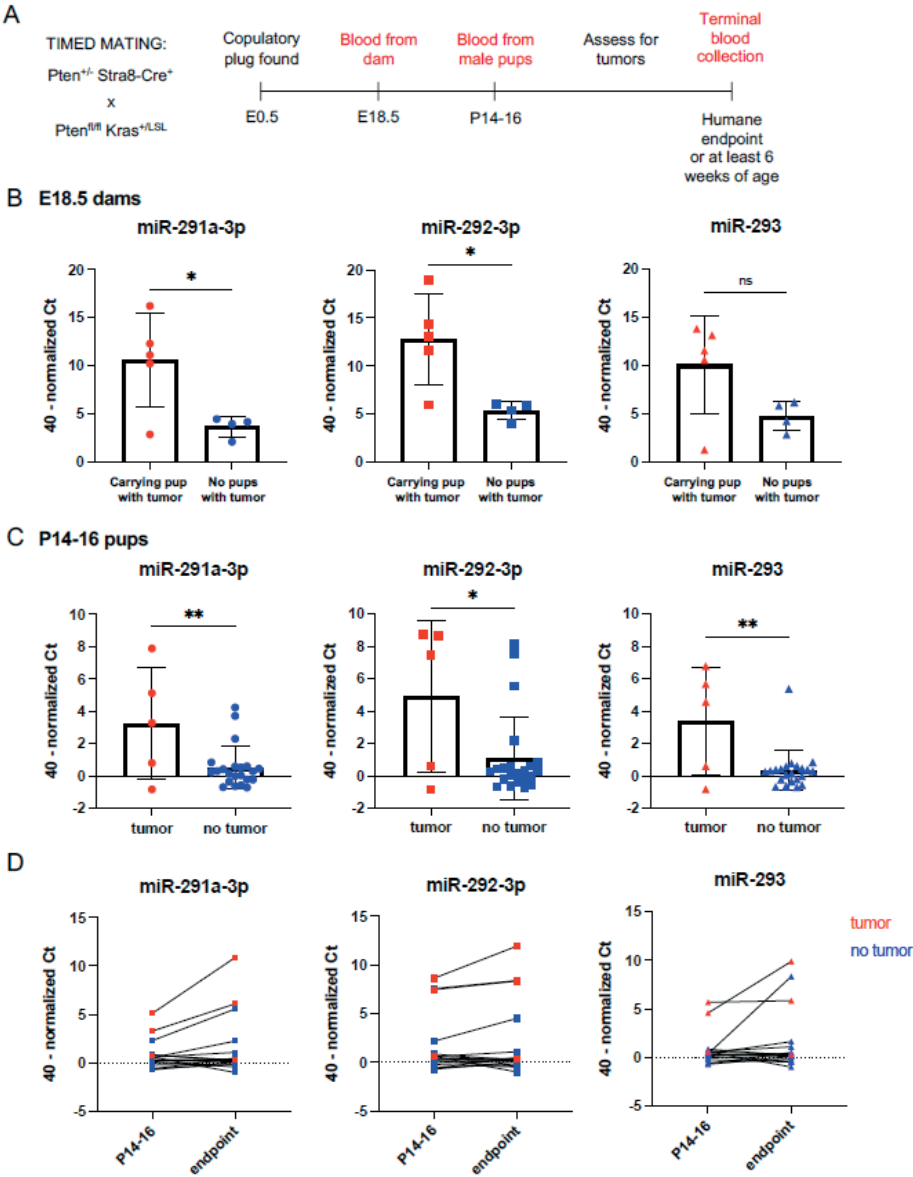


Figure 5. miR-291-293 expression predicts the presence of subclinical teratocarcinomas. (A) Schematic of experimental timeline for samples collected. (B) miR-291-293 expression in serum of pregnant dams (E18.5) carrying or not carrying a pup with a testicular tumor. (C) miR-291-293 expression in serum of 14- to 16-day old male pups that did or did not have a tumor. (D) miR-291-293 expression in serum of 14- to 16-day old mice and at endpoint (samples from the same mouse are connected by a line). ns = not significant, * $p < 0.05$, ** $p < 0.01$ (unpaired two-tailed t-test).

DISCUSSION

Just as miR-371-373 are accurate biomarkers for malignant TGCTs in humans, we have found that miR-291-293 can serve as biomarkers of malignant TGCTs in mice, providing further evidence that the gPAK TGCT model closely resembles the human disease. Here, we have shown that both *in vitro* and *in vivo*, EC cells express and secrete miRNAs from the miR-290-295 cluster. Cultured EC cells derived from murine TGCTs express and secrete miR-291-293, and this expression is lost following differentiation by TR or SAL. This suggests that miR-290-295 expression is specific to the pluripotent state. It has previously been shown that the miR-290-295 cluster is a direct transcriptional target of OCT4, SOX2, and NANOG-- all key regulators of pluripotency.⁴⁸ Additionally, miR-290-295 expression enhances the efficiency of somatic cell reprogramming to iPS cells by OCT4, SOX2, and KLF4, but does not improve reprogramming efficiency in the presence of C-MYC because these miRNAs are downstream effectors of C-MYC.⁴⁹ Therefore, pluripotency and miR-290-295 expression are intimately linked.

Not only are miR-290-295 expressed under the control of pluripotency-associated transcription factors, but they promote pluripotency themselves by regulating the expression of genes involved in multiple biological processes. Our results implicate miR-290-295 in regulating gene expression in cultured EC cells, as predicted targets of this miRNA cluster were upregulated in differentiated cells in which miR-290-295 expression is lost. In ES cells, members of the miR-290-295 cluster directly target and suppress multiple negative regulators of the G1/S transition, including *Cdkn1a* (encoding p21), *Rbl2*, and *Lats2*, thereby promoting proliferation.²³ *Cdkn1a* and *Lats2* were significantly upregulated in TR3 and TR11 cells as compared to their parental EC cell lines, and *Rbl2* was significantly upregulated in TR11 cells. This suggests that these genes are being suppressed in EC cells to support progression through the G1/S transition and cell proliferation. After TR-mediated differentiation and loss of miR-290-295, expression of these cell cycle regulators increased. Consistent with this, TR-differentiated cells show moderately reduced proliferation compared to their respective parental EC cell line.²⁸ The EC14 line is partially resistant to TR-mediated differentiation, with TR having less pronounced effects on proliferation, and accordingly the impacts of TR on miR-290-295 target gene expression were limited in this cell line.

miR-291-293 also were detected in the serum of mice bearing tumors containing EC cells. Allografts derived from cultured EC cells expressed miR-291-293 and secreted these miRNAs into the serum. Mice that received injections of differentiated cells, as well as wild-type 129S6 adult male mice, did not have elevated serum levels of miR-291-293. Interestingly, although EC-derived tumor tissue did have significantly higher expression of some of the miRNAs compared to normal testis tissue, the difference in expression between these tissue types was much smaller than the difference in miR-291-293 levels in the serum of the same mice. It has been previously shown that spermatogonia

express miR-290-295, accounting for the expression in adult testis.²⁷ It is possible that the spermatogonia that express miR-291-293 do not secrete it into circulation. Alternatively, the miRNAs could be secreted by spermatogonia but rapidly degraded while miRNAs secreted by EC cells into the serum are protected by extracellular vesicles (EVs). It is known that circulating miRNAs are often protected from endogenous RNases by association with protein complexes or encapsulation in EVs.⁵⁰ A previous study showed that the human seminoma-derived cell line, TCam-2, secretes exosomes, which are small EVs, that contain miR-371a-3p.⁵¹ The functional roles for secreted miRNAs, including miR-371-373, in intercellular communication among TGCT cells or between TGCT cells and their microenvironment are currently unknown.

Consistent with previous findings that pure teratomas in humans do not express miR-371a-3p,¹⁵ we found that miR-291-293 expression was minimal in testicular teratoma tissue from *Dazl*^{-/-} mice and undetectable in serum from teratoma-bearing mice. This suggests that miR-371-373 and miR-291-293 expression in humans and mice with TGCTs is specific to the malignant cells within the neoplasms. We also found that mammary adenocarcinomas from *MMTV-PyMT* mice did not express miR-291-293, confirming that expression of these miRNAs is not a common feature of malignant somatic cells.

Serum-based detection of EC cell markers in gPAK TGCTs could be an important tool in testing experimental therapeutics that aim to target EC cells, as these are the tumor-propagating cancer stem cells within these tumors. We previously showed that TR, an inducer of cell differentiation, significantly extended mouse survival in a human EC xenograft model.²⁸ Here, we show that TR modestly increased the survival of tumor-bearing gPAK mice, and except for one non-responder, eliminated the OCT4-positive EC cells within tumors, suggesting that the increase in survival is due to the loss of the highly malignant EC compartment. In the gPAK model, mice develop spontaneous testicular tumors that are palpable around 21 days of age on average; however there is much variation in the age at which tumors are detectable.⁴ Because the size of tumors cannot be readily measured without advanced imaging tools when they are within the abdominal cavity, we started TR administration at 21 days of age in all treated mice, a time point at which the malignancy can be quite advanced. The variation in tumor size and disease progression at the time of treatment may explain why we did not detect a significant increase in survival with TR treatment in this study.

Paralleling EC loss following TR treatment, serum miR-291-293 levels were significantly reduced in TR-treated mice except for one non-responsive outlier. miR-291-293 expression was not significantly reduced in tumor tissue from TR-treated mice compared to that from control mice. This suggests that only tumors with an EC component secrete miR-291-293 into the serum at high levels. It is possible that low levels of miR-291-293 expression in tumor tissue from both control and TR-treated mice is from normal germ cells; however, the gPAK TGCTs usually lack all normal testicular

architecture. Correlating the OCT4-positive area of a tumor with the miR-291-293 levels in the serum of the mouse bearing that tumor or in the tumor tissue itself, revealed that there is a clear diagnostic threshold of serum miR-291-293 abundance, above which it is predictive of the presence of an EC-containing tumor.

One of the most exciting potential applications of the miR-371a-3p biomarker in humans is as a screening tool to identify individuals with GCNIS lesions or localized TGCTs. If TGCTs are detected at an early enough stage, individuals can undergo surgery and active surveillance without the need for adjuvant chemotherapy or radiation², highlighting the value of screening adolescent and young adult men in high-risk groups for GCNIS or otherwise undetectable TGCT lesions using the serum miR-371a-3p biomarker. However, in one study, miR-371a-3p levels were detectably increased in only 52% of patients with GCNIS lesions.⁵² Here, we found that miR-291-293 expression significantly increased in P14-16 mice with TGCTs that were not yet clinically detectable (Figure 5C). However, a larger sample size is needed to determine the sensitivity of this assay in detecting subclinical disease. Additionally, possibly due to the very small sample volume that can be collected from mice at this young age, miR-291-293 levels appeared to be increased in a few mice that did not have a tumor, reflecting potential specificity limitations of the assay in this specific context. It is unknown whether gPAK TGCTs have a GCNIS-like state of dormancy, so the subclinical detection of gPAK TGCTs may not accurately reflect detection of human GCNIS lesions, but rather early malignant TGCTs. It is possible that by using this mouse model, we could also discover ways to increase sensitivity in detecting GCNIS lesions. For example, if miR-291-293 are shed by EC cells in EVs, EVs could be isolated from human serum to enrich for miR-371a-3p. Improving the sensitivity of this assay may also allow for earlier detection of relapsing disease after treatment.

Since TGCTs initiate during embryogenesis in the gPAK mouse model, as they do in humans, we sought to determine if miR-291-293 could be detected in the serum of pregnant dams carrying a fetus that has initiated TGCT development. Indeed, maternal serum had significantly higher levels of miR-291a-3p and miR-292-3p when carrying a fetus with a TGCT compared to pregnant dams with no tumor-bearing pups. In only one out of five serum samples from dams carrying tumor-bearing pups did the assay fail to detect increased levels of these miRNAs. Additionally, none of the pregnant dams that were not carrying a tumor-bearing mouse had elevated levels of miR-291-293 (no false positives), which suggests that screening pregnant dams has even better specificity than screening P14-16 mice. It is possible that these very early TGCT lesions at E18.5 are more undifferentiated than they are at P14-16, and therefore express miR-291-293 at greater levels. Therefore, screening pregnant women whose sons would be at high risk for developing a TGCT (for example, due to a family history of TGCTs)⁵³, may be more successful than the attempts made to screen men for GCNIS. This approach also might be informative for non-testicular malignant GCT diagnosed at early age as well.⁵⁴ One

caveat is that miR-371-373 are thought to be expressed by the placenta, as they are expressed by some trophoblast cell lines.⁵⁵ This may obscure the miR-371-373 expression from early TGCTs developing in utero, but it is probable that TGCT expression of these miRNAs would far exceed the basal expression by the placenta, still making the assay diagnostically useful.

Together, these results further validate the gPAK mouse model as being representative of human TGCTs, highlighting its translational potential. Like malignant TGCTs in humans, gPAK TGCTs arise during embryonic development, express pluripotency markers, are sensitive to chemotherapy, and express mouse homologs of human miR-371-373. The finding that miR-291-293 can be used as serum biomarkers of malignant TGCTs in mice may facilitate *in vivo* drug screening to discover new therapies for TGCT treatment, particularly those aimed at targeting EC. Additionally, this mouse model can be utilized to better understand how miR-290-295 and miR-371-373 may contribute to TGCT pathogenesis. Finally, this model demonstrates the promise for future studies aimed at refining the miR-371-373 assay into a screening tool for malignant TGCT early detection.

METHODS

Cell culture

Murine EC cell lines were cultured and differentiated as previously described.²⁸ For miRNA detection, cells at similar passage were plated, media was changed the following day, and 24 hours later the conditioned media was collected and centrifuged at 1500 rpm for 5 minutes to remove any cellular debris. The cells were pelleted and both the cells and conditioned media were stored at -80 °C prior to miRNA expression analysis.

RNA sequencing and data analysis

RNA sequencing of EC3 and TR3 cells (*Pten*^{-/-} *Kras*^{+/+} *Stra8-Cre*^{Tg} *OCT4-gfp*^{Tg}) was performed as previously described.²⁸ RNA sequencing of EC11 and TR11 (*Pten*^{-/-} *Kras*^{+/+} *Stra8-Cre*^{Tg}) and EC14 and TR14 cells (*Pten*^{-/-} *Kras*^{G12D} *Stra8-Cre*^{Tg} *OCT4-gfp*^{Tg}) was performed in a previous study.²⁸ Raw, un-normalized counts were filtered for expressed genes, defined by a minimum count value of 100 in at least one group. Standard differential analysis was done on the filtered genes using DESeq2 (v1.30.1)⁵⁶ in R (v4.0.2) with R studio. Results for each cell line were extracted by comparing the EC cell line to its matched TR-differentiated derivative, using a false discovery rate cutoff of 0.05. Data were visualized using the *ggplot2* (v3.3.6), *dplyr* (v1.0.8), and *ggrepel* (v0.9.1) packages in R studio. *Gene Set Enrichment Analysis*. DESeq2 normalized count values per gene were averaged across three independent replicates per group, and log2 fold change values were calculated per gene to compare each TR-differentiated cell line to its parental EC cell line. Data

were filtered to include only expressed genes, as defined by a minimum normalized count value of 100 in at least one group. Gene lists pre-ranked by log2 fold change were then created for each of the three comparisons. Pre-ranked gene lists and miRDB gene sets were used for Gene Set Enrichment Analysis, which was performed with 1000 permutations and a classic enrichment statistic.^{29–31}

Mouse strains and husbandry

All animals included in this study were handled in accordance with federal and institutional guidelines, under Institutional Animal Care and Use Committee-approved protocols. Mice were housed in facilities accredited by the Association for the Assessment and Accreditation of Laboratory Animal Care International and were cared for in compliance with the Guide for the Care and Use of Laboratory Animals.⁵⁷ gPAK mice were generated as previously described.^{4,58} 129S6 and *MMTV-PyMT* mice were bred and maintained at Cornell University. *Dazl*^{-/-} (*Dazl-1L*) mice were generated as previously described⁴⁷ and backcrossed to the 129S4 genetic background.

Genotyping

DNA was extracted from mouse tail snips and genotyped by PCR using primers specific for *Pten* and *Kras* alleles and the *Strat8-Cre* transgene as previously described.⁵⁸ *Dazl*^{-/-} mice were genotyped as previously described.⁴⁷

Subcutaneous cell transplantations

Tumor tissue derived from subcutaneous transplantation of cultured EC and differentiated cells into immunocompromised mice as well as serum from those mice were obtained from an experiment reported in a previous study.²⁸

Thioridazine treatment of gPAK mice

At 21 days of age, gPAK mice were randomly assigned to control or TR treatment groups. TR-treated mice were injected intraperitoneally with 25 mg/kg thioridazine hydrochloride (Sigma) dissolved in sterile 0.9% NaCl and sterile filtered, every 3 days for 3 weeks for 7 doses total or until humane endpoint criteria were met. Control mice received an equal volume of sterile 0.9% NaCl in the same manner. All mice were monitored regularly and euthanized by CO₂ asphyxiation upon meeting humane endpoint criteria (loss of over 20% body weight, tumor greater than 2 cm in diameter, severe abdominal distension, displaying signs of pain such as hunching and piloerection) or after reaching 70 days of age. TR-treated or control mice that did not develop testicular tumors were excluded from the study (about 25% of gPAK mice do not develop tumors).⁴

Serum and tissue collection

Blood was collected from pregnant females and neonates via the facial vein. For blood collection at endpoint, blood was obtained via intracardiac puncture immediately following euthanasia. Blood was allowed to clot at room temperature, then centrifuged at 5500 rpm for 10 minutes to separate serum from cellular components. Serum was transferred to a new tube and stored at -80 prior to miRNA expression analysis. Immediately after blood collection, tissue was dissected and flash frozen in liquid nitrogen, then stored at -80 prior to miRNA expression analysis.

Immunohistochemistry and quantification

OCT4 immunohistochemistry was performed on one tissue section per tumor as previously described.²⁸ OCT4-positive area per section was quantified using QuPath by manually selecting and annotating the areas of OCT4-positive staining and dividing the total OCT4-positive area by the total area of the entire tumor section.

RNA isolation from serum and conditioned media

RNA from 100 μ L of serum (35 μ L for samples from pregnant dams and 15 μ L for samples from P14-16 pups) or 200 μ L conditioned media was isolated using the miRNeasy Serum/Plasma Advanced Kit (Qiagen) according to the manufacturer's instructions. To increase RNA yield, MS2 carrier RNA (Roche) was added to a final concentration of 1.25 μ g/mL. During lysis of the samples, a non-mammalian spike-in external control, cel-miR39 (5.6x10⁸ copies), was added to each sample in order to monitor RNA recovery. RNA was eluted from columns with 50 μ L of nuclease-free water.

RNA isolation from cells and tissues

Total RNA was extracted from tumor, testis, or spleen tissue or cell pellets using TRIzol Reagent (ThermoFisher) according to the manufacturer's instruction. RNA quantity and quality were assessed using the Nanodrop One (Isogen Lifescience) and Qubit 4 fluorometer (ThermoFisher).

miRNA expression analysis via TaqMan MicroRNA Assay

5 μ L of purified RNA from serum or conditioned media samples or 10 ng of total RNA from tissue or cells was reverse transcribed using the TaqMan MicroRNA Reverse Transcription Kit (ThermoFisher) and the target-specific RT primer from the cel-miR39-3p (ID 000200), hsa-miR30b-5p (ID 000602), mmu-miR291a-3p (ID 002592), mmu-miR292-3p (ID 002593), and mmu-miR293-3p (ID 001794) TaqMan MicroRNA Assays (ThermoFisher). The final volume of 15 μ L for each reaction underwent reverse transcription using a BioRad T100 Thermal Cycler at 16 °C for 30 min, 42 °C for 30 min, followed by a final step of 85 °C for 5 min. For the final TaqMan PCR, for each of the aforementioned TaqMan MicroRNA

Assays, 1.5 μ L of the cDNA product was added to 10 μ L of 2X TaqMan Fast Advanced Master Mix (ThermoFisher) and 1 μ L of 20X TaqMan Assay (including the TaqMan probe and PCR primer set) and brought up to a final reaction volume of 20 μ L. All reactions were performed in duplicate. Ct values were measured on a QuantStudio 12K Flex device. “Undetected” calls were assigned a Ct value of 40 (maximum number of cycles) so that quantification was possible. The cel-miR39-3p assay was performed for serum and conditioned media samples as a quality control check to monitor RNA recovery. For normalization, endogenous reference miR-30b-5p was used. Targets were corrected for average miR-30b-5p levels across biological replicates to correct for deviations in the endogenous levels of miR-30b-5p. $40 - \Delta Ct$ transformation was used to represent miRNA expression levels.

Statistical analysis and visualization

Except for analysis of RNA sequencing data, all other statistical analyses were performed using GraphPad Prism. Data were visualized using GraphPad Prism.

ACKNOWLEDGEMENTS

A.R.L. was funded by NCI F30 CA247458. D.M.T., A.J.M.G. and L.H.J.L. were financially supported by the Princess Máxima Center for Pediatric Oncology through KiKa funding. The authors would like to thank Jen Grenier from the Transcriptional Regulation and Expression facility at Cornell University for RNA sequencing and assistance with data analysis, Thao. T. Pham for genotyping of *Dazl* mice, and Praveen Sethupathy and Andrew Grimson for helpful discussions.

REFERENCES

1. National Cancer Institute, DCCPS, Surveillance Research Program. Surveillance, Epidemiology, and End Results (SEER) Program (www.seer.cancer.gov) SEER*Stat Database (2015–2019). (2022).
2. Cheng, L., Albers, P., Berney, D. M., Feldman, D. R., Daugaard, G., Gilligan, T. & Looijenga, L. H. J. Testicular cancer. *Nat Rev Dis Primers* **4**, 29 (2018).
3. Baroni, T., Arato, I., Mancuso, F., Calafiore, R. & Luca, G. On the Origin of Testicular Germ Cell Tumors: From Gonocytes to Testicular Cancer. *Front Endocrinol (Lausanne)* **10**, 343 (2019).
4. Pierpont, T. M., Lyndaker, A. M., Anderson, C. M., Jin, Q., Moore, E. S., Roden, J. L., Braxton, A., Bagepalli, L., Kataria, N., Hu, H. Z., Garness, J., Cook, M. S., Capel, B., Schlafer, D. H., Southard, T. & Weiss, R. S. Chemotherapy-Induced Depletion of OCT4-Positive Cancer Stem Cells in a Mouse Model of Malignant Testicular Cancer. *Cell Rep* **21**, 1896–1909 (2017).
5. Sperger, J. M., Chen, X., Draper, J. S., Antosiewicz, J. E., Chon, C. H., Jones, S. B., Brooks, J. D., Andrews, P. W., Brown, P. O. & Thomson, J. A. Gene expression patterns in human embryonic stem cells and human pluripotent germ cell tumors. *Proceedings of the National Academy of Sciences* **100**, 13350–13355 (2003).
6. Bloom, J. C., Loehr, A. R., Schimenti, J. C. & Weiss, R. S. Germline Genome Protection: Implications for Gamete Quality and Germ Cell Tumorigenesis. *Andrology* **7**, 516–526 (2019).
7. Andrews, P. W., Matin, M. M., Bahrami, A. R., Damjanov, I., Gokhale, P. & Draper, J. S. Embryonic stem (ES) cells and embryonal carcinoma (EC) cells: opposite sides of the same coin. *Biochemical Society Transactions* **33**, 5 (2005).
8. Dieckmann, K.-P., Frey, U. & Lock, G. Contemporary diagnostic work-up of testicular germ cell tumours. *Nat Rev Urol* **10**, 703–712 (2013).
9. Javadpour, N. The Role of Biologic Tumor Markers in Testicular Cancer. *Cancer* **45**, 1755–1761 (1980).
10. Lange, P. H. & Winfield, H. N. Biological markers in urologic cancer. *Cancer* **60**, 464–472 (1987).
11. Almstrup, K., Lobo, J., Mørup, N., Belge, G., Rajpert-De Meyts, E., Looijenga, L. H. J. & Dieckmann, K.-P. Application of miRNAs in the diagnosis and monitoring of testicular germ cell tumours. *Nat Rev Urol* **17**, 201–213 (2020).
12. O'Brien, J., Hayder, H., Zayed, Y. & Peng, C. Overview of MicroRNA Biogenesis, Mechanisms of Actions, and Circulation. *Front Endocrinol (Lausanne)* **9**, 402 (2018).
13. Gillis, A. J. M., Stoop, H. J., Hersmus, R., Oosterhuis, J. W., Sun, Y., Chen, C., Guenther, S., Sherlock, J., Veltman, I., Baeten, J., van der Spek, P. J., de Alarcon, P. & Looijenga, L. H. J. High-throughput microRNAome analysis in human germ cell tumours. *J Pathol* **213**, 319–328 (2007).
14. Palmer, R. D., Murray, M. J., Saini, H. K., van Dongen, S., Abreu-Goodger, C., Muralidhar, B., Pett, M. R., Thornton, C. M., Nicholson, J. C., Enright, A. J., Coleman, N., & Children's Cancer and Leukaemia Group. Malignant germ cell tumors display common microRNA profiles resulting in global changes in expression of messenger RNA targets. *Cancer Res* **70**, 2911–2923 (2010).
15. Dieckmann, K.-P., Radtke, A., Geczi, L., Matthies, C., Anheuser, P., Eckardt, U., Sommer, J., Zengerling, F., Trenti, E., Pichler, R., Belz, H., Zastrow, S., Winter, A., Melchior, S., Hammel, J., Kranz, J., Bolten, M., Krege, S., Haben, B., Loidl, W., Ruf, C. G., Heinzelbecker, J., Heidenreich, A., Cremers, J. F., Oing, C., Hermanns, T., Fankhauser, C. D., Gillessen, S., Reichegger, H., Cathomas, R., Pichler, M., Hentrich, M., Eredics, K., Lorch, A., Wülfing, C., Peine, S., Wosniok, W., Bokemeyer, C. & Belge, G. Serum Levels of MicroRNA-371a-3p (M371 Test) as a New Biomarker of Testicular Germ Cell Tumors: Results of a Prospective Multicentric Study. *J Clin Oncol* **37**, 1412–1423 (2019).

16. Spiekermann, M., Belge, G., Winter, N., Ikogho, R., Balks, T., Bullerdiek, J. & Dieckmann, K.-P. MicroRNA miR-371a-3p in serum of patients with germ cell tumours: evaluations for establishing a serum biomarker. *Andrology* **3**, 78–84 (2015).
17. Fankhauser, C. D., Christiansen, A. J., Rothermundt, C., Cathomas, R., Wettstein, M. S., Grossmann, N. C., Grogg, J. B., Templeton, A. J., Hirschi-Blickenstorfer, A., Lorch, A., Gillissen, S., Moch, H., Beyer, J. & Hermanns, T. Detection of recurrences using serum miR-371a-3p during active surveillance in men with stage I testicular germ cell tumours. *Br J Cancer* **126**, 1140–1144 (2022).
18. Belge, G., Grobelny, F., Radtke, A., Bodes, J., Matthies, C., Wülfing, C. & Dieckmann, K.-P. Serum levels of microRNA-371a-3p are not elevated in testicular tumours of non-germ cell origin. *J Cancer Res Clin Oncol* **147**, 435–443 (2021).
19. Wu, S., Aksoy, M., Shi, J. & Houbaviy, H. B. Evolution of the miR-290–295/miR-371–373 Cluster Family Seed Repertoire. *PLoS One* **9**, e108519 (2014).
20. Houbaviy, H. B., Murray, M. F. & Sharp, P. A. Embryonic Stem Cell-Specific MicroRNAs. *Developmental Cell* **5**, 351–358 (2003).
21. Suh, M.-R., Lee, Y., Kim, J. Y., Kim, S.-K., Moon, S.-H., Lee, J. Y., Cha, K.-Y., Chung, H. M., Yoon, H. S., Moon, S. Y., Kim, V. N. & Kim, K.-S. Human embryonic stem cells express a unique set of microRNAs. *Developmental Biology* **270**, 488–498 (2004).
22. Lichner, Z., Páll, E., Kerekes, A., Pállinger, É., Maraghechi, P., Bősze, Z. & Gócsa, E. The miR-290–295 cluster promotes pluripotency maintenance by regulating cell cycle phase distribution in mouse embryonic stem cells. *Differentiation* **81**, 11–24 (2011).
23. Wang, Y., Baskerville, S., Shenoy, A., Babiarz, J. E., Baehner, L. & Blelloch, R. Embryonic stem cell-specific microRNAs regulate the G1-S transition and promote rapid proliferation. *Nat Genet* **40**, 1478–1483 (2008).
24. Zheng, G. X. Y., Ravi, A., Calabrese, J. M., Medeiros, L. A., Kirak, O., Dennis, L. M., Jaenisch, R., Burge, C. B. & Sharp, P. A. A latent pro-survival function for the mir-290–295 cluster in mouse embryonic stem cells. *PLoS Genet* **7**, e1002054 (2011).
25. Tang, F., Kaneda, M., O'Carroll, D., Hajkova, P., Barton, S. C., Sun, Y. A., Lee, C., Tarakhovsky, A., Lao, K. & Surani, M. A. Maternal microRNAs are essential for mouse zygotic development. *Genes Dev* **21**, 644–648 (2007).
26. Medeiros, L. A., Dennis, L. M., Gill, M. E., Houbaviy, H., Markoulaki, S., Fu, D., White, A. C., Kirak, O., Sharp, P. A., Page, D. C. & Jaenisch, R. Mir-290–295 deficiency in mice results in partially penetrant embryonic lethality and germ cell defects. *Proceedings of the National Academy of Sciences* **108**, 14163–14168 (2011).
27. Hayashi, K., Chuva de Sousa Lopes, S. M., Kaneda, M., Tang, F., Hajkova, P., Lao, K., O'Carroll, D., Das, P. P., Tarakhovsky, A., Miska, E. A. & Surani, M. A. MicroRNA biogenesis is required for mouse primordial germ cell development and spermatogenesis. *PLoS One* **3**, e1738 (2008).
28. Loehr, A. R., Pierpont, T. M., Gelsleichter, E., Galang, A. M. D., Fernandez, I. R., Moore, E. S., Guo, M. Z., Miller, A. D. & Weiss, R. S. Targeting Cancer Stem Cells with Differentiation Agents as an Alternative to Genotoxic Chemotherapy for the Treatment of Malignant Testicular Germ Cell Tumors. *Cancers (Basel)* **13**, 2045 (2021).
29. Subramanian, A., Tamayo, P., Mootha, V. K., Mukherjee, S., Ebert, B. L., Gillette, M. A., Paulovich, A., Pomeroy, S. L., Golub, T. R., Lander, E. S. & Mesirov, J. P. Gene set enrichment analysis: a knowledge-based approach for interpreting genome-wide expression profiles. *Proc Natl Acad Sci U S A* **102**, 15545–15550 (2005).

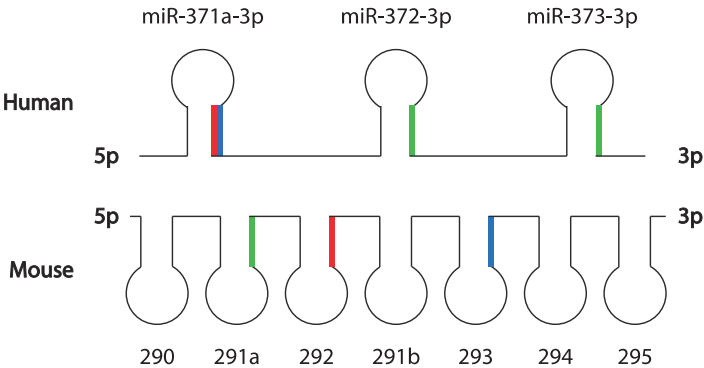
30. Liu, W. & Wang, X. Prediction of functional microRNA targets by integrative modeling of microRNA binding and target expression data. *Genome Biology* **20**, 18 (2019).
31. Chen, Y. & Wang, X. miRDB: an online database for prediction of functional microRNA targets. *Nucleic Acids Res* **48**, D127–D131 (2020).
32. Guo, W.-T., Wang, X.-W., Yan, Y.-L., Li, Y.-P., Yin, X., Zhang, Q., Melton, C., Shenoy, A., Reyes, N. A., Oakes, S. A., Belloch, R. & Wang, Y. Suppression of epithelial-mesenchymal transition and apoptotic pathways by miR-294/302 family synergistically blocks let-7-induced silencing of self-renewal in embryonic stem cells. *Cell Death Differ* **22**, 1158–1169 (2015).
33. Zovoilis, A., Smorag, L., Pantazi, A. & Engel, W. Members of the miR-290 cluster modulate in vitro differentiation of mouse embryonic stem cells. *Differentiation* **78**, 69–78 (2009).
34. Lüningschrör, P., Stöcker, B., Kaltschmidt, B. & Kaltschmidt, C. miR-290 Cluster Modulates Pluripotency by Repressing Canonical NF- κ B Signaling. *Stem Cells* **30**, 655–664 (2012).
35. Kaspi, H., Chapnik, E., Levy, M., Beck, G., Hornstein, E. & Soen, Y. Brief report: miR-290–295 regulate embryonic stem cell differentiation propensities by repressing pax6. *Stem Cells* **31**, 2266–2272 (2013).
36. Gong, Z., Wang, D., Zhu, S., Xia, Y., Fan, C., Zhao, B. & Jin, Y. miR-290 contributes to the low abundance of cyclin D1 protein in mouse embryonic stem cells. *Acta Biochim Biophys Sin (Shanghai)* **49**, 635–642 (2017).
37. Goldberger, N., Walker, R. C., Kim, C. H., Winter, S. & Hunter, K. W. Inherited Variation in miR-290 Expression Suppresses Breast Cancer Progression by Targeting the Metastasis Susceptibility Gene *Arid4b*. *Cancer Research* **73**, 2671–2681 (2013).
38. Cao, Y., Guo, W.-T., Tian, S., He, X., Wang, X.-W., Liu, X., Gu, K.-L., Ma, X., Huang, D., Hu, L., Cai, Y., Zhang, H., Wang, Y. & Gao, P. miR-290/371-Mbd2-Myc circuit regulates glycolytic metabolism to promote pluripotency. *The EMBO Journal* **34**, 609–623 (2015).
39. Kanellopoulou, C., Gilpatrick, T., Kilaru, G., Burr, P., Nguyen, C. K., Morawski, A., Lenardo, M. J. & Muljo, S. A. Reprogramming of Polycomb-Mediated Gene Silencing in Embryonic Stem Cells by the miR-290 Family and the Methyltransferase *Ash1l*. *Stem Cell Reports* **5**, 971–978 (2015).
40. Schaefer, M., Nabih, A., Spies, D., Hermes, V., Bodak, M., Wischnewski, H., Stalder, P., Ngondo, R. P., Liechti, L. A., Sajic, T., Aebersold, R., Gatfield, D. & Ciaudo, C. Global and precise identification of functional miRNA targets in mESCs by integrative analysis. *EMBO reports* **23**, e54762 (2022).
41. Akshaya, N., Srinaath, N., Rohini, M., Ilango, R. & Selvamurugan, N. Parathyroid Hormone-regulation of Runx2 by MiR-290 for Matrix Metalloproteinase-13 Expression in Rat Osteoblastic Cells. *Current Molecular Medicine* **22**, 549–561
42. Sangokoya, C. & Belloch, R. MicroRNA-dependent inhibition of PFN2 orchestrates ERK activation and pluripotent state transitions by regulating endocytosis. *Proceedings of the National Academy of Sciences* **117**, 20625–20635 (2020).
43. Lu, L., Wang, X., Zhao, H., Jiang, F., Li, Y., Yao, Y., Shi, C. & Yang, Y. MiR-291a/b-5p inhibits autophagy by targeting Atg5 and Becn1 during mouse preimplantation embryo development. *RSC Adv.* **9**, 9331–9341 (2019).
44. Wu, D.-R., Gu, K.-L., Yu, J.-C., Fu, X., Wang, X.-W., Guo, W.-T., Liao, L.-Q., Zhu, H., Zhang, X.-S., Hui, J. & Wang, Y. Opposing roles of miR-294 and MBNL1/2 in shaping the gene regulatory network of embryonic stem cells. *EMBO reports* **19**, e45657 (2018).
45. Oliveto, S., Mancino, M., Manfrini, N. & Biffo, S. Role of microRNAs in translation regulation and cancer. *World J Biol Chem* **8**, 45–56 (2017).

46. Boellaard, W. P. A., Gillis, A. J. M., van Leenders, G. J. L. H., Stoop, H., van Agthoven, T., Dorssers, L. C. J., Dinkelman-Smit, M., Boormans, J. L. & Looijenga, L. H. J. Cellular origin of microRNA-371a-3p in healthy males based on systematic urogenital tract tissue evaluation. *Andrology* **7**, 463–468 (2019).
47. Nicholls, P. K., Schorle, H., Naqvi, S., Hu, Y.-C., Fan, Y., Carmell, M. A., Dobrinski, I., Watson, A. L., Carlson, D. F., Fahrenkrug, S. C. & Page, D. C. Mammalian germ cells are determined after PGC colonization of the nascent gonad. *Proceedings of the National Academy of Sciences* **116**, 25677–25687 (2019).
48. Marson, A., Levine, S. S., Cole, M. F., Frampton, G. M., Brambrink, T., Johnstone, S., Guenther, M. G., Johnston, W. K., Wernig, M., Newman, J., Calabrese, J. M., Dennis, L. M., Volkert, T. L., Gupta, S., Love, J., Hannett, N., Sharp, P. A., Bartel, D. P., Jaenisch, R. & Young, R. A. Connecting microRNA genes to the core transcriptional regulatory circuitry of embryonic stem cells. *Cell* **134**, 521–533 (2008).
49. Judson, R. L., Babiarz, J. E., Venere, M. & Blelloch, R. Embryonic stem cell-specific microRNAs promote induced pluripotency. *Nat Biotechnol* **27**, 459–461 (2009).
50. Hoy, A. M. & Buck, A. H. Extracellular small RNAs: what, where, why? *Biochem Soc Trans* **40**, 886–890 (2012).
51. Lobo, J., Gillis, A. J. M., van den Berg, A., Dorssers, L. C. J., Belge, G., Dieckmann, K.-P., Roest, H. P., van der Laan, L. J. W., Gietema, J., Hamilton, R. J., Jerónimo, C., Henrique, R., Salvatori, D. & Looijenga, L. H. J. Identification and Validation Model for Informative Liquid Biopsy-Based microRNA Biomarkers: Insights from Germ Cell Tumor In Vitro, In Vivo and Patient-Derived Data. *Cells* **8**, 1637 (2019).
52. Radtke, A., Cremers, J.-F., Kliesch, S., Riek, S., Junker, K., Mohamed, S. A., Anheuser, P., Belge, G. & Dieckmann, K.-P. Can germ cell neoplasia in situ be diagnosed by measuring serum levels of microRNA371a-3p? *J Cancer Res Clin Oncol* **143**, 2383–2392 (2017).
53. Kratz, C. P., Mai, P. L. & Greene, M. H. Familial Testicular Germ Cell Tumors. *Best Pract Res Clin Endocrinol Metab* **24**, 503–513 (2010).
54. Oosterhuis, J. W. & Looijenga, L. H. J. Human germ cell tumours from a developmental perspective. *Nat Rev Cancer* **19**, 522–537 (2019).
55. Morales-Prieto, D. M., Chaiwangyen, W., Ospina-Prieto, S., Schneider, U., Herrmann, J., Gruhn, B. & Markert, U. R. MicroRNA expression profiles of trophoblastic cells. *Placenta* **33**, 725–734 (2012).
56. Love, M. I., Huber, W. & Anders, S. Moderated estimation of fold change and dispersion for RNA-seq data with DESeq2. *Genome Biol* **15**, 550 (2014).
57. National Research Council. *Guide for the Care and Use of Laboratory Animals: Eighth Edition*. (The National Academies Press, 2011).
58. Lyndaker, A. M., Pierpont, T. M., Loehr, A. R. & Weiss, R. S. A Genetically Engineered Mouse Model of Malignant Testicular Germ Cell Tumors. *Methods Mol Biol* **2195**, 147–165 (2021).

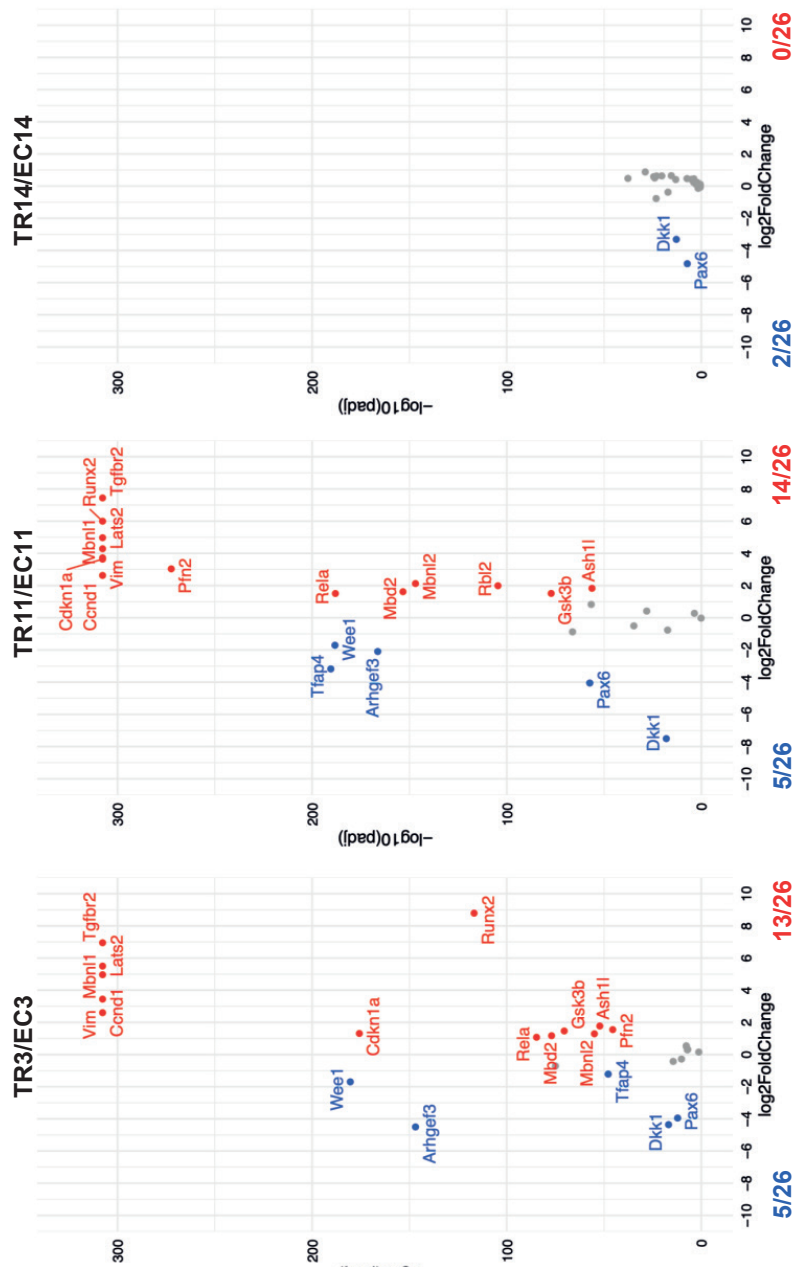
SUPPLEMENTAL MATERIALS

Supplemental Table 1. Genes that were experimentally proven to be direct targets of the miR-290-295 cluster and their associated publication.

Mouse gene name	Reference
<i>Tgfbir2</i>	Guo et al. 2015 ³²
<i>Gsk3b</i>	Guo et al. 2015 ³²
<i>Arhgef3</i>	Guo et al. 2015 ³²
<i>Fndc3a</i>	Guo et al. 2015 ³²
<i>Vim</i>	Guo et al. 2015 ³²
<i>Cdkn1a</i>	Wang et al. 2008 ²³
<i>Rbl2</i>	Wang et al. 2008 ²³
<i>Lats2</i>	Wang et al. 2008 ²³
<i>Casp2</i>	Zheng et al. 2011 ²⁴
<i>Ei24</i>	Zheng et al. 2011 ²⁴
<i>Wee1</i>	Lichner et al. 2011 ²²
<i>Fbxl5</i>	Lichner et al. 2011 ²²
<i>Dkk1</i>	Zovoilis et al. 2009 ³³
<i>Rela</i>	Lüningschrör et al. 2012 ³⁴
<i>Pax6</i>	Kaspi et al. 2013 ³⁵
<i>Ccnd1</i>	Gong et al. 2017 ³⁶
<i>Arid4b</i>	Goldberger et al. 2013 ³⁷
<i>Mbd2</i>	Cao et al. 2015 ³⁸
<i>Ash1l</i>	Kanellopoulou et al. 2015 ³⁹
<i>Tfap4</i>	Schaefer et al. 2022 ⁴⁰
<i>Runx2</i>	Akshaya et al. 2022 ⁴¹
<i>Pfn2</i>	Sangokoya and Blelloch 2020 ⁴²
<i>Atg5</i>	Lu et al. 2019 ⁴³
<i>Becn1</i>	Lu et al. 2019 ⁴³
<i>Mbnl1</i>	Wu et al. 2018 ⁴⁴
<i>Mbnl2</i>	Wu et al. 2018 ⁴⁴



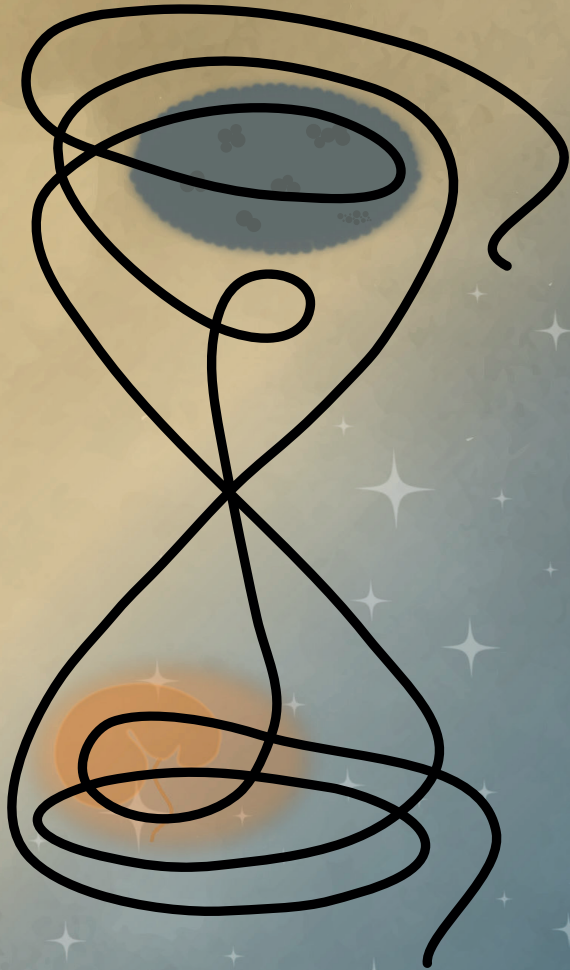
Supplemental Figure 1. Homology of the miR-371-373/miR-290-295 cluster family. Mouse miR-291a-3p is homologous to human miR-372-3p and miR-373-3p, whereas miR-292-3p and miR-293 are homologous to different isoforms of human miR-371a-3p.



Supplemental Figure 2. Volcano plots of 26 experimentally proven direct target genes of the miR-290-295 cluster (see Supplemental Table 1). Genes that are significantly upregulated in TR-differentiated cells are in red, genes that are significantly downregulated in TR-differentiated cells are in blue, and genes that are not significantly differentially expressed between the cells are in grey. Significance is defined as an adjusted p value (padj) < 0.05.

Chapter

8



Chapter 8

General discussion

DISCUSSION

Introduction

Within this thesis we have touched upon multiple patho-biological as well as clinically relevant aspects of (T)GCT research, the most important being biomarkers and tumor resistance. After reviewing the role of *TP53* in both ES cells and GCTs in **Chapter 2**, we used CRISPR Cas-9 to introduce mutations in *TP53* in two GCT cell lines and reported a role for *TP53* in (T)GCT resistance in **Chapter 3**. Continuing along the lines of (T)GCT resistance, in **Chapter 4** we used a larger set of GCT cell lines, both parental and resistant isogenic subclones and found a common amplification of the short arm of chromosome 3 (band p.25.3) in all independently generated resistant subclones. The presence of unique breakpoints proved the induced and not pre-selected nature of them. Further analysis in publicly available datasets illustrated that this region is a significant marker for (T)GCT resistance and therefore, poor prognosis. From **Chapter 5** on, we switched our focus to (T)GCT liquid biopsy biomarkers, first looking at some technical aspects of (T)GCT biomarker miR371a detection using different isolation techniques and starting material. Hereafter, we elucidated the functional role of the miR371a-3 cluster in two (T)GCT cell lines using a CRISPR-Cas9-mediated knockout approach in **Chapter 6**. Finally, using a well-established *in vivo* (T)GCT mouse-model, we investigated (T)GCT differentiation and the detection of the mouse 371a-3 cluster homologue miRs, the miR291a-5 cluster, in **Chapter 7**. Using the knowledge from the various projects, this discussion will evolve around the central themes described in the scope of this thesis; 1) what are the underlying mechanism(s) of treatment resistance in (T)GCTs, and 2) what are the possibilities as well as limitations of using the miR371a-3 cluster as biomarker for (T)GCTs.

Aim of this thesis

Ever since the discovery of cisplatin as chemotherapeutic modality for TGCT patients in the 80s (Higby et al., 1974; Einhorn and Donohue, 1977), research into treatment resistance has been hampered due to the assumption that these cancers can be considered “curable”. However, the idea of curability is not considering the sheer number of patients that get these malignancies and coincidentally, the clinically significant number of patients that do not respond to treatment and will eventually succumb to their disease (Siegel *et al.*, 2022). Not only is (T)GCT resistance still not fully understood, but the lack of knowledge also is the fundamental limitation in the discovery of additional salvage (targeted) treatment options for treatment resistant patients. Part of this thesis is therefore dedicated to this gap in knowledge, focusing mainly on patient stratification and elucidating mechanisms of resistance in *in vitro* and *in vivo* model systems.

Moreover, patient diagnosis and follow-up can be improved as well. Especially in patients that have undergone treatment and/or surgical intervention it can be challenging to determine if their remaining mass is necrotic or is still containing viable tumor. Unfortunately, current clinical biomarkers (AFP, β -HCG and LDH) are only usable in ~60% of patients and their diagnostic and prognostic power is limited due to false positives and low serum levels in smaller or residual lesions (Almstrup *et al.*, 2020; Leão *et al.*, 2022). The miR371a-3 cluster has been proven to outperform these classical clinical markers, additionally being informative during treatment response and patient follow-up (Gillis *et al.*, 2007; Murray *et al.*, 2011; Rijlaarsdam *et al.*, 2015; Syring *et al.*, 2015; van Agthoven *et al.*, 2017; Dieckmann *et al.*, 2019; Mego *et al.*, 2019; Almstrup *et al.*, 2020; Leão *et al.*, 2022). The second part of this thesis therefore focusses on these miRs, looking at methods of detection and isolation, their functional role in (T)GCTs and comparability between human and mouse.

Germ cell tumors and TP53

One of the main similarities between (T)GCTs and ES cells, which distinguishes them from other solid malignancies, is their wild-type *TP53* status. In **Chapter 2** we focused on the similarities between ES cells and (T)GCTs based on their *TP53* status and therefore hypersensitive DNA-damage and apoptotic response (Kersemaekers *et al.*, 2002; Oosterhuis and Looijenga, 2005; Bauer *et al.*, 2010; Koster *et al.*, 2011; Gutekunst *et al.*, 2011; Gutekunst *et al.*, 2013; Bagrodia *et al.*, 2016; Oosterhuis and Looijenga, 2019). We argued, that because (T)GCTs so closely resemble ES cells, their hypersensitivity to cytotoxic DNA damaging compounds, like cisplatin, is related to their embryonal origin and that these cells are therefore wired to protect their genome by undergoing apoptosis over (error-prone) DNA repair (Kersemaekers *et al.*, 2002; Fillion *et al.*, 2009; Bauer *et al.*, 2010; Gutekunst *et al.*, 2011; Gutekunst *et al.*, 2013; Koster *et al.*, 2011; Jacobsen and Honecker, 2015; Bloom *et al.*, 2019). Following this work, we try to prove the other side of the same coin in **Chapter 3**. If the wild-type *TP53* status is indeed one of the main causes of chemotherapy sensitivity in (T)GCTs, will *TP53* (T)GCT knock-out cells acquire resistance? Using CRISPR-Cas9 in two common (T)GCT cell lines, 2102Ep (testicular) and NCCIT (mediastinal), harboring both parental and isogenic cisplatin resistant subclones, we demonstrated that resistant clones benefit from loss of *TP53* and become more resistant to cisplatin than their wild-type counterparts (**Chapter 3**). Although this might seem obvious based on the vast amount of work on P53 in many cancers, often indicating a worse prognosis upon loss or mutation of *TP53*, this is not as evident in (T)GCTs, where *TP53* is rarely mutated (Bagrodia *et al.*, 2016; Shen *et al.*, 2018). Paradoxically, even though cells become more resistant to cisplatin upon artificially induced loss of *TP53* (**Chapter 3**), and (T)GCT patients, although this is relatively rare, that harbor *TP53* generally do worse

in the clinic (Bagrodia *et al.*, 2016), it still seems that the embryonal origin of these cancers dominates their behavior, genome protection over loss of P53. When *TP53* is mutated or lost, (T)GCTs respond like other malignancies. The loss or mutation benefits the cancer and therefore worsens the prognosis of the patients. However, the selective pressure on maintaining a wild-type P53-status seems to be dominant (Bagrodia *et al.*, 2016). This discovery, although mechanistic, could be important for patient stratification, that is, (T)GCT patients already harboring *TP53* mutations (or even loss) in either their primary tumor, relapse, or metastasis, might no longer benefit from cisplatin-based treatment. While often the number of options will be limited, this could still benefit a small number of patients for whom there is both the option of surgical intervention and systemic treatment. Unfortunately, a limiting factor of this finding is the lack of drugs targeting *TP53* mutations. As with many loss-of-function (or complete loss) of tumor suppressor genes, it remains challenging to find targeted therapies reactivating mutated genes or replacing their function.

Cisplatin resistance

As mentioned in the previous paragraph, (T)GCT resistance is an important issue in the clinic. (T)GCTs account for approximately 1% of male cancers world-wide and of this clinically meaningful number, roughly 5% of patients will not survive, mainly due to resistant primary or relapsed disease (Trabert *et al.*, 2015; Siegel *et al.*, 2022). In **Chapter 3 and 4** we address this topic, first showing that *TP53* can be involved in (T)GCT resistance, like discussed above, and secondly studying CNAs in both (T)GCT cell line and publicly available patient datasets to find a common chromosomal amplification (3p25.3) responsible for (T)GCT resistance in non-seminomas. Up until this point many studies have tried to identify common chromosomal rearrangements within (T)GCTs that could explain tumor resistance (Ma *et al.*, 2011; Bakardjieva-Mihaylova *et al.*, 2019; Singh *et al.*, 2019; Loveday *et al.*, 2020). Combining the knowledge that (T)GCTs (Type II) often harbor gain of the short arm of chromosome 12 (i12p) (Geurts van Kessel *et al.*, 1989; Van Echten *et al.*, 1995; Oosterhuis and Looijenga, 2019), and that (T)GCTs are known to undergo tetraploidization early in the disease onset (Oosterhuis *et al.*, 1989; de Jong *et al.*, 1990; Looijenga *et al.*, 1991; Dorssers *et al.*, 2019; Oosterhuis and Looijenga, 2019), one can understand why CNAs seem a likely target to explain treatment resistance. **Chapter 4** demonstrates for the first time a common chromosomal rearrangement significantly distinguishing between sensitive and proven resistant (T)GCTs (non-seminoma Type II male (T)GCTs) in large clinical datasets (Korkola *et al.*, 2008; Bagrodia *et al.*, 2016; Zehir *et al.*, 2017; Shen *et al.*, 2018). Not only does the 3p25.3 amplification faithfully mark treatment resistant patients, but it is also an independent predictor of treatment response adding to the current clinical IGCCCG staging model, while outperforming other

stratifying markers like *TP53* mutations or *MDM2* amplifications. Moreover, this CNA can be found back in several other (T)GCTs, like Type I male (T)GCTs, (Type II) germinomas and dysgerminomas, as well as YST and CC of the ovary. This finding has significant clinical applications as patients could be faithfully stratified based on a single genomic rearrangement. Especially for young patients, for whom treatment with cisplatin can be associated with many long-term side-effects, this upfront stratification could save them from harmful treatment with compounds that their cancer is known to be resistant to. Finally, these findings can also be instrumental to find new treatment strategies. For example, by single or combination drug screening 3p25.3 amplified cells to find compounds that either kill or sensitize these known resistant cells. This could furthermore aid in establishing new treatment regimens for clinical trials.

Liquid-biopsy based biomarkers

Finally, it is important to find the least invasive and most informative ways of diagnosis, follow-up and (early) relapse detection. Classical STMs that have been in the clinic for decades are informative for approximately 60% of patients, with large variations in informative power based on histology and stage of the disease (Almstrup *et al.*, 2020; Leão *et al.*, 2022). Even though the miR371a-3 cluster as suitable biomarker for (T)GCTs (teratomas excluded) has been reported over one decade ago, and many studies have already shown its superiority over classical STMs, this biomarker has not made it to the clinic yet (Gillis *et al.*, 2007; Murray *et al.*, 2011; Rijlaarsdam *et al.*, 2015; Syring *et al.*, 2015; van Agthoven *et al.*, 2017; Dieckmann *et al.*, 2019; Mego *et al.*, 2019; Almstrup *et al.*, 2020; Leão *et al.*, 2022). Although there are several reasons why this marker has not made it to clinic yet, one is certainly that it can be very challenging to change existing clinical protocols based solely on promising preclinical or retrospective studies without a prospective proof of principle, of which the first trials are currently running (NCT04914026). Secondly, the fact that the miRs “only” identify malignant components of (T)GCTs (all histologies except teratomas) could be considered limiting, and although many studies have tried to identify specific liquid-biopsy based teratoma markers, none have been confirmed prospectively (Lobo *et al.*, 2019; Lafin *et al.*, 2021; Nappi *et al.*, 2021). Finding STMs for residual teratoma has a high clinical need as often, post-chemotherapy, it is hard to distinguish if the remaining mass is viable tumor tissue (differentiated teratoma tissue) or remaining necrotic tumor mass solely based on imaging. Finding STMs for teratoma tissue can aid in the decision making between surgical intervention, systemic treatment, or active surveillance. Of note, one study reported that combining detection for (hyper) methylated RASSF1A with the detection of the miR371a-3 cluster can faithfully detect teratoma tissue, however this data needs to be validated prospectively (Lobo *et al.*, 2021). To aid in this process it is important to standardize research into these biomarkers. In

Chapter 5 we demonstrated that there is virtually no difference between using either serum or plasma as starting material for measuring the levels of these miRs. Furthermore, we show that although a bead-capture based method can be more sensitive, both bead-capture and kit based total RNA extraction can be used for the detection of the miRs. Additionally, in **Chapter 6** we demonstrate that this miR-cluster is not required for (T)GCT cell growth and xenograft tumor formation. Using CRISPR-Cas9 we generated several miR371/2/3 knock-out combinations. We demonstrate that although growth rates may vary upon knock-out, (T)GCT cells survive and behave normally after removal of the miRs. This indicates that the expression of the miRs is likely a passenger effect of the oncogenic development of these tumors. More specifically, these cells possibly never lose the expression of the miRs due to lack of positive selection on loss of the cluster. Finally, by using an *in vivo* mouse model that develops inducible (T)GCTs, we show in **Chapter 7** that we can detect the miR homologues of the miR371a-3 cluster in mice with (T)GCTs as well and, more interestingly, that they behave the same as in human. Most importantly, we show that we can detect elevated miR levels in pregnant dams carrying tumor bearing offspring, indicating it might be possible to screen mothers carrying children with risk of (T)GCT development.

Cell lines in cancer research

One important take home message from the work presented in this thesis is that (cancer) cell lines are still powerful as model systems in (cancer) research. A recent study by Salvadores and colleagues screened 614 cancer cell lines and matched them to tumor types based on classifiers from roughly 9000 tumors (Salvadores *et al.*, 2020). They report that only a fraction of these cell line (~5%) do not represent the tissue and cancer of origin, indicated that most cell lines are faithful models of their cancer of origin (Salvadores *et al.*, 2020). In **Chapters 3, 4 and 6** cell lines are still one of the main drivers behind key discoveries; 1) P53 is involved in cisplatin resistance, 2) 3p25.3 amplification is involved in cisplatin resistance and 3) the miR371a-3 cluster is not essential for (T)GCT cell survival. The strength of this model system lies in the rapid output and clean genetic background. For example, in **Chapter 3** we hypothesized the knock-out of *TP53* might result in more genomic aberrations over time, as P53 is an important protector of genome integrity (**Chapter 2**). However, Global Sequencing Array (GSA) indicated that *TP53* isogenic knock-out clones had virtually the same genetic copy number constitution as their parental counterparts, possibly due to the embryonic origin of these cell lines. Additionally, we obtained similar results in **Chapter 4**, where the isogenic resistant clones, apart from their 3p25.3 amplification had similar recognizable copy number patterns as their parental counterparts. From a mechanistic point of view, the generation of isogenic subclones from the same cell line harbors the most direct informative power. It is interesting to note

that these cell lines have been derived roughly 40 years ago (Wang *et al.*, 1980; Teshima *et al.*, 1988) and yet were detrimental in the above-mentioned discoveries, indicating the strength of basic *in vitro* work for fundamental pre-clinical research.

Importance of publicly available datasets

Moreover, this thesis illustrates the strengths of publicly available datasets. In **Chapter 3** we used the cBioPortal platform to demonstrate that P53-pathway alterations are dependent on anatomical location in (T)GCTs, mediastinal tumors more often harbor *TP53* mutations while testicular tumors are more likely to have *MDM2* amplifications. Furthermore, in **Chapter 4** we used both large datasets from the MSKCC (Korkola *et al.*, 2008; Bagrodia *et al.*, 2016; Zehir *et al.*, 2017) as well as data from the TCGA (Shen *et al.*, 2018) to confirm that the 3p25.3 amplification was indeed present in (T)GCT patients and was a marker of tumor resistance. Without public availability and access to such datasets some key implications of these works could not be validated, highlighting the importance of data sharing and the re-use of data generated by others.

Questioning published data and common beliefs

Lastly, we demonstrated in this thesis that questioning common beliefs (dogmas) can lead to new discoveries. The NCCIT cell line, described in **Chapters 3, 4 and 6**, was considered to harbor no P53 pathway activity due to the presence of a hemizygous mutation in the *TP53* allele relatively distal in the protein. However, specifically in the resistant subclone of NCCIT harboring the same hemizygous mutation, we demonstrated that introducing a mutation more proximal in the gene caused a significant increase in cisplatin resistance of this cell line. This result indicated that even mutated, P53 still had a function in sensitizing this clone to cisplatin. Furthermore, in **Chapter 5** we discussed the technical aspects of detection of liquid-biopsy based biomarkers in serum and plasma. This study was partially initiated by discrepant results reported in the field regarding a marker for the detection of teratoma, of which varying results between groups were accounted to a difference in starting materials (serum vs plasma). The strength of this chapter is that it faithfully reports on an important assumption that was present in the field: serum and plasma can give varying results regarding (T)GCT biomarkers. Although simple in set-up, studies like this are detrimental in empirically supporting or rejecting certain assumptions, opening the discussion of discrepant results to a more scientific approach. Of note, questioning the field and looking for gaps in knowledge can also lead to challenging avenues that perhaps have not been explored for reasons. **Chapter 6** started out with the question: is the miR371a-3 cluster an oncogenic driver or a mere passenger effect in (T)GCTs? As this question had not been sufficiently answered we

generated numerous knock-out models in our common (T)GCT cell lines, eventually demonstrating that indeed the expression of the cluster is likely a passenger effect probably due to the lack of positive selection pressure on active loss of this cluster. This indicates that simple questions can lead to challenging projects.

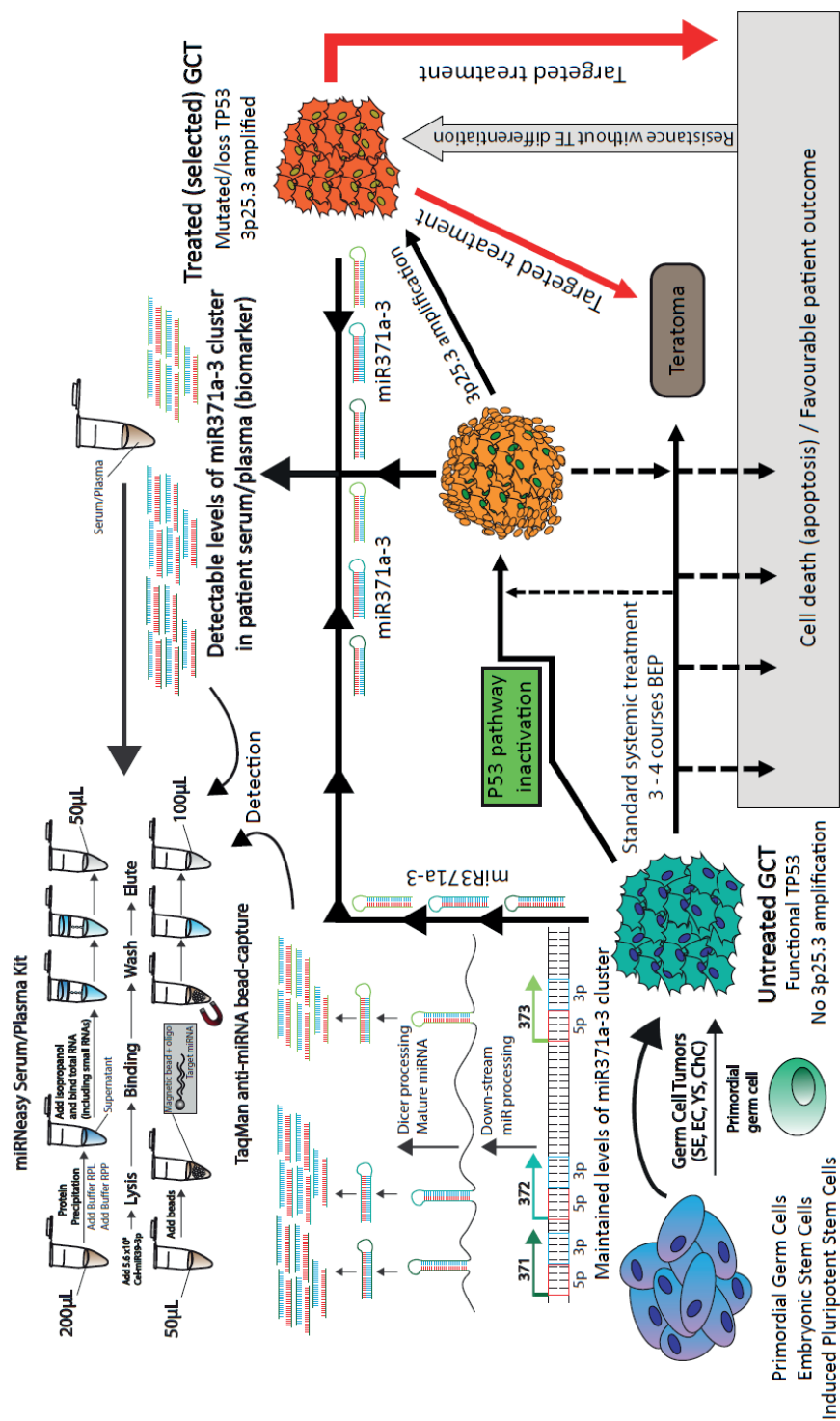
Personal perspective and future ideas

This thesis is a balanced combination of fundamental and pre-clinical research in which one study paves the way for another. While fundamental research will always prove to be important to understand the mechanisms behind disease that can then lead to new therapies and treatments, pre-clinical research has more direct implications. **Chapter 4** is an example of such a direct implication, where screening for this chromosomal amplification can immediately, if independently validated, lead to better patient stratification and identification of resistant disease. Unfortunately, the connection between clinic and research, although very close in the Princes Máxima Center, often requires more than just solid pre-clinical data. This is similar for the miRs, although the discovery that these miRs are suitable as biomarkers for (T)GCTs has been made almost two decades ago, the first steps towards clinical implications have only been taken recently with the start of prospective trials and development of commercial kits. Secondly, although not presented in this thesis, screening compounds on these (T)GCT cell lines (high-throughput and pilots) formed the foundation for many of these projects. Albeit no real alternative targeted treatments could be identified in the compounds screened so far, they still lead to new ideas and mechanisms, and eventually the works presented in this thesis. As the goal is to eventually help cancer patients survive their disease with optimal quality of life, screening compounds should play an important part in any form of cancer research, clinical trials, pre-clinical research, and fundamental research. Finally, it is important to note that the rarity or curability of a cancer should not determine the relevance of its research. (T)GCTs once were considered curable, however they are cancers with the most years of life lost, opposed to for example pons gliomas, that are incredibly rare but virtually no patient survives these cancers.

Conclusion

Once the high curability of (T)GCTs with cisplatin was demonstrated in the late 70s, (T)GCT were considered curable. These assumptions did not consider two important aspects of this disease 1) the age of the patients and incidence of the cancer associated loss of life years and 2) the possibility of patients with cisplatin resistant disease for whom no alternative treatment is available. We describe two clear factors important for cisplatin resistance, one the one hand P53 status linked to anatomical location and origin

of the cancer and on the other a chromosomal amplification located on chromosome 3p marking resistant patients. Moreover, as these tumors are often small, can occur in young patients and can leave behind necrotic or differentiated teratoma tumor mass post-treatment, biomarkers are incredibly important in diagnosis and monitoring of this disease. We describe a standardized way to measure these biomarkers, a possible function for these miRs in the tumor cells and, using an *in vivo* mouse model, a way to possibly screen pregnant women carrying at risk children. Although this work is only a fraction of the work necessary to fully cure this disease, it indicates that it is possible earn the term “curable” for these tumors with the right people, drive, and ideas.



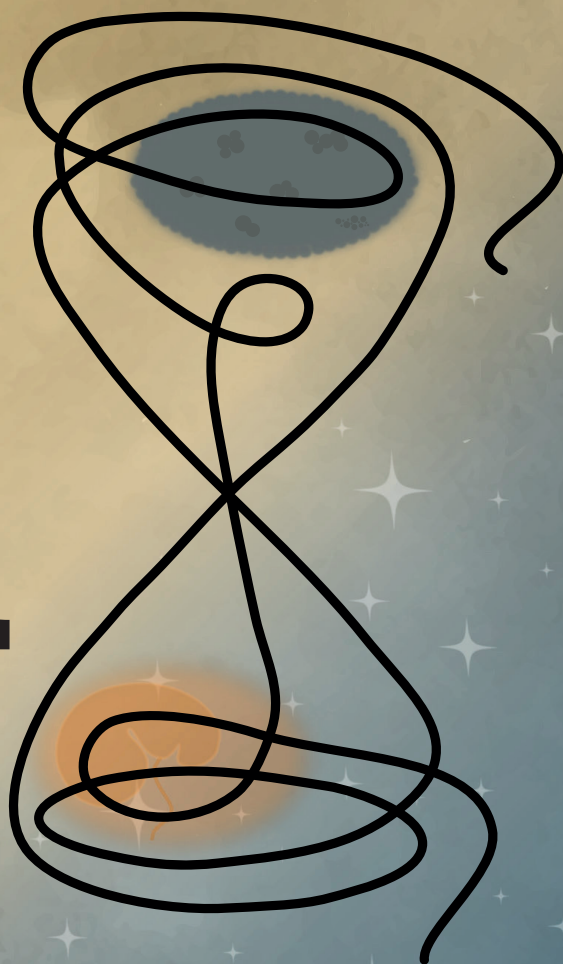
REFERENCES

1. Almstrup K, Lobo J, Mørup N, *et al.* Application of miRNAs in the diagnosis and monitoring of testicular germ cell tumours. *Nat Rev Urol.* 2020;17(4):201-213.
2. Bagrodia A, Lee BH, Lee W, *et al.* Genetic determinants of cisplatin resistance in patients with advanced germ cell tumors. *JCO.* 2016;34(33):4000-4007.
3. Bakardjieva-Mihaylova V, Skvarova Kramarzova K, Slamova M, *et al.* Molecular basis of cisplatin resistance in testicular germ cell tumors. *Cancers (Basel).* 2019;11(9):1316.
4. Bauer S, Mühlenberg T, Leahy M, *et al.* Therapeutic potential of mdm2 inhibition in malignant germ cell tumours. *European Urology.* 2010;57(4):679-687.
5. Bloom JC, Loehr AR, Schimenti JC, Weiss RS. Germline genome protection: implications for gamete quality and germ cell tumorigenesis. *Andrology.* 2019;7(4):516-526.
6. De Jong B, Oosterhuis JW, Castedo SM, Vos A, te Meerman GJ. Pathogenesis of adult testicular germ cell tumors. A cytogenetic model. *Cancer Genet Cytogenet.* 1990;48(2):143-167.
7. Dieckmann KP, Radtke A, Geczi L, *et al.* Serum levels of microRNA-371a-3p (M371 test) as a new biomarker of testicular germ cell tumors: results of a prospective multicentric study. *J Clin Oncol.* 2019;37(16):1412-1423.
8. Dorssers LCJ, Gillis AJM, Stoop H, *et al.* Molecular heterogeneity and early metastatic clone selection in testicular germ cell cancer development. *Br J Cancer.* 2019;120(4):444-452.
9. Einhorn LH, Donohue J. Cis-diamminedichloroplatinum, vinblastine, and bleomycin combination chemotherapy in disseminated testicular cancer. *Ann Intern Med.* 1977;87(3):293-298.
10. Filion TM, Qiao M, Ghule PN, *et al.* Survival responses of human embryonic stem cells to DNA damage. *J Cell Physiol.* 2009;220(3):586-592.
11. Geurts van Kessel A, van Drunen E, de Jong B, Oosterhuis JW, Langeveld A, Mulder MP. Chromosome 12q heterozygosity is retained in i(12p)-positive testicular germ cell tumor cells. *Cancer Genet Cytogenet.* 1989;40(1):129-134.
12. Gillis A, Stoop H, Hersmus R, *et al.* High-throughput microRNAome analysis in human germ cell tumours. *J Pathol.* 2007;213(3):319-328.
13. Gutekunst M, Oren M, Weilbacher A, *et al.* P53 hypersensitivity is the predominant mechanism of the unique responsiveness of testicular germ cell tumor (Tgct) cells to cisplatin. Gartel AL, ed. *PLoS ONE.* 2011;6(4):e19198.
14. Gutekunst M, Mueller T, Weilbacher A, *et al.* Cisplatin hypersensitivity of testicular germ cell tumors is determined by high constitutive noxa levels mediated by oct-4. *Cancer Research.* 2013;73(5):1460-1469.
15. Higby DJ, Wallace HJ, Albert DJ, Holland JF. Diaminodichloroplatinum: a phase I study showing responses in testicular and other tumors. *Cancer.* 1974;33(5):1219-1215.
16. Jacobsen C, Honecker F. Cisplatin resistance in germ cell tumours: models and mechanisms. *Andrology.* 2015;3(1):111-121.
17. Kersemaekers AMF, Mayer F, Molier M, *et al.* Role of p53 and mdm2 in treatment response of human germ cell tumors. *JCO.* 2002;20(6):1551-1561.
18. Korkola JE, Heck S, Olshen AB, *et al.* In vivo differentiation and genomic evolution in adult male germ cell tumors. *Genes Chromosomes Cancer.* 2008;47(1):43-55.

19. Koster R, Timmer-Bosscha H, Bischoff R, Gietema JA, de Jong S. Disruption of the MDM2–p53 interaction strongly potentiates p53-dependent apoptosis in cisplatin-resistant human testicular carcinoma cells via the Fas/FasL pathway. *Cell Death Dis.* 2011;2(4):e148–e148.
20. Lafin JT, Kenigsberg AP, Meng X, *et al.* Serum small rna sequencing and mir-375 assay do not identify the presence of pure teratoma at postchemotherapy retroperitoneal lymph node dissection. *Eur Urol Open Sci.* 2021;26:83–87.
21. Leão R, Albersen M, Looijenga LHJ, *et al.* Circulating micrornas, the next-generation serum biomarkers in testicular germ cell tumours: a systematic review. *European Urology.* 2021;80(4):456–466.
22. Lobo J, Gillis AJM, van den Berg A, *et al.* Identification and validation model for informative liquid biopsy-based microrna biomarkers: insights from germ cell tumor in vitro, in vivo and patient-derived data. *Cells.* 2019;8(12):1637.
23. Lobo J, van Zogchel LMJ, Nuru MG, *et al.* Combining hypermethylated rassf1a detection using ddpcr with mir-371a-3p testing: an improved panel of liquid biopsy biomarkers for testicular germ cell tumor patients. *Cancers (Basel).* 2021;13(20):5228.
24. Looijenga LH, Oosterhuis JW, Ramaekers FC, *et al.* Dual parameter flow cytometry for deoxyribonucleic acid and intermediate filament proteins of residual mature teratoma. All tumor cells are aneuploid. *Lab Invest.* 1991;64(1):113–117.
25. Loveday C, Litchfield K, Proszek PZ, *et al.* Genomic landscape of platinum resistant and sensitive testicular cancers. *Nat Commun.* 2020;11(1):2189.
26. Ma YT, Cullen MH, Hussain SA. Biology of germ cell tumors. *Hematol Oncol Clin North Am.* 2011;25(3):457–471, vii.
27. Mego M, van Agthoven T, Gronesova P, *et al.* Clinical utility of plasma miR-371a-3p in germ cell tumors. *J Cell Mol Med.* 2019;23(2):1128–1136.
28. Murray MJ, Halsall DJ, Hook CE, Williams DM, Nicholson JC, Coleman N. Identification of microRNAs From the miR-371~373 and miR-302 clusters as potential serum biomarkers of malignant germ cell tumors. *Am J Clin Pathol.* 2011;135(1):119–125.
29. Nappi L, Thi M, Adra N, *et al.* Integrated expression of circulating mir375 and mir371 to identify teratoma and active germ cell malignancy components in malignant germ cell tumors. *Eur Urol.* 2021;79(1):16–19.
30. Oosterhuis JW, Castedo SM, de Jong B, *et al.* Ploidy of primary germ cell tumors of the testis. Pathogenetic and clinical relevance. *Lab Invest.* 1989;60(1):14–21.
31. Oosterhuis JW, Looijenga LHJ. Testicular germ-cell tumours in a broader perspective. *Nat Rev Cancer.* 2005;5(3):210–222.
32. Oosterhuis JW, Looijenga LHJ. Human germ cell tumours from a developmental perspective. *Nat Rev Cancer.* 2019;19(9):522–537.
33. Rijlaarsdam MA, van Agthoven T, Gillis AJM, *et al.* Identification of known and novel germ cell cancer-specific (Embryonic) miRs in serum by high-throughput profiling. *Andrology.* 2015;3(1):85–91.
34. Salvadores M, Fuster-Tormo F, Supek F. Matching cell lines with cancer type and subtype of origin via mutational, epigenomic, and transcriptomic patterns. *Sci Adv.* 2020;6(27):eaba1862.
35. Shen H, Shih J, Hollern DP, *et al.* Integrated molecular characterization of testicular germ cell tumors. *Cell Rep.* 2018;23(11):3392–3406.
36. Siegel RL, Miller KD, Fuchs HE, Jemal A. Cancer statistics, 2022. *CA A Cancer J Clinicians.* 2022;72(1):7–33.

37. Singh R, Fazal Z, Freemantle SJ, Spinella MJ. Mechanisms of cisplatin sensitivity and resistance in testicular germ cell tumors. *Cancer Drug Resist.* 2019;2(3):580-594.
38. Syring I, Bartels J, Holdenrieder S, Kristiansen G, Müller SC, Ellinger J. Circulating serum miRNA (Mir-367-3p, mir-371a-3p, mir-372-3p and mir-373-3p) as biomarkers in patients with testicular germ cell cancer. *J Urol.* 2015;193(1):331-337.
39. Trabert B, Chen J, Devesa SS, Bray F, McGlynn KA. International patterns and trends in testicular cancer incidence, overall and by histologic subtype, 1973-2007. *Andrology.* 2015;3(1):4-12.
40. Teshima S, Shimosato Y, Hirohashi S, *et al.* Four new human germ cell tumor cell lines. *Lab Invest.* 1988;59(3):328-336.
41. van Agthoven T, Eijkenboom WMH, Looijenga LHJ. Microrna-371a-3p as informative biomarker for the follow-up of testicular germ cell cancer patients. *Cell Oncol (Dordr).* 2017;40(4):379-388.
42. van Echten J, Oosterhuis JW, Looijenga LH, *et al.* No recurrent structural abnormalities apart from i(12p) in primary germ cell tumors of the adult testis. *Genes Chromosomes Cancer.* 1995;14(2):133-144.
43. Wang N, Trend B, Bronson DL, Fraley EE. Nonrandom abnormalities in chromosome 1 in human testicular cancers. *Cancer Res.* 1980;40(3):796-802.
44. Zehir A, Benayed R, Shah RH, *et al.* Mutational landscape of metastatic cancer revealed from prospective clinical sequencing of 10,000 patients. *Nat Med.* 2017;23(6):703-713.

A



Addendum

ENGLISH SUMMARY

Malignant germ cell tumors (GCTs) account for approximately 1% of male cancers worldwide and are the most common solid malignancy among males ages 15 to 44 years old. While the majority of GCTs are of testicular origin, they can also occur extra-testicular anywhere in the midline of the body, for example in the (retro)peritoneum, the mediastinum, and intracranially, in the brain. Of all diagnosed GCT patients roughly 5% will succumb to their disease and as these cancers often occur in relatively young patients (young males but also pediatrically) they are, when considering potential years of life lost, the highest-ranking cancer.

GCTs come in many flavors, but the most important distinction is between the embryonic type GCT elements and the fully differentiated teratomas. As GCTs closely resemble embryonal germ and stem cells, the cells that form us as organisms from the first stages of fertilization, the various intermediates as well as the fully differentiated components (teratomas) are present at different developmental stages of a healthy individual. Just like embryonal germ and stem cells, GCT cells are overall, with the consistent exception of teratomas, very sensitive to DNA-damage and therefore the main treatment modality for GCTs is platin-based (cisplatin in adults). Cisplatin is a DNA-damaging chemotherapeutic agent discovered in the late 70s. Even though cisplatin is effective for treatment in the majority of GCT patients, its efficacy is almost fully diminished in treatment resistant patients, rendering them with limited options and, in ~50% of cases, death because of their disease. Furthermore, cisplatin is highly toxic, and the price of treatment often comes with many side-effects like chronic fatigue, heart-disease, kidney disease and loss of hearing (ototoxicity), of which the severity is also age dependent. This demonstrates a high clinical significance to understand GCT resistance not only to improve treatment but also improve upfront patient stratification, avoiding overtreatment of intrinsically resistant patients, resulting in severe impact on quality of life.

There are currently a few clinical biomarkers in place for the early detection, diagnosis, and surveillance of GCTs (teratoma excluded). Good biomarkers are for example hormones and/or proteins that are detectable in bodily fluids (liquid-biopsy based) that specifically mark the presence of disease while not being present in healthy individuals. Unfortunately, the total set of biomarkers currently used in the clinic have about 60% accuracy, which means that only roughly 60% of people that have a GCT have elevated levels of these markers. Additionally, some healthy individuals might have elevated levels of these markers, called false positives, warranting improvement. The microRNA cluster 371a-3 has been reported some two decades ago to faithfully mark GCTs (teratomas excluded), meaning that no or limited healthy individuals show detectable levels of these microRNAs. The majority of patients (>95%) display elevated levels, making them excellent biomarkers for GCTs with a high potential to be clinically applicable.

Lastly, it is important to mention *TP53*, an important gene in many cancers. This gene is considered the ‘guardian of genome’ because under normal circumstances one of its main functions is protect genomic integrity and assure that only cells harboring intact, damage-free DNA undergo full cellular division. Consequently, this gene appears mutated or lost in many solid cancers, essentially giving cancers a “license to divide”. The rule of thumb is that patients harboring cancers with *TP53* mutations generally do worse in the clinic. Additionally, considering all solid cancers, *TP53* is either lost or mutated (or both) in roughly 50% of cases, making it one of the most important known cancer associated genes. Interestingly, *TP53* is rarely mutated in GCTs, likely due to the embryonal origin of these cancers. One can imagine that embryonal germ and stem cells, the cells responsible for the germ cell lineage as well as the development of the entire organism, need to maintain the utmost genomic integrity and therefore *TP53* is one of the key players in facilitating genome protection in these early embryonic cells. It is unknown whether loss of *TP53* can confer cisplatin resistance in GCTs.

This thesis focuses on two main topics in GCT research **1)** what causes GCT resistance and **2)** what is the role of the microRNA 371a-3 cluster in GCTs. We focus on resistance, both in the light of *TP53* mutations as well as other factors, in **Chapters 2, 3 and 4** and on the microRNAs in **Chapters 5, 6 and 7**.

In **Chapters 2 and 3** we discuss *TP53*. First, we study the available literature and report on the role of *TP53* in embryonal stem cells and speculating about a possible role for it in GCTs. We continue along this line in **Chapter 3**, empirically demonstrating a potential role for *TP53* in GCT cell lines by introducing artificial mutations in the gene using the CRISPR-Cas9 technology. Initially we show that even though being rare, *TP53* mutations can occur in GCTs by investigation of a large publicly available dataset. We find that the presence of *TP53* mutations almost always coincides with treatment resistance and that this furthermore seems to be dependent on the anatomical location where the cancer resides. Next, we demonstrate that by introducing defined mutations in the *TP53* gene, rendering it virtually non-functional, cells become more resistant to cisplatin treatment, illustrating that even though they are rare, *TP53* mutations can contribute to cellular resistance in GCTs.

In **Chapter 4** we expand upon the topic of GCT resistance by demonstrating that in an independently generated set of sensitive and cisplatin resistant GCT cell lines all independently generated resistant clones share the same chromosomal gain, located on the short arm of chromosome 3. Additionally, we use several publicly available datasets to demonstrate that not only is the specific gain present in GCTs, but it is also significantly enriched in the group of GCTs diagnosed in patients who show cisplatin-based treatment resistance. Lastly, we demonstrate that stratifying patients based on the chromosomal gain adds diagnostic value to the already in-place staging systems currently used in the clinic (IGCCCG classification). These findings are highly relevant for the clinic as patients

could be stratified upfront, avoiding over-treatment of patients harboring intrinsically or relapsed resistant tumors.

Finally, **Chapters 5, 6 and 7** focus on the microRNAs. In **Chapter 5** we compare two methods for this molecular biomarker detection, coming from different starting materials (serum and plasma). We show that there is virtually no difference between serum and plasma and the two detection techniques, demonstrating that both can be used to detect the microRNAs faithfully. This is a significant contribution to the field in the context of development of a clinically applicable test. **Chapter 6** is a mechanistic study into the microRNA cluster. Again, using the same technique as in **Chapter 3** we genetically mutate the various microRNAs located in this cluster to study their function in GCT cell lines. We find that removing the microRNAs in GCT cell lines has little to no effect on their survival indicating that the expression of the microRNAs is likely a passenger effect that occurs during early oncogenic development of these cancers. Finally, in **Chapter 7** we use a mouse model for GCTs to illustrate that we detect the mouse homologue (same versions of the same gene in a different animal) of the microRNA cluster in these GCT bearing mice. Furthermore, we can detect elevated levels of the microRNAs in pregnant mice carrying pups that have GCTs, indicating that mothers carrying at risk children could be screened for the presence of GCTs in their babies using the microRNAs.

In conclusion, this thesis reports on several aspects of GCT research, being significant contributions to the current field. Although this work is only a fraction of the necessary work to fully characterize these cancers with the aim to cure all GCT patients, it paves a way to new avenues to be explored. The key findings in this work are the involvement of *TP53* in GCT resistance, the chromosomal gain on the short arm of chromosome 3 as marker for GCT resistance, the comparability of serum and plasma and various techniques for detection of microRNA371a, the mechanistic work illustrating that the microRNAs are likely passenger effects and lastly the fact that mice can be used to study various aspects of these specific biomarkers further related to various clinically relevant parameters. The latter even suggests the possibility to screen pregnant women for the presence of the malignancy during intra-uterine development. However, so far, no informative biomarker has been found to identify teratoma, which remains an area of potential investigation.

NEDERLANDSE SAMENVATTING

Kwaadaardige kiemceltumoren (GCTs) vertegenwoordigen ongeveer 1% van de mannelijke kankersoorten wereldwijd en zijn de meest voorkomende solide maligniteit bij blanke mannen tussen de 15 en 44 jaar oud. Hoewel de meerderheid van de GCTs van testiculaire oorsprong is, kunnen ze ook extra-testiculair voorkomen op elke plaats in de middenlijn van het lichaam, bijvoorbeeld in het (retro)peritoneum, het mediastinum en in de hersenen. Ongeveer 5% van alle gediagnosticeerde GCT-patiënten overlijdt aan hun ziekte, en omdat deze kankers vaak voorkomen bij relatief jonge patiënten (jonge mannen maar ook pediatrische patiënten), zijn ze, wanneer dit bekeken wordt vanuit de potentiële verloren levensjaren, de hoogst scorende kanker.

GCTs komen in verschillende varianten voor, maar het belangrijkste onderscheid is de embryonale type GCT-elementen en de volledig gedifferentieerde teratomen. GCTs lijken sterk op embryonale kiem- en stamcellen, dat zijn de cellen verantwoordelijk voor de kiemlijn en de ontwikkeling van het hele organisme vanaf het moment van bevruchting. Hierdoor kunnen deze tumoren kenmerken hebben van zowel extra-embryonale structuren (dooierzak, amnionzak) maar ook weefsel wat lijkt op volledig gedifferentieerde cellen (teratoom). Net als embryonale kiem- en stamcellen zijn GCT-cellen over het algemeen, met de consistente uitzondering van teratomen, zeer gevoelig voor DNA-schade, en daarom is de belangrijkste behandeling voor GCTs een platina-gebaseerde chemotherapie (cisplatine bij volwassenen). Cisplatine is een DNA-beschadigend chemotherapeutisch middel dat eind jaren 70 is ontdekt. Hoewel cisplatine effectief is bij de behandeling van de meerderheid van de GCT-patiënten, is diezelfde werkzaamheid vrijwel volledig verdwenen bij patiënten die resistent zijn voor de behandeling. Bij patiënten met resistente kankers zijn de opties beperkt en in ongeveer 50% van de gevallen overlijden ze als gevolg van hun ziekte. Bovendien is cisplatine giftig en de behandeling gaat vaak gepaard met bijwerkingen zoals chronische vermoeidheid, hartziekte, nieraandoeningen en gehoorverlies (ototoxiciteit), waarvan de ernst ook afhankelijk is van de leeftijd. Dit toont het grote klinische belang aan van het begrijpen van GCT-resistentie. Dit niet alleen om de behandeling te verbeteren, maar ook om het selecteren van het optimale behandelplan van patiënten vooraf te verbeteren. Hierdoor kan overbehandeling van intrinsiek resistente patiënten, maar ook mogelijk onder behandelen, voorkomen worden, wat de kwaliteit van leven van de individuele patiënt zal verbeteren.

Op dit moment zijn er enkele klinische biomarkers voor vroege detectie, diagnose en monitoring van GCTs (teratoma uitgezonderd). Goede biomarkers zijn bijvoorbeeld hormonen en/of eiwitten die detecteerbaar zijn in lichaamsvloeistoffen (gebaseerd op vloeibare biopsie) en specifiek de aanwezigheid van de ziekte markeren zonder aanwezig te zijn bij gezonde individuen. Helaas heeft de totale set biomarkers die momenteel in de kliniek wordt gebruikt bij GCT-patiënten een nauwkeurigheid van ongeveer 60%, wat

betekent dat slechts ongeveer 60% van de mensen met een GCT verhoogde niveaus van deze markers heeft. Bovendien kunnen sommige gezonde individuen verhoogde niveaus van deze markers hebben, ook wel valse positieven genoemd. Het microRNA-cluster 371a-3 is zo'n twintig jaar geleden gerapporteerd als een mogelijk betrouwbare marker voor GCT's (teratoma uitgezonderd), wat betekent dat geen of weinig gezonde individuen detecteerbare niveaus van deze microRNAs vertonen. Vele studies zijn uitgevoerd, en hieruit blijkt dat de meerderheid van de patiënten (>95%) verhoogde niveaus vertoont. Hierdoor zijn deze embryonale microRNAs uitstekende biomarkers voor de aanwezigheid van een GCT met een grote potentie voor klinische toepasbaarheid.

Tot slot is het belangrijk om *TP53* te noemen, een belangrijk gen bij veel kankersoorten. Dit gen wordt beschouwd als de "bewaker van het genoom" omdat het onder normale omstandigheden één van de belangrijkste functies heeft om genomische integriteit te behouden en ervoor te zorgen dat alleen cellen met intact, schadevrij DNA volledige celdeling ondergaan. Als gevolg hiervan is dit gen gemuteerd of verloren in veel solide tumoren, waardoor kankers als het ware een "licentie om te delen" krijgen. Als vuistregel geldt dat patiënten met kankers met *TP53*-mutaties over het algemeen een slechter klinisch gedrag vertonen. Bovendien is *TP53* in ongeveer 50% van de gevallen verloren of gemuteerd (of beide) bij alle solide tumoren, waardoor het één van de belangrijkste bekende genen geassocieerd met kanker is. Interessant is dat *TP53* zelden gemuteerd is in GCTs, waarschijnlijk vanwege de embryonale oorsprong van deze tumoren. Men kan zich voorstellen dat embryonale kiem- en stamcellen, de hoogste genomische integriteit moeten handhaven en daarom is *TP53* een van de belangrijkste spelers bij het faciliteren van genoombescherming in deze vroege embryonale cellen. Het is onbekend of het verlies van *TP53* cisplatine resistentie kan veroorzaken bij GCTs.

Dit proefschrift richt zich op twee hoofdonderwerpen in GCT-onderzoek: **1)** wat veroorzaakt GCT-resistentie en **2)** wat is de rol van het microRNA-cluster 371a-3 in GCTs. Dit werk focust zich op resistentie, zowel in het licht van *TP53*-mutaties als andere factoren, in **Hoofdstukken 2, 3 en 4**, en op de microRNAs in **Hoofdstukken 5, 6 en 7**.

In **Hoofdstukken 2 en 3** bespreken we *TP53*. Eerst bestuderen we de beschikbare literatuur en rapporteren we over de rol van *TP53* in embryonale stamcellen en speculeren we over een mogelijke rol in GCTs. We gaan verder op deze lijn in **Hoofdstuk 3**, waar we een mogelijke rol voor *TP53* in GCT-celkweken aantonen door kunstmatige mutaties in het gen te introduceren met behulp van de CRISPR-Cas9-technologie. In eerste instantie laten we zien dat, hoewel zeldzaam, *TP53*-mutaties kunnen voorkomen bij GCTs door onderzoek beschikbaar in een publieke dataset. We ontdekken dat de aanwezigheid van *TP53*-mutaties bijna altijd samengaat met resistentie tegen behandeling en dat dit bovendien lijkt af te hangen van de anatomische oorsprong van de kanker. Vervolgens tonen we aan dat door gedefinieerde mutaties in het *TP53*-gen te introduceren in laboratorium modellen waardoor het eiwit niet-functioneel wordt, cellen resistenter

worden tegen cisplatine-behandeling. Dit toont aan dat hoewel *TP53*-mutaties zeldzaam zijn, ze kunnen bijdragen aan cellulaire resistentie bij GCTs.

In **Hoofdstuk 4** breiden we het onderwerp van GCT-resistentie uit. We tonen aan dat in een onafhankelijk gegenereerde set van gevoelige en cisplatine resistente GCT-cellen alle onafhankelijk gegenereerde resistente klonen dezelfde chromosomale amplificatie hebben, gelegen op de korte arm van chromosoom 3. Bovendien gebruiken we verschillende publiek beschikbare datasets om aan te tonen dat niet alleen de specifieke amplificatie aanwezig is in GCTs, en dat deze significant verrijkt is in de groep GCTs die resistentie vertonen tegen cisplatine-behandeling. Ten slotte tonen we aan dat het stratificeren van patiënten op basis van de chromosomale amplificatie, prognostische waarde toevoegt aan de al gebruikte stadiëringssystemen in de kliniek (IGCCG-classificatie). Deze bevindingen zijn relevant voor de kliniek, omdat patiënten van tevoren zouden kunnen worden gestratificeerd, waardoor overbehandeling van patiënten met intrinsiek resistente of teruggekomen ziekte wordt voorkomen.

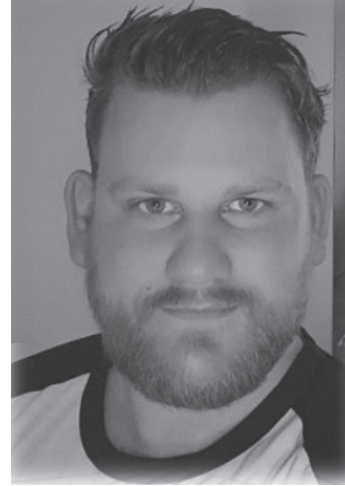
Hoofdstuk 5, 6 en 7 richten zich op de microRNAs. In **Hoofdstuk 5** vergelijken we twee methoden voor de detectie van deze moleculaire biomarker, afkomstig van verschillende startmaterialen (serum en plasma). We tonen aan dat er vrijwel geen verschil is tussen serum en plasma en de twee detectietechnieken, wat aantoont dat beide gebruikt kunnen worden om de microRNAs betrouwbaar aan te tonen. Dit is een belangrijke bijdrage aan het vakgebied in het kader van de ontwikkeling van een klinisch toepasbare test. **Hoofdstuk 6** beschrijft een fundamentele studie naar het microRNA-cluster. Opnieuw gebruiken we dezelfde techniek als in **Hoofdstuk 3** om de verschillende microRNAs in dit cluster genetisch te muteren om hun functie in GCT-cellen te bestuderen. We ontdekken dat het verwijderen van de microRNAs in GCT-celculturen weinig tot geen effect heeft op hun overleving, wat aangeeft dat de expressie van de microRNAs of een neveneffect is wat optreedt tijdens de vroege ontwikkeling van deze tumoren of enkel belangrijk is tijdens de eerste stadia van het ontwikkelen van deze kanker. Ten slotte gebruiken we in **Hoofdstuk 7** een muismodel voor GCTs om aan te tonen dat we het muis-homoloog (dezelfde versies van hetzelfde gen in een ander dier) van het microRNA-cluster kunnen detecteren in deze muizen met GCTs. Bovendien kunnen we verhoogde niveaus van de microRNAs detecteren bij zwangere muizen die pups dragen die een GCT hebben, wat aangeeft dat moeders die kinderen met een risico op een GCT dragen, gescreend zouden kunnen worden op de aanwezigheid van een GCT bij hun baby's met behulp van de microRNAs.

Samengevat onderzoekt deze scriptie de mechanismen van GCT-resistentie en de rol van het microRNA-cluster 371a-3 bij deze kankers. Het identificeert *TP53*-mutaties als een mogelijke oorzaak van resistentie en toont aan dat een chromosomale amplificatie op de korte arm van chromosoom 3 geassocieerd is met cisplatine resistentie. Bovendien laat het zien dat het microRNA-cluster 371a-3 een veelbelovende biomarker is voor de

detectie en prognose van GCTs zonder duidelijke belangrijke functies voor het overleven van deze tumoren. Deze bevindingen dragen bij aan een beter begrip van GCTs en kunnen bijdragen aan verbeterde behandelingen en klinische besluitvorming.

CURRICULUM VITAE

Dennis Michael Timmerman was born in Dordrecht, the Netherlands, on September 23, 1995. In 2013 he obtained his high school degree (Christelijk College Nassau Veluwe). Later that year, he started his Bachelor's program Biomedical Sciences at University Utrecht in Utrecht and obtained his degree in 2016. In the same year he started his Master's program Cancer, Stem Cells and Developmental Biology also at the University Utrecht in Utrecht, specializing in cell biology and colorectal cancer. During his Master's he performed his first internship called 'Drug screens on STAR organoids' in the group of Dr. Hugo Snippert under supervision of Dr. Koen Oost at the UMC Utrecht. His second internship, called 'Treatment of



Early Tumor Stem Cells with DNA-damaging Agents', was performed in the group of Prof. Dr. Owen Sansom under supervision of Dr. Michael Hodder at the CRUK Beatson Institute in Glasgow. He obtained his Master's degree in 2018. In 2019 he joined the lab of Prof. Dr. Leendert Looijenga at the Princess Máxima Center in Utrecht. The results of his PhD project 'Germ cell tumor treatment resistance and liquid biopsy-based microRNA biomarkers' are presented in this thesis.

PHD PORTFOLIO

Discipline-specific educational activities	# ECTS
Gene Expression, Epigenetics and Disease	3
Cell Organization in Health and Disease	1.5
Introduction to Stem Cells	2.4
CS&D Masterclass December 12/13 2019	1
CS&D Masterclass November 18 2021	0.5
CS&D Masterclass September 29/30 2022	1
CS&D Retreat March 26 2021	1
CS&D Retreat June 15/16/17 2022	1
CS&D Seminars	4

General educational activities	
RISE EU Madame Curie exchange project Trento (2 months full-time)	2.5
PMC Retreat 2021 (Oct 27/28)	0.6
PMC Retreat 2022 (Oct 5/6)	0.6

Symposia/conferences (oral/poster presenter) and other activities	
PhD symposium PMC	0.6
Scientific symposium PMC (2 full days)	0.6
TOTAL NUMBER OF ECTS	20.3

STUDENT SUPERVISION

- **Master internship** (Tessa Remmers, 9 months)
- **Writing assignment** (Tessa Remmers, +/- 3 months)
- **Writing assignment** (Maarten Pops, +/- 3 months)
- **Master internship** (Sanne Hillenius, 8 months)
- **Master internship** (Carlijn Friedrichs, 8 months)
- **Master internship** (Marit Buiting, 9 months)

DANKWOORD

Daar is het dan, het is klaar. Het voelt alsof ik aan de noodrem van een sneltrein heb getrokken en ineens stil sta. Ik wist sinds de 2^e klas al dat ik een PhD wilde doen, en die PhD moest zijn in kankeronderzoek. Nu, terwijl ik dit dankwoord schrijf, realiseer ik me pas hoe de afgelopen jaren in een waas aan me voorbij zijn gevlogen om te kunnen bereiken wat ik toen al wilde doen. Nu voor het eerst, hier aan het eind van mijn jeugddroom, vind ik mezelf op een plek zonder blik vooruit, voor het eerst zonder plan voor de toekomst. In September 2013 begon ik met mijn bachelor biomedische wetenschappen en nu, bijna 10 jaar later (het is vandaag 20 Juli 2023) ben ik begonnen aan het dankwoord van mijn thesis. Wat een geweldig avontuur was dit! Ik heb ook mixed feelings over het afronden van mijn PhD tijd, want ik vond dit, het zijn van een PhD student, toch het allermooiste wat ik tot nu toe heb mogen doen in mijn academische carrière. Aan de andere kant ben ik natuurlijk ook enorm blij dat mijn proefschrift af is en ik deze periode van vallen en opstaan af kan sluiten. Er zijn zoveel mensen die dit tot zo'n leuke tijd hebben gemaakt en zonder wie ik nooit tot dit punt was gekomen en die mensen wil ik hier graag bedanken.

Allereerst, mijn promotor Prof. Dr. **Leendert Looijenga. Leendert**, er staat hier promotor maar ik zag je eerder als mijn mentor, want wat heb ik ongelooflijk veel van jou mogen leren. Vanaf moment één was er voor mij een klik, want ik voelde dat jij je oprecht bekommerde om mij én mijn carrière. Jij hebt altijd in mij geloofd, ook op de momenten dat ik dit niet deed. Sterker nog, op veel momenten voelde het alsof jij meer in mij zag dan ik zelf kon zien. Ik wil je hier enorm voor bedanken. Al was het eerste jaar turbulent, het afkrijgen van de eerste versie van het paper, het 'werk' van onze oude postdoc en een interne scoop van je oude PhD-student, we hebben altijd de communicatie kort gehouden en samengewerkt naar een oplossing. Je zei dat we hier tijdens mijn promotie nog wel om gingen lachen en ik denk dat we dat onderweg al meerdere keren hebben gedaan. Ook wil ik je bedanken dat je altijd achter me stond. Waar we naar mijn mening een makkelijke verhouding hadden, vaak op één lijn zaten en eigenlijk nooit conflicten hebben gehad, hield je me, als het nodig was, altijd de hand boven het hoofd. In onze meetings was er ruimte voor discussie, maar ook emotie, en als ik ergens niet uitkwam was je altijd oplossingsgericht zonder veroordelingen. Je hielp me het beste uit mezelf te halen, mijn grenzen te zoeken (en ze te vinden), maar was ook daar voor rust en reflectie als ik mezelf voorbij was gelopen. Ik ben enorm dankbaar voor mijn tijd in jouw groep en de dingen die wij samen hebben bereikt en ik ben trots om onder jou te mogen promoveren.

Beste leden van de beoordelings- en leescommissie, hartelijke dank voor de tijd die jullie hebben genomen om mijn proefschrift te lezen en zitting te nemen in mijn commissie. Ik kijk er naar uit om met jullie van gedachten te wisselen over mijn werk.

Sruthi... I know I promised you a full page, although I am not sure if I will manage, you deserve a full book worth of thanks. Even though we haven't always seen eye to eye (actually, we rarely have), I always seen our connection as an accelerated siblinghood, because you are like a sister to me. In the first year of our PhD we were young and although we liked each other, moods could rapidly swing from love to hate and vice versa. During the second year we hit puberty, we tested each other, but immediately had each other's back when something external happened. In the final years we've grown mature and patient towards each other. Still thinking 'why is he/she being so dramatic' but texting "hey, it's going to be okay". Saying you were my rock would be an understatement, because Sruthi, if it weren't for you, I think there would be times where I wouldn't have had the faith in myself to continue in this journey. You made bad days manageable, and you made good days great. You always brought great 'tea', and I will never forget our million looks every time something odd happened the office or I gave you the "let's have coffee nod". Thank you for everything Sruthi, and I am sure, if your absurdly full calendar allows it, we will see each other many more times.

Beste **Ad**, nog zo iemand zonder wie ik mijn PhD niet had kunnen doen. Want Ad, wat heb jij enorm veel data voor mij gegenereerd. qPCRs, DNA-isolatie, PCR, RNA-isolatie, conditioned medium, zo lang ik maar het ML-I gedeelte deed, draaide jij nooit je hand om voor een assay. Verder hebben elkaar ook goed kunnen vermaken over frikandellen samples en de befaamde jaarlijks uitgave van de gouden frikandel. Heel erg bedankt voor alles.

Thomas, de redder in nood, niet de postdoc die we verdiende maar de postdoc die we nodig hadden. Na het fiasco van jouw voorganger kwam jij als nuchtere factor in onze groep. Jouw "ik kan wel wat met R" werd al snel omgezet naar de bio informaticus van de groep. Jouw kritische blik heeft me altijd geholpen om meer uit mijn werk te halen en een betere onderzoeker te worden. Je was altijd available om te sparren over gaande proeven en projecten en we hebben samen een paar keurige papers geschreven. Ik ben ook blij dat je tussen je drukke werk-privé leven ook een paar keer de tijd hebt gevonden om lekker bier te drinken, heb me altijd kostelijk met je vermaakt!

Lieve **Tessa**, jij was mijn allereerste student en kwam midden in de chaos van het 3p project binnen. Ik was nog een piepkleine baby-PhD die net 6 weken begonnen was en samen hebben wij zo belachelijk veel proeven gedaan. Lange dagen in de ML-I, maar wel altijd gelachen, drankjes op vrijdag en uiteindelijk samen ook twee papers mogen schrijven, we hebben de tijd goed gevuld. Heel erg bedankt voor de leuke tijd en je inzet!

Lieve **Sanne**, eerst mijn student en nu sinds kort mijn collega. Ook jij hebt zoveel werk verzet tijdens je stage, wat ook resulteerde in dezelfde twee papers. Ik ben blij dat je na al mijn adviezen toch uiteindelijk de keuze hebt gemaakt om een PhD te gaan doen. Je bent mega slim dus dat moet helemaal goed komen.

Lieve **Carlijn**, het voelt meteen al raar om Carlijn te zeggen, hier moet natuurlijk “Lieve **Lino**” staan. Ik kan hier wel zeggen dat je goed gewerkt hebt en dat we ook samen één paper hebben geschreven, maar jij weet natuurlijk zelf ook wel dat ik je vooral wil bedanken voor de toptijd, en nog beter, de good vibes (en roddels). Vanaf moment een hadden we echt perfecte klik, niet gebaseerd op research, maar om onze gedeelde liefde om te geiten. Heel erg bedankt voor de leuke maanden, ik wens jou en Hedel veel geluk toe (en natuurlijk binnenkort de baby Cisplatino).

Lieve **Lotte** (Lotsjj Potsjj), ik weet dat jij hier eigenlijk niet thuishoort (wel in mijn dankwoord, maar niet tussen de studenten), maar ik doe het lekker toch. Want lieve Lotte, je voelde toch wel een beetje als mijn student, maar nog veel belangrijker, een hele leuke collega en vriendin. Lekker hitjes draaien in de ML-I, drankjes doen, oh ja, soms ook hier een daar een proefje. Ik ben heel blij dat als ik dit boekje aan je mag overhandigen je gewoon weer terug bent in Utrecht om naar Ferrari te luisteren (en er een potje van te maken). Heel erg bedankt voor de leuke tijd op lab en nu nog steeds erbuiten!

Lieve **Marit** (Malibu/Mehek), onze tijd samen begon een beetje raar, ik zat in Trento en jij zat half zonder begeleider. Ik merkte al wel direct, zowel vanuit Trento als toen ik terug was, dat jij extreem zelfstandig bent op het lab. Ik had pas later door hoe grappig je bent als persoon. Je had altijd de laatste nieuwsroddels of andere goeie tea voor me paraat. Na werk lekker bij Oorlof, in jouw prachtige tuin of mijn balkon zitten, of de Boys kijken (helaas toch net niet afgekregen voor het eind van je stage). Heel erg bedankt dat jij de laatste periode van mijn PhD zo leuk hebt gemaakt en voor je hulp en lieve woorden om te helpen los te laten. Je bent van een student naar een van mijn beste vriendinnen gegaan en daar ben ik heel blij mee.

Dear **Ziqin**, without you I wouldn't have been able to complete some of the simplest tasks. How is it possible that someone who started only one month after me, literally knows everything about anything going on in the Maxima Center. There is literally no question you cannot answer, no experiment you do not know. You are one of the most driven and smartest people I know, and I am very grateful for our times and discussions in the ML-I/coffee corner/office. You are a great guy, just try to go home and sleep once in a while.

Joaquin, my lab brother from another mother (or more colleague from another PI but that sounds less catchy). I had the privilege to get to know you about one year into my project and things immediately clicked. We shared ideas, projects, half a group and quite some beers. I think you are a very clever dude but moreover, you are funny as hell man. Appreciate you.

Thijs (Thieske), onze avonturen begonnen allemaal rondom de beste machine in het Maxima, de multidrop! Ik kan hier vanalles zeggen maar niemand zal ooit begrijpen wat een band samen multidroppen schept, het vergt een speciaal soort persoon. Na je master stage kwam je gelukkig terug voor een PhD en hebben we nog op 2 retreats een kamer mogen delen. Ik weet dat je jezelf nu al moet verdelen over 2 groepen maar voor mij ben je altijd onderdeel geweest van onze groep (als adoptiestudent).

Kostas, salam aleikum ya akhi. I took the time to learn some of your language to greet you. You obviously belong here as well. Although you were spread thin between your 7+ institutions, it was always nice to see you around the Maxima (and even nicer to see you outside the Maxima). Let me know if you are done with your million trips so we can finally hang out again.

Lieve **Eugenie**, waar zou ik (en eigenlijk iedereen in de research) zijn zonder jou. Niet alleen verzorg je ons dagelijks van onze bestellingen en nieuwe materialen, maar hielp je me ook nog eens persoonlijk aan spullen, zeker in tijden van schaarste, tijdens Covid. Heel erg bedankt voor al je harde werk en hulp (vooral alle Cell Titre Glo potjes en 96-wells platen die je voor me bewaarde!).

To any **other colleagues** I forgot to mention by name, you know who you are, there is just too many people to all mention here. Thank you everyone, especially from the 3rd floor ML-I for all the fun times, nice conversations, problem solving, ranting, tips, tricks, and laughs. I appreciate you all and will miss the ML-I vibes.

Dear **Katie**, thank you for all your support from the start and along the way. I really appreciate it.

Lieve **Mams**, jij hebt altijd in mij geloofd, ondanks dat je niet altijd akkoord ging met mijn manier van studeren, wist je dat ik altijd op mijn plek zou komen. Ik weet hoe trots je op me bent en daar ben ik dankbaar voor.

Lieve **Vadert**, ook jij bedankt voor je onvoorwaardelijke vertrouwen in mij. Ik weet dat je niet altijd even goed begreep wat ik nou deed maar je toonde altijd interesse en heb altijd gevoeld hoe trots je op me was, dankjewel.

Lieve lieve lieve **Kimmie**, laat je niet misleiden dat jij pas hier staat, de beste bedankjes bewaar ik voor het laatst. Allereerst wil ik jou bedanken voor de prachtige voorkant van dit boekje (en overige artwork), het is echt heel mooi geworden en dat was het zonder jou nooit gelukt. Verder wil ik je bedanken voor alle lieve woorden van support en vertrouwen op welk moment ik dat ook nodig had. Jij hebt me er echt doorheen getrokken wanneer ik het even niet meer zag zitten, niet alleen de afgelopen 4 jaar, maar altijd. Van kleine belletjes tot nummers opnemen, jij staat altijd voor me klaar. Ik ben zo gelukkig en trots om jou mijn zusje te mogen noemen, je bent echt goud.

Lieve **Maarten** (het Paard), begonnen als fulltime student en nu fulltime maat, ik spreek jou nog steeds dagelijks en daar ben ik enorm dankbaar voor. Je bent een schat van een mens, zorgzaam naar iedereen om je heen maar soms niet zo voor jezelf. Je hebt me zoveel geholpen met struggles zowel op werk als privé, je bent een van de liefste mensen die ik ken.

Crazy Louis **Laurens** (Lulu), mijn god wat ben jij ook inderdaad crazy. Maar ik denk dat als ik jou niet had leren kennen tijdens Covid ik zelf ook lachend gek was geworden. Dagen op het lab werden ingeruild voor bier drinken op het dak en iets als een 'schoolnight' was meer een suggestie. Wat hebben wij er toch een heerlijke bende van gemaakt in de Casa in die tijden dat de rest zich heeft mogen vervelen. Ik waardeer ook heel erg onze diepgaandere gesprekken, jouw volwassenheid en geduld en natuurlijk onze holy trinity (gym, fortnite, bier).

Lieve **Yousef**, dit dankwoord zou niet compleet zijn zonder jou, want waar zou ik überhaupt ergens in het leven gekomen zijn door jouw oeroude wijsheid en serene innerlijke stilte en rust. Op de meeste dagen waren de gym sessies genoeg om mijn hoofd leeg te maken, maar ik kreeg er altijd gratis een therapie sessie van jou bij. Jouw adviezen hebben me oprecht geholpen mijn weg te vinden zonder mezelf daarin compleet te verliezen. Ik ben echt heel erg blij dat ik jou ken. Als laatste wil ik je hierbij wel nog met klem verzoeken een agenda te kopen of desnoods dit boekje te gaan gebruiken als planner. Oh ja, kom ook eens terug uit Rotterdam, heb je toch liever permanent in Utrecht.

Brian, je wilde niet in dit dankwoord, ik heb geen idee waarom, maar ik hoop dat als je dit leest je ook zelf beseft dat jij helemaal niks te zeggen hebt over mijn boekje. Ik zou je hier graag willen bedanken voor de warme gesprekken, de woorden van motivatie, de steun in tijden dat het tegen zat, de “het komt wel goed schatje”. Echter is onze vriendschap geen Roosvicee reclame en is dat ook niet voor jou weggelegd. Toch had je wel altijd tijd om me te laten weten wanneer ik me aanstelde, ondanks dat ik weet dat je druk was met je eigen dingen en leven. Ik blijf je toch nog steeds, zelfs na 12 jaar, enorm waarderen, en ik ben oprecht dankbaar om je mijn beste vriend (kennis) te mogen noemen.

Lieve **Ruth**, mijn allerliefste lievelingsmens. Wat ben jij toch een lief en zorgzaam persoon. Ik kan jou alles vertellen en je hoort ook alles. Ik ben zo ontzettend dankbaar, gelukkig en trots om jouw vriend te mogen zijn. Samen alles met je te mogen delen en te weten dat je er altijd voor me bent. Je hebt me altijd gesteund, zeker in de laatste fasen heb ik zoveel op jou kunnen en mogen leunen. Je weet hoe ik over je denk, hoe gelukkig ik met je ben en hoe ik op kijk tegen jou als persoon. Ik heb in de afgelopen twee jaar minstens zoveel van jou geleerd als ik tijdens mijn PhD heb gedaan. Nu lekker samen verder kijken naar de volgende stap en genieten van ons prachtige nieuwe paleisje. Ik hou van jou.

